Water flow and solute transport modeling in structured porous media. A review

Francois Lafolie

Water Flow and Solute Transport Modeling in Structured Porous Media.

A Review.

F. Lafolie

Institut National de la Recherche Agronomique,
Station de Science du Sol, Domaine St Paul,
Montfavet, France.

Report made during a stay at the U.S. Salinity Laboratory, Riverside, Ca.

TABLE OF CONTENTS

INTRODUCTION

In our industrial and agricultural environment, pollution sources for groundwater are diverse and numerous. Industrial wastes which are in constant growth and accidental spreads of chemical substances constitute potential and effective contamination risks. Fertilizers and pesticides are used in large quantities by a more and more intensive agriculture, and up to the last few years little interest was borne to their behavior. With the new problem of radioactive wastes storage an increased interest has been borne to the understanding of transport mechanisms through porous media and to the prediction of solutes movement in the saturated and unsaturated zones. This growing concern for groundwater recharge, pollution problems and environmental protection has resulted in an increasing number of studies and models attempting to describe and predict the physical and chemical behaviors of water and solutes transported through heterogeneous porous media.

Early studies have focused primarily on solute movement through soil laboratory columns made up of uniformly packed disturbed materials. Solutes transport through these porous media is modeled by the convection–dispersion equation (C–D). Although this approach is restricted to uniform field soils, the convection–dispersion equation has been and is still widely used to describe the transport of dissolved substances. In fact, it appeared that the simple convection diffusion equation was not an appropriated tool when applied to undisturbed materials, and that a lot of physical mechanisms was not accounted for in this model. The C–D model is a macroscopic one, assuming that local heterogeneities in pore–water velocities due to pore geometry and pore–size distribution and occurring at a microscopic level can be lumped into an average pore–water velocity and dispersion coefficient. These assumptions are reasonable for soils which exhibit a narrow pore–size distribution and hence a relatively uniform velocity field.

In fact, for natural undisturbed materials a large pore–size distribution often exists, ranging from a porosity referred as micro–porosity or textural porosity to a size of pores corresponding to large voids often referred as macro–porosity or structural porosity. These pores corresponding to cracks in swelling soils, inter–aggregates voids, earthworm or gopher channels, old roots holes, are preferential pathways for water and applied solutes, and that not only for drastic boundary conditions. Thus, it is obvious that a large fraction of applied water and solutes is going to be transported through these ways and that the classical approach will fail to predict soil water contents as well as solute distributions. A lot of experimental studies have highlighted and underlined the important role played by macropores in the hydraulic working of the soil, Anderson et al. (1977 a,b), Bouma et al. (1977,1979,1982, 1984), Trudgill et al. (1983), Smettem et al. (1985 a,b,c).

Until about ten years ago, very little work was done to account for the different transport mechanisms operating in soils with large pores. Up to that time, however, several potentially useful models were formulated and used in both chemical and petroleum engineering literature, Rosen (1952), Turner (1958), Coats ans Smith (1964), Pellet (1966), Babock et al. (1966), Villermaux and van Swaay (1969). During the last years, following the way opened by these peoples, several models have been proposed in the soil science and civil engineering literature to simulate solute transport in structured soils. From a conceptual point of view all these models are

very similar. The main common assumption being that the velocity field can be a function of the space variables but is independent of time. One of the purposes of this report is to present and discuss these models, their hypothesis, solutions ans usefulness. The possibility to obtain analytical solutions through an extensive use of Laplace transforms, among other mathematical techniques, has been one of the reasons of the popularity and success of this approach in the last years. However, many people recognize now that numerical methods are needed to deal with complex real situations, Huyakorn (1983a,b).

As it has been said, the different available models have in common the steady–flow assumption. This is a limitation to their field application. In natural conditions and in the saturated–unsaturated zone this hypothesis is barely acceptable. We are there more concerned with a succession of transient flows of variable intensities and durations. In fact the hypothesis of steady–state flow can be released if we are not restricted to obtain analytical solutions. However, the prediction of water flow characteristics in an heterogeneous media is not easy and the coupling of water and solute transport in such conditions is still a very open research subject.

If we want to be able, not only to identify all the different mechanisms involved in solute transport, but also to predict the behavior of these substances in real situations and for management purposes, a coupling between water flow and solute transport models is necessary. As referred above, some approaches have been developed for solute transport assuming the knowledge of the velocity field. In homogeneous media where DARCY'S law is assumed valid, the velocity field can be easily obtained through the resolution of RICHARDS' equation. In heterogeneous conditions, many problems arise. DARCY'S law is no longer applicable and conceptually different approaches have to be developed to model saturated–unsaturated water flow in such media. Until now, very little works have been done in this domain. They are restricted to well defined geometry media, single crack or network of cracks, and thus can easily account for the flow in the macroporosity. They are mainly used to demonstrate the importance of preferential pathways on runoff, pollution risks and deep migration of fertilizers. An important problem arising when dealing with water flow in heterogeneous media is to take into account the possible modifications of the medium geometry and hence the modification of its hydraulic characteristics with time. This is done in saturated flow models by assuming deformations law for the porous media based on the elasticity theory, Jouanna and Louis (1984). At our knowledge, very little has been published to accounted for modifications of the structural porosity with time for unsaturated flows in swelling soils, Jarvis et al. (1987a). Only available models are concerned with water flow in homogeneous deformable media.

Even if it appears that a lot remains to be done in the field of solute transport and water flow modeling (water flow in particular), many models and solutions have been published in the past years and our modeling capacity has been improved.

This report aim at providing an overview of what is the actual state of the research in water flow and solute transport modeling through heterogeneous media. Special attention has been paid to present the different available models and their physical hypothesis in a form as detailed as possible so as the reader can easily appreciate the degree of sophistication and have an immediate and easy comparison between the different available approaches. A discussion of the different application conditions and hypothesis is presented with each model or group of models. Associated applications and field experiments are also presented when available. When analytical solutions are involved, which is frequently the case for solutes transport models, a complete expression of the solution is given, directly in the text or in annex, in such a way that the reader can readily use it. When numerical solutions are used, it is assumed that the reader is sufficiently familiar with numerical basic techniques, so that only the main steps leading to the numerical scheme are given.

In this report water flow models for saturated fractured media are presented first. Two different approaches are developed. One will be referred as *deterministic* and the other as *stochastic*. The particular meaning of these terms will be explained later. Then are discussed the different approaches and works published to deal with unsaturated flows in heterogeneous media. This part will cover models for single crack or pore, networks of cracks, double porosity models, and kinematic waves based models. An extension to non rigid media will end this part.

Solute transport will be split into three parts. The first will present the models developed for well defined geometry media. Equations and analytical solutions will be derived for spherical aggregates, and extensions presented for other types of geometry, planar voids and planar aggregates, cylindrical voids and cylindrical macropores. The notion of aggregate shape factor will provide a link between the different geometries. Special attention will be payed to analytical solutions and Laplace transform inversion problems. The macroscopic approach will be the second part. The concept of mobile–immobile water is at the base of this type of approach. Relations will be established between the parameter controling the interphase transport rate in these models and the geometry of the porous blocks or aggregates in the former ones. The concept of Block–Geometry–Function which appears to provide a new and inovative way to model solute transport will be fully developed. Its links with previous models will be also fully discussed. At the end of this part will be presented the transfer function approach developed by Jury (1982) to cope with spatial variability of transfer processes. Finally the coupled water flow, solute transfer problem will be considered.

1. SATURATED FLOW IN HETEROGENEOUS POROUS MEDIA

1.1 INTRODUCTION

Simulation of saturated water flow in fractured porous media has been and still continues to be an important research subject in areas such as petroleum engineering or karst hydrology. The problem of underground nuclear wastes storage and the assessment of assossiated groundwater contamination risks arose in the past few years and gave a new dimension and importance to this field of research. In this part of the report we review some models lately proposed for saturated water flow modeling in fractured media. At first, it may seem that this problem is not of great interest from the point of view of agronomic research. In fact it is a first step toward unsaturated water flow modeling in heterogeneous media and in particular can provide useful ideas in order to model the interaction between the fractures or more generally the macroporosity and the porous matrix. The models which have been developed for saturated water flows are of two types and usually referred as *Discrete approach* models and *Double porosity* models, **Narasimhan (1982a,b,c,d), Huyakorn (1983a).** These two approaches will be developed in the following paragraphs. These models are based on physical laws for saturated water flow in the macroporosity and microporosity. As such, they will be referred as *deterministic.* Hereafter, we present two of the last published models which seem to best illustrate these two concepts.

Others techniques can be used to simulate water flow through fractured media. Among them, random walk methods and particles tracking techniques proved to be useful. This last method has been used to study the response of a fractured media to a step injection when a constant hydraulic gradient exists throughout the medium. Particles tracking through a network of cracks in which water velocity is calculated by a numerical model provides a useful tool to estimate the influence of fissuration characteristics on the transport. Because of the probabilistic generation of the crack networks, these models will be referred as *Stochastics,* **Smith and Schwartz (1984), Smith et al. (1985), Schwartz et al. (1983),** Schwartz and Smith (1985). This technique can also be very interesting and useful for solute transport modeling. However, a strong limitation is that the models based on random networks of cracks can only be used for theoretical studies. Some examples are given at the end of the part treating of solute transport, (Ch. 4)

1.2 DETERMINISTIC MODELING.

As mentioned before this paragraph deals with the so called *Single crack* and *Double porosity* approaches. **Duguid and Lee (1977)** have proposed a complete mathematical derivation of the flow and stress equations for a confined fractured media. The resulting set of equations can be viewed as a double porosity model. Later, **Huyakorn (1983a)** published the finite element solutions for different sets of equations corresponding to a double porosity model with different formulations for the coupling term modeling the intrephase transport rate. A model was also proposed for a single crack by the same author. **Narasimhan (1982a,b,c,d)** has proposed a model based on the IFDM (Integrated Finite Difference Method) numerical method and capable of performing flow simulations using either the double porosity concept, the discrete crack approach or both. In the following paragraph we describe in detail the models of **Duguid and Lee (1977)** and **Huyakorn et al. (1983a).** The model proposed by **Narasimhan (1982a,b,c,d)** is more briefly reviewed. Applications are presented later.

1.2.1 DERIVATION OF THE GOVERNING EQUATIONS.

Duguid Model

In this model, developed by **Duguid and Lee (1977),** the fractured porous

media is treated as an elastic media which contains two kinds of porosity. The *primary* porosity assumed isotropic and also refered as *microporosity,* and a *secondary* porosity called *macroporosity,* which characteristics, anisotropic among others, depend on the spatial distribution of the cracks. Water is allowed to flow from one porosity system to the other in response to changes occuring in their respective pressure head distributions. Since the system is assumed to be elastic and always saturated, modifications in the two porosity systems occur when water is removed from or injected into the global system. If we note $\varphi_1$and φ_2 the two porosities ,σ_1 and σ_2 the pressures coresponding to these two domains, and β the compressibility coefficient of water, we can write the two equations:

$$\frac{d\varphi_1}{dt} = \varphi_1\,\varphi_2\,\beta\frac{d\sigma_2}{dt} - (1-\varphi_1)\,\varphi_1\,\beta\frac{d\sigma_1}{dt} \qquad [1.1]$$

$$\frac{d\varphi_2}{dt} = \varphi_1\,\varphi_2\,\beta\,\frac{d\sigma_1}{dt} - (1-\varphi_2)\,\varphi_2\,\beta\frac{d\sigma_2}{dt}\,. \qquad [1.2]$$

Given a surface S enclosing a volume V containing fluid and solid, the continuity equation for the fluid phase is :

$$\frac{d}{dt}\int_V \rho_f\varphi_f dV = \int_V \frac{\partial}{\partial t}(\rho_f\varphi_f)dV + \int_V n.\rho_f\varphi_f<v_f>dS = 0 \qquad [1.3]$$

where $<v_f>$ is the space–average velocity of the fluid, and ρ_f the mass density of water. Writing $<v_s>$ the space–average velocity of the solid phase and $<v_{fs}>$ the space–average velocity of the fluid relative to the solid phase we have:

$$<v_{fs}> = <v_f> - <v_s>\,. \qquad [1.4]$$

Substituting [1.4] into [1.3] and applying the divergence theorem, one obtains the following continuity equation:

$$\frac{\partial\rho_f\varphi_f}{\partial t} + \nabla.(\rho_f\varphi_f<v_s>) + \nabla.(\rho_f\varphi_f<v_{fs}>) = 0 \qquad [1.5]$$

or

$$(d/dt)(\rho_f\varphi_f) + \rho_f\varphi_f\nabla.<v_s> + \nabla.(\rho_f\varphi_f<v_{fs}>) = 0 \qquad [1.6]$$

where: $(d/dt) = (\partial/\partial t) + <v_s>.\nabla$.

Let Γ be the mass of fluid which flows from the microporosity into the macroporosity per unit of time and volume unit of the medium. Γ is sometimes referred as the leakage term. It can be seen that changing the sign of Γ, the inverse phenomena is accounted for. If we take into account Γ, the continuity equations for the two fluid phases (macroporosity and microporosity) and for the solid phase are now:

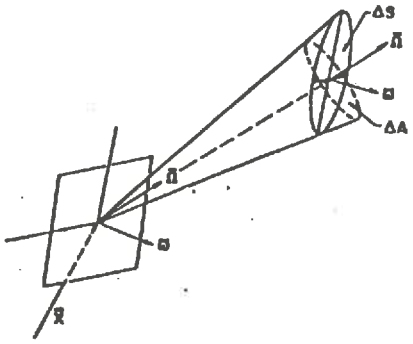

Fig. 1.1 Relation between Ω and ω
[after *Duguid and Lee, 1977*]

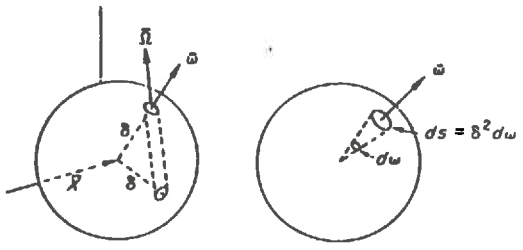

Fig. 1.2 Volume element [after *Duguid and Lee, 1977*]

$$\frac{\partial \rho\varphi_1}{\partial t} + \nabla.(\rho\varphi_1 <v_s>) + \nabla.(\rho\varphi_1 <v_{1s}>) + \Gamma = 0 \qquad [1.7]$$

$$\frac{\partial \rho\varphi_2}{\partial t} + \nabla.(\rho\varphi_2 <v_s>) + \nabla.(\rho\varphi_2 <v_{2s}>) - \Gamma = 0 \qquad [1.8]$$

$$[\partial(\rho_s\varphi_s)/\partial t] + \nabla.(\rho_s\varphi_s <v_s>) = 0 \qquad [1.9]$$

where subscripts $_1$ and $_2$ respectively stand for the fluid phase associated with the microporosity and for the fluid phase associated with the macroporosity. The subscript $_s$ stands for the solid phase. Motion equations are all we need now to complete the model. To derive these equations some assumptions have to be made regarding the geometry of the phase associated with the macroporosity.

Heterogeneities are idealized as a set of tubules of elliptic sections such that the length and the major axis of a tubule are significantly larger than its minor axis. Fluid flow in a tubule is then governed by the Navier–Stokes equation:

$$\rho(dv_2/dt) = \rho g - \nabla p_2 + \mu\nabla^2 v_2 \,. \qquad [1.10]$$

where μ is the fluid viscosity. Using the relation $v_2 = v_s + v_{2s}$, where v_s is the velocity of the solid phase and v_{2s} the fluid velocity relative to the solid phase, Eq. [1.10] becomes:

$$\frac{\partial v_s}{\partial t} + \frac{\partial v_{2s}}{\partial t} + (v_s+v_{2s}).\nabla(v_s+v_{2s}) = \rho g - \nabla p_2 + \mu\nabla^2(v_s+v_{2s}) \qquad [1.11]$$

As the velocity of the solide phase, v_s, is supposed to be small as compared to the fluid velocity, the terms in v_s of highest order are neglected and equation [1.11] is simplified to:

$$\rho(\partial v_{2s}/\partial t) = \rho g - \nabla p_2 + \mu\nabla^2 v_{2s} \,. \qquad [1.12]$$

This is the motion equation for one tubule. But as the medium is made up of many fractures, an average over a representative volume must be performed before [1.12] applies to the entire medium. Remark that at this point it is implicitely assumed that a macroscopic law can be derived that accurately describes the saturated flow in the macroporosity continuum. The validity of this implicit hypothesis is discussed later in the part reserved to stochastic models. (See §1.3.2)

Here is introduced the notion of ***pore matrix function*** $f(x,\Omega)$. The pore matrix function is statistically defined as the number of oriented tubules per unit area per unit solid angle. The dependence on x allows to account for the inhomogeneity and the dependence on Ω allows to account for the anisotropy. This concept is clarified by Fig. 1.1 . Considering a direction defined by the vector Ω, and the surface ΔA orthogonal to Ω, the solid angle sustaining ΔA about the point x is noted $d\Omega$. Hence, according to the definition of the pore matrix function, the number of tubules ΔN oriented within the solid angle $d\Omega$ about the direction Ω is given by:

$$\Delta N = f(x,\Omega)\ \Delta A\ d\Omega\ .$$

But if we look at the number of tubules passing through the surface $\Delta S.\omega$ we have :

$$\Delta N(x,\Omega,\omega) = f(x,\Omega)\Omega.\omega\Delta S d\Omega.$$

Now, if we want to know the total number of tubules passing through ΔS regardless of their orientations we have to perform a solid angle integration, and we obtain:

$$\Delta N(x,\Omega,\omega) = \Delta S \int_0^{2\pi} f(x,\Omega)\Omega.\omega\ d\Omega\ . \qquad [1.13]$$

If we suppose that the velocity in a tubule is colinear to Ω and of module U_{2s}, then the motion equation (Eq. [1.12]) can be written:

$$\rho(\partial/\partial t)(U_{2s}\Omega) = \rho g.\Omega\Omega - \nabla p_2.\Omega\Omega + \mu\nabla^2(U_{2s}\Omega). \qquad [1.14]$$

In order to apply equation [1.12] to the entire medium we must obtain an average value of the velocity over an elementary volume of the medium. This is performed integrating the velocity in a single tubule over the entire solid angle (4Π). Hence, the flux is given by the following expression:

$$\langle q_{2s}(x)\rangle = \varphi_2\langle v_{2s}(x)\rangle = \frac{1}{\tau}\int_{\tau_2} U^0_{2s}\Omega\ d\tau \qquad [1.15]$$

where U^0_{2s} is the average velocity of the fluid in an elliptic section, τ is a spherical volume element, and τ_2 the volume of fluid in the tubules of that element. τ has to be chosen such that its radius δ is much greater than the tubule spacing or the major axis. In fact τ is a R.E.V for the fluid phase associated with the macroporosity. But, the expression we derived for the flux is valid for a volume of fluid and not for a volume including the solid phase. Thus, we must now establish a relation between an integral over τ_2 and an integral over τ. Considering Fig. 1.2 one can see that the length of a tubule oriented along Ω and passing through an elementary surface ω is: $2\delta\Omega.\omega$, and that its volume is: $2\delta\Omega.\omega\pi bc$. If we consider a surface $dS = \delta^2 d\omega$, the number of tubules oriented along Ω and passing through dS is given by:

$$\Delta N(x,\Omega,\omega) = f(x,\Omega)\Omega.\omega d\Omega\delta^2 d\omega\ .$$

Thus, for any scalar function Q depending on the position x and the vector Ω we can write the following formula:

$$\int_{\tau_2} Q(x,\Omega)\ d\tau = \frac{1}{2}\{2\delta^3 \oint [\int_0^{2\pi} \pi bc Q(x,\Omega)f(x,\Omega)(\Omega.\omega)\ d\Omega]\ d\omega\} \qquad [1.16]$$

where the first integral in the right hand side is taken over the entire solid angle, (4Π). As the pore matrix function is point symmetric, this integral is simplified to:

$$\int_{\tau_2} Q(x,\Omega)d\tau = \frac{\delta^3}{2}\oint \omega\omega\, d\omega \int_0^{2\pi} \pi bc\, Q(x,\Omega) f(x,\Omega)\Omega\Omega\, d\omega \qquad [1.17]$$

Given that $\Omega\Omega = I$, the identity tensor, and $\oint \omega\omega\, d\omega = 4\pi I/3$ equation [1.17] becomes:

$$\int_{\tau_2} Q(x,\Omega)d\tau = \oint \pi bc\, Q(x,\Omega) f(x,\Omega)\, d\Omega\,. \qquad [1.18]$$

Now, for an elliptical tubule the velocity verifies the relation

$$\nabla^2(U_{2s}(\Omega)) = \lambda\,[-GU^0_{2s}(\Omega)] \qquad [1.19]$$

where: $G = 4(b^2 + c^2)/b^2c^2$. Substituting [1.18] into [1.14] we obtain an expression for the average velocity in a tubule:

$$U^0_{2s}(\Omega)\Omega = \frac{1}{\lambda\mu G}[-\rho(\partial/\partial t)U_{2s}(\Omega)\Omega + \rho g.\Omega\Omega - \nabla p_2.\Omega\Omega] \qquad [1.20]$$

Using [1.15] an expression for the flux is derived:

$$\langle q_{2s}\rangle = \frac{1}{\mu\lambda G\tau}\int_{\tau_2} [-\rho\frac{\partial U_{2s}}{\partial t}(\Omega)\Omega + \rho g.\Omega\Omega - \nabla p_2.\Omega\Omega]\, d\tau. \qquad [1.21]$$

We can now use [1.18] to obtained an expression of the flux over any volume in the medium:

$$\langle q_{2s}\rangle = -\frac{1}{\mu}\oint \frac{\pi b\, c}{2\lambda G} f(x,\Omega).(-\rho g + \nabla p_2 + \rho\frac{\partial v_{2s}}{\partial t}).\Omega\Omega\, d\Omega. \qquad [1.22]$$

In a similar way space–averaged values for pressure gradients and acceleration can be defined. It comes

$$\nabla\langle p_2\rangle \oint f(x,\Omega).\Omega\Omega\, d\Omega = \oint \nabla p_2.f(x,\Omega).\Omega\Omega\, d\Omega \qquad [1.23]$$

and

$$\frac{\partial}{\partial t}\langle q_{2s}\rangle \oint f(x,\Omega).\Omega\Omega\, d\Omega = \oint \frac{\partial v_{2s}}{\partial t}.f(x,\Omega).\Omega\Omega\, d\Omega \qquad [1.24]$$

respectively. Now, if we define the intrinsic permeability by:

$$K_2 = \oint \frac{\pi bc}{8\lambda}\frac{b^2c^2}{(b^2+c^2)} f(x,\Omega).\Omega\Omega\, d\Omega \qquad [1.25]$$

a general form of Darcy's law is obtained from equation [1.22]:

$$<q_{2s}> = -(K_2/\mu)[\nabla\sigma_2 + \rho(\partial/\partial t)<q_{2s}>] \quad . \qquad [1.26]$$

Since Darcy's law is assumed to apply for the fluid flow in the microporosity, the flux $<q_{1s}>$ is given by

$$<q_{1s}> = -(K_1/\mu)(\rho g + \nabla\sigma_1) = \varphi_1 <v_{1s}> \qquad [1.27]$$

where K_1 is the permeability of the porous matrix. Combining equations [1.1], [1.7], [1.9] and Darcy's law we obtain the flow equation for the fluid phase in the microporosity. The equation for the flow in the macroporosity continuum is derived in a similar way using equations [1.2], [1.8], [1.9]. It comes respectively,

$$(1-\varphi_2)\varphi_1\beta\frac{\partial\sigma_1}{\partial t} + (1-\varphi_2)\varphi_2\beta\frac{\partial\sigma_2}{\partial t} + (1-\varphi_2)\nabla.v_s + \frac{\Gamma}{\rho} = \frac{K_1}{\mu}.\nabla^2\sigma_1 \qquad [1.28]$$

$$(1-\varphi_1)\varphi_1\beta\frac{\partial\sigma 1}{\partial t} + (1-\varphi_2)\varphi_2\beta\frac{\partial\sigma 2}{\partial t} + (1-\varphi_1)\nabla.v_s - \frac{\Gamma}{\rho} + \nabla.<q_{2s}> = 0 \quad . \qquad [1.29]$$

It remains now to define the interaction term Γ. This is done using the flow equation in the porous matrix. In order to derive an expression for the leakage term Γ, the authors assume that the microporosity continuum is made up of porous blocks for which Richards' equation can be solved. Notice that for a rigid and saturated media, Richards' equation in fact reduces to the Laplace equation and is a particular case of Eq. [1.28]. Assuming a simple form for the geometry of the blocks and appropriated boundary conditions, analytical expressions can be derived from which it is easy to obtain Γ. If for example we assume that the macroporosity consists of a set of plane fractures we have the following flow equation in the microporosity:

$$\partial\sigma/\partial t = (K_1/\phi_1\beta\mu)\ \nabla^2\sigma \quad . \qquad [1.30]$$

By means of Darcy's law, a solution of this equation will provide an estimation of the flow rate between the two phases per unit surface of crack. Now, in Eq. [1.28] and [1.29], the term Γ is a leakage term per volume unit of the medium. Hence, we have to convert the flow rate into the macroporosity which is expressed in unit volume of fluid per unit surface of fracture in a flow rate expressed in unit fluid volume per unit of the total volume. Again, the pore matrix function is used in a way similar to the one followed to derive the continuity and motion equations. Given an elementary volume τ and the hypothesis of elliptic tubules, it can be shown that the following relation holds: $S_2/\tau = 4\ \varphi_2/(\pi c)$ where S_2 is the surface developed by the fractures contained in τ. Thus, the coupling term is defined by:

$$\Gamma = \frac{4\ \varphi_2\ \rho\ <q_{1s}>}{\pi\ c} \qquad [1.31]$$

where $<q_{1s}>$ is the flux at the interface calculated from Darcy's law and the solution of Richards equation. (For example [1.30] for plane fractures.) The main problem in this approach is the choice of the boundary conditions for equation [1.30].

At this stage of the calculation, Duguid and Lee (1977) make the hypothesis that the porous blocks are parallelepipeds, and use an analytical solution of equation [1.30] to derive an expression for Γ. With this geometry, the flow is one–dimensional in the porous blokc. The analytical solution they have used corresponds to

Dirichlet–type conditions at both boundaries. In this case the Dirichlet condition applied in the center of the blocks is not very well appropriated. An analytical solution with a Neumann–type boundary condition at the center of the block should have been used. Other sets of boundary conditions and other ways to couple the two phases will be presented within the models of Huyakorn et al. (1983a) and Narasimhan (1982a,b,c,d).

The pore matrix function introduced, under assumption of cracks with elliptic section, and applied to obtain a permeability tensor and to link the leakage rate by area unit to a leakage rate per volume unit is a general and theoretically attractive tool. Particular cases will appear in the following models and later for solute transport models.

Huyakorn Models

The double porosity models hereafter described use for the flow in the macroporosity a formulation different of that developed by Duguid and Lee (1977). No compression of the porous matrix is accounted for and the flow equation used for the macroporosity phase is consequently slightly different regarding the storage term. Using the concept of REV, the following equation is used:

$$\frac{\partial}{\partial x_i}\left(T \frac{\partial h}{\partial x_i}\right) = S \frac{\partial h}{\partial t} - \Gamma - q \quad i=1,2 \qquad [1.32]$$

where h is the hydraulic head in the fractures, T and S are the fracture transmissivity and storage coefficients respectively, Γ is the volumetric rate of fluid flow from the porous blocks to the fractures per unit area, and q is the volumetric rate of fluid flow per unit area via sinks or sources. The leakage term, Γ, can be defined as before from a solution of the flow equation in porous blocks of well defined geometry. Beside that approach, an other definition of Γ, more simple but less accurate, has been proposed by Barenblatt et al. (1960), that does not require a geometrical conceptualization of the porous blocks. Let us first define Γ, in that way independent of the geometry.

Models based on this approach are called, *Quasi–Steady Fracture Flow Models,* and assume that Γ depends only on the gradient existing between the pressure head in the macroporosity and an "average" pressure head in the microporosity. The mathematical formulation derived by Barenblatt et al. (1960) is:

$$\Gamma = \Pi \sigma^2 (h'-h) \qquad [1.33]$$

where, Π is a leakage parameter assumed constant, σ is the specific surface of fractures defined as the surface area of fractures per unit of volume of the medium, and h' is the average head in the porous matrix. The model is completed using a mass balance equation for the fluid phase in the porous blocks

$$S' \frac{\partial h'}{\partial t} = \Pi \sigma^2 (h-h') = -\Gamma \qquad [1.34]$$

where S' is the storage coefficient. This equation is easily solved using the Laplace transform, Streltsova (1976). Noting $\omega = \Pi\sigma^2/S'$, Γ is given by

$$-\Gamma = S' \omega \int_0^t \frac{\partial h}{\partial t} e^{-\omega(t-\tau)} d\tau \ . \qquad [1.35]$$

A second way to derive a coupling term is to assume a network of parallel fractures. In this case, as a geometrical representation of the media is assumed, the leakage term is more rigorously obtained. In the porous blocks bounded by plane surfaces, the following set of equations is solved:

$$K'\frac{\partial^2 h'}{\partial z^2} = S_s'\frac{\partial h'}{\partial t}, \qquad h'=h_0' \text{ at } t=0$$

$$h'=h \text{ at } z=0, \qquad \frac{\partial h'}{\partial z} = 0 \text{ at } z=a$$

This approach is very close to the one developed by Duguid and Lee (1974). However, the boundary condition at the center of the block is different. Duguid and Lee used a Dirichlet condition, Huyakorn a more realistic Neuman boundary condition deriving from the symmetry of the system. An analytical solution of this set of equations can be obtained for constant boundary conditions. *Duhamel's* theorem allows to obtain the solution for a time–dependent boundary condition from the solution for a constant boundary condition. The velocity at the matrix–fracture interface is then given by:

$$V_n = K'\frac{\partial h'}{\partial z}\Big|_{z=0} = -\frac{2K'}{a}\sum_{n=0}^{\infty}\int_0^t \frac{\partial h}{\partial \tau} e^{-\alpha_n(t-\tau)}\, d\tau \qquad [1.36]$$

where: $\alpha_n = \pi^2(2n+1)^2K'/(4S'a^2)$. The coefficients α_n come from the solution of the Laplace equation expressed as a series. Solutions of Laplace equation for various geometries and boundary conditions can be found in Carslaw and Jaeger (1959). The specific surface of the flow between porous matrix and fractures is: $\sigma = 1/a$, where 2a is the width of the porous blocks. So, if H is the thickness of the aquifer and b the half of the fracture aperture, Γ is given by:

$$\Gamma = \left(\frac{H}{a} + \frac{a}{b}\right) V_n\, \sigma \qquad [1.37]$$

The third approach is based on the assumption of a medium made up of parallelepiped shaped blocks separated by three sets of planar fractures. These blocks are regarded as spheres for transport modeling, and the interaction term is derived as for the planar previous model by solving the flow equation in spherical coordinates with appropriated boundary conditions. The outward normal velocity is founded to be:

$$V_n = K'\frac{\partial h'}{\partial r}\Big|_{r=0} = -\frac{2K'}{a}\sum_{n=1}^{\infty}\int_0^t \frac{\partial h}{\partial \tau} e^{-\alpha_n(t-\tau)}\, d\tau \qquad [1.38]$$

where: $\alpha_n = \pi^2 n^2 K'/(S'a^2)$. The specific surface of the flow between porous matrix and fractures is: $\sigma=3/a$, where a is the radius of idealized spherical porous blocks. So, if H is the thickness of the aquifer and b the half of the fracture aperture, Γ is given by:

$$\Gamma = \left(\frac{H\ a}{a\ +\ b}\right).V_n.\sigma \qquad [1.39]$$

It can be seen that for these three approaches a convolution integral appears in the formulation of the coupling term. This is due to the analytical method used to solve the flow equation in the porous matrix blocks and to the use of *Duhamel's* theorem to accomodate time–dependent boundary conditions. If we don't use an analytical solution a set of two coupled partial differential equations results. Thus, one have the choice between two strategies to numerically solve the problem. A comparison between the two methods is presented in §1.2.2.. The numerical solutions developed by Huyakorn use a finite element solution for equation [1.32] and the coupling is handled either calculating the convolution integrals or using a finite difference algorithm to solve the flow equation in the porous matrix. The solutions obtained by both methods are very close and this is not surprising as the finite difference solution of a linear equation is well known to converge to the analytical one when the space step is sufficiently refined. In fact the finite difference based algorithm avoids the problems involved in summing infinite series who's convergence rates can be slow and strongly dependent on the characteristic of the porous medium, (conductivity, storage coefficient,..), and of the time. For future extensions, the finite difference approach offers more possibilities to incorporate variable boundary conditions. However, finite differences are not very well suited to handle sharp gradients, often present at early times. An other advantage of the convolution integral approach, not reported in this study, will cleraly appear with the concept of BGF developed in Chap. 4.

Narasimhan Model

The model developed by **Narasimhan (1982d)** is essentially based on the IFDM numerical method presented by **Narasimhan and Witherspoon (1976)**. This numerical method can of course be used to solve the different conceptual flow models proposed before. In fact the equations derived by **Narasimhan** (1982d) are not specifically based on one of the currently used approaches, double porosity for example. The IFDM method, using a set of equations directly derived from the mass conservation equation, allows to calculate the flow in a medium composed of porous blocks of arbitrary shapes separated or not by plane cracks. The immediate drawback of this approach is the very detailed description of the medium which is required. Thus, it is not a predictive tool which is developed but an analysis one. Let us first presented the IFDM method, and then look how **Narasimhan's** model compares with others.

The basic mass conservation law is applicable to any elemental volume l of the flow region whether that elemental volume comprises a portion of fracture, a portion of porous matrix or both. Thus, for any elemental volume l surrounded by a surface Γ_l we can write the following equation:

$$\rho_l G_l + \int_{\Gamma_l} \rho\, \mathbf{K}\cdot\nabla\phi.\mathbf{n}\, d\Gamma = \frac{\partial M_{w,l}}{\partial t} \qquad [1.40]$$

where G_l is a volumetric rate of fluid due to sources or sinks, K is the hydraulic conductivity, $\phi = z + \psi$ is the fluid pressure head, n is unit vector normal to Γ_l and oriented outward, and $M_{w,l}$ is the mass of water in l. The specific storage coefficient of the material is defined as:

$$S_{s,l} = \rho_l g(n\beta + m_{v,l}) \qquad [1.41]$$

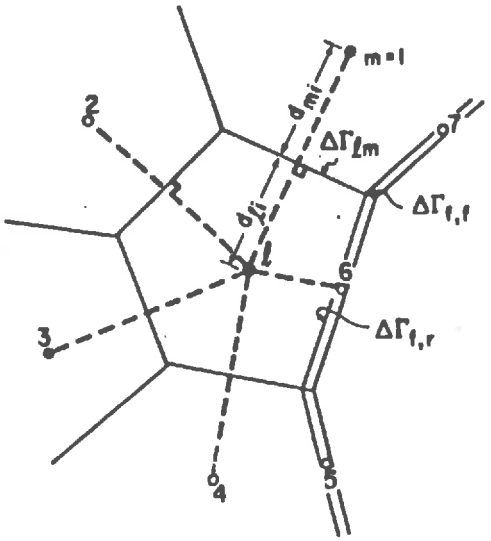

Fig. 1.3 Example of discretization for the integral finite difference method. Nodes 5, 6 and 7 are located in a crack [after *Narasimhan 1982*]

where n is the porosity, β is the water compressibility coefficient, and $m_{v,l}$ is the rate of change of the porosity according to the external pressure. The fluid mass capacity of the element l is then given by:

$$M_{c,l} = \rho_l V_l S_{s,l} \qquad [1.42]$$

where, V_l is the volume of l. In equation [1.40] the surface Γ_l can either be completely interior to l or coincide with parts of the external boundary of the total system. So, separating these two kind of boundaries, equation [1.40] can be written:

$$\rho_l G_l + \int_{\Gamma_{l,m}} \rho K \nabla\phi.n \, d\Gamma + \int_{\Gamma_{l,b}} \rho K \nabla\phi.n \, d\Gamma = M_{c,l} \frac{\partial M_{w,l}}{\partial t} \qquad [1.43]$$

The discrete equations are directly derived from this expression. As in others numerical methods the flow domain is subdivided into small domains, and a discrete form of equation [1.43] is derived transforming integrals in discrete sums and approximating first order derivatives by finite difference formulas. It is obvious that the size of elemental volumes, l, has to be small enough in order to insure convergence and precision in the calculations. Figure 1.3 gives a local example of the spatial discretization with both porous matrix and fractures elemental sub–domains. Given an element, l, equation [1.43] is approximated by:

$$\rho_l G_l + \sum_m \rho_{lm} K_{lm} (\nabla\phi.n) \Delta\Gamma_{lm} + \sum_b \rho_{lb} K_{lb} (\nabla\phi.n) \Delta\Gamma_{lb} = M_{cl} \frac{\Delta\phi_l}{\Delta t} \qquad [1.44]$$

where $_m$ denote all interior surface elements and $_b$ all exterior surface elements (elements in contact with the boundary of the system), $\Delta\Gamma_{lm}$ is the area of the interface between two elements and K_{lm} is the conductivity at the interface.

In previous double porosity models, the fluxes between porous matrix and fractures were treated as sinks or sources for the global flow equation and were calculated using a discrete formula. The result was weighted by a coefficient related to the geometry of the crack network or to the specific surface by volume unit developed by the heterogeneities. Moreover, this coefficient was supposed constant all over the domain, which is a probably strong and quite irreal hypothesis. Of course many different weighting coefficients can be fitted according to the assumed geometry. In the IFDM method the fluxes between fractures and porous matrix blocks are explicitly calculated. The pressure head gradients between the two sub–domains, regardless of their location (fracture or porous matrix elements), are approximated by:

$$\nabla\phi.n|_{l,m} \approx \frac{\phi_m - \phi_l}{D_{l,m}} \qquad [1.45]$$

where $D_{l,m}$ is the distance between the nodal points l and m. Equation [1.45] assumes implicitely that the line joining l and m is orthogonal to $\Delta\Gamma_{lm}$. In Fig. 1.3, $D_{l,m}$ is equal to $d_{l,i} + d_{m,i}$. Using [1.45] in [1.44] for all the nodal points, we obtain the following set of differential equations of time:

$$\rho_l G_l + \sum_{m \neq l} U_{l,m} (\phi_m - \phi_l) + \sum_b U_{l,b} (\phi_b - \phi_l) = M_{c,l} \frac{\Delta\phi_l}{\Delta t} \quad l = 1,2,3,...,L \qquad [1.46]$$

where the conductances, $U_{l,m}$ and $U_{l,b}$ are given by:

$$U_{l,m} = \frac{\rho K_{l,m} \Delta\Gamma_{l,m}}{D_{l,m}} \text{ and } \qquad U_{l,b} = \frac{\rho K_{l,b} \Delta\Gamma_{l,b}}{D_{l,b}} . \qquad [1.47]$$

Attention has to be payed to the signification of the parameters. First, calculating the conductance for an interface fracture–porous matrix, the following formula is used:

$$U_{f,r} = \frac{\rho K_r \Delta\Gamma_{f,r}}{d_{r,i}} \qquad [1.48]$$

where, K_r is the porous block conductivity and d_{ri} the distance from the nodal point to the interface. The second important parameter is the storage parameter for a fracture element. The amount of water released from or inject into the fractures for a unit change in pressure head is given by:

$$M_{c,l} = \frac{d(V_{v,f}\rho)}{d\psi} = V_{v,f}\frac{d\rho}{d\psi} + \rho\frac{dV_{v,f}}{d\psi} \qquad [1.49]$$

where, V_{vf} is the volume of voids in the fracture element. Normalizing with reference to the bulk volume, V_{bf}, of the fracture and since $p = \rho g \psi$ we have:

$$M_{c,l} = V_{b,f}\rho g[n_f\beta + m_{v,f}] \qquad [1.50]$$

where n_f is the porosity of the fracture element, and $m_{vf} = -\,dn/dp$ is the coefficient of volume change. Finally, the conductivity of the fractures is related to their apertures by the classic formula:

$$K_f = \frac{(2b)^2 \rho g}{12\mu} \qquad [1.51]$$

where, 2b is the aperture, and μ the viscosity of water. The validity of this law has been extensively discussed by **Wilson (1970)** and **Witherspoon (1980)**. As the flux through the fracture is related to $(2b)^3$, this expression is often referred as the *cubic law*. Time integration of Eq. [1.46] is then performed by a mixed implicit–explicit scheme.

As said before, the double porosity concept can be hold by the IFDM method. To develop a double porosity concept based model, some assumptions have to be made in order to obtain coupling terms between the two phases. In Huyakorn model, several geometries for the heterogeneities have been assumed leading to different coupling terms. In the model of **Duguid and Lee (1977)**, the interaction term is derived using the porous matrix function which in fact provides a statistical and geometrical description of the medium. For **Narasimhan (1982d)**, the double porosity model is based on a representation of the macroporosity continuum by a set of parallel fractures. This situation has already been described and discussed for the model of **Huyakorn**. Let us give only the set of equations for the IFDM:

$$\begin{aligned} -\mathrm{div}(\rho K_f \nabla\phi_f) + \rho\alpha K_r(\phi_r - \phi_f) &= \rho S_{sr}\frac{\partial\phi_f}{\partial t} \\ -\rho\alpha K_r(\phi_r - \phi_f) &= \rho S_{sr}\frac{\partial\phi_r}{\partial t} \end{aligned} \qquad [1.52]$$

where α is a parameter related to the specific surface developed by the porous blocks.

1.2.2 DISCUSSIONS AND CONCLUSIONS.

These models are in fact mainly studying tools and cannot be really considered as predictive. They have been principaly used to study the effects of various heterogeneity geometries when pumping tests are conducted for an aquifer. Principal studied cases involve horizontal fractures, vertical fractures, sets of both.

In his paper, **Huyakorn (1983a)** compared numerical and analytical solutions for the three different conceptual double porosity models he developed. Numerical simulations are used to demonstrate the effects on draw–down curves of various leakage factors (Π in Eq. [1.33]) related to fractures network geometry. An improved interpretation of pumping tests may result from this study. Similar problems are solved by Narasimhan to show the efficiency of the IFDM. More interesting is the numerical solution developed by **Huyakorn (1983a)** and the treatment of the convolution integral.

In fact, going through the bibliography, one realizes that trying to set up a meaningful model, we are facing several kinds of problems. Of course the more rigorous approach is provided by models fully accounting for the geometry of the media and using known and reliable transfer laws. However, even for these models, some physical laws are only roughly approached. For example the "cubic law" relating the flux in a fracture to its aperture is only an approximation since the cracks do not have a constant aperture all along the flow pattern and in addition have rough surfaces. Recognizing that these models are powerful analysis or studying tools but obviously without great interest concerning real situations simulations since they require an irrealistic degree of detail in the description of the media, an other approach is required. The logical step when dealing with transport phenomena is to try to derive macroscopic physical laws which combined with a continuity equation provide a mathematical model for the flow problem. This reasoning has led to the concept of equivalent porous media. It is now well recognized that this approach fails to provide a useful tool in many cases, and is only applicable to particular situations.

The physical laws we are looking for have to be derived for a macroscopic elemental volume. The question is then: is it possible according to microscopic or local properties and local phenomena to derive a meaningful expression modeling the flow at a larger scale? The response was clearly no for the simpleminded equivalent porous media concept. The following step has been to introduce the double porosity concept. The meaning of this concept, its utility and its applicability have been discussed at long by **Narasimhan (1982d)**, who call this model *" a truly mathematical approximation whose exact relation to physics is ill defined"*. It is recognized now that it produces, via different formulations for the coupling term, a useful tool to analyse flow in real situations and for example, pumping tests. The double porosity conceptual models we have presented, use to simulate the flow in the macroporosity continuum a macroscopic law analog to Darcy's law, assuming laminar flow and cracks of small apertures (e.g. the averaging procedure developed by **Duguid and Lee (1977)**, or equation [1.32] in the model of **Huyakorn (1983a)**). The conditions where Darcy's law can be used to simulate the flow in the macroporosity continuum are discussed later, (see §1.3.2). Progresses remain to do for Bingham fluids and non–Darcian flows.

The formulation of the coupling term constitutes certainly another weak point of these approaches. This one is usually defined from geometrical assumptions and the solution of Richards' equation in the microporosity. Several formulations are obtained according to the geometry of the flow assumed to hold in the porous blocks. This restriction to simple geometries is a limitation. An extension of this approach and release of the geometrical constraint is developed in chapter 4. (See the The

Block Geometry Function concept). Notice that the coefficient, σ, accounting for the "density of fissuration" and appearing in the formulation of the coupling term is typically a fitting parameter.

The double porosity model which interphase transport rate is modeled as simple first order process, Eq. [1.33], lacks of physical background. It is obvious that the first order rate process based on a gradient between the pressure in the macroporosity continuum and an average pressure in the porous blocks only rawly approximates the water uptake process obeying Darcy's law. The same kind of approach has been used for unsaturated flow and also for solute transport in aggregated or fractured media. A full disccusion of this model, its relation with the real physical process and its applicability are given in Chap. 3. (§3.6)

In fact as noticed by Narasimhan (1982a,b,c,d), the double porosity concept is only a particular case of a more general concept involving several interacting media. An attempt has been made by Pruess and Narasimhan (1985) to use this concept for coupled heat transfer and water flow simulations in a fractured media. In fact, the proposed approach, named MINC, (Multiple Interacting Continuum), based on the IFDM method, is very close to the ***"Unsteady Blocky Fracture Flow Model"*** developed by Huyakorn (1983a) and discussed above. In the MINC approach the medium is split in ideal cubes delimited by planar cracks. The different continuums are defined by their distance to the nearest crack. Thus, we have a set of smaller and smaller nested cubes whose distance to the nearest crack is larger and larger. Fluxes and mass balances between and for each element are calculated in the way described for the IFDM. One can see that this approach is in fact quite equivalent to solve a transport equation in cubic porous blocks, a "finite difference grid" being provided by the faces of the nested cubes. This approach is slightly more general than Huyakorn's model, as many different discretizations of the space can be used, and as the flow in the macroporosity is explicitly calculated.

However, one can see that this is not a fully multi continuum approach as a continuum i is only connected with continua i—1 and i+1. A truly multiple continuum approach would allow direct coupling between different continuums or all the continuums, without introducing a hierarchy based on geometrical considerations. This kind of modeling is still to be developed.

In fact it seems that the two kinds of models, double porosity and geometrically based models, have not really been compared and used together in order to define for example what kind of coupling term is more adapted for a given crack network characterized by some geometrical parameters such that connectivity, isotropy, irregularity of apertures distribution, etc... Huyakorn's work only, presents the influence of the coupling term on model responses, but only from a qualitative point of view. The power of the IFDM could be used to simulated flows in randomly defined cracks networks. Useful indications on the sensibility of the interphase transport term to geometrical parameters.

Networks of fractures with varying lengths, aperture, spatial distribution, etc.. can be easily generated. Deterministic simulations conducted on these networks offer an interesting theoretical way to analyse the problems arising when it comes to decide if macroscopic laws such as for example Darcy's law or Fick's law can be applied to the macroporosity continuum. The following paragraphs present some works using this technique to analyse the phenomena of dispersion and the validity of Darcy's law for saturated water flow in fractured media. This approach has also been followed for solutes transport and will be reported later.

1.3 STOCHASTIC APPROACHES.

As said before, this approach use randomly generated networks of cracks and as such has been referred as *stochastic*. Initially, it has been developed to study the dispersion in a fractured medium, and in which way the macroporosity continuum in a fractured media can be replaced by an equivalent porous medium as far as saturated water flow is concerned, **Long et al. (1982)**. Hence, this modeling approach appears as more related to solute transport problems. But as the first studies were not accounting for the diffusion in the matrix and were rather focusing on the calculation of the flow and the dispersion of a particles swarm, we chose to present this work in this part of the report. An extension of the hereafter presented approaches, accounting for the matrix diffusion, will be presented later.

1.3.1 METHODS

The models developed by **Long et al.** (1982), **Smith and Schwartz** (1980–1984), **Schwartz and Smith** (1985) **Schwartz et al.** (1983), **Smith et al.** (1985) and **Andersson et al.** (1986) are closely related and particular cases of the percolation theory, developed by **Broadbent and Hammersley** (1957). In a synthesis article, **Guyon et al** (1984), have summarized some usefull results concerning the critical percolation thresholds for random networks of cracks in two or three dimensions.

The first step in this approach is the generation of the network. Several methods can be used to generate a set of cracks in a bounded domain. We have to distinguish between two problems. The first one is to choose the kind of distributions that should be used to characterize the length, aperture and orientation of the cracks. This choice can be done according to some available experimental data.

The second problem, more related to the percolation theory, is to decide what type of spatial distribution should be used to distribute the cracks in the domain. They can be uniformely distributed, in a clustered way, randomly, or according to some combination of these distributions. Obviously this choice will have a non–negligible weight on the results. For example the connectivity of the system and its critical percolation thresholds can be quite different. The residence time of a solute will probably also depend on this choice. Here too, experimental data can help to decide. Usually a random distribution is chosen.

Even though most of the published works are concerned with 2–D networks, some papers exist for three dimensional networks. In those cases, the cracks are either represented by pieces of plane or by disks. Particularly, **Baecher and Lanney** (1978) developed a conceptual crack geometry model, using circular disks randomly distributed in the space. Later, **Long et al.** (1985), Elsworth (1986), and Andersson and Dverstorp (1987), each proposed three–dimensional models to simulate water flow and mass transport in fissured rocks. What follows concerns 2–d networks unless otherwise specified.

It seems that according to experimental data, the lenght of the cracks can be determined by sampling a negative exponential distribution. The probability density function of this distribution is given by:

$$g(l_f) = \lambda\, e^{-\lambda l_f} \qquad [1.53]$$

However, lognormal distributions are also found in the literature. Apertures are usually obtained by sampling lognormal distributions.

Fractures orientations data are certainly the best understood of all geometrical properties recorded. A computerized method for analysing cluster orientation has been developed, **Mathab et al (1972)**. An hemisherical normal distribution is used to represent these data. The cumulative probability function of this distribution is :

$$P(\theta) = [1 - \exp[k(\cos\theta - 1)]]/[1 - \exp(k)] \qquad [1.54]$$

where k is the dispersivity coefficient.

Simulations in three dimensions are only available at our knowledge for networks generated with strong hypothesis on the shape and orientation of the cracks. Calculations on general networks have only been done in two dimensional domains. The generation of the network generally proceeds as follows:

1– Definition of a background rectangular grid whose nodes will be used to locate the middle of the cracks. The spacing between the nodes and the size of the domain give the number of nodes in both directions.

2– Random determination of a set of nodes and sampling of the different distributions to define the characteristics of the cracks associated with these nodes. In the works of **Schwartz et al. (1983), Smith et al.** (1984) the background grid has usually between two thousands and three thousands points while less than one hundred cracks are generated.

Once this is done, one have the choice to keep or eliminate dead–end segments. It is obvious that if we are only interested in estimating the dispersivity of the network, or the flow developing under a pressure head gradient applied at the boundaries of the domain, we are allowed to eliminate the dead–end segments. Of course, if we want to account not only for convection but also for diffusion inside the cracks and from the cracks into the matrix, the dead–end segments cannot be eliminated as they represent a non negligible part of cracks volume and exchange surfaces.

The next step, common to all approaches, is to calculated the pressure field generated by a hydraulic gradient applied at two opposite boundaries. Usually, on a rectangular domain no flux conditions are applied on the two other boundaries, **Schwartz et al. (1983). Long et al. (1982)** use a slightly different set of conditions to create a constant hydraulic gradient along the two boundaries parallel to the flow. Notice that the pressure head distribution throughout the network obeys the Laplace equation. In order to calculate pressure head and flux distributions, **Long et al.** (1982) use a finite element model developed by Wilson (1970) in which the cracks are considered as line finite element and the cubic law mentioned before, **Narasimahan model** (§1.2.1), is used to calculate the fluxes. To solve the flow problem in the crack network, **Schwartz et al.** (1983), and **Smith et al.** (1984) use a finite difference model similar to the one described by **Castillo et al.** (1972a,b). For three–dimensional systems, an algorithm have been proposed by **Long et al.** (1985), based on the solution of Laplace equation in each fracture and the theory of images. This leads to a set of mass–balance equations. Later, **Elsworth** (1986) proposed a numerical algorithm combining finite element and boundary element methods to solve Laplace equation. **Andersson et al.** (1987) use a boundary element technique described in **Shapiro and Andersson** (1983, 1985).

The velocity distribution resulting from the distribution of gradients in the domain is then used in a particle tracking simulation. In this kind of simulations, a swarm of particles is instantaneously released in the domain at the upper boundary. **Schwartz et al.** (1983) use a single fracture to release the totality of the swarm, thus simulating a point source. Other choices are possible. The particules are then individually through the domain according to the velocity field. Here also many choices are possible. Some authors use the background grid as a guide to move the particles from one node to the other. In this case a particle is moved for a time equal to a base time step Δt, in a series of small steps corresponding to a mesh size of the background grid. Each of these small step take a time Δt_i, calculated according to the flow velocity. The particle is moved until the base step time Δt is completed. Then the particle is stopped somewhere in a crack and not necessarily at the intersection of two cracks. This is repeated for all the particles and as many times as

required to move the swarm all through the domain.

When a particle arrives at an intersection, the direction followed is determined from probabilities weighed according to the relative amount of flow moving away from the intersection in each fracture. Thus, a macroscopic dispersion is modeled in a realistic way. In these models, mixing effects related to small scale dispersion and diffusion are expected to be much less important than those related to fracture connections geometry and heterogeneity of the distribution of velocities.

The last step of the simulation to get a Monte–Carlo method is to repeat a sufficient number of times the generation of the network and the particule tracking simulation. For example, **Schwartz et al. (1983)** use five hundred particles and three hundred realizations of the process.

The steps followed for threedimensional simulations are quite similar. In the work of **Smith et al. (1985)**, planar fractures are generated sampling distributions for their aperture and length. In this case the network is composed of two sets of parallel cracks. Then the flow equation is solved by a finite element method, in which the macroporosity continuum is discretized using triangular elements. The particle tracking technique proceeds as for the two–dimensional case.

1.3.2 APPLICATIONS AND RESULTS.

It is generally recognized that this approach is unlikely to be used for prediction purpose and simulation of real situations. So the main developed applications are concerned with sensitivity studies and numerical experimentations. However, **Schwartz et al. (1985)** have given an extension of their approach allowing to cope with realistic domains. This technique involving a connection between continuum and discrete concepts is described at the end of this paragraph.

An important problem in modeling water transfer in heterogeneous media is to choose an appropriate conceptual model according to the medium characteristics. Particularly the question is: *are we allowed to use the continuum approach and the related equations ?* Numerical experimentation is typically very well suited to study this problem and furnish some qualitative information and quantitative thresholds. **Long et al. (1982)** have used a simulation technique very close to that described in the preceding paragraph to determine when a crack network can be replaced by an equivalent continuum porous medium. The precise question being: is it possible to find a symmetric conductivity tensor such that water flow in the medium can be simulated using a continuity equation and Darcy's law ?

Numerical experiences consist in generating a network of cracks by sampling some distributions for their length, aperture and orientation. Two different pressure heads are applied at two opposite boundaries and a constant gradient is imposed on the two boundaries parallel to the flow. Then the steady–flow through this artificial medium is calculated using a finite element technique, **Wilson (1970)**. Using Darcy's law, an equivalent saturated hydraulic conductivity can then be calculated. By rotating the flow region (rotation of the direction of the gradient) and keeping the network fixed, different output flow rates will be obtained, and hence different values of the hydraulic conductivity which will reveal the anisotropy of the network. If the medium is homogeneous and anisotropic the values of $1/\sqrt{K}$ plotted against φ, the angle measuring the rotation, must approximately lie on an ellipse. If it is not the case the medium is heterogeneous and the flow cannot be modeled by Darcy's law. Of course, in all these simulations, the macropore continuum only is considered and all interactions with the porous matrix are neglected.

Long et al. (1982) have studied the effects of fracture density, fracture spacing and fracture orientation on the $K(\varphi)$ relationship. One can retain the following conclusions. Increasing the fracture density leads to a medium behaving more like a homogeneous medium. However, a quite dense network of cracks is required.

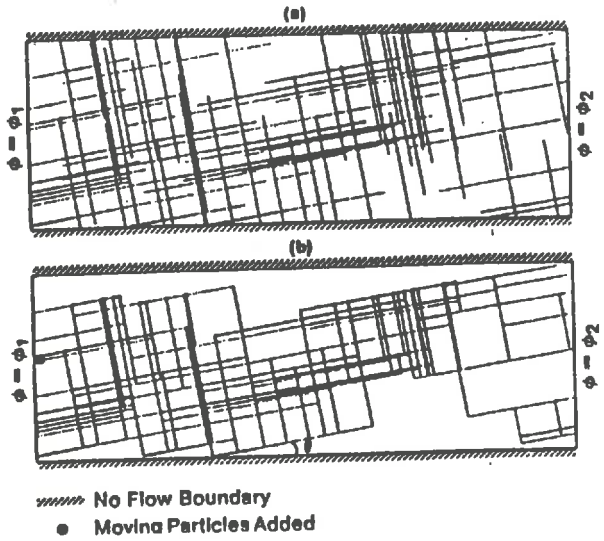

Fig. 1.4 (a) Example of a fracture network before removing dead–end segments. (b) Network remaining after dead–end segments are removed. θ is the angle between the first set of fractures and the direction of the hydraulic gradient [after *Schwartz et al. 1983*]

Acceptable results are obtained for a flow region of 25×25 cm in which one hundred fractures with lengths of 10 or 20 cm and uniform aperture are randomly distributed. The same network expanded in a 40×40 cm region gives erratic results. If the aperture of the crack is not homogeneous, a dramatic increase in the heterogeneity results. Of course the effects are magnified by the cubic law relating the flux to the aperture. Finally for a given set of fractures, the spreading of the orientation improves the homogeneity. Of course these qualitative conclusions are not surprising; but the results of the numerical simulations show that really dense networks are needed for one can use an equivalent porous media approach for the macropore continuum. **Long and Billaux (1986)** have also discussed the relationships existing between the degree of interconnection and the permeability of a crack network.

Following a quite similar scientific approach, the first works of **Schwartz et al. (1983)** and **Smith et al. (1984)** tried to bring a response to the question: *can the dispersion process in a fracture network be modeled by a classical dispersion equation*? Their calculations are restricted to networks of orthogonal fractures having all the same aperture. In the paper of **Schwartz et al. (1983)**, the only varying parameter was the orientation of the network relative to the main flow direction. An example of the type of network used by the authors is given Fig. 1.4. The network is presented before and after elimination of the dead–end segments. Their first simulations with θ=0, show that the longitudinal mass distributions from one realization to another can be very different. Some realizations show spreading of the mass over 90% of the domain before the beginning of the breakthrough. The distributions have a quite complex form and can be multimodal. The breakthrough curves exhibit very long tails and the recovering of all the mass can take a very long time. This behaviour is related to the large differences existing between the velocities in the two orthogonal sets of cracks. While the velocity distribution in the first set, fractures parallel to the flow, is very narrow, it is much more spread for the second set of fractures orthogonal to the flow. Obviously, such a fractured domain does not behave as an equivalent porous medium. Increasing θ, means and standard deviations of the velocity distributions in the two sets of cracks become more similar. This results in a diminution of the spreading of the mass through the domain. The initial breakthrough time is not modified, but significant reductions of the times at which 25%, 50%, 75% and 90% of the mass is recovered are noted. For example the time lag between the thresholds 25% and 75% is quite divided by 3 for θ passing from 0 to 33 degrees. A chi–square analysis of the mass distributions shows that more and more realizations exhibit a Gaussian distribution when θ increases. In order to get a more reliable index on the possibility to represent the dispersion process by a diffusion equation, **Schwartz et al. (1983)** have analysed $(d\sigma^2/dt)$ the time variation of the variance of the longitudinal mass distribution. If a single value of the dispersivity exists, this derivative will be constant. Analysing the simulation results, it appeared that the dispersivity coefficient was never constant or even time–dependent. This indicates that the diffusion model for the dispersion can only be applied in very few cases. However, since these results have been obtained for networks of orthogonal fractures, one may wonder if the conclusions may be extended to more general networks.

Smith at al. (1984) have studied on an identical network and with a θ–angle equal to zero, the influence of the mean aperture of the second set, the influence of the number of fractures forming each set, the influence of the length of the fractures and the influence of the source loading. Their conclusion is that mass transport characteristics are directly related to the connectivity of the network. This is a rather general result of the percolation theory obtained on more general networks. The discussion of the different simulations and the sensibility analysis being rather painful, we refer the interested reader to the mentioned paper.

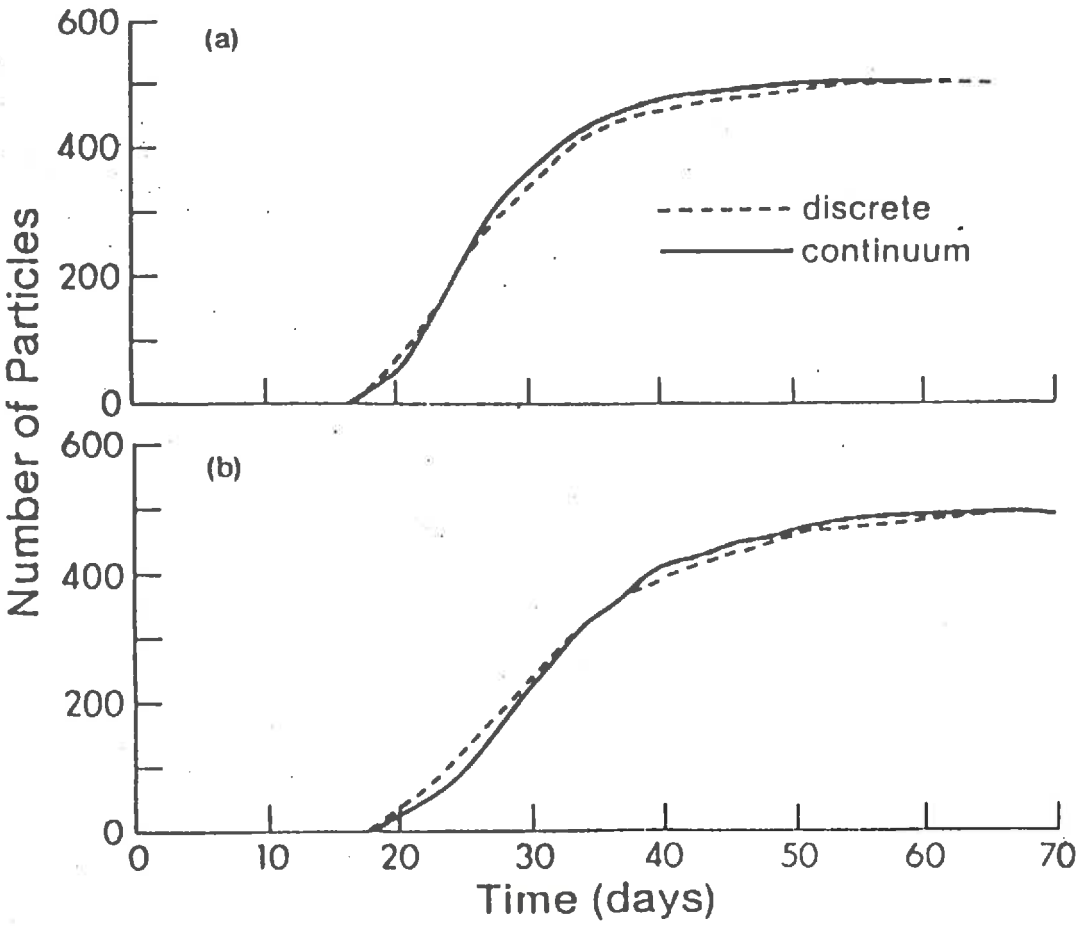

Fig. 1.5 Two examples of breakthrough curves obtained using discrete and continuum (type 2) approaches [after *Schwartz and Smith 1985*].

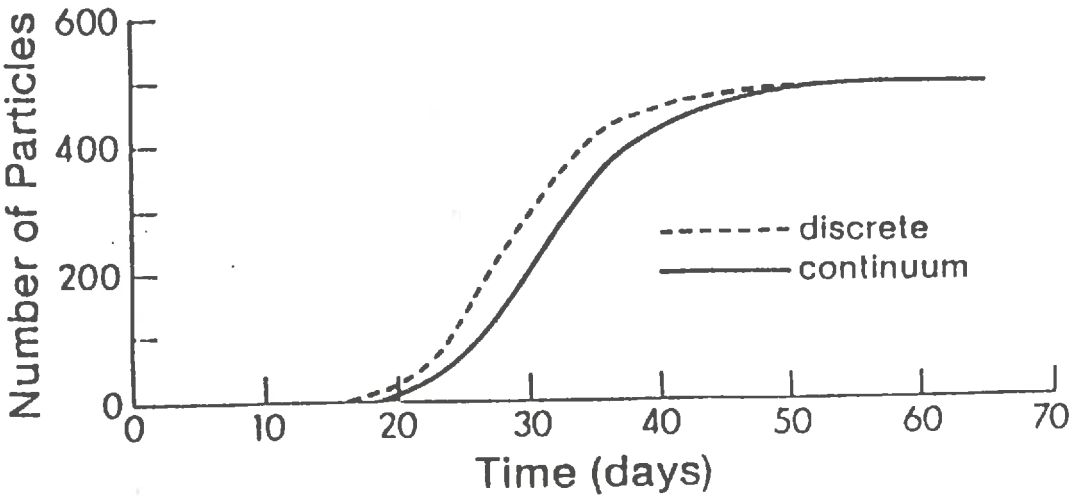

Fig. 1.6 Breakthrough curves obtained using discrete and continuum (type 1) approaches [after *Schwartz and Smith 1985*].

An interesting extension of this discrete approach has been proposed by Schwartz and Smith (1985). The basic idea of the method is to model the spread of the contaminant by a random walk method. The characteristics of this process are determined from deterministic mass transport simulations carried out on discrete fracture networks. Practically, a small part of the flow domain is used for deterministic simulations from the results of which the characteristics of the random walk will be derived. With this approach one must require the flow realizations used to derive the characteristics of the random walk process to be ergodic. This means that the flow realizations are not dependent on the local geometry of the network, but are representative of the overall statistical features of the network. Practically, this means that a sufficiently dense network has to be used. In other words, ergodicity imposes the sub–domain on which the deterministic simulations are conducted to be sufficiently large to represent an average behavior of the entire flow domain.

The characteristics of the random walk process are collected from statistics elaborated on the entire swarm of particules. Two methods are possible. The first one is to derive the probability distributions for the velocity in the three directions, upward, downward and downstream, directly from all the velocities experienced by all the particles. The second is to calculate the mean and the standard deviation of the velocity distribution experienced by each particle and for each direction. The means obtained with the two methods are evidently equal but the variances are different. In fact the mean of the standard deviations calculated on a particle basis is smaller than the standard deviation calculated for the entire swarm which reveals a certain deviation from the assumption of ergodicity.

If we note $-v_1$, $-v_2$, $-v_3$, the log–mean of the velocity in the three directions, and $-v_e$ the equivalent log–mean velocity across the domain derived from the mean travel–time of the particules, then the mean values of the distributions used for the random walk are:

$$-v_i = -v_e \, v_i / v_e \quad i = 1,2,3 \qquad [1.55]$$

where v_e is the equivalent velocity for the porous medium calculated from the effective conductivity K_e, the effective porosity θ_e and the hydraulic gradient. The values of the velocity used in the random walk (Eq. [1.55]) are slightly modified if the second approach is used to calculate the statistics of the velocity distribution. We refer to the paper by Schwartz and Smith (1985) for more details.

In order to check the methods, the continuum approach is applied to the domain used to derive the velocity. The random walk method with velocities calculated by the second approach restitutes very closely the breakthrough curve calculated with the particule tracking technique. Particularly, the long tails that can develop in such media are well reproduced, Fig 1.5. As well, the beginning of the breakthrough is perfectly restituted which is not the case for the random walk simulations using the velocity determined from global statistics, Fig. 1.6. In consequence, if the subdomain used to calibrate the random walk algorithm is representative of the entire domain, the movement of the particules can be simulated with a very rapid algorithm and overall does not require a geometrical description of the fractured media. In fact, the procedure developed above allows to pass from a local level of simulation requiring a detailed description of the media to a macroscopic scale since in the random walk method all that matters is a velocity in the three directions.

1.3.3 CONCLUSIONS

Several approaches have been proposed to simulate saturated water flows in heterogeneous media. They range from the equivalent porous medium concept to more sophisticated multi–continuum approaches. It is now recognized that in most of natural conditions the equivalent porous continuum approach leads to poor results and is unlikely to provide a useful frame to take up this problem.

Double porosity models have been introduced to account for physical situations where two fluid phases with very different characteristics are interacting. Namely, one fluid phase with high velocity and small capacity and the other with high capacity and very small velocity. In these models there is implicitely a phase playing the role of a vector and a phase used for storage. This partionning of the roles will be perhaps too strict for situations where the heterogeneities does not closely verify the conditions mentioned before (strict separation of the roles).

Among all double porosity models, one can distinguish between two kind of approaches. First the models trying to ignore the precise geometry of the discontinuities and the flow in the porous blocks. The interphase transport rate is then modeled by a first–order process. In this case the parameter controling the transport rate integrates at the same time the geometrical characteristics of the media and its transport characteristics. This type of approach has been initially developeded by **Barenblatt et al. (1960)**. The other way to define a coupling term between the two phases, **Duguid and Lee (1977)**, **Narasimhan (1982a,b,c,d)**, **Huyakorn (1983a)**, is to assume that the microporosity is made up of porous blocks having a simple geometrical shape and consequently to solve Richards' equation in these domains. This approach leads to various coupling terms according to the geometry retained. For these simple geometries, analytical solutions can be obtained since Richards' equation reduces to Laplace equation for saturated flows. Making use of Duhamel's theorem, the coupling terms take the form of convolution integrals. A partial differential equation is used in addition to model the flow in the macroporosity domain.

The other possible approach needs a precise description of the cracks network but there is no restriction on the geometry of the porous blocks. In this approach developed by **Narasimhan (1982a,b,c,d)**, the transport rates between the two phases and the pressure head distribution in each phase are explicitly calculated. The IFDM numerical method developed by **Narasimhan and Witherspoon (1976, 1977, 1978)** allows to handle any type of fracture networks.

Long et al. (1982) have provided a useful study and methodology to decide if the macroporosity continuum in a fissured medium can be approximated, for saturated water flow modeling, by an equivalent porous medium or what is equivalent if an analog to Darcy's law can be used at a sufficiently large scale. Similarly, in order to study the dispersion properties of a cracks network, **Smith and Schwartz** have developed a model based on Monte–Carlo simulations and randomly generated networks to simulate the movement of a swarm of particules. In these models the macroscopic dispersivity of the medium is shown up by using a particle tracking technique simulation and by explicitly calculating potential and flux distributions in the network. No exchanges between micro and macro porosities are accounted for. Their studies restricted to sets of orthogonal fractures, but varying a lot of parameters characteristic of the geometry, show that such a medium is unlikely to behave like a homogeneous porous media from the point of view of dispersivity properties.

2. WATER TRANSFER IN SATURATED–UNSATURATED MEDIA.

2.1 INTRODUCTION

It is now well recognized that a sufficiently precise modeling of the different chemical and physical processes occurring within the unsaturated zone is absolutely necessary in order to provide reliable predictions and risk assessments for all the environmental and agricultural problems we are facing. Water table recharge, leaching of fertilizers, accidental or continuous pollution by Nitrates, heavy metals or other substances (bacteria, virus), are now recognized as very dependent on all the transport phenomena occurring through the unsaturated zone. During the transport through the unsaturated zone, water fluxes and water content are two fundamental parameters directly controlling the movement of solute species, convection and diffusion, and indirectly the biological and chemical processes (aerations, reaction sites,...) in which they are involved.. Thus an understanding and a prediction as precise as possible of saturated–unsaturated water flow through the vadose zone is required.

For many years, Richards' equation based on Darcy's law has been widely used to build up models in order to study water table recharge, to provide fluxes for solute transport models or to predict infiltration and runoff. Usually, good agreements are obtained between simulation and laboratory experiments. Applying these models to field situations many deviations are recorded between calculated and observed data, if not a complete unability of the model to provide reasonable results. Consequently, it is clear that using these models in uncontrolled conditions may sometimes lead to a very bad estimation and description of water fluxes. If we are interested not only in water distribution but also in dissolved substances behavior, it is clear that very poor predictions may result.

In fact, looking for explanations, people have rediscovered the importance of preferential pathways such as, cracks, wormholes, structural porosity, moles and ants holes, dead roots, etc... on water flow. The role played by macropores on water circulation in the soil is not a recent discovery. More than one hundred years ago, Schumacher (1864) wrote:

"*..the permeability of a soil during infiltration is mainly controlled by big pores, in which the water is not held under the influence of capillary forces*".

Some years later, **Lawes et al. (1882)** reported:

"*The drainage water of a soil may thus be of two kinds: it may consist (1) of rainwater that has passed with but little change in composition down the open channels of the soil; or (2) of the water discharged from the pores of a saturated soil*".

Finally, Hursh (1944) noted:

"*Here porosity is not a factor of individual soil particle size but rather of structure determined by soil aggregates which form a three–dimensional lattice pattern. This structure is permeated throughout by biological channels which themselves also function as hydraulic pathways. A single dead–root channel, worm–hole or insect burrow may govern both the draining of water and escape of air through a considerable block of soil.*"

In the last years an increased interest for water flow modeling in heterogeneous media appeared. At the same time many experimental works have been done in order to better understand the basic physical processes involved in water flow through soil heterogeneities. A useful survey has been given by Bouma (1981) and Beven and German (1982).

Some of the published papers give experimental evidences of preferential flows, Thomas and Phillips (1979), Kneale and White (1984). Nitrate and chloride are used to show up the preferential flow of water in the heterogeneities, Quisenberry and Phillips (1976). Guennelon et al. (1981) have illustrated the importance of convective unsaturated flows taking place in the structural porosity. In their experiments, a

combined utilization of Phosphorus and Nitrate was very clearly showing the presence of two interacting flow processes. Due to precipitation in the calcareous clay soil on which the experiments were conducted and to its very low diffusion coefficient, the phosphorus was dying the convective pathways. Soil samples revealed the presence of very sparse convective paths and the arrival of the phosphorus at large depths (1 m). Inversely, the relative homogeneity of nitrate distributions in the soil profile were clearly illustrating the importance of the diffusion from the structural porosity into the porous matrix. Dying techniques are also largely used, associated with micromorphological observations in order to define where water is flowing, **Ritchie et al. (1972), Bouma et al. (1977), Bouma and Wosten (1979), Bouma (1981), Bouma et al. (1982), Bouma and Wosten (1984).**

Many measurement techniques have been developed. **Topp et al. (1981)** have applied the time–domain reflectometry technique to detect the occurrence of water flow in cracks. **Bouma et al. (1977)** have used dying techniques associated with image analysis to characterize the role played by different type of macropores. Estimations of the area developed by the cracks were also derived under controlled conditions. Field measurement techniques for saturated conductivity have also been proposed by **Bouma (1980)**. An extension to measurement of the unsaturated conductivity in the vicinity of the saturation is also given. Morphological methods have been developed to characterize the macrostructure of the soil. **Jarvis et al. (1987)**, presented a simple infiltrometer to apply water at low potentials (ψ between –0.5 and –9 cm) at the soi surface and used it to estimate unsaturated infiltration rates in a cracked clay soil. **Germann and Beven (1981a)** also presented a device to follow the drainage of initially saturated undisturbed soil samples.

For modeling purposes, many useful indications concerning the physic of the flow in macropores of different geometries can be obtained from these studies. Using dying techniques and image analysis, **Bouma et al. (1977)** distinguished between three types of macropores: cylindrical, planar and intermediate. They observed that under saturated conditions at the soil surface, they were equally used as preferential pathways. One important observation was that under these conditions, only a small part of the surface offered by the macroporosity was marked by the flow. It is clear that the amount of water reaching a given depth is among other parameters a function of the exchange surface between the porous matrix and the macroporosity, developed by the flow. Thus, this percentage is clearly an important parameter for any model. **Bouma (1980)** and **Bouma and Dekker (1978)**, also reported the fact that in their experiments the preferential flow was not occuring on all the surface offered by the cracks. They remarked that the flow took place along narrow bands and that the number of these bands depended on the rain intensity and duration. The same results are reported by **Kneale et al (1984)**. For sprinkling intensities varying from 1 to 10 they recorded an outflow ranging from 0 to 60 per cent of the input. The absorption rate of the matrix was then multiplied by 5. They concluded to the increase of absorption areas with the intensity of the input. Usually this increase in the contact area is said to be related to an increase in the number of pathways and probably not to an increase of the width of the stripes. This is a very important affirmation. From this affirmation it immediately appears that a two–dimensional simulation of the phenomena in a single crack or pore will be theoretically impossible. The phenomena is completely three–dimensional.

Most of the time the heterogeneities of the porous medium are due to swelling and shrinking properties of the material. These modifications of the geometry and thus of the hydraulic properties of the medium result in experimental and modeling problems. Many observations are reported in the literature regarding the difficulty there is to measure a saturated hydraulic conductivity for a swelling soil or to use the same sample for several infiltration trials. For the modeler the problem is to relate swelling or shrinking to a quantitative modification of the hydraulic characteristics of

the macropores and likely also of the porous matrix. Bouma et al. (1977) have studied the effects of swelling on water flow for four different macrostructures of the peds. They distinguished between structures where the prisms had *rough irregular* vertical faces and peds with *smooth* faces. Three of their samples had linear extension coefficients at saturation equal to .138. The last had a coefficient of .092. The linear extension coefficient at saturation is defined by:

$$LE_{sat} = [(V_s/V_d)-1]^{1/3} \qquad [1.1]$$

where, V_s is the volume at saturation and V_d is the stove dry volume. They showed that regarding flow characteristics a consistent difference existed between the two types of structure for a same linear extension coefficient. The peds having *smooth* faces exhibited a strong diminution of the crack surface used by the flow after swelling. The peds with *rough* faces had the opposite behavior. They explained that by the fact that upon swelling the *smooth* faces offer a better contact and thus more effectively close the cracks. With *rough* faces the contact is not so good and an important percentage of cracks surface remains available for preferential flows. In an other paper, Bouma and Wosten (1979) have studied for two types of macrostructure and upon continuous swelling, the evolutions of the saturated conductivity and chloride breakthrough curves. Their samples had identical linear extension coefficients. The faces of the peds were *rough* for the first set and *smooth* for the second set. After five months of swelling they found a very small decrease in the saturated conductivity for the first set and a strong diminution for the second set. Here also, the *smooth* faces provided a better contact between the peds. Correlated with this swelling phenomena, a gradual modification in the shape of the breakthrough curves was noted for the second set of samples. Longer tails and slower variations of the concentration at the beginning of the breakthrough are explained by a modification of the pores radius distribution.

Thus, one can see that for modeling purpose, and if we want to account for effects of swelling or shrinking on the flow, some indications on the morphology of the medium are required. In this case classical physical characterizations alone are probably not sufficient.

Several approaches can be outlined among the models proposed for saturated–unsaturated water flow modeling in heterogeneous media. First the models simulating water flow in a single crack or pore and diffusion in the surrounding matrix. They are based on Richards' equation for the porous matrix. This problem does not require any equation to describe the flow in the macroporosity although a model due to Yeh and Luxmoore (1982) uses one. This last characteristic is very important since the derivation of an equation modeling the flow in the macroporosity is actually a fundamental problem. An attempt to generalize this type of model to a entire soil profile by including an equation for the flow in the macropore continuum has been made by Jarvis et al. (1987a,b). A complete different approach based on the kinematic wave theory has been proposed to model the flow in the macroporosity continuum. In that case a simple coupling term is accounting for the interactions between macro– and microporosity flows. By analogy with the models presented for saturated flows in fractured media, these last two models will be called double–porosity models.

2.2 FLOW IN A SINGLE CRACK OR PORE.

Edwards et al. (1979) proposed a model for transient infiltration in a pore. A very similar approach was developed by Nieber (1981) for the same problem with a plane crack instead of a pore. For infiltration from saturated cracks two models have been proposed by Davidson (1984, 1985a). One use a Green–Ampt approach and the

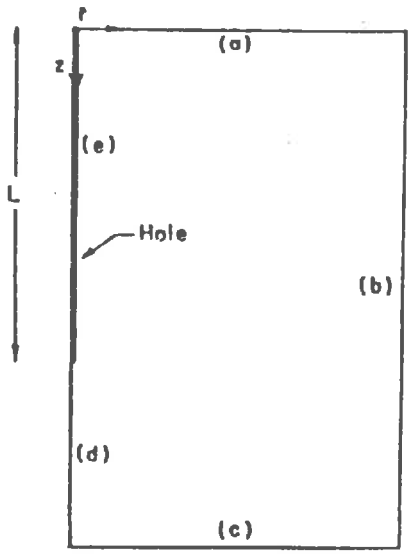

Fig. 2.1 Schema of the infiltration domain and boundaries. (a) soil surface, (b) column side, (c) bottom, (d) axis of symmetry and (e) vertical cylindrical hole with length L [after *Edwards et al. 1979*]

other a finite difference based numerical solution. An extension to a one–dimensional Green–Ampt approach to asymptotic infiltration in a cracked profile has also been proposed by Davidson (1985b,1987)

Edwards Model (1979)

This model considers a single vertical pore of length L, surrounded by a porous matrix. The symmetry is thus cylindrical and Richards' equation will be solved in a radial plane. This implicitly assumes that all the surface of the cylindrical macropore is used by the flow when the rain intensity exceeds the porous matrix infiltrability and water starts entering the macropore. If we note R the radius of the soil column and H its height, the flow equation in $\Omega = [0,R]\times[0,H]$ is in cylindrical coordinates:

$$\frac{\partial\theta}{\partial t} = \frac{1}{r}\frac{\partial}{\partial r}\left(Kr\,\frac{\partial H}{\partial r}\right) + \frac{\partial}{\partial z}\left(K\,\frac{\partial H}{\partial z}\right) \qquad [2.2]$$

where H is the total head (cm), z is depth oriented downwards, r is radial distance, θ is the water content of the porous matrix, and t is the time. Initially, a flux boundary condition is imposed at the surface of the soil. As long as the porous matrix infiltrability through the column surface is greater than the rain intensity no flow occurs along the macropore walls. As soon as saturation occurs at the top of the column the water may enter the macropore. Let us note t_1 this time. Thus the boundary conditions at the soil surface (a) Fig 2.1 are given by:

$$-K\,\frac{\partial H}{\partial z} = F \quad \text{for} \quad t \le t_1 \qquad\qquad H = 0 \quad \text{for} \quad t \ge t_1\,. \qquad [2.3]$$

On the boundaries (b), (c), (d), no–flux boundary conditions are imposed. The algorithm used to handle the runoff along the macropore wall is similar to the one used by **Brandt et al.** (1971) to calculate the extension of the saturated zone under trickle irrigation. As long as there is no runoff ($t \le t_1$), a null–flux condition is used on (e):

$$-Kr_h\,\frac{\partial H}{\partial r} = 0 \qquad [2.4]$$

where r_h is the pore radius. When water flows along the macropore walls the algorithm used is as follow:

– Calculate the flow rate entering the pore

– If z_t is the depth of the wet zone along the pore wall, apply a Dirichlet condition corresponding to saturation and calculate the flux through this zone using an approximation of the hydraulic gradient.

– If all the flux entering the macropore doesn't completely diffuse through the wet zone then increase z_t, else go to next time step.

If we note t_2 the time at which water reaches the bottom of the macropore, the boundary conditions corresponding to this physical situation, holding for $t \in [t_1,t_2]$ are:

$$\begin{array}{rcl|l} H = -z & & & 0 \le z \le z_t \\ -Kr_h\,\dfrac{\partial H}{\partial r} = i & \Big| & t_2 \le t \le t_2 & z = z_t \\ -Kr_h\,\dfrac{\partial H}{\partial r} = 0 & & & z_t \le z \le L \end{array} \qquad [2.5]$$

If the rain lasts long enough, the water accumulating at the bottom of the hole may reach the surface of the soil at a time we note t_3. During the time interval $[t_2,t_3]$ the boundary conditions along (e) are:

$$\left.\begin{array}{l} H = -z \\ H = -W \end{array}\right] t_2 \leq t \leq t_3 \left[\begin{array}{l} 0 \leq z \leq W \\ W \leq z \leq L \end{array}\right. \qquad [2.6]$$

where W is the depth of the water table below the soil surface. Once the water table in the hole has reached the soil surface the boundary condition becomes:

$$H = 0 \text{ for } t \geq t_3 \text{ and } 0 \leq z \leq L \qquad [2.7]$$

and the runoff at the soil surface starts. The finite difference based numerical solution of this set of equations was carried out using the CSMP package. This model was used by Edwards et al. (1979) to study the effects on runoff time of start and intensity of depth, radius, and number of holes by unit area.

Beside the fact that all the surface of the hole is used which seems to be in contradiction with observations, the main critic which can be done is that the algorithm used to estimate the amount of water diffusing radially from the macropore wall into the porous matrix is very badly suited for this physical situation. This algorithm has already been discussed by Lafolie et al. (1988) and shown to give bad estimations in many cases for trickle irrigation. Concerning the problem of evaluation of fluxes at a boundary, see also the remarks by Huyakorn et al. (1983a). In this case we are typically facing a situation where very large gradients of potential exist all along the macropore wall, which is the worst possible configuration. Furthermore, in clay soil the diffusivity is very weak and thus, only the immediate vicinity of the pore will be wetted. Therefore, very small spatial steps must be used if we want to correctly estimate radial fluxes. In their calculations, Edwards et al. (1979) used a step of 5. cm which is obviously too large and probably leading to large errors in cumulative infiltration estimations. Reasonable steps should be of some millimeters near the macropore wall. Finally, in the cases studied by Edwards et al. (1979) infiltration lasts approximately half an hour, and it is precisely at the beginning of the process that estimation errors mentioned before are the largest. Typically, for high intensity short storm simulations, which is the case reported by Edwards et al. (1979), the model will probably give poor estimations of runoff starting time and intensity.

Concerning the utilization of the model to evaluate the global infiltrability of the soil and the runoff, an important problem is the choice of the area which contributes to the flow in the macropore. Since the runoff at the soil surface is largely conditioned by the microtopography, one can expect certain holes to be bypassed and others to receive a much more important contribution than the one evaluate from a simple ponderation of the area of the field. Hence, it is difficult to extrapolate the results obtained for one macropore or crack to a much larger area. In addition, remark that the percentage of the surface of the cracks used by the flow is also certainly related to the runoff pattern at the soil surface.

The model developed by Nieber (1981) for infiltration into cracks is very similar to the one proposed by Edwards et al. (1979). It resolves Richards' equation with the same boundary conditions with a finite element method. The algorithm handling the runoff along the crack wall is identical with the one used by Edwards et al. (1979) and thus suffers from the same defaults. Thus, we are not going to further develop this model. The main difference between the two models is that Nieber (1981) has tried to incorporate in his model the banding effect reported by Bouma et Dekker (1978). As remarked by the author the simulation is then theoretically

three—dimensional. The way the banding is introduced is in fact not very clear. For the same reasons as for Edwards' model the conclusions derived from the simulations are not very reliable.

Model of Yeh and Luxmoore

Yeh and Luxmoore (1982) proposed a different model for the same problem. Instead of assuming that the flow in the macropore is controled by the uptake rate from the walls of the macropore, they used the following equations to model the flow in the macropore

$$\beta' \frac{\partial \psi}{\partial t} = \nabla.(K \frac{d\varphi}{d\ell} \vec{n}_\ell) \qquad [2.8]$$

when the pore is saturated, and

$$\frac{\partial \theta}{\partial t} = \frac{dz}{d\ell} \vec{n}_\ell \nabla K \qquad [2.9]$$

when the pore is unsaturated. β' is the modified compressibility of water; K is the equivalent hydraulic conductivity in the pore; ψ,φ, and θ are the pressure head, total head ($\varphi=\psi+z$), and water content, respectively, in the pore. ℓ is the distance from a reference point along the longitudinal direction of the pore indicated by the vector $\vec{n}_\ell$. If we note R the radius of the macropore and R—r the thickness of the liquid film, then, the water content and hydraulic conductivity of the pore are

$$\theta = 1-r^2/R^2 \qquad [2.10]$$

and

$$K(\theta) = [\rho g R^2/(8\mu)][1 + 3(1-\theta)^2 - 4(1-\theta) + 4(1-\theta)^2 \ell n(1/\sqrt{1-\theta})], \qquad [2.11]$$

respectively, where μ is the viscosity of water, ρ the density, and g the gravity acceleration. Similarly, if we note W the aperture of a plane crack and w the thickness of the film of water, the water content and the hydraulic conductivity are

$$\theta = 2w/W \qquad [2.12]$$

$$K(\theta) = [\rho g W^2/(12\mu)]\theta^3, \qquad [2.13]$$

respectively. Darcy's law is used to model the flow in the porous matrix, and continuity of the pressure head is imposed across the interface macropore microporosity. Boundary conditions must be suppied either in terms of water content if the pore is unsaturated. When the pore is completely saturated the boundary condition at the soil surface is $\psi=0$. Applied to the simulation of simultaneous infiltration from the soil surface and macropore walls, the model gives essentially the same results as earlier obtained by Edwards et al. (1979).

Davidson Model. The Green—Ampt approach

For the infiltration from a saturated crack, Davidson (1984,1985a) proposed two solutions for the problem, respectively based on a Green—Ampt model and a finite difference solution of Richards' equation.

The Green–Ampt model assumes that water advances in a sharp wetting front at which water potential is constant and behind which hydraulic conductivity and moisture content are also constant. This concept has been largely used to model classical one–dimensional infiltration.

Let us consider a two–dimensional representation of a soil profile (Fig. 2.2) containing regularly spaced vertical cracks. The length of each crack is a and the spacing between two cracks, b. The initial moisture content is assumed uniform, and at t=0 the saturation is assumed over all the crack wall and at the surface of the soil. No–flux boundary conditions are imposed everywhere else. The constant conductivity in the wet zone is noted K, and ϕ the total pressure head is given by $\phi = \psi + z$, where ψ is the matrix potential. Assuming Darcy's law in the wet region the flow velocity **u** is given by:

$$\mathbf{u} = -K\nabla\phi \ . \qquad [2.14]$$

Combining with the continuity equation, Laplace's equation is obtained in the wet zone:

$$\nabla^2\phi = 0 \quad \text{in R} \ . \qquad [2.15]$$

The potential at the front is given by: $\phi = \psi_c - z$, where ψ_c is negative and can take an arbitrary value. The boundary conditions are, Fig 2.2:

$$\begin{aligned} &\phi = 0 \ ; z = 0 \quad x \in [0,b] \\ &\phi = 0 \ ; x = 0 \quad z \in [0,a] \\ &\frac{\partial\phi}{\partial x} = 0 \ ; x = 0 \ , z \geq a \quad \text{and } x = b \ , z \geq 0 \ . \end{aligned} \qquad [2.16]$$

Let us note C the wetting front and N the normal to C. Then any point (x,z) on C moves according to the kinematic equations:

$$\frac{dx}{dt} = -U_n \sin\chi \qquad \frac{dz}{dt} = U_n \cos\chi \qquad [2.17]$$

where χ is the angle between N and the z axis, and U_n the velocity normal to the wetting front given by:

$$U_n = (-K\frac{\partial\phi}{\partial N} - K_0\cos\chi)/f \qquad [2.18]$$

K_0 is the conductivity ahead the front and f the difference in moisture contents between the wet and dry zones. As K_0 is usually very small in a initially dry soil, U_n is simplified to

$$U_n = -\frac{K}{f}\frac{\partial\phi}{\partial N} \ . \qquad [2.19]$$

The first stage of the solution is to transform the physical domain where Dirichlet conditions are imposed on two orthogonal boundaries in a domain where only one boundary has a Dirichlet condition. This is done using a conformal transform. If $\Omega = x + iz$ is the physical complex plane Fig 2.2, and ω=p+iq the

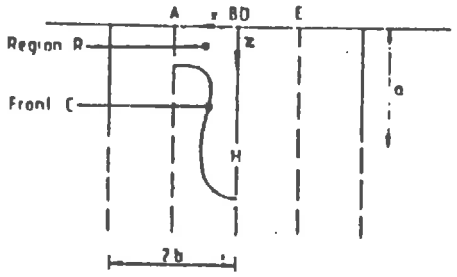

Fig. 2.2 Schematic representation of the physical domain, Ω, containing regularly spaced cracks with depth a and spacing $2b$. Dashed lines are symmetry axis for the flow [after *Davidson 1984*]

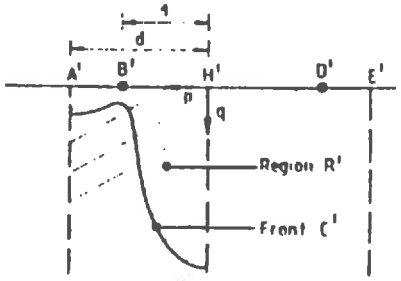

Fig. 2.3 Schematic representation of the transformed domain, ω, containing regularly spaced cracks with depth a and spacing $2b$. Dashed lines are symmetry axis for the flow [after *Davidson 1984*]

transformed complex plane Fig 2.3, the conformal transform mapping ω in Ω is given by:

$$\Omega = \frac{i\,b}{\pi}\left\{ \log\left[\frac{\cos(\pi\omega/2d)}{\sin(\pi/2d)} + \left(1 - \frac{\sin^2(\pi\omega/2d)}{\sin^2(\pi/2d)} \right)^{1/2} \right] \right.$$

$$\left. - \log\left[\frac{\cos(\pi\omega/2d)}{\sin(\pi/2d)} - \left(1 - \frac{\sin^2(\pi\omega/2d)}{\sin^2(\pi/2d)} \right)^{1/2} \right] \right\} \qquad [2.20]$$

where d is defined by: $\sin(\pi/2d) = \tanh(\pi a/2b)$. With this transformation, the boundary sections A'–B', B'–H', H'–D', D'–E' in the plane ω are mapped into A–B, B–H, H–D, D–E in the plane Ω. If we note R' the wet region and C' the front in the ω plane, the flow equation remains:

$$\nabla^2\phi = 0 \text{ in } R' \qquad [2.21]$$

with

$$\phi = 0 \text{ on } q = 0. \qquad [2.22]$$

The other boundary conditions are :

$$\phi = \psi_c - z(p,q) \text{ on } C' \qquad [2.23]$$

$$\frac{\partial\phi}{\partial p} = 0 \quad \text{for } p = 0 \text{ or } p = d\,. \qquad [2.24]$$

For a conformal mapping, the normal derivatives are related by:

$$\frac{\partial\phi}{\partial N} = \frac{\partial\phi}{\partial n} \Big/ \left|\frac{d\Omega}{d\omega}\right| \qquad [2.25]$$

$$e^{i\chi} = \frac{d\Omega}{d\omega} e^{i\theta} \Big/ \left|\frac{d\Omega}{d\omega}\right|$$

where n is the outward normal to C' and ω the angle between n and the positive q axis. Thus the kinematic conditions [2.17] becomes:

$$dp/dt = -U_n \sin\theta \qquad dq/dt = U_n \cos\theta \qquad [2.26]$$

where

$$U_n = U_n \Big/ \left|\frac{d\Omega}{d\omega}\right| = \frac{-K}{f} \frac{\partial\phi}{\partial n} \Big/ \left|\frac{d\Omega}{d\omega}\right|^2 . \qquad [2.27]$$

The second stage of the solution is to calculate in the ω–plane the movement of the wetting front. Let us define $\phi_1 = \psi - \psi_c$, so that ϕ_1 equals zero on the wetting front. Note that ϕ_1 satisfies equations [2.15] or [2.21]. We note G(P;Q) a Green's function with field and source points P and Q respectively. A Green's function satisfying:

$$\nabla^2 G = \delta(p-\xi)\delta(q-\eta) \qquad [2.28]$$

in the semi–infinite stripe $0 \le p$; $0 \le q$; $\xi \le d$; $\eta \le \infty$, together with the homogeneous boundary conditions [2.22] and [2.24] is given by:

$$G(p,q;\xi,\eta) = \frac{1}{4\pi}\log[\cosh\frac{\pi}{d}(q-\eta) - \cos\frac{\pi}{d}(p+\xi)][\cosh\frac{\pi}{d}(q-\eta) - \cos\frac{\pi}{d}(p-\xi)]$$

$$-\frac{1}{4\pi}\log[\cosh\frac{\pi}{d}(q+\eta) - \cos\frac{\pi}{d}(p+\xi)][\cosh\frac{\pi}{d}(q+\eta) - \cos\frac{\pi}{d}(p-\xi)] \ . \qquad [2.29]$$

To solve the kinematic equations we need U_n and thus $\partial\phi_1/\partial n$. An expression for $\partial\phi_1/\partial n$ is derived using Green's theorem:

$$\int_{R'}(\phi_1\nabla^2 G - G\nabla^2\phi_1)dQ = \int_{\partial R'}(\phi\frac{\partial G}{\partial n(Q)} - G\frac{\partial\phi_1}{\partial n(Q)})ds(Q) \ . \qquad [2.30]$$

Applying formula [2.30], together with [2.21], [2.22], [2.23], [2.24], [2.28], gives:

$$\phi_1(P) = -\int_{C'} G(P;Q)\frac{\partial\phi_1}{\partial n(Q)}ds(Q) + \int_0^d \{[\psi_c - z(Q)]\frac{\partial G}{\partial\eta}\}_{|\eta=0}d\xi \qquad [2.31]$$

This expression is transformed by **Davidson (1984)**, and the final integral equation giving $\partial\phi_1/\partial n$ is:

$$\frac{\partial\phi_1}{\partial n(P)}[\int_{C'}(\eta - q)\frac{\partial G}{\partial n(Q)}ds(Q) - q] = \cos\theta(P)\,[z(P) - qb/d - \psi_c]$$

$$+\int_{C'}[\cos\theta(Q)\frac{\partial\phi_1}{\partial n(P)} - \cos\theta(P)\frac{\partial\phi_1}{\partial n(Q)}]Gds(Q) \qquad [2.32]$$

for P lying on C'. When C' is a single–valued function q(p,t), its motion can be expressed by:

$$\partial q/\partial t = U_n\cos\theta \ . \qquad [2.33].$$

The aim is then to numerically follow the movement of the front, solving equations [2.32] and [2.33]. The solution is sought along equally spaced lines $p = p_j$ $j=1,...,N$. Time integration is performed by a Adams–Bashforth–Moulton scheme, and the quadrature of integrals in [2.32] by Simpson's rule. A cubic spline is used to calculate the slopes of C'. The solution in the physical Ω–plane is obtained by mapping C'into C through [2.20].

Davidson Model. The finite difference solution.

Davidson (1985) has also provided a finite difference based numerical solution for the same problem. Using Kirchoff transformation, the equations of the problem are:

$$\nabla^2 V = 0 \text{ in the saturated zone and}$$

$$\frac{d\theta}{dV}\frac{\partial V}{\partial t} = \nabla^2 V - \frac{\partial K}{\partial z} \text{ in the unsaturated zone } (v \leq 0)$$

where V is defined by:

$$V(\psi) = \int_0^{\psi} K(\psi')\, d\psi'. \qquad [2.34]$$

The physical boundary conditions are the same as for the Green–Ampt model and easily transformed for the new variable, V. The Laplace operator and the first derivative $\partial K/\partial z$ are approximated by three points and two points centered formula, respectively. A fully implicit scheme is used to advance in time. This results in the following system of non–linear equations:

$$\frac{V^{n+1}_{i+1,j} - 2V^{n+1}_{i,j} + V^{n+1}_{i-1,i}}{(\Delta x)^2} + \frac{V^{n+1}_{i,j+1} - 2V^{n+1}_{i,j} + V^{n+1}_{i,j-1}}{(\Delta z)^2} = 0 \quad \text{for} \quad V^{n+1}_{i,j} \geq 0$$

$$" = \left(\frac{d\theta}{dV}\right)^{n+1}_{i,j} \frac{V^{n+1}_{i,j} - V^{n+1}_{i,i}}{\Delta t} + \frac{K^{n+1}_{i,j+1} - K^{n+1}_{i,j-1}}{2\Delta z} \quad \text{if} \quad V^{n+1}_{i,j} \leq 0 \qquad [2.35]$$

where:

$$\left(\frac{d\theta}{dV}\right)_{i,j} = \frac{\theta^{n+1}_{i,j} - \theta^{n}_{i,i}}{V^{n+1}_{i,j} - V^{n}_{i,j}} \quad \text{if} \quad V^{n+1}_{i,j} \neq V^{n}_{i,j}$$

$$\left(\frac{d\theta}{dV}\right)_{i,j} = \frac{d\theta}{dV}\left(V^{n}_{i,j}\right) \quad \text{if} \quad V^{n+1}_{i,j} = V^{n}_{i,j}. \qquad [2.36]$$

This system is written in the form:

$$V^{*}_{i,j} = V^{n+1}_{i,j} = f(V^{n+1}_{i+1,j}, V^{n+1}_{i-1,j}, V^{n+1}_{i,j+1}, V^{n+1}_{i,j-1}, \left(\frac{d\theta}{dV}\right)^{n+1}_{i,j},$$

$$K^{n+1}_{i,j+1}, K^{n+1}_{i,j-1}, V^{n+1}_{i,j}) \qquad [2.37]$$

and solved with a sur–relaxation iterative scheme:

$$V^{n+1}_{i,j} = V^{n+1}_{i,j} + \omega\,(V^{*}_{i,j} - V^{n+1}_{i,j}). \qquad [2.38]$$

Davidson (1985) uses a correction technique due to Hirt and Harlow (1967) to prevent accumulation of iteration errors with time.

Both models have been used to test the effects of different geometrical parameters such that cracks spacing and cracks depth. Changes due to variations in

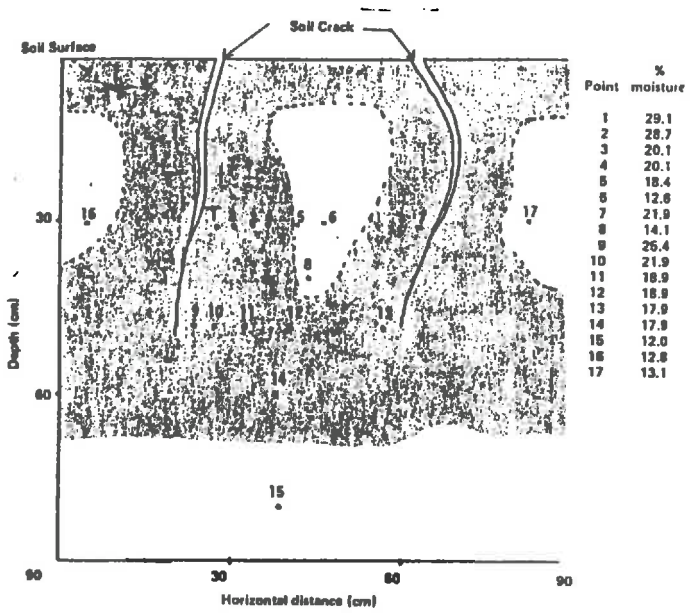

Fig. 2.4 Moisture distribution in a clay soil after a 90 mm rain. Shaded area indicates the part of the profile that appears to have been moistened [after *Lewis 1977*]

the hydraulic characteristics have been estimated with the numerical model. Water content profiles, cumulative infiltrations and infiltration rates, functions of time are given in **Davidson (1984, 1985a)** for different configurations of the cracks. The different results agree well with those of **Edwards (1979)** and those of **Nieber (1981)**. The **Green–Ampt model** fails to provide results for b/a lower than .5, which is the case of a set of relatively close cracks. In this case as soon as the wetted zone developing at the bottom of the crack touches the symmetry axis, the numerical calculation breaks down. So the occurrence of a dry zone surrounded by a wet zone between two cracks is never shown up. With the numerical model the calculus is possible and a dry zone appears. For illustration purpose an experimental water content distribution drawn from **Lewis (1977)** and illustrating this phenomena is given Fig 2.4

Asymptotic Behaviour.

The aim of this study, **Davidson (1985b,1987)**, was to derive a one–dimensional **Green–Ampt** model for infiltration in a soil containing cracks or holes. As presented before, **Davidson (1984)** has derived a two–dimensional **Green–Ampt** model for infiltration from a single saturated crack, whose solution process involved a conformal transform. In this case the conformal transform is not necessary. The Green function (Eq. [2.29]) is used again and the problem is then defined by:

$$\begin{array}{l|l} \nabla^2\phi = 0 \text{ in } R & \nabla G = \delta(x-\xi)\delta(z-\eta) \\ \partial\phi/\partial x = 0 \quad x=0,\ z\geq a;\ x=b,\ z\geq 0 & \partial G/\partial x = 0 \quad x=0,\ x=b,\ z\geq 0 \\ \phi = 0 \quad z=0,\ x\in[a,b],\ x=0,\ z\in[0,a] & G = 0 \quad z=0,\ x\in[0,b]\ . \end{array}$$

Applying Green's theorem to functions ϕ and G the following expression is obtained:

$$\phi(x,z) = z(\partial\phi/\partial z)_{|L} + \int_0^a (G\ \partial\phi/\partial\xi)_{|\xi=0}\, d\eta \qquad [2.39]$$

since $G \longrightarrow -z/b$ when $\eta \longrightarrow \infty$ with z finite. For (x,z) belonging to the crack, this expression reduces to:

$$-z(\partial\phi/\partial z)_L = \int_0^a g_c(z,\eta)\,\partial\phi(0,\eta)/\partial\xi\, d\eta \qquad [2.40]$$

where

$$g_c(z,\eta) = G(0,z,0,\eta)\ . \qquad [2.41]$$

Another relationship connecting the gradients of potential on the front to those along the crack can be obtained by applying Green's theorem to the function $z\nabla^2\phi - \phi\nabla^2 z$. Then we have:

$$(\partial\phi/\partial z)_{|L} = \frac{1}{L}\left(\frac{1}{b}\int_0^a z\,\partial\phi(0,z)/\partial x\, dz + \psi_c - L\right) \qquad [2.42]$$

where L is the depth of the wetting front assumed to be horizontal. L is supposed to be large enough so that $\partial\phi/\partial z$ can be taken constant along the front. One can expect the gradients to decrease when L increases. Thus we can express these gradients in series of negative powers of L

$$(\partial\phi/\partial z)_L = a_0 + a_1 L^{-1} + a_2 L^{-2} + \ldots\ldots$$

$$\partial\phi(0,z)/\partial x = Q_0(z) + Q_1(z)L^{-1} + Q_2(z)L^{-2} + \ldots\ldots \qquad [2.43]$$

Using these expressions in equations [2.40] and [2.42], and equating the terms of like order, we get:

$$a_0 = -1 \qquad [2.44]$$

$$a_1 = \psi_c + \frac{1}{b}\int_0^a z Q_0(z)\, dz \qquad [2.45]$$

$$a_n = \frac{1}{b}\int_0^a z.Q_{n-1}(z)\, dz \quad (n\geq 2) \qquad [2.46]$$

$$-a_n z = \int_0^a g_c(z,\eta) Q_n(\eta)\, d\eta \ . \qquad [2.47]$$

Multiplying [2.47] by $Q_0(z)$ and integrating gives:

$$-a_n \int_0^a z Q_0(z)\, dz = \int_0^a Q_n(\eta) \int_0^a g_c(z,\eta) Q_0(z)\, dz d\eta \ . \qquad [2.48]$$

The integral on the left hand side can be evaluated using [2.45], and the integral on the right by [2.47] with n=0. Thus [2.48] becomes:

$$-a_n\,(a_1 - \psi_c)b = \int_0^a \eta Q_n(\eta)\, d\eta \qquad [2.49]$$

and hence, using [2.46] we have:

$$a_{n+1} = (\psi_c - a_1)a_n \quad n \geq 1 \ . \qquad [2.50]$$

Defining $L_0 = \psi_c - a_1$ we have the following relation:

$$a_n = -L_0^{n-1}\,(L_0 - \psi_c) \quad n \geq 1 \ . \qquad [2.51]$$

Summing [2.43a] gives:

$$(\partial\phi/\partial z)_L = \frac{\psi_c - L}{L - L_0} \qquad [2.52]$$

which is a one–dimensional Green–Ampt form for an infiltration from a supply surface located at L_0 below the surface. L_0 is given by:

$$L_0 = -\frac{1}{b}\int_0^a zQ_0(z)\,dz\,. \qquad [2.53]$$

In the case of a cylindrical hole a different Green's function is needed satisfying the equation:

$$\nabla^2 G_h = \frac{1}{r}\frac{\partial}{\partial r}\left(r\frac{\partial G_h}{\partial r}\right) + \frac{\partial^2 G_h}{\partial z^2} = \frac{1}{2\pi r}\delta(r-\rho)\,\delta(z-\eta)\,. \qquad [2.54]$$

This function is given by Davidson (1985b):

$$G_h(r,z;\rho,\eta) = \frac{1}{2\pi r_1^2}\left(|z-\eta| - |z+\eta|\right)$$

$$-\sum_{n=1}^{\infty}\left[\exp(-\lambda_n|z-\eta|) - \exp(-\lambda_n|z+\eta|)\right]\frac{J_0(\lambda_n r)\;J_0(\lambda_n\rho)}{2\pi r_1^2\;\lambda_n . J_0^2(\lambda_n r_1)} \qquad [2.55]$$

where the λ_n are the roots of: $J_1(\lambda_n r_1) = 0$. J_0 and J_1 are Bessel functions of first kind. Applying the same reasoning as for the case of a crack, an expression is derived for L_0 and it is shown that a one dimensional Green–Ampt formulation can be derived. In this case L_0 is given by:

$$L_0 = -\frac{2\pi r_0}{r_1^2}\int_0^a zQ_0(z)\,dz \qquad [2.56]$$

where:

$$2\pi r_0\int_0^a g_h(z,\eta)Q_0(\eta)\,d\eta = z \qquad 0 \le z \le a\,. \qquad [2.57]$$

The calculation of L_0 is performed by standard techniques, quadrature of the integral and collocation to obtain a set of linear algebraic equations. The following transformation is applied before numerical calculations to avoid any difficulties associated with the logarithmic singularity of g:

$$\int_0^a g(z,\eta)Q_0(\eta)d\eta = \int_0^a g(z,\eta)(Q_0(\eta)-Q_0(z))d\eta + \int_0^a g(z,\eta)d\eta \qquad [2.58]$$

Some results are presented by **Davidson (1985b)** comparing infiltration rates calculated by the two–dimensional model and the present approach. For large times the two models give the same results. To apply this approach one have to wait for the front to be quite horizontal, namely for the infiltration front to be well below the crack depth. It is obvious that this can only occur if the flooding of the surface lasts sufficiently, which is as outlined in his conclusion by Davidson (1985b), unlikely to occur in natural conditions. L_0, the virtual null potential surface ordinate, is always lower than a the depth of the crack, and is only related to the geometry of the system. Tabulated values of L_0/a function of b/a are given by Davidson (1985b), where b is the half crack spacing. For cylindrical holes, L_0/a depends on the ratios r_1/a and r_1/r_0, where r_1 is the radius of the soil column associated with the macropore and r_0 the radius of the hole.

As said at the beginning these models are restricted to infiltrations from saturated cracks instantaneously filled by a storm and hence are not really applicable to field situations. In fact it seems that all the authors who worked on this problem have always assumed that it was necessary to have a high input rate at the soil surface (storm or flooding) to have a flow in the macroporosity.(cf the different hypothesis of Davidson). Particularly, all the range of rain intensities progressively filling the cracks or even just involving some runoff along their walls cannot be simulated with this model. Another restriction comes from the hypothesis of an initially very dry soil, thus eliminating all the physical situations resulting from a succession of infiltrations and redistributions. How the wetting front develops under more wet initial conditions ? Is the mushrooming effect more or less important ? For what configuration an enclosed relatively dry pocket appears ? What are the effects on infiltration rates ? All these questions cannot be taken up by these two models.

The models of **Edwards et al. (1977), Nieber (1981), Davidson (1984–1985)** are all restricted to a single crack or cylindrical macropore, and extensions needed for infiltration simulations in a heterogeneous profiles. Some attempts have been made by **Hoogmoed et al. (1980), Bouma et al. (1982), Bouma and Wosten (1984)** to extend these modeling approaches to field situations and to compare calculated and measured water content distributions. The most interesting work lately proposed, is a model by **Jarvis and Leeds–Harrison (1987a)** to simulate water flow in a structured and drained clay soil.

2.3 A DOUBLE POROSITY MODEL

This model comes naturally as an extension of the various approaches developed for flows in single cracks or pores. To be able to use an approach simulating at the same time the flow in the cracks and water uptake by the peds the authors assume that the soil is made up of cubic porous blocks of known size (d) separated by a network of plane cracks with width (w). This assumption enalbles them to calculate a structural porosity (e_t) and a crack surface per unit of soil volume (A). In addition they distinguish between a dynamic structural porosity (e_d) and a stable structural porosity (e_s). The stable structural porosity is related to the volume of cracks remaining in a fully swollen material; this is a parameter to be fixed by the user. The dynamic structural porosity is related to the volume of cracks disappearing upon swelling of the peds. Thus, the total structural porosity at any time is given by $e_t = e_s + e_d$. According to the authors, $e_d = \theta_f - \theta$, where θ_f is the water content at field capacity and θ the initial water content. Assuming isotropy of shrinkage and swelling properties the volume of vertical cracks and their area per unit of soil volume are defined by $e_v = 2e_t/3 = 2w/d$ and $A_v = 2A/3 = 4/d$, respectively. Hallaire (1987) gave evidences that isotropy of shrinkage and swelling are reasonable hypothesis for aggregates isolated from their environment, but that for a layer of soil the process is certainly more complicated. However, even if it is in a relatively crude

way, the model of **Jarvis et al. (1987a)** is at our knowledge the the first to introduce the processes of srinkage and swelling in a water flow model.

Water uptake by the peds and at the surface of the soil is in their model controled by the sorptivity. Thus assuming that the gravitational component of the flow is negligible in the peds, the water uptake rate at the soil surface is given by

$$I_v = S/2\sqrt{t} \qquad [2.59]$$

As in previous models, the flow is assumed to start in the cracks when ponding occurs at the soil surface. According to the equation above, the ponding time t_p is given by

$$t_p = (S/2R)^2 \qquad [2.60]$$

where R is the rain intensity assumed constant over the period of application. The input rate into the cracks is then defined by: $I_c = R - I_v$. As soon as the rain stops the input rate into the cracks goes to 0.

To simulate horizontal adsorption by the peds, the soil profile is discretized into n layers with width (Δz), each characterized by a surface of cracks per unit volume of soil, $A_{v,i}$. According to the experimental results reported in previous paragraphs, it is assumed that water uptake by the peds occurs through a fraction only of the total surface offered by the cracks. Thus, a paremeter α_i is introduced to account for this phenomena. In consequence, the global horizontal water uptake rate for the whole profile is

$$I_l = \sum_{i=1}^{n} (f_i \Delta z)(\alpha_i A_{v,i})(S_i/2)\sqrt{t - t_i} \qquad [2.61]$$

where f_i is the fractional wetted depth for the layer i, S_i is its sorptivity and t_i the time at wich water reached that layer. Remark that f_i is equal to 1 for all the layers between the soil surface and the wetting front, has a value between 1 and 0 for the layer in which is located the front, and is equal to zero for all the layers below. Normally, a nonlinear relationship holds between the sorptivity and the water content. In the model a linear relationship is assumed with a sorptivity equal to 0 at field capacity. The initial sorptivity must be supplied by the user.

The flow in the cracks is based on the cubic law presented before. For a laminar flow in a completely filled crack the flux q is, $q = (\rho g/12\eta)w^3\nabla\varphi$, where g is the acceleration due to gravity, $\nabla\varphi$ is the hydraulic gradient and ρ and η are the density and viscosity of water respectively. Since the model is applied to a drained profile the hydraulic gradient is taken equal to 1. The flux q* per unit volume of soil for the orthogonal network of cracks is then

$$q^* = (\rho g/12\eta)w^2 e_v \qquad [2.62]$$

since the distance between two cracks is d. To reflect factors such that pore connectivity, roughness, tortuosity, and account for the degree of saturation of the cracks, Eq. [2.62] giving the flux q* is modified as follows

$$q^* = (\rho g/12\eta)w^2 e_v S_c^n \qquad [2.63]$$

where S_c is the degree of saturation of the craks and n is an empirical exponent. The

authors assume that water flowing in a crack which is not full does so by "bridging" over the crack. With this assumption it follows that $S_{c,i} = \alpha_i$. Hence, there is now a way to couple the flux in the cracks, Eq. [2.63], to the uptake of water by the peds, Eq. [2.61]. In the following, (§2.5), is proposed by Germann and Beven a derivation of a law $q^* = bS_c^a$, thus in fact identical to [2.63], and based on the assumption that the flow takes place under the form of thin liquid films on each faces of the cracks.

In their approach, the authors assume that the degree of sturation in the cracks is the same for all the layers participating in the flow. Thus, if L is the depth of the wetting front, the amount of water stored in the cracks above the water table is

$$C = S_c e_v L. \qquad [2.64]$$

The coupling between the two flows is provided by the following mass balance equation

$$\int_{t_p}^{t} I_c \, dt = \int_{t_p}^{t} I_l \, dt + C \qquad [2.65]$$

Assuming that the wetting front is located in the layer j, an iterative procedure is used that adjusts the value of S_c and update f_j according to

$$f_j(t) = f_j(t - \Delta t) + (\Delta t q^*/\Delta z) \qquad [2.66]$$

The height of the water table in the crack is controled by a mass balance equation. During a time step Δt, the variation ΔH of the height of the water table is given by

$$\Delta H = (I_c - Q - I_l)\Delta t / e_f \qquad [2.67]$$

where Q is the rate of loss to the drain and $e_f = e_t - (e_v S_c)$.

Remark that the structural porosity, e_v, and the crack width, w, of the layer in which is located the wetting front control the flow rate in the cracks. It is also assumed that for the layers below the water table, α is equal to 1. For the layers in the saturated zone, the flow of water from the cracks into the peds is assumed to occur through all the surface offered by the cracks. Thus, A_v is replaced by A. Identically, all the structural porosity is assumed occupied in the saturated zone. This is important since it controls the raise of the water table. It is also assumed that no vertical flow occurs between the peds, except if they are at field capacity, in which case the excedent of water is instantaneously transferred vertically down into the layer below.

In the model the rate of loss to the drains is assumed to be $Q = 8E/D^2$ where D is the drain spacing and E is

$$E = \int_0^{z_1} K_1(H_z - z)dz + \int_{z_1}^{z_2} K_2(H_z - z)dz + \ldots + \int_{z_{k-1}}^{z_k} K_k(H_z - z)dz \qquad [2.68]$$

In this equation, K_i is the effective conductivity of the ith layer above the drain; layer one being the layer just above the drain. Z_i refers to the height of the top of each layer above the drain and H_z is the height of the water table in the crack.

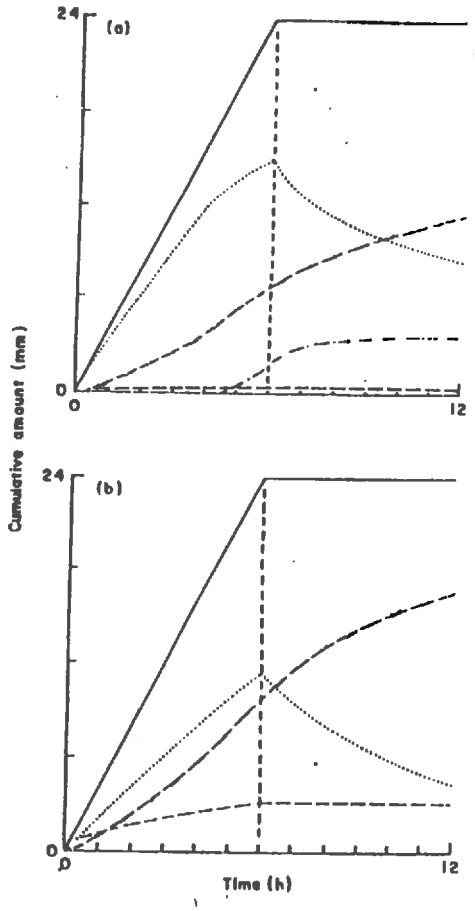

Fig. 2.5 Examples of model outputs. (a) wet initial situation, (b) dry initial situation. Cumulative input (——), drain outflow (–.–.–) (a) only, water storage in the cracks (....), ped water uptake from the surface (– – –) and laterally from the cracks (— — —) [after *Jarvis and Leeds–Harrison 1987*].

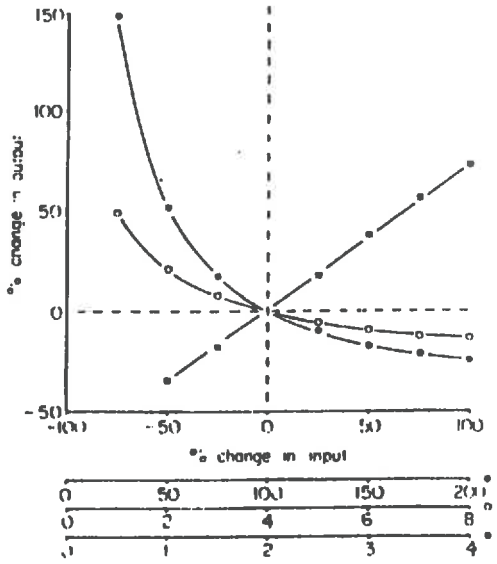

Fig. 2.6 Sensitivity of the amount of water stored at 0–25 cm to changes in crack spacing (black dots), rainfall intensity (open dots), tortuosity factor (n) (black squares) [after *Jarvis and Leeds–Harrison 1987*].

In their paper the authors present the results of a simulation involving a 4 mm/h rain lasting 6 h and applied to a dry (θ=.4) and wet (θ=.46) initial situation, respectively. The water content at field capacity was .47, the water table was assumed to be at 75 cm depth and the drains were at 50 cm depth with a 2m spacing. Other characteristics of interest are in table 2.1. The results clearly illustrate the importance of the horizontal absorption by the porous matrix from the cracks. The evolution in time of some variables of interest is plotted for two different initial water content, Fig. 2.5. The amount of water stored in the first 25 cm was chosen as variable of interest for the sensitivity analysis. Fig 2.6 shows the sensitivity of that variable to variation of n, the rainfall intensity and the crack spacing, respectively. The total structural porosity was assumed to remain the same during these calculations. Hence, the diminution of distance between the cracks resulted at the same time, in an increase of the exchange area per unit of soil volume and in a decrease of the width of the cracks which in addition led to a lower value of the flux in the cracks.

Parameter		Value	
		Dry soil	Wet soil
Soil water content	θ (m^3m^{-3})	0.40	0.46
SWC at field capacity	θ_f (m^3m^{-3})	0.47	0.47
Dynamic crack porosity	e_d (m^3m^{-3})	0.07	0.01
Stable crack porosity	e_s (m^3m^{-3})	0.02	0.02
Total crack porosity	e_t (m^3m^{-3})	0.09	0.03
Crack spacing	d (mm)	100	100
Crack width	w (mm)	3	1
Sorptivity	S (mm $h^{-1/2}$)	1.4	0.2
Effective hydraulic conductivity	K (mm h^{-1})	150	50

Tab. 2.1 Characteristics of the runs for a dry and wet initial situation, respectively.

2.4 APPLICATION TO EXPERIMENTS ANALYSIS.

As a matter of fact, except for the model lately proposed by Jarvis et al. (1987a,b), no general simulation model is actually available for infiltration into a cracked soil. We first analyse an application of the model presented by Jarvis and Leeds–Harrison (1987b) to an experiment conducted on a lysimeter. Many other field or laboratory experiments anterior to this work can be found in the literature. Since these works correspond to less general physical situations and problems, and also lead to less interesting conclusions, they will be reported more briefly.

Jarvis and Leeds–Harrison (1987b) applied their model to analyse a series of irrigations conducted on clay soil (Evesham clay). The soil profile was 1 m depth and drained at 50 cm depth with a drain spacing of 2m. Four neutron access tubes were used to obtain volumetric water content profiles. As the model also predicts the drainage, this one was recorded. The lysimeter on which the experiments were conducted is 2 by 2 m large and was 2–3 years old by the time of the experiment. Since the water table was always between 0.5 and 1 m depth and since the saturated conductivity of large soil samples continuously saturated was of about .4 mm/h, it was assumed that over small period of time the flux of water at the bottom of the lysimeter was negligible.

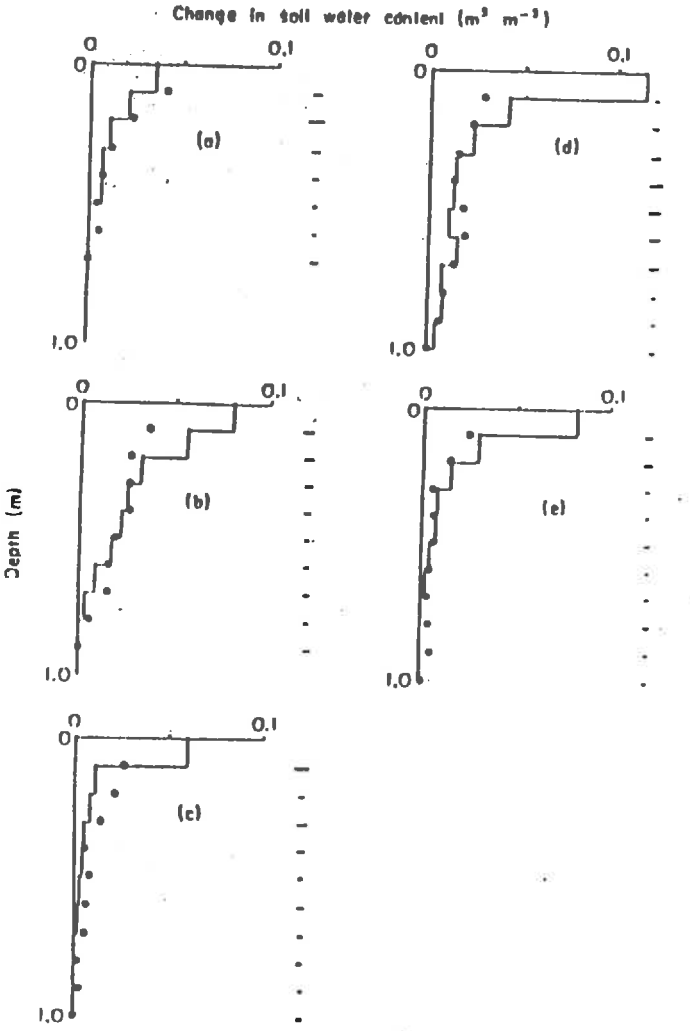

Fig. 2.7 Plots of observed (dots) and calculated (—) soil water recharge profiles [after *Jarvis and Leeds–Harrison 1987*]

Parameter	Value
No. layers	10
Layer thickness	0.1 m
Time interval	0.1 h
Drain depth	0.5 m
Drain spacing	2.0 m
Tortuosity factor	1.9

Tab. 2.2 Parameters with a fixed value for each irrigation [after *Jarvis and Leeds–Harrison 1987*]

Date	Irrigation amount (mm)	Irrigation intensity (mm h^{-1})	Initial depth to water table (mm)
10/04/85	23.2	4.1	500
06/08/85	24.4	3.5	999
18/09/85	9.4	2.8	999
22/10/85	28.2	3.9	750
30/10/85	14.8	4.5	750
12/12/85	28.8	7.2	500
17/03/86	23.4	3.9	500
21/03/86	17.5	3.6	500

Tab. 2.3 Irrigations intensities and amounts of water applied. [after *Jarvis and Leeds–Harrison 1987*]

Before each irrigation, the initial water content profile was obtained by means of the neutron probe. Water content profiles for comparison with model predictions were also obtained with the neutron probe.

Regarding the parameters needed by the model, all were measured but the tortuosity factor, n, which was fitted. A value of 1.9 gave the best fit for the rain event considered. The stable structural porosity, e_s, and the water content at field capacity, θ_f, were measured for ten distinct layers. The size of the peds was also given to the model for each layers. The conductivities required to evaluate the drainage rate were obtained from anterior experiments which yielded a linear relation between the flow in the drain and the hydraulic condcutivity. The sorptivity of the porous matrix was assumed to depend linearily on the water content. A value of 0 was assumed at field capacity. For a low initial water content, the sorptivity is estimated from infiltration rates measured with an infiltrometer allowing to supply water at negative pressure heads, thus excluding the role of possible macropores. For an initial water content of .29, a value of 3.2 mm/$\sqrt{h}$ was obtained for the sorptivity with a standard error of .3. Regarding the width of the cracks, it is assumed that a constant crack spacing holds all along the experiments. Thus, any variation in structural porosity is entirely transmited to the width of the cracks. This assumption was used to calculate the width of the cracks at the start of each experiment. An experiment with a green dye, (Powdered Lissamine) allowed to estimate, α, the percentage of crack surface involved in the flow. This experiment yielded a value of about 20% . Some other fixed parameters of the simulations are given Tab. 2.2 .

Initial water content profiles and water content distibutions after the irrigations were obtained with the neutron probe. Eight irrigations with various intensities and durations, Tab. 2.3, have been applied over a period of almost 1 year. A relatively broad range of initial sitiations correspond to these irrigations. However, the presence of the water table at a shallow depth prevent from obtaining very contrasted initial situations.

Calculated drainage hydrographs compare quite well with that measured. However, from the strict point of view of water flow modeling, it is much more enlightening to compare the water content profiles which reflect more precisely the capabilities of the model. Comparison on drainage hydrographs is not so intersting because too many processes are integrated and interact. Calculated and observed water content variations for the first 5 irrigations are plotted, Fig. 2.7. One can observe a quite close agreement, with some evidence of overestimation of the amount of water stored in the first layer and at the same time an underestimation of the recharge of deep layers. A characteristic of these irrigations is that the amount of water applied is always but one case larger than the amount of water stored in all the profile. Thus, it is difficult to judge of the quality of the transport model for the macropore phase. Remark that for the 3rd irrigation, corresponding to a relatively dry initial situation and deep water table (1 m), and where a small amount of water was applied, the simulated water content profile largely underestimates the penetration of the wetting front. Remark also that when large amounts of water are applied and whatever are the initial conditions, the flow will reach the water table and hence large errors which would appear on a deeper profile are less easy to detect or less apparent. A limiting case beeing an irrigation lasting long enough to completely recharge the profile, in which case any model gives good predictions regarding the final situation. Thus, disregarding the prediction of drainage, and in order to evaluate more completely the capacity of the model with respect to unsaturated water flow modeling, more contrasted initial situations should be used with irrigations doses and intensities allowing to evaluate in particular the part of the model dealing with the macropore continuum. In this regard, an hydrograph more direct than a drain output rate would be of a great help.

All the calculations and comparisons with field data reported hereafter have been conducted in very particular situations. Models used for these comaparisons were all very dependent upon characteristics of the flow measured at the experiment location. For example none of the hereafter presented works use an algorithm to calculate the runoff along the crack walls. All need in–situ measured physical quantities determining the boundary conditions at the extremities of the soil column. Thus, the models used in what follows to analyse experiments are quite for from the theoretical works of Edwards et al. (1979) and Nieber (1981).

Hoogmoed et al. (1980) have compared simulated and measured drainage rates for a 20 cm long column and very high intensity application rates. The model simulates vertical infiltration with the following boundary conditions:

$$\begin{cases} z = 0 & \begin{cases} -K.\partial H/\partial z = R & 0 \le T \le T(P) \\ 0 \le H \le w & T(P) \le T \le T(C) \\ H = w & T(C) \le T \end{cases} \\ z = 20 & -K.\partial H/\partial z = \text{cte} \end{cases} \qquad [2.69]$$

where, R is rainfall intensity, w a threshold value for surface ponding depth (.2cm), T(P) is ponding time ,T(C) is the time at which the flow starts in cracks when ponding reaches the threshold w, and H is the total pressure head. The model used is a reservoir one, and Darcy's law is applied to calculate the fluxes. In fact as the rainfall intensities used in the calculations are very high, respectively 22cm/day and 77 cm/day, the authors assume that as soon as the runoff starts all the length of the crack is used for horizontal absorption. The length of the soil column, 20 cm, is also one of the characteristics allowing this simplification. One can see that the physical system is quite simplified compared to the studies presented before. The horizontal infiltration in the pedons is modeled by:

$$\frac{\partial}{\partial x}\left[D(\theta)\frac{\partial H}{\partial x}\right] = \frac{\partial H}{\partial t} \qquad [2.70]$$

subject to boundary conditions:

$$\begin{cases} x=0 & \dfrac{\partial \theta}{\partial t} = 0 \quad T \ge T(C) \\ x \ge x_t & \dfrac{\partial \theta}{\partial t} = 0 \quad T \ge T(C) \end{cases} \qquad [2.71]$$

where x_t is the horizontal penetration of the wetting front at time t. When the flow rate into the cracks exceeds horizontal infiltrability, the drainage starts at the bottom of the soil column. Therefore, no water accumulation is allowed in the cracks. To account for the banding effect, a function S(T) describing the increase of the contact area with time is included in the model. This function has been estimated according to in–situ observations using different stained water application rates and different durations, Bouma and Dekker (1978). Model predictions are compared to measured drainage rates for two rainfall intensities, 22 and 77 cm/day and two initial moisture contents correspondingto a water pressure heads of .1 bar and 15. bars, respectively. Drainage rates are very high. Expressed in percentage of the application rate they are usually over 90% for the highest application rate and over 97% in the case of a initially wet soil. For the lowest application rate and for a initially dry soil, measured

and predicted values are respectively of 88% and 79%. Due to incertitudes in S(T), to all the simplifications made in the modeling, to the characteristics of the numerical solution employed, to the high application rates, to the length of the column, and to all the interactions between the different parameters it is difficult to say if the agreement between calculated and measured drainage rates is good or not, and what are the origins of the discrepancies.

Another experimental study has been reported by Bouma and Wosten (1984). The same soil was used. Two samples were carved out in–situ. A first estimation of the structural porosity used by the flow was given by measuring the amount of water necessary to instantaneously filled up the cracks. This volume is noted V_1. Then, a flux noted q_1 was monitored so as to just keep the cracks filled and the surface of the sample slightly flooded. This flux, which corresponds to the uptake of water by the peds and the subsoil, reaches a constant value very quickly. After this steady–state has been reached, gypsum is poured into the cracks and the sample removed to measure the infiltration rate of the subsoil. This flux is noted q_2. The block is then sectioned and the pattern of the cracks stained by the gypsum recorded. The area of the cracks used by the flow, A, and the length of these cracks, L, are obtained by image analysis. The authors found a good agreement between the volume V_1 and the quantity A×H, where H is the height of the sample. Equations [2.70] and [2.71] are used to simulate horizontal infiltration. Using L×H+S where S is the sample surface, an estimation of the total amount of water diffusing into the peds is obtained at the end of the experiment. The amount of water lost in the subsoil can be estimated according to q_2. So a comparison is possible between the amount of water given by the model and a good estimation of the amount of water really stored in the microporosity. Starting with a dry soil, 15 bars, a very good agreement is found by the authors.

The last experiment we want to report has been conducted by Bouma et al. (1982), in order to study the infiltration through and from worm holes. In this experiment, tensiometers are installed in the soil columns five centimeters below the infiltration surface. Two cup sizes were used. The experiment consist in filling up the worm hole and applying two centimeters of water at the surface. The redistribution is followed. The simulation model account for the infiltration through the surface but not for the horizontal infiltration from the wall of the hole. The amount of water flowing through the worm hole is accounted for assuming a given value for the flow rate. This value is obtained from experiments where infiltrations are monitored through single macropores. The main result of this study is that large cup tensiometers lead to erroneous values, as there is a high probability for they intercept preferential pathways where free water is available. A relatively good agreement is founded between calculated potentials and values given by small cup tensiometers.

One interesting and important problem when simulating water flow and solutes transfer in heterogeneous media is to obtain or assess the contact area, macropore–porous matrix, developed by the flow taking place in the macropore continuum. Until now this has only been done by measuring in–situ stained surfaces. Another possible way would be to determine the area of interest as solutions of an inverse problem. In this approach a numerical model, to be developed, would be used to simulate the drainage rates for different initial water contents, different rainfall intensities, and different durations. Then, an objective function to be minimized could be as for solutes transport the sum of the squares of the differences between observed and calculated outflow rates. In this case the minimization problem has only one unknown if we assume that the exchange surface per unit of soil volume is independent of the depth. Otherwise, the minimization problem corresponds to the estimation of a distributed parameter. This approach has obviously many advantages when compared to the measurement techniques usually employed. However, some

difficulties exist which must not be ignored. First, from an experimental point of view, it will be difficult to obtain a uniform water content distribution inside the soil samples. This problem is already present in all the experimental studies presented before. Another problem would be to obtain in–situ hydrographs. From a theoretical point of view, the uniqueness of the solution of the inverse problem has to be studied. The "breakthrough" curves are certainly not sufficient alone if we assume a distributed parameter. Another problem arising is the influence of errors in soil characteristics and numerical calculations. The great advantage of the inverse problem approach is that it allows to numerically study the influence of errors in different parameters as for example, non uniform initial water content, sensibility to hydraulic characteristics, etc... Therefore, best experimental conditions, water content, rainfall intensity, duration, etc.., can be selected. Experimental results of **Bouma and Wosten (1984)** are encouraging in this regard. Let us remark that the knowledge of this surface would be very helpful for solutes transport simulation in such media.

Many modeling approaches have been developed for saturated water transfer in media where two porosity systems can be shown up. Probably most of these approaches could be used for unsaturated water transfer modeling. In particular it should be possible to adapt the different double porosity models developed by **Duguid and Lee (1974)**, **Huyakorn (1983a)** and **Narasimhan (1982a,b,c,d)**. The main difficulty as for the precedent inverse problem is certainly the derivation of an equation modeling the flow through the macroporosity. A possibility would be to use a kinematic wave approach such that developed by **Germann and Beven** (see §2.5). Once this done, the different geometries and coupling approaches could be readily applied.

Based on the *double porosity concept* a new approach using a kinematic waves equation for the flow in the macroporosity and a simple coupling term between the two porosity systems has been proposed to model infiltration in a heterogeneous profile. This approach is developed in the following paragraph.

2.5 KINEMATIC WAVE APPROACH

A Double Porosity Model.

In a set of papers, **German and Beven (1981a,b)**, **Beven and Germann (1981)** have presented various laboratory experiments carried out on large undisturbed soil cores and demonstrating the effects of different macropore structures on water flow through a soil profile. At the same time they developed a double porosity model in which water flow through the macroporosity is modeled by a kinematic wave equation. The model assumes that two interacting continuums corresponding respectively to the macroporosity and the microporosity are superposed. Richards' equation is classically used to model the flow in the microporosity continuum:

$$C_{mi} \frac{\partial \varphi_{mi}}{\partial t} = \frac{\partial}{\partial z} \left(K(\theta_{mi}) \frac{\partial \varphi_{mi}}{\partial z} \right) + S \qquad [2.72]$$

where φ is the total water potential, θ is the water content, K is the conductivity, C is the capillary capacity, z is the depth, t is the time and S is the coupling term with the macroporosity flow. The subscript $_{mi}$ stands for *microporosity*. Let us immediately remark that the flow in the microporosity is modeled in the vertical direction, which means that the "constraints" are applied at the surface and not at the interface with the macroporosity. This approach is therefore quite different as compared to the models presented for saturated flow or to the model of **Jarvis and Leeds–Harrison (1987a)**. For the flow in the macropore continuum a continuity equation can be written:

$$\frac{\partial \theta_{ma}}{\partial t} = -\frac{\partial}{\partial z}(Q_{ma}) - S \qquad [2.73]$$

where θ_{ma} is the water content in the macroporosity and Q_{ma} the volume flux density (cm/s) in the macropore. As for equation [2.72] the coupling term S appears in the right hand side but with a minus sign. Two relations are needed now to complete the model. First an expression linking θ_{ma} and Q_{ma}, and second a physically acceptable formulation for S.

Beven and Germann (1981) assume that the flux in the macropore continuum is related to the thickness of the film of water. An extension of the cubic law for the cracks and an extension of Poiseuille law for cylindrical pores are used:

$$q_p = \frac{\pi \rho g}{2\mu}\left(\frac{R^4}{4} + \frac{3}{4}r^4 - r^2R^2 + r^4 \ln R - r^4 \ln r\right) \qquad [2.74]$$

$$q_c = \frac{4}{3} L \frac{\rho g}{2\mu} d^3 \qquad [2.75]$$

where in the case of the pore (index p), R is the radius of the pore, r the thickness of the water film, μ the dynamic viscosity, ρ the density of water; and in the case of the crack (index c), L is the length of the crack, and d the thickness of the film of water. If D is the crack aperture the classical formula is founded for $d = D/2$. The authors assume that the pore size distribution is made up of a set of N class sizes of circular pores containing each n_i pores of average radius R_i, and M class sizes of cracks containing each m_j cracks of average width D_j and length L_j. For a macropore continuum as described above, we have the two following expressions giving the flux and the water content:

$$Q = \frac{1}{A}\left[\sum_{i=1}^{N}\sum_{j=1}^{n_i} q_p + \sum_{i=1}^{M}\sum_{j=1}^{m_i} q_c\right] \qquad [2.76]$$

$$\theta_{ma} = \frac{1}{A}\left[\sum_{i=1}^{N}\sum_{j=1}^{n_i} q_p\, \pi(R_j - r_j) + \sum_{i=1}^{M}\sum_{j=1}^{m_i} 2L_j d_j\right] \qquad [2.77]$$

Different theoretical systems made up of parallel cracks and pores with different width and radius were used in calculations carried out with Eq. [2.76] and [2.77]. The results suggested that a power function can be used to relate flux and water content in the macropore continuum. **Beven and Germann (1981)** have proposed the following expression:

$$Q = a(\theta_{ma})^b \qquad [2.78]$$

If Q_{sat} is the fully saturated flow predicted from [2.76], and K_{ma} the saturated conductivity, then the flux in the macropore, Q_{ma}, is obtained by applying the following scaling relation:

$$Q_{ma} = K_{ma}\frac{Q}{Q_{sat}} \qquad [2.79]$$

The continuity equation [2.73] can be written:

$$\frac{\partial \theta_{ma}}{\partial Q_{ma}} \frac{\partial Q_{ma}}{\partial t} = - \frac{\partial Q_{ma}}{\partial z} - S \qquad [2.80]$$

and we have:

$$\frac{\partial Q_{ma}}{\partial \theta_{ma}} = b[K_{ma} \frac{a}{Q_{sat}}]^{1/b} Q_{ma}^{1-1/b} = c \qquad [2.81]$$

Thus the equation for the flow in the macropore continuum takes the following form:

$$\frac{\partial Q_{ma}}{\partial t} = -c[\frac{\partial Q_{ma}}{\partial z} + S] \qquad [2.82]$$

The coupling term S is defined by:

$$S = - K(\theta_{mi}) \frac{\Delta \Psi}{\Delta \chi} \qquad [2.83]$$

where $\Delta\Psi$ is the difference of potential between the two phases, and $\Delta\chi$ is an average distance between two distinct macropores. Equation [2.82] is a non–linear hyperbolic equation requiring a careful control of integration. It is in essence very different from the usual non–linear parabolic Richards' equation.

Obviously in this formulation the term $\Delta\chi$ is very ill defined. Identically, the signification of $K(\theta_{mi})$ is not consistent as very large horizontal water content gradients can appear at a given depth in the microporosity continuum during an infiltration. In fact, even if it is not said, this approach assumes that in response to a solicitation, at the surface or due to S, an immediate pressure head equilibrium is obtained in the microporosity. Obviously, this assumption is violated as it can be shown with numerical calculations or experimentally. It is highly probable that this formulation of the interphase exhange process will give a very bad estimation of what is the real amount of water diffusing in the microporosity. This approach can be related to that called "*Quasi –Steady flow model*" by Huyakorn et al. (1983a) for saturated flows. The parameter $\Delta\chi$ is certainly a function of z and play the role of a matching factor in this model since it controls the gradient between the two phases.

In the algorithm proposed by Beven and Germann (1981), the flow starts in the macropores as soon as the rain intensity exceeds the soil infiltrability. The boundary condition at the surface for the kinematic equation is then the flux corresponding to this difference. The model controls the level of the water table in the macropore system, and S is hence calculated according to:

$$\begin{aligned} &\Delta\Psi/\Delta\chi = 0 && , \theta_{ma} = 0 \ , \ \theta_{mi} \le \theta_{mi,sat} \\ &\Delta\Psi/\Delta\chi = (\Psi(\theta_{mi})-0)/\Delta\chi && , 0 \le \theta_{ma} \le \theta_{ma,sat} \\ &\Delta\Psi/\Delta\chi = (\Psi(\theta_{mi})-d_w)/\Delta\chi \ , && \theta_{ma} = \theta_{ma,sat} \end{aligned} \qquad [2.84]$$

where d_w is the depth below the water table. In their calculations Beven and Germann (1981) used a $\Delta\chi$ of 10.4 cm, for the simulation of a rain lasting 266 s. This value for $\Delta\chi$ can be compared to the various experimental results of Bouma et al. presented before and to the numerical simulations of Edwards et al. (1979) and Nieber (1981). In all these studies the water front penetration from a macropore was never greater than two or three centimeters during the period the flow was effectively

taking place in the macroporosity. This means that for all the duration of the rain, the term S is probably largely underestimated. Of course water redistribution in the microporosity is not accounted for in the model of Beven and Germann (1981). The consequences on the water distribution in the profile are clear. Different runs were made in which the hydrodynamic characteristics of the soil varied, but no study of the sensibility of the results to $\Delta\chi$ variations was presented by the authors.

As a matter of fact, $\Delta\chi$ which is presented as a measure of the average distance between the macropores, should be rather considered as the distance between the wetting front in the microporosity and the macropore, for the term S has a more physical signification. This means that $\Delta\chi$ would not only be a function of z but also a function of the time. We are there very close to a Green–Ampt model. In fact unless making assumptions on the geometry of the media as done by Huyakorn et al. (1983a) in the case of saturated media transfers there is no way to relate $\Delta\chi$ to the time. Assuming a geometry could lead to an estimation of $\Delta\chi(t)$ via a resolution of Richards' equation.

To close this paragraph, let us underline some differences existing between the double porosity models developed for saturated flows in the engineering and petroleum literature, and this double porosity approach. In models such those of Narasimhan, Huyakorn,... the *"constraints"* applied at the domain boundaries are transmitted to the micropore phase through the macropore continuum and the flow equation for the microporosity continuum is only solved at a local level, essentially in order to furnish the fluxes between the two phases. This is possible because hydraulic conductivities in both phases are expected to be very different and the physical connections between porous blocks negligible. The roles played by the two continuums are completely dissociated. One plays the role of a vector and the other the role of a storage. For physical situations where one cannot ignore the microporosity flow induced by external constraints, the modeling problem is more complicated. Both flow phases must be superposed over all the domain. The problem is then to define a coupling term. It clearly appears an inconsistency between a mono–dimensional approach to microporosity flow and the multi–dimensionality of the physical process. It seems obvious that if we stand at a one–dimensional simulation level for the microporosity flow, it will be difficult to introduce a coupling approach related to geometrical considerations, and simulating necessarily multidimensional water diffusion from the cracks into the porous matrix. This leads to the question: is it possible to apply a fully dissociated approach as those defined before, that is to say, can we release or reasonably ignore the microporosity flow induced by external constraints? For example in the case of a heterogeneous profile, this means: can we consider that no vertical flow occurs in the microporosity? As a matter of fact, in structured soils for example, it is quite impossible to ignore the connections existing between the different porous blocks, and allowing the microporosity flow to occur throughout the domain. In addition the distribution of pore radius probably do not allow to distinguish between two porosity domains playing very different roles. The problem of the influence of the boundary conditions applied at the surface of the soil has not been considered either. It is highly probable that for this kind of porous media the constraints applied at the boundaries, in addition to the intrinsic charcateristics of the media, largely determine the type of flow. However, physical situations exist, crusted surface, clay soils with a very low conductivity, strongly defined structure, compacted profiles, where necessary hypothesis to the application of a model with two very well defined phases are quite well approximated. In these cases, coupling terms as those based on geometrical considerations, for example average shape of the porous blocks, can be defined. For physical situations where this is not the case, the right model to apply is probably strongly dependent on parameters such that, boundary conditions (rain intensity, duration) or initial conditions.

A Kinematic Wave Model with a Sink Term.

A simplified approach to water flow modeling in structured media is to ignore the flow in the microporosity and to define the sink term S in equation [2.82] as a function of the water content variation in the macropore continuum only. This has been developed in a set of papers by Germann (1985), Germann and Beven (1985), and Beven and Germann (1985). In this case equation [2.48] becomes:

$$\frac{\partial q}{\partial t} + c\frac{\partial q}{\partial z} + cr\theta = 0 \qquad [2.85]$$

where q is the volume flux density (m/s), c the kinematic wave velocity (m/s), θ the water content in the macropore continuum, and r the term describing the losses in the matrix (1/s). Equation [2.78] is assumed to hold between θ and q. Thus the kinematic wave velocity c defined by $c = dq/d\theta$ can also be written:

$$c = dq/d\theta = ab^{1/a}\, q^{(a-1)/a} = ab\theta^{(a-1)} \qquad [2.86]$$

The sorbance function is defined, Germann and Beven (1985), by:

$$r = -\frac{1}{\theta(t)}\frac{d\theta}{dt} = -1/(aq)\ dq/dt \qquad [2.87]$$

This simple formulation of the problem allows to obtain analytical solutions from the theory of characteristics. As a solution of the kinematic wave equation can be readily obtained for a pulse of given duration and constant intensity, the main idea is to approximate the input signal, usually the rain intensity, as series of constant intensity pulses. Then a procedure to handle the interferences which can occur between several pulses allows to calculate the behaviour of any input signal. Let us first derive the solution for a square pulse when r=0.

Case without matrix absorption

This is the case of a quasi–saturated matrix, and hence the sink term r is equal to 0. The conditions at the surface are defined by:

$$\begin{aligned} q &= q_s \quad t \in [0,t_s] \\ q &= 0 \quad t \geq t_s \end{aligned} \qquad [2.88]$$

We note $z_w(t)$ the location of the wetting front defined by a discontinuity in the water content profile in the macroporosity. The water content is constant and equal to θ_w behind the wetting front and equal to 0 in front of it. So the water content profile is defined by:

$$\begin{aligned} \theta(z,t) &= \theta_w \quad 0 \leq z \leq z_w(t)\ ;\ t \in [0,t_s] \\ \theta(z,t) &= 0 \quad z \geq z_w(t) \quad ;\ t \in [0,t_s] \end{aligned} \qquad [2.89]$$

If we note c_w the velocity of the wetting front, which is constant since r=0, we have $z_w(t) = c_w t$. The velocity c_w is defined by: $c_w = dq/d\theta$ which is equal to q_s/θ_w. Using [2.78] we obtain the following expression for the velocity of the wetting front:

$$c_w = q_s^{1-1/a}\, b^{1/a} \qquad [2.90]$$

When the input stops ($t \geq t_s$), the water content at the surface drops to zero and a draining front develops. We note c_d its velocity, and $z_d(t)$ its position. These two quantities are related by:

$$z_d(t) = c_d(t-t_s) \qquad [2.91]$$

At the level of the draining front we have $q=q_s=b\theta_w^a$. For any value of θ between θ_w and 0 the corresponding depth is given by: $z(w) = c(w)(t-t_s)$, where $c(w)= dq/dw$. But we have also: $c(w) = z(w)/(t-t_s)$ and $c(w) = dq/dw = a.b.\theta^{a-1}$. Thus combining these two expressions the following equation is obtained which relies the water content to the depth:

$$\theta = z^{1/(a-1)}\, [ab(t-t_s)]^{1/(1-a)} \qquad [2.92]$$

Combining [2.91] and [2.92] we get the water content at the draining front:

$$\theta = c_d^{1/(a-1)} [a.b]^{1/(1-a)} \qquad [2.93]$$

But as at the draining front we have $q_s = b.\theta_w^a$ we obtain :

$$q_s = b c_d^{a/(a-1)} [a.b]^{a/(1-a)} \qquad [2.94]$$

from which comes the speed of the draining front:

$$c_d = q_s^{1-1/a}\, b^{1/a}\, a = a c_w \qquad [2.95]$$

As the parameter **a** is greater than 1, we can see from [2.95] that the draining front moves faster than the wetting front. The interception time is easily obtained from the equations of the movement:

$$t_i = a t_s/(a-1) \qquad [2.96]$$

and the depth at which interception occurs is easily derived:

$$z_i = \frac{a}{a-1}\, q_s^{(a-1)/a}\, b^{1/a}\, t_s \qquad [2.97]$$

After the draining front overlapped the wetting front, a peak with decreasing velocity and water content moves through the domain. The characteristics of its movement are determined introducing the mass balance expression:

$$\int_0^{z_p(t)} \theta(z,t)\, dz = q_s t_s \qquad [2.98]$$

As expression [2.92] giving $\theta(z,t)$ still holds, integrating by parts [2.98] gives:

$$z_p(t) = [q_s t_s \frac{a}{a-1}]^{(a-1)/a} [ab(t-t_s)]^{1/a} \quad [2.99]$$

The water content at the peak and its velocity are then readily obtained:

$$\theta_p(t) = [q_s t_s]^{1/a} [(a-1)(t-t_s)b]^{-1/a} \quad [2.100]$$

$$c_p(t) = (t-t_s)^{(1/a-1)} ab^{1/a} [q_s t_s/(a-1)]^{(1-1/a)} \quad [2.101]$$

Case with matrix absorption. Infiltration of a square pulse.

Now, if we consider the case with absorption by the porous matrix, it is obvious that the wave velocity and the water content profile will not be constant, but that we have a water content profile and a flux distribution both decreasing with depth between the soil surface and the wetting front. For a square pulse, the flux profile is obtained by combining [2.84], [2.78], [2.87], and integrating with respect to the following boundary and initial conditions:

$$\begin{array}{lll} t < 0 & 0 \le z \le \infty & q(z,t) = 0 \\ 0 \le t \le t_s & & q(0,t) = q_s \\ t_s < t & & q(0,t) = 0 \end{array} \quad [2.102]$$

The flux profile obtained behind the front for the first stage, ($t \le t_s$), is:

$$q(z) = q_s[1-rz(a-1)/c_s]^{a/(a-1)} \quad [2.103]$$

where $c_s = ab^{1/a}.q_s^{(a-1)/a}$.

It exists a depth z^* under which no macropore flow will ever occur due to complete sorbance of the input by the soil matrix. This depth is, according to [2.103],:

$$z^* = c_s/[r(a-1)] \quad [2.104]$$

Thus, the flux profile can be written:

$$q(z) = q_s(1-z/z^*)^{a/(a-1)} \quad [2.105]$$

Using the relation $q=b\theta^a$ and setting $q_s=b\theta_s^a$ the water content profile is obtained from [2.105]:

$$\theta(z) = \theta_s(1-z/z^*)^{1/(a-1)} \quad [2.106]$$

The front velocity is given by $c_w=q/\theta_w$. Using [2.105] and [2.106] the following expression is derived :

$$c_w(z) = c_s[1-z_w/z^*]/a = dz_w/dt \qquad [2.107]$$

Hence, integrating [2.107] subject to $z_w(0)=0$, we obtain the equation of the movement for the wetting front:

$$z_w(t) = z^*[1-\exp(-tr(a-1)/a] \qquad [2.108]$$

During the second stage, as for the case without matrix absorption, the water content at the surface drops to zero as soon as the input stops and a draining front moves through the domain. The velocity of this front is noted c_d and is given by:

$$c_d = c_s(1-z/z^*) = dz_d/dt \qquad [2.109]$$

Note that here, as for the case without matrix absorption, c_w and c_d are also related by: $c_d = a\ c_w$. Then proceeding as for the wetting front, the equation of the movement is readily derived:

$$z_d(t) = z^*[1-\exp(-(t-t_s)r(a-1))] \qquad [2.110]$$

The time at which the two fronts overlap is given by [2.96] since the velocities verify the same relation as in the case without absorption. The depth corresponding to this time is derived combining [2.96] and one of the movement equations. We obtain:

$$z_i = z^*[1-\exp(-t_s r)] \qquad [2.111]$$

The flux profile behind the draining front is obtained combining equations, [2.110] and [2.69]. The final expression is:

$$q(z,t) = \left[zr(a-1)/[b^{1/a}\ a\ \exp(-(t-t_s)r(a-1))]\right]^{a/(a-1)} \qquad [2.112]$$

Case with matrix absorption. Movement of two square pulses.

Let us consider now the following boundary conditions:

$$\begin{array}{llll} t<0 & q(0,t)=0; & t_1<t\leq t_s & q(0,t)=q_2 \\ t<t1 & q(0,t)=q_1; & t_s<t & q(0,t)=0 \end{array} \qquad [2.113]$$

where q_2 is greater than q_1. The second wave starts to move with a speed:

$$c_j(0,t_1) = [q_2-q_1]/[\theta(q_2)-\theta(q_1)] \qquad [2.114]$$

The velocity profile is obtained combining [2.114], [2.103] and [2.78].

$$c_j(z) = [b^{1/a}[(q_2{}^{(a-1)/a} - zp)^{a/(a-1)} - (q_1{}^{(a-1)/a} - zp)^{a/(a-1)}]]$$

$$/[(q_2{}^{(a-1)/a} - zp)^{1/(a-1)} - (q_1{}^{(a-1)/a} - zp)^{1/(a-1)}]] \qquad [2.114]$$

with $p = r(a-1)/(ab^{1/a})$. An expression for $c_j(t)$ is obtained combining [2.114] and

[2.87].

$$c_j(t) = c_j(0,t_1)\exp(-r(a-1)(t-t_1)) \qquad [2.116]$$

Because $c_j(t) = dz_j/dt$, the characteristic of the second wave is obtained upon integrating [2.116] with respect to time,

$$z_j(t) = c_j(0,t_1)/[r(a-1)](1-\exp(-r(a-1)(t-t_1)) \qquad [2.117]$$

As the second wave moves faster than the first one, interception will occur at a time $t_{1,2}$ and depth $z_{1,2}$. Germann and Beven have not found a general analytical procedure to solve either for time or depth of interception. Numerical procedures have to be applied. In the case of a two step input with q_2 lower than q_1, the second wave follows a draining front and equations like those derived for the second stage of the single square pulse must be obtained.

For the case of a monotonically increasing input rate at the surface, this one is decomposed in a series of square pulses which intensities are given by:

$$q_k = 1/\Delta t \int_{(k-1)\Delta t}^{k\Delta t} q_s(t)\,dt \quad k = 1,N \qquad [2.118]$$

where q_s is defined by:

$$q_s(t) = q^* - (S\sqrt{t} + A) \qquad [2.119]$$

S is the sorptivity, A is the final infiltration rate, and q* is the rain intensity. The characteristics of the different jumps initiated by the increasing intensity pulses at the surface are calculated according to equations [2.114] to [2.117].

As it can be seen, the derivation of the solution is not easy in a general case with time dependent input rates. In addition, the theoretical calculations of Germann and Beven are restricted to monotonically increasing input rates. Furthermore, in order to derive their analytical solutions a simple expression for the absorption rate by the matrix has been chosen. A numerical solution of this convection equation would allow to handle any input rate function, and to use in the model a great variety of adsorption terms. A sink term calculated from a solution of Richards' equation would be possible.

Parameters Estimation

In this approach, as for the double porosity model developed by Germann and Beven (1981) (cf.§ 2.4 "*A double porosity model*") parameters *a* and *b* are unknown, and *r* as well as $\Delta\chi$ in the former double porosity model are fitting parameters. It is experimentally difficult to obtain a good estimation of *a* and *b*. Ehlers (1975), Germann and Beven (1981), Smettem and Collis–George(1985a) report some experiments and data analysis trying to provide estimations for these two parameters. According to the different authors, *a* is found between 2 and 4.5. Therefore, the only remaining way to asses *a* and *b* is to use a non–linear estimation method. Two studies are reported, Germann and Beven (1985) and Germann (1985).

Germann (1985) was working with a saturated block of polyester consolidated sand. Hence, *r* was equal to zero and *a* and *b* only had to be estimated. Experiments consisted in several runs with different sprinkling intensities and durations.

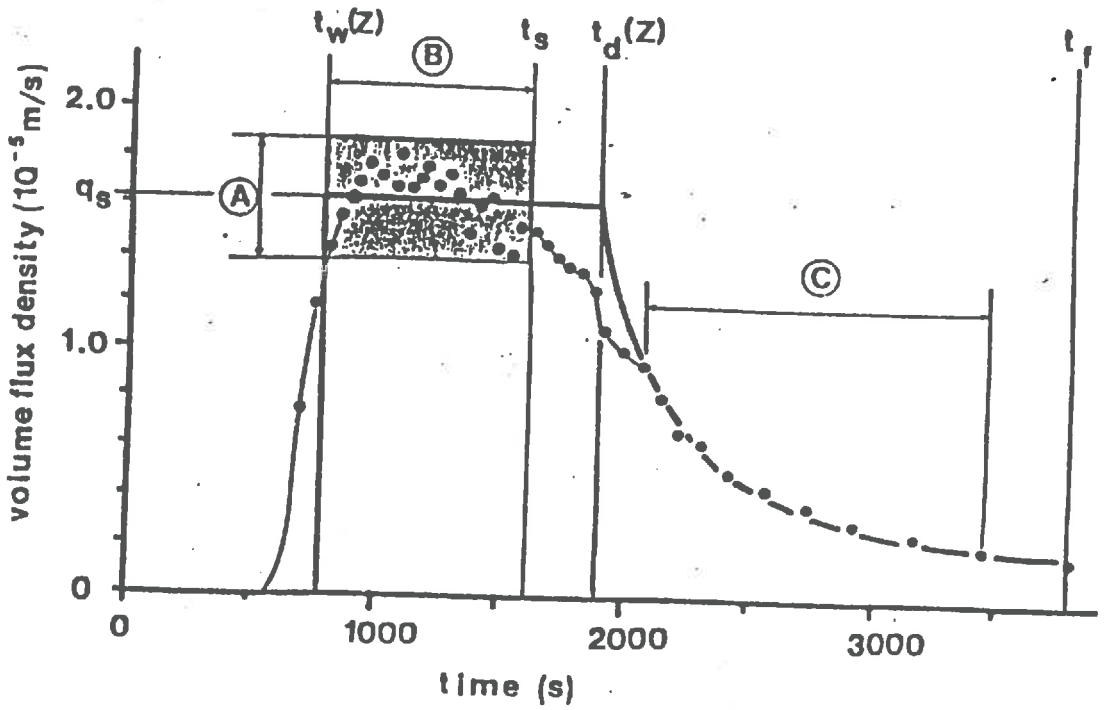

Fig. 2.8 Observed (dots) and modeled hydrograph (solid line). The time of arrival of the wetting and drainage fronts are noted t_w and t_d, t_s indicates the duration of the square pulse input, q_s is the sprinkling intensity [after *Germann 1985*].

Parameter	1	2	3	4
t_s (s)	1340	1800	4087	1621
q_s (m/s)	$5.32\ 10^{-5}$	$1.96\ 10^{-5}$	$3.92\ 10^{-6}$	$1.62\ 10^{-5}$
$t_w(z)$ (s)	580	710	1790	780
$t_d(z)$ (s)	1494	2035	4641	1895
t_f (s)	4185	4861	7140	3813
a	3.758	3.016	3.233	2.848
b (m/s)	2.679	1.2856	5.244	0.754

Tab. 2.4 Data and fitted parameters for four infiltration–sprinkling experiments [after *Germann 1985*].

Parameters a and b were adjusted so as calculated and observed drainage rates fit as closely as possible. In that case the solution for the case without matrix absorption is used. The different values obtained for a and b are reported Tab. 2.4, with runs characteristics. An example of observed and fitted outflow curves is given Fig. 2.8. Several remarks can be made. First, it appears that a and b are strongly dependent on "external constraints" for a given and fixed heterogeneity pattern. This means for example that no unique value of a and b can be found and used for a same experimental plot with different input rates or initial conditions. This seems to be somewhat in contradiction with the assumption implicitely made by **Jarvis and Leeds–Harrison (1987)**. In their model a and b are taken constant whatever are the initial conditions and the input rates. Hence, it is for now difficult to say if a and b can be considered as intrinsic properties of the medium. The sensibility to variations in a–values has been tested for the cumulative drainage. Variations of approximately 10% are recorded for a ranging from 2 to 4 which indicates a relative insensitivity of the model to a. However, the simulated cumulative drainage is always but one case underestimated compared to the measured one. Remark also, Fig. 2.5, that the physical dispersion is not accounted for by the model and that the areas under the simulated and recorded outflow curves are slightly different.

In the other experiment, **Germann and Beven (1985)**, a .1×.3×.9 m undisturbed unsaturated soil sample was used. The sprinkling rate was 2.92 10^{-5} m/s and was lasting 5040 s. The drainage hydrograph was recorded by continuously weighting the output. As the infiltration occurs also through the surface of the block the parameters A and S (equation [2.119]) must be estimated together with a,b and r. Observed and modeled drainage hydrographs obtained by **Germann and Beven (1985)** are given Fig. 2.9. As it can be seen the agreement is fairly good. However, one can remark that the long tail of the observed hydrograph is not restituted by the model and that the drainage peak is not as closely approached as in the precedent case. **Germann and Beven (1985)**, explain the discrepancies observed on the tail of the hydrograph by the fact that no dispersion is included in the model. One can remark that for the precedent fitting case the tail was perfectly reproduced. Therefore, one can think that the lack of dispersion is perhaps not the only explanation to be put forward.

The authors observed that a uniform macropore system with unique flow characteristics was implicitly assumed in their model. In fact the multitude of the different possible pathways is not accounted for. A more realistic approach including this notion needed to be developed. A distributed channeling flow model has been proposed by **Beven and Germann (1985)**. This approach will be presented later. Notice also that due to interaction between vertical infiltration from the surface of the soil and horizontal diffusion from the macropore, the parameters S and A fitted to determine the amount of water entering the macropore continuum are not the sorptivity and saturated hydraulic conductivity, respectively.

A sensitivity analysis has been done by Germann and Beven (1985). The sensitivity to variations in a,b and r values of, the time of the initial breakthrough, the time of the maximum discharge rate (peak), and the volume flux density at the peak, have been estimated. It appears that in the case studied, the three characteristic of the flow retained for sensitivity analysis are very little sensitive to variations of r. The first two are absolutely not sensitive to r and the last one has a variation of 4% when r is multiplied by 3. The characterictics of the flow are more sensitive to parameters a and b, the largest sensitivity being obtained for variations of a. Table 2.5 taken from (Germann and Beven 1985) presents the different values obtained.

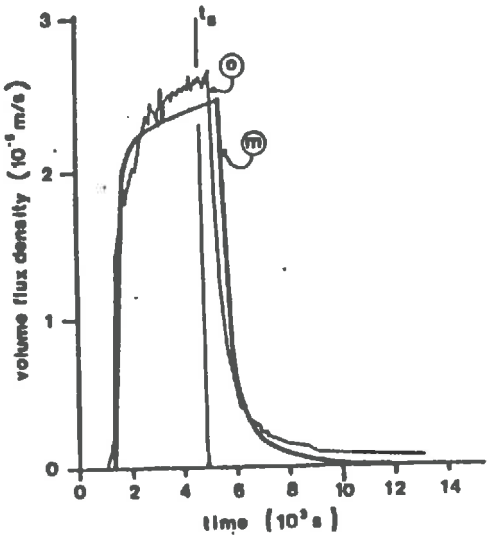

Fig. 2.9 Calculated (m) and observed (o) hydrographs. The end of the square pulse input is noted t_s. The input rate is 2.92 10^{-5} m/s. [after *Germann and Beven 1985*]

a	b, m/s	r, 1/S	Time of Hydrograph Beginning, s	Time to Peak, s	Relative Volume Flux Density at Peak	Comment
2.20	0.06	4.0×10^{-3}	1396	5513	1.0	Table 1
1.10	0.06	4.0×10^{-3}	98	5067	1.04	sensitivity of *a*
1.65			513	5233	1.03	
2.75			2607	5819	0.956	
3.30			4031	6070	0.907	
2.20	0.03	4.0×10^{-3}	1827	5691	0.985	sensitivity of *b*
	0.045		1559	5580	0.994	
	0.075		1284	5467	1.003	
	0.090		1197	5433	1.007	
2.20	0.06	2.0×10^{-3}	1388	5511	1.021	sensitivity of *r*
		3.0×10^{-3}	1392	5512	1.011	
		5.0×10^{-3}	1400	5515	0.989	
		6.0×10^{-3}	1404	5516	0.979	

Table 2.5 Results of the sensitivity analysis.

A Distributed Channeling Flow Model Based on the Kinematic Wave Approach.

In the previous approaches a unique relation was assumed to hold between the flux and the water content in the macropore system: $q = b\, w^a$. In the following approach the flow is assumed to take place through a multitude of pathways with different geometric characteristics. In each of them the previous power law is assumed to hold with a different value for *b*. The objective is then to estimate the distribution of the parameter *b*. One more time this is done by comparing observed and calculated drainage hydrographs. Before describing the algorithm and the results obtained by Beven and Germann (1985), let us derive the relations we need. The flow equation is still

$$\frac{\partial q}{\partial t} + c\frac{\partial q}{\partial z} = cs \qquad [2.120]$$

where, $c=dq/d\theta$, and s is the term describing the losses in the matrix. In this case s is defined by:

$$s = -r\theta \qquad [2.121]$$

Notice that the sink term depends linearly on the water content in the macropore continuum. It has been shown, [2.104], [2.105], [2.106], that the water content at the wetting front was:

$$\theta_w = \theta^*[1-r(a-1)z/c^*]^{1/(a-1)} \qquad [2.122]$$

where θ^* is the macropore water content at the surface ($\theta^*=(q^*/b)^{1/a}$), $c^*=ab\theta^{*(a-1)}$, and q^* in the input rate into the macropore continuum. Integrating the wetting front movement equation: $dz_w/dt = b\theta_w^{a-1}$, gives:

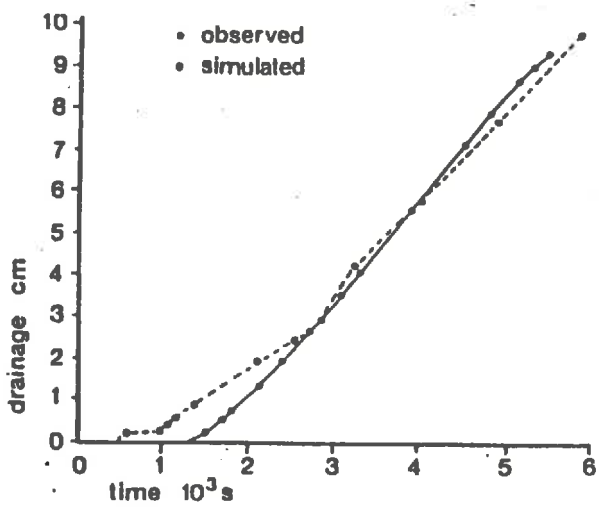

Fig. 2.10 Observed drainage rate and best fit as calculated with the channeling flow model. [after *Beven and Germann 1985*]

$$z_w(t) = \frac{c^*}{r(a-1)}[1 - \exp(\frac{-r(a-1)t}{a})] \qquad [2.123]$$

In order to estimate the distribution of the values of b the following algorithm was set up by the authors. The hypothesis are:

1) that the same input rate is applied to all the pores.
2) the values of a and r are the same for all the paths. The value a=2 was chosen.

The idea of **Beven and Germann** is to calculate the coefficients b_i corresponding to the times t_i of the observed drainage hydrograph. The values of b_i are calculated inverting equation [2.123]. The following expression is obtained:

$$b_i = q^{*(1-a)}[dr(\frac{a-1}{a})/(1-\exp(-r(\frac{a-1}{a})t_i)]^a \qquad [2.124]$$

where, d is the length of the soil column, and t_i the i^{th} time sampling point on the breakthrough curve. The probability weighting $p(b_i)$ is calculated by equating the observed incremental drainage flux between two consecutive times to the calculated one given by:

$$q(b_i) = q^*(1-r(a-1)d/c^*)^{a/(a-1)} \qquad [2.125]$$

The value of r is adjusted until one obtains:

$$\sum_i p(b_i) = 1 \qquad [2.126]$$

One can remark that this way to calculate b_i implicitly assumes that several wetting fronts corresponding to different pathways are travelling through the medium, and that an increment in the output flux is due to the arrival of a new front at the bottom of the soil column. Using formula [2.123] to calculate b_i implicitly assumes that the beginning of the breakthrough for a pathways occurs at the level of the front and consequently that the dispersion will be only a consequence of the spreading of b. Thus it is evident that in this approach the part of the drainage hydrograph after the peak can't be used to fit b. The part of the hydrograph up to the peak only can be used

For values of a varying between 1.5 and 2.5 the distribution function for b is shifted by one to two powers of ten towards higher values. Comparing adjusted and observed drainage hydrographs (Fig. 2.10) a large underestimation of the beginning breakthrough time appears. In the previous fitting procedure with a model employing a unique value for b it was the inverse; the early part of the breakthrough curve was not simulated correctly. In the present case, the curve seems to be quite correctly reproduced for the larger times, which may indicate that the parameter r describing the losses in the matrix has a correct value. However, no simulation or experimental results are presented for an input shape such that used in the previous model. So, one cannot say if an improvement is obtained for the simulation of the tail of the breakthrough curve after the input stops. It is quite difficult to find explanations to the relative bad agreement observed at the early times. Too many assumptions are made regarding the physics of the flow, the uniqueness of a for each path, the uniqueness of the input rate for each path, the evaluation of the input through the surface of the soil, the law modeling the uptake of water by the porous matrix. Perhaps a numerical study on networks of macropores without absorption by the

matrix could bring some elucidations.

To close this paragraph on the kinematic wave approach applied to water flow modeling in macropores, a global remark must be done. One must keep in mind that all the developments presented before (§ 2.4) rely on two main hypothesis. First, that the relation $q=b\theta^a$ holds at any time and everywhere in the macropore continuum, and secondly that interactions between both flow phases can be modeled by a simple relation. The difficulties encountered to adjust the parameters a, b and r and their dependence on experimental conditions, suggest that the kinematic approach in its actual form does not fully account for the complexity of the phenomena. However, it constitutes, with the model of **Jarvis and Leeds–Harrison (1987a)** the only macroscopic approaches actually available to model unsaturated water flows in the macroporosity continuum.

Let us mention to end, two papers, **Smith (1983)** and **Charbeneau (1984)**, in which the main ideas used by **Germann and Beven** to solve the hyperbolic equation are yet present. These papers were not specifically dealing with transport in heterogeneous media, but aimed at providing a new way to take up the problems of water flow and solute transport modeling in soils. In both papers an hyperbolic equation is substituted to **Richards** equation to model water flow. As such, these works were already providing a new approach to transport simulation in non–necessarily homogeneous soils.

2.6 EXTENSION TO NON–RIGID MEDIA

The precedent paragraphs cope with water movement in heterogeneous media, assuming that both porous matrix and heterogeneity pattern are not subject to deformations, except for the model of **Jarvis and Leeds–Harrison (1987a)**. As underlined before, heterogeneity sources are numerous; soil physical properties (clay content and clay minearlogy), biological activity, old roots, etc ... Among these different kinds of preferential pathways those resulting from biological activity (worm holes, old root channels,..) are expected to remain unchanged for large periods of time. Inversely, those resulting from material intrinsic physical properties may be expected to undergo numerous and more or less rapid changes, (pattern, width,..). These heterogeneities constitute probably the "main part" of the structural porosity (surface and volume) and that particularly in rooting and tilled zones, **Jarvis and Leeds–Harrison (1987a)**. Crack patterns resulting from wetting–drying cycles occur in many situations, even if percentage of clay is not very high. Hence, as soon as we want to deal with transport problems in heterogeneous media, it is in many cases difficult if not impossible to ignore soil deformations occurring with water content variations

Of course situations exist where this can be done. Let us recall for example the measurements reported by **Bouma et al. (1977, 1979)** concerning the evolution of the hydraulic saturated conductivity for different samples under continuous swelling. It was shown that in some cases, characterized by different soil morphologies, swelling doesn't affect saturated conductivity value. It is also evident that the time is an important factor. Ignoring time soil deformations is possible for example if one is only interested in very short term simulations, such as infiltration during a storm, or if swelling kinetic is very slow. However, for some soils such as *vertisoils* for example, swelling properties are such that cracks closing may occur so quickly that the models presented before are useless. Inversely, if we are interested in long term simulations, characterized by several wetting drying cycles, and various boundary conditions, accounting for deformation processes seems inevitable.

Swelling and shrinking basically modify hydrodynamics properties in two possible ways. First, occur modifications for the volume and the shape of the porous

matrix blocks delimited by the crack lattice. This change in volume, related t wetting or drying kinetics, induces a modification of the structural porosity pattern From a modeling point of view, this three–dimensional lattice can be characterized b different parameters, its volume, the width of the cracks and others voids, it exchange surface with the porous matrix, its connectivity, etc.... As noted before, modification of the volume of the porous blocks is not necessarily related to a drasti change in hydrodynamic characteristics, saturated conductivity in particular. So even if we can readily include in a simulation program an algorithm to account fo textural porosity modifications related to water movement, it appears difficult to handle the modifications induced for the macroporosity system and what's more its hydrodynamic properties variations.

However, if we restrict ourselves to simple cases, considering a single crack and assuming some swelling or shrinking kinetics, numerical simulations are possible. Probably, some interesting results can be obtained concerning the competition between swelling kinetic and rain intensity. Particularly, one can expect some conclusions opposite to those obtained in the case where no deformations were allowed. Amount of water infiltrating, runoff starting time, and other interesting variables are in certain cases probably very dependent not only on rain intensity but also on swelling kinetic.

Some modeling approaches to water flow in swelling soils have been given by **Smiles and Rosenthal (1968), Philip (1968,1969), Smiles (1974).** In all these studies the soil is assumed homogeneous and a diffusion equation analogous to the **Fokker–Planck** equation is derived. Although this topic is not really in the frame of this report we give below some of the relations derived by Philip, which can be useful when accounting for swelling in numerical models such as those proposed before.

Some relations for swelling soils hydrodynamics

In case of an horizontal flow and for a two phases system (soil–water) the diffusion equation is:

$$\frac{\partial e}{\partial t} = \frac{\partial}{\partial m}\left[D_m \frac{\partial e}{\partial m}\right] \qquad [2.127]$$

where D_m the diffusion coefficient efined by:

$$D_m = D(1+e)^{-3} \qquad [2.128]$$

where, $e = n/(1-n)$ and n is the porosity. m is the material coordinate defined by:

$$dm/dx = 1/(1+e) \qquad [2.129]$$

For a three–phases system (Water–Solid–Air), diffusion equation and diffusion coefficient are respectively:

$$\frac{\partial v}{\partial t} = \frac{\partial}{\partial m}\left[D_v \frac{\partial v}{\partial m}\right] \quad \text{and} \quad Dv = \frac{D(1+e - vde/dv)}{(1+e)^3} \qquad [2.130]$$

where v is the saturation index.

If one considers the case of a system where the gravity cannot be neglected, the total water potential is now defined by:

$$\phi = \Psi - z + \Omega \qquad [2.131]$$

where Ω is the overburden potential, defined by:

$$\Omega = P(z)de/dv \qquad [2.132]$$

and $P(z)$ is the total vertical stress. Noting γ_s the solid density, the wet specific gravity γ is defined by:

$$\gamma = (v + \gamma_s)/(1+e) \qquad [2.133]$$

and then $P(z)$ is given by:

$$P(z) = P(0) + \int_0^z \gamma\, dz \qquad [2.134]$$

symbolng the equilibrium equation: ϕ = cte , a differential equation relating z and v is obtained

$$dz/dv = -M(v) - N(v)z \qquad [2.135]$$

where $M(v)$ and $N(v)$ are given by:

$$M(v) = \frac{\frac{de}{dv}\frac{d\Psi}{dv} - (Z+\Psi)\frac{d^2e}{dv^2}}{\frac{de}{dv}\left[\gamma\frac{de}{dv} - 1\right]} \qquad N(v) = \frac{d^2e/dv^2}{\frac{de}{dv}\left[\gamma\frac{de}{dv} - 1\right]} \qquad [2.136]$$

A singularity exists for $de/dv = \gamma^{-1}$. **Philip** shows that this relation is satisfied only at an extremum of $\gamma(v)$, and that under relatively weak conditions on $e(v)$ there is one and only one extremum and that it is a maximum. This value is denoted by v_p. It follows that three types of moisture equilibrium profiles can be distinguished in a swelling soil. Noting v_0 the moisture ratio at the surface, we have:

1– For $v_0 > v_p$; $v > v_p$ and $dv/dz < 0$ for $z \geq 0$

2– For $v_0 = v_p$; $v = v_p$ and $dv/dz = 0$ for $z \geq 0$

3– For $v_0 < v_p$; $v < v_p$ and $dv/dz > 0$ for $z \geq 0$

Combining [2.131] and $v_r = -K\nabla\phi$ which is a more general form of Darcy' law, an expression is obtained for steady vertical flows. A second order differential equation is derived:

$$d^2z/dv^2 = -M_1(v) - N_2(v)dz/dv \qquad [2.137]$$

Philip (1969) gives a relatively lengthy discussion of the different possible configurations. We refer the reader to this paper for more details. For unsteady flows, combining equations [2.131], [2.132], [2.134] and the continuity equation, the following relation is derived:

$$\frac{\partial v}{\partial t} = \frac{\partial}{\partial m}\left[\frac{K}{1+e}\left\{\frac{d\Psi}{dv} + P(0)\frac{d^2v}{dv^2}\right\}\frac{\partial v}{\partial_m}\right]$$

$$-\frac{\partial}{\partial m}\left[K\left\{1 - \gamma\frac{de}{dv} - \frac{d^2e/dv^2}{1+e}\int_0^m \gamma(1+e)dm\,\frac{\partial v}{\partial m}\right\}\right] \qquad [2.138]$$

If the terms of order m^{-1} are neglected, a diffusion equation is obtained with diffusion coefficient D^*:

$$D^* = \frac{K}{1+e}\left[\frac{d\Psi}{dv} + P(0)\frac{d^2e}{dv^2}\right] \qquad [2.139]$$

2.7 CONCLUSIONS

A natural and physically realistic approach to unsaturated water flow modeling in heterogeneous media has been to introduce the concept of '*double porosity*' in order to separate the behavior of two water phases obviously undergoing very different processes. However, in this frame it appeared difficult to set up the equations modeling the flow in the macroporosity continuum. The other main approach developed, not attemp ting to handle the problem in his full generality, has been to consider infiltration through and from single macropores and cracks. These different ways to take up the problem have been reviewed in the precedent paragraphs.

Models based on the double porosity concept for unsaturated flows are not as developed as for saturated flows. All proposed double porosity models are in essence mono–dimensional, as they use a one–dimension equation for the macropore flow. This choice compared to two or three–dimensional models used in saturated flow studies leads to important limitations. One of these is of course that no physical problem needing a two–dimensional representation can be treated. However, this limitation should not preclude from using geometrically based expressions for the coupling term. Until now, only rough expressions have been used to describe the interaction between the two flow phases. Hypothesis included in these approaches, implicitly make irreal assumptions on the physics of the flow. A good example being the formulation used by **Beven and Germann (1981)** which implicitly assumes the establishment of an instantaneous equilibrium for the water content field inside the porous blocks over distances larger than 10 cm. Obviously, to assume that there is no pressure head gradients at a given level in the microporosity can only lead to some very bad estimations of the water fluxes from one phase to the other. This is a typical example of the kind of perturbing term which precludes for example from obtaining meaningful transfer parameters through fitting procedures.

Assuming some simple shapes for the porous blocks, the simulation of the interaction between the two phases could be made in a more realistic way and wouldn't need irreal hypothesis. The only unknown parameters would then be those characterizing the geometry. These parameters can be more or less numerous or complicated according to the type of geometrical representation chosen. Therefore, in a given case defined by initial and boundary conditions, the only parameters which would have to be fitted are those corresponding to geometrical assumptions. These parameters account in fact for the characteristics of the system such that, exchange surface, shape of porous blocks,etc... One important property of these parameters is

that they probably would not be so dependent upon initial conditions or boundary conditions as it is the case for the parameters defined by Beven and Germann.

The main difficulty is the derivation of a two–dimensional equation modeling the flow in the macropore continuum. The hyperbolic equation derived by Germann and Beven is based on a power law function linking the flux and the macropore water content. A representation of the structural porosity with vertical pores and cracks was used in conjunction with an extension of Poiseuille law to derive the relation $Q(\theta)$. In the case of a two or three dimensional flow, expressions [2.76] and [2.77] are no longer acceptable. If we consider Q not only as a function of the vertical coordinate but also as a function depending on all space coordinates, one can expect, since the flow is induced by gravity forces, a strong anisotropy of Q(x,y,z). Maximum values can be expected for orientations defined by vector (0,0,z), and probably a value equal to 0 for orientations (x,y,0). As already indicated in the text, deterministic simulations on networks could help to set up a useful relation between the flux Q, the direction considered and the water content, according to the geometrical characteristics of the network.

The different models developed for single pore or crack have the advantage of being more physically rigorous. However their usefulness is restricted to some particular studies, such that: influence of macropores on global infiltrability or on runoff intensity and starting time. As mentioned in the precedent paragraph they will certainly provide a useful way to test swelling influence on macropore continuum hydrodynamic characteristics modifications.

Let us define the problem in the following way. What are we able to do (modeling) and what kind of measurements do we need to simulate water flow in structured soils ? Actually, the only modeling approach which can be applied to field situations is the double porosity approach. In this frame one have the choice between two possible strategies. The first one is to use the model of Germann and Beven which provides an approach for macropore flow, but a very poor modeling for flow phases interaction in its actual formulation. The other possible direction is to use a model based on single crack approach, that is to say a model explicitly accounting for wall runoff and thus providing a physical simulation of phases flow interaction. Remark that the model of Jarvis and Leeds–Harrison (1987a) provides a combination of these two approaches

For the first choice a discussion of the meaning, fitting and robustness of the parameters has already been given. Needed data only consist in this case in a breakthrough curve. One have remarked that fitted parameters a and b are dependent on experimental conditions (initial and boundary conditions), and are also certainly dependent on interaction term formulation. For example in the double porosity model of Germann and Beven, a dependence on $\Delta\chi$ can be expected. One have to be conscious that even if the formulation seems to account for all physical phenomena, the coupling term used, leads in fact to consider the profile as a big black box. The fitted parameters are in fact integrating the geometrical characteristics of the macroporosity for all the profile together with other flow parameters. This approach is conceptually not very far from the transfer function model prposed by Jury (1982) for solute transport. In this modeling frame, a classical hydraulic characterization of the soil profile is also required; $\Psi(\theta)$ and $K(\theta)$ relationships.

In order to use the second possibility, a more detailed description of profile characteristics is required. Some examples of how useful can be an estimation of crack length, width, etc... obtained by image analysis, have been given in the precedent paragraphs. In this modeling frame a classical hydraulic characterization is also required. For this approach, it appears that the only parameter to be fitted will be the area used by the convective flow, expressed as a surface per unit volume of soil. The agreement between experimental and simulated results can be assessed by comparing outflow curves. A verification of the results should also be carried out by

comparing the water content profiles. If the comparison is made only on outflow curves one can expect the same kind of indeterminations and incertitudes on water content profiles as it is the case for the kinematic wave approach. Now if we consider the area which can be used by the convective flow not as a constant but as a function of depth one can perhaps expect a more reliable estimation of water distribution in the profile. Unfortunately it seems that an estimation of this area can only be obtained a—posteriori. However, if we accept to assume a direct relation between structural porosity and this area, the calculation is possible without to many data required and without disturbing the experimental site. We have to keep in mind that a direct relation between structural porosity and exchange surface will depend on experimental site, flow rate at the surface, and will not hold for swelling conditions in general.

The question arising in both simulation frames is then: do we have a correct or useful water fluxes estimation in order to predict solute movements ? Actually it is difficult to answer this question, although the answer is probably, no. This point will be discussed later, but let us already say that estimations of the exchange areas are of prime importance in solute transport simulation through structured soils. Thus, it appears that the second modeling approach proposed is perhaps better suited than the first one, at least in its actual form. Here it clearly appears that if a model with geometrically based coupling terms could be developed our ability to simulate solute transport in heterogeneous media would be largely improved.

Water movement simulation in structured media appears to be a difficult task to achieve. Even in the case of rigid media it is difficult to derive a mathematical model. In fact the problem seems to be that we are unable, from a transport point of view, to physically characterize the medium as it was done for homogeneous porous media. The other problem is that we have not identify transport laws in such media or at least we have not express them in a convenient way. For example we don't have a macroscopic transport law for the macropore continuum, and what's more it has been shown that a law similar to Darcy's law can't be derive in all the cases. Another example being the empirical power law proposed by German and Beven linking flux and water content in the structural porosity. Structured media do not behave as homogeneous media. In other words the problem is not only a scale change problem as it has been shown in the works of Long et al. (1982) and Schwartz and Smith (1984, 1985) for saturated conditions. Following these authors, an important work should be done on theoretical networks in order to better understand the phenomena and show up the important parameters controlling the flow in a structured media.

3. SOLUTE TRANSPORT IN HETEROGENEOUS SYSTEMS.

3.1 INTRODUCTION AND BASIC CONCEPTS

It was recognized some years ago by some scientists, see for example Nielsen and Biggar (1961), Coat et Smith (1964), Philip (1968), Passioura (1971), Passioura and Rose (1971), Van Genuchten and Wierenga (1976, 1977a,b), Gaudet (1978), working on what is considered as a homogeneous media (laboratory columns with sandy materials), that a certain percentage of the water was immobile during saturated–unsaturated flows. This stagnant water was related to the thin liquid films surrounding the particles, to the dead–end pores, to intraaggregate immobile water, or to relatively isolated regions associated with unsaturated flows. Thus, it appeared that the simple CDE (Convection Dispersion Equation) alone was not a fully appropriate tool to model solute transport in porous media. Based on this concept of mobile and immobile water, the concept of mobile and immobile solute concentrations was formulated, and the interaction between the two domains first included in the transport models under the form of a first order differential equation describing a non equilibrium exchange process. This model is usually referred as "*first–order phyical noequilibrium model*" (FO). In this report it will also be referred, for reasons later obvious, as the "*Quasi–steady state model*" (QSS). Beside, nonequilibrium conditions of chemical origin can arise and require the same kind of treatment.

In the previous chapters it was shown that at least two water phases should be considered when modeling water flow in heterogeneous porous media. It is then obvious that when it comes to model solute transport under such physical conditions the differentiation between two concentrations constitutes a modeling base. In fact, in structured soils, the transport phenomena between the two domains can barely be modeled by a simple first order differential equation. Though, this approach may still be employed with some succes, it no longer gives a realistic representation of the physical phenomena. In soils presenting well defined heterogeneities, the space dimension can no longer be ignored when modeling the exchange process from one liquid phase to the other, and the so called immobile concentration is not homogeneous at a given level. Therefore, an explicit simulation of the diffusion process occuring in the porous matrix is needed. Based on various conceptualizations of the heterogeneities, a certain number of models including this process appeared in the past few years. In the following these models will be referred as "*diffusional models*" or "*geometrically based models*". These different approaches will be reviewed in the following paragraphs, together with their solutions and applications.

In fact, these models provide usefull tools to optimize leaching strategies, and improve our understanding of the physical phenomena. Unfortunately, due to various assumptions and simplifications involved in the reduction of the system to a simple geometry and tractable mathematical form, they do not really constitute predictive tools and are not easily applied to field situations. A unifying concept appeared two or three years ago, Barker (1985a,b), named the block geometry function (BGF), and allowing to express the equations in a unique form wathever is the geometry. In fact it will be shown that by means of the BGF, any geometrical conceptualization of the physical system is readily included and more, that the geometrical constraint can be released. The other advantage is that the model applied to a given soil profile is no longer restricted to a given unique aggregate shape. It is possible through the BGF to account for any mixture of aggregates having various shapes and sizes. Though this is not explicitely expressed in the literature, the BGF could be used as a fitting parameter fully accounting for the geometry of the aggregates and only for their geometry. The BGF'S theory will be presented as a unifying concept allowing to

integrate in a single frame models based on geometrical conceptualization of the porous media as well as more simple ones such as the well known first–order physical non–equilibrium model, the local equilibrium model or models including skin effects.

An actual trend in solute transport modeling research is to seek for relations between diffusional models and more simpler ones such as the FO model or CDE–based models which can be considered as more macroscopic as they lump into a first–order process and a dispersion coefficient respectively, a physical phenomena in fact obeying a diffusion equation. Several studies have been lately dedicated to this task. Conditions where macroscopic models can be used in place of geometrically based models have been derived but at the same time the relative crude nature of these macroscopic approaches appear clearly together with their limitations.

Before really starting the description of the different equations available for solute transfer modeling in heterogeneous media we have thought it would be useful and may be necessary to first recall some basic results. We would like to amphasize on (1) the notions of *volume–average and flux–average concentrations*, (2) the problems of approprieted boundary conditions and their relations with the evaluation of breakthrough curves, (3) the different types of adsorption isotherms, resulting retardation factors and adsorption models.

Volume–average and Flux–average concentrations.

The simple convection–dispersion equation is the base of solute transport modeling in homogeneous porous media. Expressed in normalized variables this one is,

$$R\frac{\partial C}{\partial t}=\frac{1}{P}\frac{\partial^2 C}{\partial x^2}-\frac{\partial C}{\partial x} \qquad [3.1]$$

where R is called the retardation factor and P is the Peclet number defined by: P=vL/D. When applied to reacting solute transport modeling this equation is often referred as the LEA (Local Equilibrium Assumption) model. Classicaly the concentration appearing in this equation is assumed to correspond to the average concentration over a small representative elementary volume. As shown by **Kreft and Zuber (1978)**, **van Genuchten and Paker (1984)** and **Parker and van Genuchten (1984)**, it is also possible to define a flux averaged concentration, corresponding to the mean value of the flux distribution over the column section. This one is given by:

$$C_f = C_r-(D/v)(\partial C_r/\partial x) \qquad [3.2]$$

where C_r denotes the volume–average concentration also called resident concentration. If this transformation is applied to the CDE [3.1], strictly the same equation results, **van Genuchten and Parker (1984)**. The differences appear when specifying the boundary conditions. From Eq. [3.2], one see that if we apply a third type boundary condition at the surface in terms of resident concentration, this one corresponds to a first–type condition in terms of flux–averaged concentration. Identically, when a semi–infinite profile is modeled by the condition:

$$(\partial C_r/\partial x)(L,t)= 0. \qquad [3.3]$$

this one corresponds to a first–type condition in terms of flux–averaged

concentration. In fact this notion of volume–averaged or flux–averaged concentration is closely related to the problem of imposing the right boundary conditions at both extremities of the flow domain.

Boundary conditions.

Let us first consider a semi–infinite system. The mass–conservation across the inlet boundary requires, **van Genuchten and Paker (1984)**,

$$[-D(\partial C_r/\partial x) + vC_r]\Big|_{x=0^+} = vC_0 \,. \qquad [3.4]$$

This condition is valid for a system not physically connected to the soil column, as it is for example the case when the solution is trickled at the surface. This condition is also valid when the reservoir is connected to the soil, but perfectly mixed. For a semi–infinite system the boundary condition at the outlet is:

$$(\partial C_r/\partial x)(\infty,t) = 0 \,. \qquad [3.5]$$

It is pointed out, **van Genuchten and Parker (1984)**, that with these boundary conditions, Eq. [3.4] and [3.5], the analytical solution derived for equation [3.1] by **Lindstrom and Narasimham (1967)**,

$$\frac{C_r(x,t)}{C_0} = \frac{1}{2}\,\mathrm{erfc}\left[\frac{Rx - vt}{2(DRt)^{1/2}}\right] + \sqrt{\frac{v^2 t}{\pi DR}}\exp\left[-\frac{(Rx-vt)^{1/2}}{4DRt}\right]$$

$$-\frac{1}{2}\left[1 + \frac{vx}{D} + \frac{v^2 t}{DR}\right]\exp\left[\frac{vx}{D}\right]\mathrm{erfc}\left[\frac{Rx + vt}{2(DRt)^{1/2}}\right] \qquad [3.6]$$

satisfies the mass–balance requirement:

$$vC_0 t = R\int_0^\infty C_r(x,t)\,dx \,. \qquad [3.7]$$

Inversely, it is shown that for the same problem the analytical solution obtained by **Lapidus and Amundson (1952)**,

$$\frac{C_r(x,t)}{C_0} = \frac{1}{2}\,\mathrm{erfc}\left[\frac{Rx - vt}{2(DRt)^{1/2}}\right] + \frac{1}{2}\exp\left[\frac{vx}{D}\right]\mathrm{erfc}\left[\frac{Rx + vt}{2(DRt)^{1/2}}\right] \qquad [3.8]$$

with a first–type boundary condition at the inlet, Dirichlet–type condition, does not verify the mass–balance equation. The mass–balance error is shown to be quite large when dispersive transport is important compared to convective transport and/or when the solute is strongly adsorbed by the porous matrix, case of large retardation factors, R.

Now, considering a finite length soil column, appears the problem of the choice of the correct boundary condition to be imposed at the outlet. Continuity of the flux of solute across the lower boundary is a requirement that must always be satisfied. Mathematically, this is expressed by, **Brenner (1962)**, **Gaudet (1978)**, **van Genuchten and Parker (1984)**,

$$[-D(\partial C_r/\partial x) + vC_r]\Big|_{x=L} = vC_e \qquad [3.9]$$

where C_e is the concentration of the solution immediatly outside the flow domain. This condition assumes that the reservoir collecting the solution at the exit is not directly connected to the liquid phase of the column, or that diffusion–convection effects in this reservoir are negligible. Unfortunately, this condition introduces an additional unknown, C_e, and an other equation is now required to solve the problem. Usually, one requires the continuity of the concentration across the boundary, which after combination with [3.9]leads to:

$$(\partial C_r/\partial x)(L,t) = 0. \qquad [3.10]$$

One must realize that this condition is in contradiction with the third–type boundry condition applied at the surface. It assumes the macroscopic continuity of the concentration at the outlet, **Danckwerts (1953)**, Pearson (1959). However, if we accept this condition, the solution with a third–type boundary condition at the surface is given by **Brenner (1962)**,

$$\frac{C_r(x,t)}{C_0} = 1 - \sum_{m=1}^{\infty} \frac{\frac{2vL}{D}\beta_m \left[\beta_m \cos\left(\frac{\beta_m x}{L}\right) + \frac{vL}{2D}\sin\left(\frac{\beta_m x}{L}\right)\right]}{\left[\beta_m^2 + \left(\frac{vL}{2D}\right)^2 + \frac{vL}{D}\right]\left[\beta_m^2 + \left(\frac{vL}{2D}\right)^2\right]}$$

$$\exp\left(\frac{vx}{2D} - \frac{v^2 t}{4DR} - \frac{\beta_m D t}{L^2 R}\right) \qquad [3.11]$$

where the coefficients β_m are the positive roots of

$$\beta_m \cot(\beta_m) - (\beta_m^2 D/vL) + (vL/4D) = 0. \qquad [3.12]$$

The breakthrough curve resulting from the evaluation of the solution at (x=L) is,

$$\frac{C_e(T)}{C_0} = 1 - \sum_{m=1}^{\infty} \frac{2\beta_m \sin(\beta_m) \exp\left[\frac{P}{2} - \frac{PT}{4R} - \frac{\beta_m^2 T}{PR}\right]}{\beta_m^2 + \frac{P^2}{4} + P} \qquad [3.13]$$

where the β_m are the roots of,

$$P\beta_m \cot(\beta_m) - \beta_m^2 + \frac{P^2}{4} = 0$$

$$T = vt/L \qquad P = vL/D\,.$$

It is shown that this solution verifies the mass–balance requirement. The breakthrough curve can be obtained by combining the solution of **Lindstrom and Narasimham (1967)** given above (Eq. [3.6]), and the relation [3.9]. Then, the following expression is obtained:

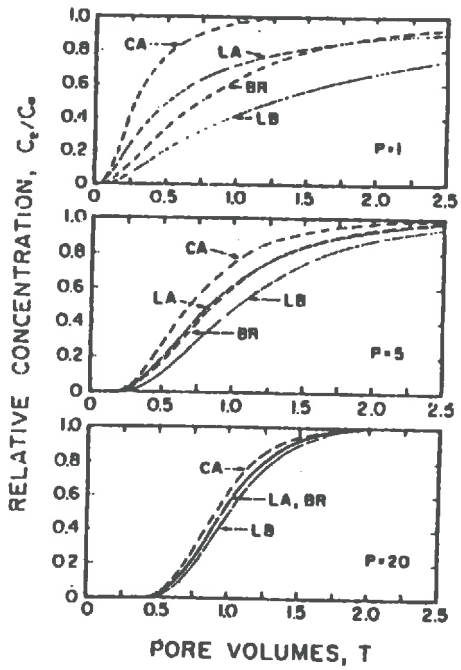

Fig. 3.1 Relative effluent concentration profiles calculated with the solutions of LA (Lapidus and Amundson 1952), CA (Cleary and Adrian 1973), LB (lindstrom et al. 1967) and BR (Brenner 1962). The curves are plotted for three different values of the column Peclet number [after *van Genuchten et al. 1984*].

$$\frac{C_e(L,t)}{C_0} = \frac{1}{2}\,\mathrm{erfc}\left[\frac{RL - vt}{2(DRt)^{1/2}}\right] + \frac{1}{2}\exp\left[\frac{vL}{D}\right]\mathrm{erfc}\left[\frac{RL + vt}{2(DRt)^{1/2}}\right] \quad [3.14]$$

which is in fact the solution of **Lapidus and Amundson (1952)** (eq. [3.8]) evaluated at (x=L). If now we consider the CDE expressed in terms of flux–averaged concentration, we immediatly see that the solution of **Lapidus and Amundson (1952)** (Eq. [3.8]) predicts the breakthrough curve in terms of flux–averaged concentration. Given the relation [3.9] and the boundary condition used at the outlet, Eq. [3.10], it is obvious that the breakthrough curves derived from the solution of **Brenner (1962)** are the same either expressed in terms of volume–averaged or flux–averaged concentrations. However, concentration profiles can be quite different. Figure 3.1 taken from **van–Genuchten and Paker (1984)**, presents the breakthrough curves obtained with four different analytical solutions. It can be seen that they drastically differ at low Peclet numbers, but that they converge to a unique curve when the Peclet number increases. This means that when the convection term is predominent, all the solutions are very close and the effects of boundary conditions are damped out.

In conclusion, when a volume–averaged based expression of the CDE is used with a first–type boundary condition at the inlet, the solution (Eq. [3.8]) of **Lapidus and Amundson (1952)** should be used to calculated breakthrough curves, and the solution (Eq. [3.6]) of **Lindstrom and Narasimham (1967)** obtained with a third–type boundary condition should be used to evaluated resident concentration profiles. An important point to keep in mind is that the transformation to a flux–averaged formulation is not always possible, especially when dealing with complicated systems. In these cases, the breakthrough curves should be calculated by applying equation [3.9] to the volume–averaged solution.

Adsorption Isotherms Retardation Factors and Adsorption Models

In the classical CDE equation given above appears a parameter noted R and called retardation factor. This factor is equal to one if there is no physical or chemical interactions between the applied solute and already present chemical species. This assumption is usually made when dealing whith tracers such that chloride or nitrate and when at the same time all soil water is supposed to be mobile. When chemical reactions, ions exhange processes, or isotopic exchanges occur between the applied tracer and the solid phase or the resident liquid phase, some other differential equations describing these processes must be added to the simple CDE modeling the transport phenomena. In fact many complex processes can be involved such that precipitation, dissolution, isotopic exchange, etc...As well, it might then become necessary to model the behavior of different chemical species involved in the different reactions and transported by the flow.

Let us for now consider the case of a single chemical product reacting with the solid phase of the porous media. Inclusion of this process in the transport model have been done by several ways. The simplest one is usually denoted (LEA) for local equilibrium assumption. This approach is based on the hypothesis of local reversible sorption reactions and thus of local chemical equilibrium. This notion of equilibrium is in fact not absolute but relative to the flow process. **Valocchi (1985)** expressed that by: "*..if the microscopic processes are 'fast enough' with respect to the bulk fluid flow rate then, reversible ...*" This means that experimental conditions are not too different from batch ones.

If nonequilibrium conditions exist, a LEA based model will exhibit less dispersion than the real process and a breakthrough occuring too late. The problem of dealing with nonequilibrium conditions is not restricted to reactive

tracers. When two distinct water phases are present, one mobile and the other immobile, nonequilibrium conditions correspond to the fact that equilibrium between both phases is not instantaneous. The incapacity of the LEA model to reproduce long tailings with nonreactive tacers is a manifestation of physical nonequilibrium conditions.

Making use of the LEA results in considerable simplifications. In particular adsorption isotherms can be determined from batch experiments, and one does not need to describe the microscopic pathways towards reaction sites. This is to say that a geometrical conceptualization of the sorbent or a two–regions model are not required. Usually, batch experiments are fitted to a non–linear Freundlich isotherm,

$$S = k\, C^N \qquad [3.15]$$

where S is the concentration of the adsorbed phase expressed in (μg/gsoil), C the concentration of the solution, k is the adsorption constant and N a constant. When adsorption on the solid phase is accounted for, the transport phenomena is modeled by the following equation:

$$\frac{\rho}{\theta}\frac{\partial S}{\partial t} + \frac{\partial C}{\partial t} = D\,\frac{\partial^2 C}{\partial z^2} - v\frac{\partial C}{\partial z} \quad . \qquad [3.16]$$

Deriving equation [3.15] we obtain,

$$\frac{\partial S}{\partial t} = kNC^{N-1}\frac{\partial C}{\partial t} \quad . \qquad [3.17]$$

Using [3.16] in [3.17], equation [3.1] is obtained where the retardation factor R, is given by:

$$R = 1 + \rho kNC^{N-1}/\theta \quad . \qquad [3.18]$$

Most of the time N is taken equal to one and thus a linear isotherm results, with R given by: $R = 1 + \rho k/\theta$.

As remarked by Valocchi (1985), very few works are concerned with the validity of the LEA. James and Rubin (1979), performed laboratory experiments at different flow rates and found that the LEA failed at the higher fluxes. Using a model, they derived the rather qualitative conclusion that the LEA is valid when the ratio of the hydrodynamic dispersion coefficient to the diffusion coefficient is close to one. As Valocchi (1985) pointed out, the LEA proved to be valid for experimental conditions where the hydrodynamic dispersion was significantly greater than the diffusion coefficient. However, in many recent papers, van Genuchten et al. (1974), Rao et al. (1979), Nkeddi–Kizza et al. (1983), Schulin et al. (1987), Selim et al. (1987), Southworth et al. (1987), non–equilibrium conditions have been noticed at high velocities. These nonequilibrium conditions of physical origin imply that adsorption and equilibrium constants determined from batch experiments are not applicable within the LEA model. This appears very clearly when comparing the retardation factors obtained from batch experiments (Eq. [3.17]), with those obtained from the fitting of calculated breakthrough curves on experimental ones, Southworth et al. (1987). The same phenomena is reported by Jardine et al. (1988) for transport of several anions and cations through undisturbed soil

columns. Valocchi (1985), comparing the first moments of the breakthrough curves obtained with different models, analysed and quantified the conditions under which the LEA is valid. We shall expose later the results he obtained. Let us say for now that his conclusions aggree with the rather qualitative statements exposed above involving the respective chemical reaction and flow rates.

Most of the time, in order to obtain analytical solutions, the non–linear Freundlich isotherm is approximated by a linear isotherm by assuming N=1. Numerical solutions can be carried out for non–linear isotherms, Lai and Jurinak (1972), van Genuchten et al. (1974), van Genuchten and Wierenga (1976), Selim et al. (1987). An other limitation to the utilization of analytical solutions is that not only N can be different from one but that isotherm parameters can be different for adsorption and desorption processes. For a pesticide, 2,4,5–T (2,4,5–trichlorophenoxyacetic acid), van Genuchten and Wierenga (1977b) reported a N_{ads}/N_{des} ratio of 2.3, desorption constants ranging from 1.3 to 2.03, and an adsorption constant of .616. However, he found little differences between the breakthrough curves obtained with a numerical model accounting for irreversibility and non–linearity of the adsorption process, and the breakthrough curves calculated with his analytical solution assuming local equilibrium (LEA).

Beside the model resulting from the LEA, several other adsorption models have been proposed to deal with nonequilibrium conditions of chemical origin. Three different are reviewed by van–Genuchten et al. (1974) for pesticide movement simulation. Beside the LEA model used with a non–linear Freundlich isotherm, the two following expressions are also proposed.

$$\frac{\partial S}{\partial t} = \left[k_2 \exp(bS) \right] \left[\frac{k_1}{k_2} \exp(-2bS) \frac{\theta C}{\rho} - S \right] \qquad [3.19]$$

$$\frac{\partial S}{\partial t} = k_2 \left[\frac{k_1 \theta}{k_2 \rho} C^N - S \right] \qquad [3.20]$$

where S is the concentration of the adsorbed phase, C the concentration of the solution, and k_1 and k_2 are the forward and backward adsorption constants, (not the same in both expressions), respectively. The second expression is often referred as the kinetic chemical non–equilibrium model. It has been used by Lapidus and Amundson (1952), Ogata(1964), Oddson et al. (1970), Lindstrom and Narasimham (1973), van–Genuchten et al. (1974), Rao et al. (1979), Rasmuson (1981b, 1985a,b), Southworth et al. (1987).

However, it was remarked by many people that owing to the flow pattern and to the various kind of reaction sites available in the profile, adsorption phenomena could certainly not be modeled using only one isotherm and adsorption model. A first step toward a better representation of the reality has been to distinguish between two kind of adsorption sites. One type where the chemical equilibrium assumption (LEA) is assumed valid and a second type where adsorption is assumed to be controled by a kinetic non–equilibrium model such as described by Eq. [3.20], Cameron and Klute (1977), Rao et al. (1979), Nkeddi–Kizza et al. (1984). These models are usually called two–sites models. Combining these two adsorption models, and still assuming that at equilibrium the relation between adsorbed and in solution concentrations is linear, $\partial S/\partial t$ is as follows

$$\frac{\partial S}{\partial t} = \frac{\partial S_1}{\partial t} + \frac{\partial S_2}{\partial t} = k_1 \frac{\theta}{\rho} C_s - k_2 S_1 + k_3 \frac{\theta}{\rho} \frac{\partial C_s}{\partial t} \qquad [3.22]$$

where k_1 and k_2 are respectively the adsorption and desorption rates often referred as forward and backward rates, and k_3 is the equilibrium constant. This adsorption model has been used by **Selim et al. (1976)**, and **Rao et al. (1979)**. **Cameron and Klute (1977)**, applied this model to pesticide and phosphorus transport. A very good agreement was obtained in both cases.

3.2 MODELING THE TRANSPORT PROCESS IN STRUCTURED MEDIA

3.2.1 INTRODUCTION

Natural soil aggregates and peds occur in a wide range of sizes and shapes. **Brewer (1964)** proposed a schema for classifying the geometrical shapes of the aggregates based on the relative length of their three principal axis. Modeling solute diffusion in natural aggregates is difficult if not impossible due to their irregular shapes. Though the diffusion equation can be solved in any geometrical domain, using some powerfull numerical technique, it is of little interest to do so and the first step of the modeling work is to choose a geometrical form allowing to solve the mathematical problem without too many difficulties and being also reasonabely close to natural aggregate shapes. From the modeling point of view, the natural question arising is then: can any natural aggregate be replaced by a geometrically simple aggregate and if yes how ? The following natural question to answer to being: what happen when the soil profile is composed of a mixure of aggregates having different shapes and sizes? These questions will be addressed further in this report. We present first the modeling approach and its solutions for media made up of uniform and regularly shaped aggregates, prisms, cylinders and spheres respectively. An approximation of this problem, spherical particles, has been considered and treated at the begenning of the fifties in the chemical engineering literature. These results have only recently been improved and applied to the field of solute transport modeling in heterogeneous or structured soils.

3.2.2 GOVERNING EQUATIONS

First–Order Physical Nonequilibrium Model

One of the ways to derive the equations for solute transport modeling in a media made up of regularly shaped aggregates is to use those of the two–regions model also known as physical non–equilibrium model formulated by **van Genuchten and Wierenga (1976)**. Let us first recall why these equations were introduced, how they are obtained and then how they are modified when applied to media made up of regular aggregates.

Extensive tailings were noticed on breakthrough curves obtained with unsaturated materials, **Turner (1958)**, **Nielsen and Biggar (1961)**, **Deans (1963)**, **Coats and Smith (1964)**, and this phenomena was related to an increase of the proportion of regions isolated from the flow, immobile water, and which rely on a diffusive process to reach equilibrium. Extensive tailing were also recorded in aggregated media, **Biggar and Nielsen (1962)**, **Green et al. (1972)**, **McMahon and Thomas (1974)**. Several experiments, **Biggar and Nielsen (1962)**, **Villermaux and van Swaay (1969)**, **Skopp and Warrick (1974)**, indicated that the tailing was also more important when the pore–water velocity was decreasing. The concept of mobile–immobile water and diffusional exchange between these two phases was then proposed to explain this tailing phenomena, and was modeled by a first–order rate process, **Deans (1963)**, **Coats and Smith (1964)**.

Let us note θ_m and θ_{im}, the mobile and immobile water contents, respectively. Associated with these two phases are the two concentrations respectively noted, C_m and C_{im}. We also assume that adsorption on the solid

phase occur for the two phases, and we note S_m and S_{im} the two adsorbed concentrations. It appears here that we need to partition the solid phase into a dynamic region associated with the mobile water phase and a static region associated with the immobile water phase. As the amount of solute sorbed is dependent on the area offered by the solid phase, this partitionnement should be based on estimations of the solid areas assossiated with the two flow domains. However, some problems appear. First, this estimation is not easy to obtain. Secondly, most of the time the bigger pores corresponding to the mobile water phase are coated with highly reactive materials, such that hydroxydes or aluminium, thus preventing from considering both regions as having the same adsorption capacity. A partition coefficient based on mass considerations has been proposed by **van–Genuchten et al. (1984)**. Given these difficulties, this coefficient noted, *f*, is most of the time adjusted or taken close to the partition coefficient used for the water content.

It is assumed that the flow in the mobile phase is characterized by a velocity, V_m, and a dispersion coefficient, D_m. Assuming that the transport can be modeled by a convection–dispersion equation, the following formulation results after application of the continuity equation:

$$\frac{\partial}{\partial t}(\theta_m C_m) + \frac{\partial}{\partial t}(\theta_{im} C_{im}) + \frac{\partial}{\partial t}(f\rho S_m) + \frac{\partial}{\partial t}(1-f)\rho S_{im} =$$

$$\frac{\partial}{\partial z}(\theta_m D_m \frac{\partial C_m}{\partial z}) - \frac{\partial}{\partial z}(\theta_m V_m C_m) \; . \qquad [3.23]$$

Assuming that the water content in the two phases is constant in time and space, that the velocity, the dispersion coefficient and *f* also are constant, the following equation is derived:

$$\theta_m \frac{\partial C_m}{\partial t} + \theta_{im} \frac{\partial C_{im}}{\partial t} + f\rho \frac{\partial S_m}{\partial t} + (1-f)\rho \frac{\partial S_{im}}{\partial t} = \theta_m D_m \frac{\partial^2 C_m}{\partial z^2} - \theta_m v_m \frac{\partial C_m}{\partial z} \qquad [3.24]$$

At this point, if instantaneous local equilibrium and non–linear Freundlich adsorption isotherms are assumed for both phases, replacing the time derivatives of S_m and S_{im} in [3.24] leads to,

$$(\theta_m + f\rho k N C_m^{N-1}) \frac{\partial C_m}{\partial t} + [\theta_{im} + (1-f)\rho k N C_{im}^{N-1}] \frac{\partial C_{im}}{\partial t} =$$

$$\theta_m D_m \frac{\partial^2 C_m}{\partial z^2} - \theta_m v_m \frac{\partial C_m}{\partial z} \; . \qquad [3.25]$$

The first–order equation modeling the diffusional exchange process between the two phases is,

$$\theta_{im} \frac{\partial C_{im}}{\partial t} + (1-f)\rho \frac{\partial S_{im}}{\partial t} = \alpha(C_m - C_{im}) \qquad [3.26]$$

which, using the Freundlich isotherm, results in

$$[\theta_{im} + (1-f)\rho k N C_{im}^{N-1}] \frac{\partial C_{im}}{\partial t} = \alpha(C_m - C_{im}) \qquad [3.27]$$

where α is a first–order coefficient controling the transport rate. Note that the dimension of α is that of the inverse of a time. Remark also that the total water content of the media is given by: $\theta = \theta_m + \theta_{im}$. Defining the dimensionless variables,

$$\begin{aligned} T &= v\,t\phi/L \\ x &= z/L \\ \phi &= \theta_m/\theta \\ P &= v_m L/D \\ \omega &= \alpha L/(v_m \theta_m) \end{aligned} \qquad [3.28]$$

the following set of equations results,

$$R_m \frac{\partial C_m}{\partial t} + (1-\phi) R_{im} \frac{\partial C_{im}}{\partial t} = \frac{1}{P} \frac{\partial^2 C_m}{\partial z^2} - \frac{\partial C_m}{\partial z} \qquad [3.29]$$

$$(1-\phi) R_{im} \frac{\partial C_{im}}{\partial t} = \omega (C_m - C_{im}) \qquad [3.30]$$

where the retardation factors R_m and R_{im} are given by

$$R_m = 1 + \frac{\rho f k N C_m^{N-1}}{\theta_m} \qquad R_{im} = 1 + \frac{\rho (1-f) k N C_{im}^{N-1}}{\theta_{im}} . \qquad [3.31]$$

At this point, if a linear adsorption isotherm is assumed, (N=1), equations [3.29] and [3.30] are as follows:

$$\beta R \frac{\partial C_m}{\partial t} + (1-\beta) R \frac{\partial C_{im}}{\partial t} = \frac{1}{P} \frac{\partial^2 C_m}{\partial z^2} - \frac{\partial C_m}{\partial z} \qquad [3.32]$$

$$(1-\beta) R \frac{\partial C_{im}}{\partial t} = \omega (C_m - C_{im}) \qquad [3.33]$$

where $\beta = \theta_m R_m / \theta R$ and [3.31] evaluated with (N=1). A third–type boundary conditions is imposed at the surface and a semi–infinite media is assumed. In dimensionless variables, and for a square pulse, these conditions are expressed by:

$$\lim_{x \to 0^+} \left(C_m - \frac{1}{P} \frac{\partial C_m}{\partial x} \right) = \begin{cases} 1 & 0 \le T \le T_1 \\ 0 & T \ge T_1 \end{cases} \qquad [3.34]$$

$$\lim_{x \to \infty} [C_m(x,T)] = 0 \qquad [3.35]$$

Assuming uniform initial conditions $C_m(0,x)=C_{im}(0,x)=0$, an analytical solution for equations [3.32], [3.33], [3.34] and [3.35] was derived by van–Genuchten and Wierenga (1976). This solution in given in annex, (A1).

Dealing with tracers reacting with the porous matrix, an other possible approach proposed in the litterature has been to consider that all the water was mobile and to assume that regarding adsorption two types of adsorption sites could be distinguished. (cf. 3.1 ***Adsorption Isotherms and Retardation Factors***).

These models are called two–site chemical nonequilibrium models. Nkedi–Kizza et al (1984) proved that the above two–regions model in which linear Freundlich isotherms are assumed was mathematically equivalent to the two–sites chemical nonequilibrium model. Thus, the two–region model can be viewed as a model where local equilibrium assumption is valid in both phases, but where accessibility of certain sorption sites is diffusion controled.

On a physical basis, if we accept the presence of two water phases it would be more logical to associate with the mobile phase a kinetic adsorption model since the instantaneous equilibrium assumption is likely to be violated in this zone, while the hypothesis of local equilibrium at least do not suffer from physical limitations in the immobile zone.

The problem arising when using the two–regions model is the complex dependency of α upon physical conditions such that, shape of immobile regions, flow velocity, diffusion coefficient, etc... This problem can be overcame by assuming that immobile water is located inside geometrically well defined regions delimitated by the macroporosity. Spherical porous blocks or aggregates are one of the most commonly used geometrical conceptualization of the media.

Extension to spherical aggregates

Considering a media made up of uniform spherical aggregates containing the immobile water, the immobile concentration is the average concentration in the aggregates and is given by:

$$C_{im}(z,t) = \frac{3}{a^3} \int_0^a r^2 C_a(z,r,t)\, dr \qquad [3.36]$$

where a is the radius of the aggregates, and C_a is called the local or intraaggregate concentration. Solute transfer inside the aggregates is governed by the diffusion equation expressed in spherical coordinates,

$$R_{im} \frac{\partial C_a}{\partial t} = \frac{D_a}{r^2} \frac{\partial}{\partial r}\left(r^2 \frac{\partial C_a}{\partial r}\right) \qquad r \in [0,a] \qquad [3.37]$$

where D_a is the diffusion coefficient inside the aggregate (e.g. the diffusion coefficient of the soil matrix). At this point equation [3.30] is no longer needed to couple the two phases. The coupling will now occur through the natural boundary conditions arising from this geometrical conceptualization of the medium, for example continuity of the concentration at the interface aggregate–macroporosity. Equations [3.32], [3.36] and [3.37] constitute the transport equations for the spherical aggregates model. This approach could be repeated for any aggregate with a simple geometrical shape. However, a set of general equations can be derived without assuming any special aggregate shapes and then adapted to particular cases.

Derivation of equations for the general case

The sets of equations presented aboved and derived from the two–region physical non–equilibrium model can also be obtained by a straightforward analysis of the physical system. Let us consider a media characterized by a macroporosity, ϵ_m, also called fracture porosity or structural porosity. In our case ϵ_m represents the percentage of the total porosity where the convective transport takes place. We define in addition ϵ_p, the porosity of the immobile zone. ϵ_p can be viewed as the aggregate or porous blocks porosity. Therefore the total

porosity of the system is given by:

$$\epsilon = \epsilon_m + (1-\epsilon_m)\epsilon_p \ . \qquad [3.38]$$

Let us remark that these porosities can be function of depth and will probably for a soil profile depend on parameters such that, flow pattern, water content, etc... The transport equation in the macro–porosity can be written:

$$\epsilon_m \frac{\partial C_m}{\partial t} = \epsilon_m D_m \frac{\partial^2 C_m}{\partial z^2} - \epsilon_m v_m \frac{\partial C_m}{\partial z} + \epsilon_m \Gamma - \lambda \epsilon_m C_m \qquad [3.39]$$

where D_m is the dispersion coefficient and Γ a source/sink term modeling the exchanges between the two phases. Γ is expressed in mass of solute per unit time per unit volume of flowing fluid. λ is a decay constant for radionuclides transport. Let us assume we have a media made up of arbitrarily shaped porous blocks delimitated by a network of "macropores". The term "macropore" is intentionally vague and in fact stands for any kind of void where the convective flow occurs. In addition the size of the porous block is assumed to be small compared to the overall flow domain. We define two functions noted S(z) and S'(z).

S(z) is defined as '*the surface area of porous matrix involved in the exchange process per unit volume of macroporosity at a given depth, z* '.

S'(z) is defined as '*the surface area of porous matrix involved in the exchange process per unit volume of porous matrix at a given depth z*'.

Let us remark that while S(z) depends for a given aggregate shape on the arrangement of these aggregates, S'(z) is a more intrensic property only related to the shape and volume of the aggregates. Let $<\nabla C_p>$ denote the average gradient at the interface macro– micro–porosity at a depth z. Then if, D_p is the diffusion coefficient of the porous blocks and C_p the concentration profile in the porous matrix, the sink term, Γ, is given by

$$\Gamma = S(z)\epsilon_p D_p <\nabla C_p> \ . \qquad [3.40]$$

The problem when using this expression and some geometrical shape for the aggregates is that the function S(z) which depends upon their arrangement is not easily evaluated. The idea is to use S'(z) which is more intrinsically related to the shape of the porous blocks and therefore easily evaluated. Let us consider a unit volume of porous matrix noted, Ω. Inside this block, solute movement is controlled by the diffusion equation written:

$$\epsilon_p \frac{\partial C_p}{\partial t} = \mathrm{div}(\epsilon_p D_p \overrightarrow{\mathrm{grad}}\, C_p) \ . \qquad [3.41]$$

Let $\overline{C}_p$ denotes the average concentration inside the porous blocks at the depth z. Integrating each sides of the previous equation over Ω and applying the divergence theorem give,

$$\epsilon_p \frac{\partial \overline{C}_p}{\partial t} = \int_{\partial\Omega} \vec{F}.\vec{n}\ d\gamma = S'(z)<\vec{F}.\vec{n}> \qquad [3.42]$$

where F is the flux defined along $\partial\Omega$ by:

$$\vec{F} = \epsilon_p D_p \vec{\nabla} C_p \Big|_{\partial\Omega} \qquad [3.43]$$

and $\langle \vec{F}.\vec{n} \rangle$ is the average value of the scalar product $\vec{F}.\vec{n}$ over $\partial\Omega$. With the assumption that the porous blocks are small compared to the macropore flow characteristic length, $\vec{F}$ is taken constant over a matrix block. So we obtain,

$$\epsilon_p \frac{\partial \overline{C}_p}{\partial t} = S'(z) \| \vec{F}(z) \| . \qquad [3.44]$$

assuming that $\vec{F}$ and $\vec{n}$ are colinear. We have already derived the following expression for Γ,

$$\Gamma = S(z) \| \vec{F}(z) \| \qquad [3.45]$$

therefore combining with equation [3.44] we obtain,

$$\Gamma = \frac{S(z)}{S'(z)} [\epsilon_p \frac{\partial \overline{C}_p}{\partial t}] . \qquad [3.46]$$

Let us consider the ratio $S(z)/S'(z)$. Considering a volume V_t of the overall flow domain at the depth z, we can write

$$S(z) = \frac{S_m}{V_m} \quad \text{and} \quad S'(z) = \frac{S_m}{V_r} \qquad [3.47]$$

where S_m is the exchange surface associated to the volume of macropore V_m and V_r the volume of the porous block associated with S_m. Therefore, $S(z)/S'(z) = V_r/V_m$ which can also be written

$$S(z)/S'(z) = (V_t - V_m)/V_m = 1/\epsilon_m - 1 . \qquad [3.48]$$

Hence, the following expression is derived for Γ,

$$\Gamma = \frac{1 - \epsilon_m}{\epsilon_m} [\epsilon_p \frac{\partial \overline{C}_p}{\partial t}] . \qquad [3.49]$$

Combining this expression with equation [3.39], the following form for the transport equation in the macroporosity is obtained,

$$\epsilon_m \frac{\partial C_m}{\partial t} + (1-\epsilon_m)\epsilon_p \frac{\partial \overline{C}_p}{\partial t} = \epsilon_m D_m \frac{\partial^2 C_m}{\partial z^2} - \epsilon_m v_m \frac{\partial C_m}{\partial z} - \lambda \epsilon_m C_m . \qquad [3.50]$$

Remark that $(1-\epsilon_m)\epsilon_p$ is in fact the porosity of the immobile phase as defined by van Genuchten and Wierenga (1976). Thus, this formulation (Eq. [3.39]) and the one presented before, Eq. [3.32], are equivalent.

The formulation explicitely involving the fluxes at the interface to express the exchange term, has the advantage to be closer to the physics of the phenomena and may be more immediately understood than the one using the average concentration in the porous blocks. On an other hand, as remarked by **Huyakorn et al. (1983b)**, when numerical solutions are required by the complexity of the problem, gradients evaluation at the boundary of the porous blocks introduces some errors. This does not constitute a problem when analytical solutions are sought. We must also remark that for the cases of a single fracture or macropore in a semi–infinite medium, it is impossible to define a function S'(z). S(z) only can be defined. The formulation presented before, eq. [3.32], and resulting from the application of the divergence theorem has the advantage to define the sink term as the time derivative of an integral which can be ~~precisely~~ evaluated and which gives a value very close to the true one since the numerical schema solving the diffusion equation can be expected to globaly conserve the mass.

In opposition to the two–region physical non–equilibrium model where the retardation factor is defined on a mass basis, (eq. [3.24]), it can now for the mobile phase be defined as a "face retardation factor", accounting for solute adsorption on the interface micro– macroporosity. Assuming linear reversible and instantaneous equilibrium, the time derivative of the adsorption term can be written,

$$\frac{\partial S_m}{\partial t} = K_f S(z) \frac{\partial C_m}{\partial t} \qquad [3.51]$$

where S_m is defined as a mass of solute per unit area. Therefore, the retardation factor is given by,

$$R = \epsilon_m + S(z)K_f = \epsilon_m + \frac{1 - \epsilon_m}{\epsilon_m} S'(z)K_f \qquad [3.52]$$

where K_f is the surface equilibrium constant. The same approach to define the retardation factor was used by **Tang et al. (1981)**, **Sudicky and Frind (1982)**, **Neretnieks et al. (1982)** for plane symmetry problems (transport in pane cracks), **Hodgkinson and Lever (1983)** for a problem with cylindrical symmetry, **Rasmuson (1984)**, **Neretnieks and Rasmuson (1984)**, **Moreno and Rasmuson (1986)** for spherical symmetry problems (transport around spherical particles). However it seems that nonequilibrium conditions will prevail most of the time in the mobile phase. Therefore, adsorption at the interface should probably be modeled by a kinetic equation. By analogy with [3.20] one could define the following adsorption model

$$\frac{\partial S_m}{\partial t} = \alpha[K_f C_m - S_m]$$

Inside the immobile zone, intraaggregate water, the assumption of local equilibrium is probably valid and a linear or nonlinear isotherm derived from batch experiments can be used. A linear or nonlinear retardation factor will result for the immobile region.

During derivation of equation [3.50], no assumptions have been made regarding the geometry of the porous blocks. However, in the following and in order to solve the diffusion equation [3.41], the regions where water is supposed to be immobile are given a geometrically simple shape. Usually, rectangular aggregates, cylindrical aggregates, and spherical aggregates are considered,

leading to respectively the plane, cylindrical and spherical symmetries for the diffusion phenomena inside the aggregates. The diffusion equation [3.41] can now be written

$$\epsilon_p \frac{\partial C_p}{\partial t} = \frac{1}{r^i} \frac{\partial}{\partial r} (r^i \epsilon_p D_p \frac{\partial C_p}{\partial r}) \qquad [3.53]$$

where $i = 0,1,2$ for, the plane, cylindrical and spherical symmetries, respectively. The average concentration over the porous blocks will then be defined according to the symmetry of the blocks. If adsorption on the solid phase occurs, the retardation factor, R_p, will be defined in the usual way (bulk density basis), assuming a linear isotherm and instantaneous and reversible equilibrium.

$$R_p = \epsilon_p + \rho_b K_m \qquad [3.54]$$

Direct coupling of both phases

As presented before for the case of spherical aggregates derived from the two–region model, the coupling between equation [3.53] and equation [3.50] can be modeled by a Dirichlet condition simply stating the continuity of the concentration at the interface, van Genuchten (1985a,b). However, an other coupling approach assuming the presence of a liquid film surrounding the particles and acting as an impedance or boundary layer is also possible, Rosen (1952). (See below, *Another coupling approach*).

For the three kinds of aggregates referred above and assuming linear (N=1) Freundlich adsorption isotherms, the set of equations in normalized variables is as follows,

$$\beta R \frac{\partial C_m}{\partial T} + (1-\beta) R \frac{\partial C_{im}}{\partial T} = \frac{1}{P} \frac{\partial^2 C_m}{\partial Z^2} - \frac{\partial C_m}{\partial Z} \qquad Z \in [0,1] \qquad [3.55]$$

$$\frac{\partial C_a}{\partial T} = \frac{\gamma_s}{\rho^i} \frac{\partial}{\partial \rho} (\rho^i \frac{\partial C_a}{\partial \rho}) \qquad \rho \in [0,1] \qquad [3.56]$$

$$C_{im} = (i+1) \int_0^1 \rho^i C_a(\rho)\, d\rho \qquad [3.57]$$

where i=0,1,2 for respectively plane, cylindrical and spherical aggregates. The dimensionless parameters are as follows,

$$T = \frac{\theta_m V_m t}{\theta L} \qquad Z = \frac{z}{L} \qquad [3.58a,b]$$

$$P = \frac{V_m L}{D_m} \qquad \rho = \frac{r}{a} \qquad [3.59a,b]$$

$$\gamma_s = \frac{D_a \theta L}{a^2 \theta_m V_m R_{im}} \qquad \beta = \frac{\theta_m R_m}{\theta_m R_m + \theta_{im} R_{im}} = \frac{\theta_m R_m}{\theta R} \qquad [3.60a,b]$$

$$\phi = \frac{\theta_m}{\theta} \qquad R = \phi R_m + (1-\phi) R_{im} \qquad [3.60c,d]$$

where T is the number of pore volumes leached through a soil profile or soil column of length L, P is a Peclet number, β is a dimensionless partitioning coefficient, and R is the total retardation factor of the soil profile. R_m and R_{im} have already been defined, (eq.[3.31] with N=1). All the concentrations are assumed to be in dimensionless form: $C = (C-C_i)/(C_0-C_i)$, where C_0 and C_i respectively denote initial and input concentrations. a alternatively denotes the half width of rectangular aggregates, or the radius of spherical or cylindrical aggregates. Note that in order to be able to use a one–dimensional equation for the diffusion inside the aggregates, one must assume that the bases of rectangular and cylindrical aggregates are sealed and thus do not participate in the exchange process. Remark also that the equations for rectangular aggregates and for a single or a set of regularly spaced plane cracks are identical. The formulation derived above can also be used for solute transport modeling in cylindrical macropores surrounded by a soil matrix of finite radius, van Genuchten et al. (1984). In that case, the average concentration in the soil matrix is given by,

$$C_{im} = \frac{2}{\rho_0^2 - 1} \int_1^{\rho_0} \rho C_a \, d\rho \qquad [3.61]$$

where ρ_0 is the ratio between the radius of the soil column and the radius of the macropore. All these equations and useful parameters are summarized in Tab. 3.1. Before giving the boundary conditions associated with these equations we first present an other way to couple the respective transport equations for the two regions.

An other way to couple macro– and micro–porosity.

The problem defined above first appeared in the chemical engineering literature, Rosen (1952), under a slightly different form for transport modeling through beds made up of spherical particles. In that work the dispersive term in equation [3.55] was neglected, but the presence of a thin liquid film surrounding the particles and acting as an impedance was accounted for. Later, Babcock et al. (1966) gave a solution of the problem including the dispersive term. This formulation of the problem is also used by Rasmuson and Neretnieks (1980, 1981), Rasmuson (1981b, 1984, 1985a,b). Their set of equations is as follows:

$$\frac{\partial C}{\partial t} + v \frac{\partial C}{\partial z} - D \frac{\partial^2 C}{\partial z^2} = -(\partial q/\partial t)/m \qquad [3.62]$$

$$\partial q_i/\partial t = D_s(\partial^2 q_i/\partial r^2 + \frac{2}{r} \partial q_i/\partial r) \qquad [3.63]$$

where m is given by $m=\epsilon/(1-\epsilon)$, and ϵ is the macroporosity, also referred in the chemical engineering literature as the porosity of the particle bed. The local concentration inside the particles is noted, q_i, and the mean concentration is noted q. Boundary and initial conditions are as follows,

$$C(z,0)=0 \qquad C(0,t)=C_i \qquad C(\infty,t)=0 \qquad [3.64a,b,c]$$

$$q_i(r,z,0)=0 \qquad \partial q_i/\partial r\big|_{r=0} = 0 \qquad [3.65a,b]$$

$$q_i(b,z,t)=q_s(z,t) \qquad [3.66]$$

and where b is the radius of the spheres, and $q_s(z,t)$ is given by:

$$\frac{\partial q}{\partial t} = \frac{3h}{b}(C-q_s/K) \; . \qquad [3.67]$$

Equation [3.67] links the two transport equations and states that the rate of variation of the mean concentration inside a particle is equal to the solute transport rate through the liquid film surrounding that particle. In this equation, K is an equilibrium constant and h is a parameter characterizing the average diffusive property of the liquid film. In particular if the liquid film surrounding each particle is not uniform, due to the flow pattern for example, the coefficient h can be chosen such that the previous equation averages the phenomena over the surface of the particle. The boundary layer introduced with this way to coupled the two phases is probably more physically founded than the simple continuity of the concentration which implicitely assumes that there are no cros–gradients of concentration in the macropore continnum. One can certainly hypothezise by analogy with the case of a single pore that there is a radial velocity gradient in the convective flow and that due to various physical and/or chemical phenomena it exists a thin film of water surrounding any aggregate through which solute must travel by diffusion before reaching the porous matrix.

It is also well known that in aggregated or fractured media, regarding either water or solute transport, the surface of the macroporosity may have, due to physical alteration or coating with highly reactive materials, transport properties quite different from the rest of the porous matrix. This differentiation leads in hydrogeological models to the introduction of a thin layer known as "fracture skin". Retardation effects in transport from the cracks to the porous matrix due to this layer are known as "skin effects". These effects are usually modeled by a first order equation. Equation [3.67] can be viewed as one of these. Relevant litterature for skin effects have been recently surveyed by Moench (1984).

So, the main difference with the previous model assuming the continuity of the concentration at the interface is the way both transport equations are coupled. Remark that no retardation factors are included in these equations. This last approach certainly more closely approximates the reality and might be offering a little more flexibility but has the disadvantage to introduce a parameter, h, which can probably not be independantly estimated or measured. Solutions of this last system can be obtained analytically or by numerical techniques.

Boundary Conditions

Boundary and initial conditions are now required for equations [3.55] and [3.56]. Let's first consider the CDE, Eq. [3.55]. Many papers deal with the type of boundary conditions to be imposed at the top or at the bottom of a soil column when modeling solute transport. Usually one have the choice between a Dirichlet and a third type condition. This problem has already been adressed in the previous paragraph. For a contaminant transport simulation model a comparison between the different porous matrix concentration profiles resulting from using a first–type or a third–type boundary condition is given by Moreno and Rasmuson (1986). As previously pointed out, it is now accepted that for the formulation using a volume–averaged concentration, the boundary condition really modeling

the physical phenomena at the top of the profile is one of the third–type, **Parker and van Genuchten (1984), van Genuchten and Parker (1984).** Expressed in the original variables this boundary condition is:

$$(C_m - \frac{D_m}{V_m}\frac{\partial C_m}{\partial z})_{|z=0} = C_0 \, . \qquad [3.68]$$

In normalized variables the following expression is derived:

$$C_m(0,T) - \frac{1}{P_m}\frac{\partial C_m}{\partial Z}(0,T) = 1 \, . \qquad [3.69]$$

The boundary condition imposed at the bottom of the profile is often that corresponding to a semi–infinite profile:

$$C_m(\infty,T) = 0 \, . \qquad [3.70]$$

When dealing with finite lenght column, the following boundary condition is imposed,

$$\frac{\partial C_m}{\partial Z}_{|Z=1} = 0. \, . \qquad [3.71]$$

This condition comes from the equilibrium equation relating the fluxes inside and outside the column at the outlet. Derivation of this condition has been already discussed. See also **Gaudet (1981)** for a derivation of this condition. The initial condition for equation [3.55] is:

$$C_m(0,Z) = 0. \quad Z \in [0,1] \, . \qquad [3.72]$$

The boundary conditions for the diffusion equation [3.56] modeling the transport inside the aggregates are:

$$C_a(Z,1,T) = C_m(Z,T) \qquad Z \in [0,1] \qquad [3.73]$$

which expresses that there is continuity of the concentration at the interface mobile–immobile water, **van Genuchten et al. (1984), van Genuchten (1985a,b),** and

$$\frac{\partial C_a}{\partial \rho}_{|\rho=0} = 0. \qquad [3.74]$$

expressing that the diffusion process inside the aggregates is symmetrical with respect to center (sphere), axis (cylinder) or symmetry plane (parallelepiped) of the aggregates. The initial condition for the concentration inside the aggregates is also assumed to be:

$$C_a(Z,\rho,0) = 0. \qquad [3.75]$$

which leads in addition to $C_{im}(Z,0)=0$. We have now the system of equations [3.55], [3.56], [3.57], with the boundary conditions [3.69], [3.70] or [3.71], [3.73], [3.74], and the two initial conditions, [3.72] and [3.75].

In the following we present the different analytical solutions proposed in

the literature for the problems described above. Numerical solutions have also been proposed. **Huyakorn et al. (1983b)**, developed a combined finite element, finite difference numerical schema for different geometries of the porous blocks, (slabs and spheres), while **Rasmuson et al. (1982)** used the TRUMP code of **Edwards (1969)** implementing the IFD method, already described in the first part of this report dealing with water flow. More references and details on these numerical solutions are provided in annex, (A2). The popularity of analytical solutions comes from the fact that as long as we are restricted to simple systems, with simple initial and boundary conditions, (typically those of laboratory experiments), they provide the best tool to analyse the physical assumptions at the base of models. Inversely, as soon as it comes to handle complex physical systems with arbitrary boundary and initial conditions, transient flow conditions, or presenting complex chemical processes, numerical approaches constitute the only really available answers. An other problem is the fact that analytical solutions are rapidly reaching a high degree of complexity when including extra processes, like decaying phenomena, or dealing with multi–dimensional problems, thus becoming less easy to handle, to evaluate and to use.

3.3 ANALYTICAL SOLUTIONS

3.3.1 CASE OF SPHERICAL AGGREGATES

We first present the solutions for the case where the particles are assumed to be surrounded by a liquid film, (cf.*An other way to couple macro– and micro–porosity*). Analytical solutions derived for the other coupling approach are presented after.

Solution of Babcock et al. (1966)

This solution is expressed in the form of an infinite integral and corresponds to the problem defined by equations [3.62]–[3.67]. A solution for the same system of equations, but without dispersive term in equation [3.62] was previously given by Rosen (1952). Conditions under which a numerical evaluation of this integral is possible are discussed below.

$$u(z,\theta) = \frac{1}{2} + \frac{2}{\pi}\int_0^\infty \exp-\{\gamma x H_1 + \frac{zD_L}{v^3}[\sigma^2\lambda^4 + \frac{2\sigma\lambda^2 H_2\gamma}{m} + \frac{\gamma^2}{m^2}(H_2^2 - H_1^2)]\}.$$

$$\sin\left\{\sigma\theta\lambda^2 - \gamma x H_2 + \frac{zD_L}{m^2}\left(\frac{2\sigma\lambda^2 H_1\gamma}{m} + \frac{2H_1H_2\gamma^2}{m^2}\right)\right\}\frac{d\lambda}{\lambda} \qquad [3.76]$$

where H_1 and H_2 are given by:

$$H_1(\lambda,\nu) = \frac{H_{d1} + \nu(H_{d1}^2 + H_{d2}^2)}{(1+\nu H_{d1})^2 + (\nu H_{d2})^2}$$

$$H_2(\lambda,\nu) = \frac{H_{d2}}{(1+\nu H_{d1})^2 + (\nu H_{d2})^2}$$

and H_{d1} and H_{d2} are defined by:

$$H_{d1} = \left[\lambda\left(\frac{\sinh 2\lambda + \sin 2\lambda}{\cosh 2\lambda - \cos 2\lambda}\right) - 1\right]$$

$$H_{d2} = \lambda\left(\frac{\sinh 2\lambda - \sin 2\lambda}{\cosh 2\lambda - \cos 2\lambda}\right).$$

γ, θ, σ, ν and x are given by:

$$\gamma = 3D_s K/b^2 \qquad \theta = t - z/v$$

$$\sigma = 2D_s/b^2 \qquad \nu = \gamma b/3h \qquad x = z/mv$$

and the solution $u(z,\theta)$ is the normalized concentration $(C–C_0)/(C_i–C_0)$.

This integral is the product of an decaying exponential with a oscillating

function (sin). Thus, the accuracy of the integration is strongly related to the rate of convergence of the integrand to zero and to the period of the oscillating term. The leading term in the exponential is γx, and mainly controls the rate of convergence to zero.

Solution of Rasmuson et Neretnieks (1980)

An other solution for the same problem has been proposed by **Rasmusson and Neretnieks (1980)**, under a slighly different form. The set of equations is strictly identical to the one given before, Eq. [3.62], [3.63], [3.64], [3.65], [3.66], [3.67]. The solution of **Babcocok et al. (1966)** was found to be limiting for low values of the dispersion coefficient, and to lead to a poor solution at early times. The following solution has served as a basis for subsequent studies.

$$C(z,t)/C_0 = \frac{1}{2} + \frac{2}{\pi}\int_0^\infty \exp\left[\frac{Vz}{2D_L} - z\frac{\sqrt{\sqrt{x'(\lambda)^2+y'(\lambda)^2}+x'(\lambda)}}{\sqrt{2}}\right]\cdot$$

$$\sin\left[\sigma\lambda^2 t - z\frac{\sqrt{\sqrt{x'(\lambda)^2+y'(\lambda)^2}-x'(\lambda)}}{\sqrt{2}}\right]\frac{d\lambda}{\lambda} \qquad [3.77]$$

where

$$x'(\lambda) = \frac{V^2}{4D_L{}^2} + \frac{\gamma}{mD_L}H_1$$

$$y'(\lambda) = \frac{\sigma\lambda^2}{D_L} + \frac{\gamma}{mD_L}H_2$$

and where H_1 and H_2 are as previously given by:

$$H_1(\lambda,\nu) = \frac{H_{d1} + \nu(H_{d1}^2 + H_{d2}^2)}{(1+\nu H_{d1})^2 + (\nu H_{d2})^2}$$

$$H_2(\lambda,\nu) = \frac{H_{d2}}{(1+\nu H_{d1})^2 + (\nu H_{d2})^2}$$

and H_{d1} and H_{d2} by:

$$H_{d1} = \left[\lambda\left(\frac{\sinh 2\lambda + \sin 2\lambda}{\cosh 2\lambda - \cos 2\lambda}\right) - 1\right]$$

$$H_{d2} = \lambda\left(\frac{\sinh 2\lambda - \sin 2\lambda}{\cosh 2\lambda - \cos 2\lambda}\right).$$

The parameters σ, γ, θ, and ν are the same as in the solution of **Babcock et al. (1966)**. **Rasmuson and Neretnieks (1980)** showed that for high values of the

Peclet number (P=zV/D) and disregarding the term of order $1/P^2$ and less the solution of **Babcock et al. (1966)** was obtained. The solution of **Rosen (1952)** (D=0) could be obtained from this approximation by letting $P \to \infty$. A complete derivation of the solution is also given by **Rasmuson and Neretnieks (1980)**.

Solution of Rasmuson (1981)

Following the solution proposed before for a system where no adsorption occurs, **Rasmuson (1981)**, gave the solution for the following system of equations, now accounting for adsorption of the tracer on the solid phase inside the aggegates. The system of equations is as follows,

$$\frac{\partial C}{\partial t} + v\frac{\partial C}{\partial z} - D\frac{\partial^2 C}{\partial z^2} = -(\partial q/\partial t)/m \qquad [3.78]$$

$$\epsilon_p \partial C_p/\partial t + \partial C_s/\partial t = D_s(\partial^2 C_p/\partial r^2 + \frac{2}{r}\partial C_p/\partial r) \qquad [3.79]$$

$$\frac{\partial C_s}{\partial t} = k_{ads}(C_p - C_s/k_a) \qquad [3.80]$$

$$\frac{\partial q}{\partial t} = \frac{3k_f}{b}(C - C_p|_{r=b}) \qquad [3.81]$$

Boundary and initial conditions are as for the previous case, without adsorption, equations [3.64] to [3.66]. It is important to remark that the adsorption rate, eq. [3.80], is modeled by a first–order kinetic process analog to equation [3.20], and therefore that instantaneous local equilibrium (LEA) is not assumed. The analytical solution is as follows,

$$C(z,t)/C_0 = \frac{1}{2} + \frac{2}{\pi}\int_0^\infty \exp\left[\frac{Vz}{2D_L} - z\frac{\sqrt{\sqrt{x'(\lambda)^2+y'(\lambda)^2} + x'(\lambda)}}{\sqrt{2}}\right]\cdot$$

$$\sin\left[\frac{k_{ads}}{k_a}\lambda^2 t - z\frac{\sqrt{\sqrt{x'(\lambda)^2+y'(\lambda)^2} - x'(\lambda)}}{\sqrt{2}}\right]\frac{d\lambda}{\lambda} \qquad [3.82]$$

where

$$x'(\lambda) = \frac{V^2}{4D_L{}^2} + \frac{\gamma}{mD_L}H_1$$

$$y'(\lambda) = \frac{k_{ads}\lambda^2}{k_a D_L} + \frac{\gamma}{mD_L}H_2$$

and where H_1 and H_2 are as previously given by:

$$H_1(\lambda,\nu) = \frac{H_{d1} + \nu(H_{d1}^2 + H_{d2}^2)}{(1+\nu H_{d1})^2 + (\nu H_{d2})^2}$$

$$H_2(\lambda,\nu) = \frac{H_{d2}}{(1+\nu H_{d1})^2 + (\nu H_{d2})^2}$$

H_{d1} and H_{d2} are given by:

$$H_{d1} = \left[\frac{\lambda_2 \sinh 2\lambda_2 + \lambda_1 \sin 2\lambda_1}{\cosh 2\lambda_2 - \cos 2\lambda_1} - 1\right]$$

$$H_{d2} = \left[\frac{-\lambda_1 \sinh 2\lambda_2 + \lambda_2 \sin 2\lambda_1}{\cosh 2\lambda_2 - \cos 2\lambda_1}\right]$$

where

$$\lambda_1 = -\sqrt{\frac{l-c}{2}}$$

$$\lambda_2 = -\sqrt{\frac{l+c}{2}}$$

$$l = \sqrt{c^2 + d^2}$$

$$c = \frac{b^2 k_{ads}}{D_s \epsilon_p} \frac{\lambda^4}{1 + \lambda^4}$$

$$d = \frac{b^2 k_{ads}}{D_s k_a}\left[1 + \frac{k_a}{\epsilon_p} \frac{\lambda^4}{1 + \lambda^4}\right]\lambda^2$$

A straitghforward extension of this solution to radionuclides transport, with decaying constant, λ_d, is given by **Rasmuson (1981)**. Given the properties of Laplace transform, and if the input boundary condition is $C(0,t) = C_1 \exp(-\lambda_d t)$, it comes,

$$(C/C_0)\big|_{\lambda_d>0} = e^{-\lambda_d t}(C/C_0)\big|_{\lambda_d=0} \qquad [3.83]$$

A different solution is obtained by **Rasmuson (1984)** if a first–type input boundary condition is used, $C(t,0) = C_1$

Extension to a two–dimensional system.

Assuming axi–cylindrical symmetry of the solute transport process, a disk surface source of finite radius *a* with a first–type boundary condition, and spherical particles, the following system of equations is obtained:

$$\frac{\partial C}{\partial t} + v\frac{\partial C}{\partial z} - D_l \frac{\partial^2 C}{\partial z^2} - D_t \frac{1}{r}\frac{\partial}{\partial r}\left(r \frac{\partial C}{\partial r}\right) = -(\partial q/\partial t)/m \qquad [3.84]$$

$$\partial q_i/\partial t = D_s(\partial^2 q_i/\partial x^2 + \frac{2}{x}\,\partial q_i/\partial x) \qquad [3.85]$$

with initial and boundary conditions as follows,

$$C(r,0,t) = C_0 \quad r \le a$$

$$C(r,0,t) = 0 \quad r \ge a$$

$$C(r,\infty,t) = 0$$

$$\partial C(0,z,t)/\partial r = 0$$

$$C(\infty,z,t) = 0$$

$$C(r,z,0) = 0$$

$$q_i(b,r,z,t) = q_s(r,z,t)$$

$$\frac{\partial q}{\partial t} = \frac{3k_f}{b}\left(C - \frac{q_s}{K}\right)$$

$$q_i(x,r,z,0) = 0.$$

Remark that in this formulation one have $q_i = \epsilon_p C_p + C_s$. Remark also that a Linear Freundlich adsorption isotherm is used and that local equilibrium is assumed. The analytical solution is as follows

$$C(z,t)/C_0 = \frac{1}{2}\exp\left[\frac{Vz}{2D_L}\right]\int_0^\infty \exp\left[-z\left[\frac{V^2}{4D_1^2} + \frac{D_t}{D_1 a^2}\xi^2\right]^{1/2}\right] J_0\left(\frac{r}{a}\xi\right)J_1(\xi)\,d\xi +$$

$$\exp\left[\frac{Vz}{2D_L}\right]\frac{2}{\pi}\int_0^\infty J_0\left(\frac{r}{a}\xi\right)J_1(\xi)\left\{\int_0^\infty \exp\left[-z\left[\frac{(x'(\lambda,\xi)^2+y'(\lambda)^2)^{1/2} + x'(\lambda,\xi)}{\sqrt{2}}\right]^{1/2}\right]\right.$$

$$\left.\sin\left[\sigma\lambda^2 t - z\left[\frac{(x'(\lambda,\xi)^2+y'(\lambda)^2)^{1/2} - x'(\lambda,\xi)}{2}\right]^{1/2}\right]\frac{d\lambda}{\lambda}\right\} \qquad [3.86]$$

with

$$x'(\lambda,\xi) = \frac{V^2}{4D_1^2} + \frac{\gamma}{mD_1}H_1(\lambda) + \frac{D_t}{D_1 a^2}\xi^2$$

$$y'(\lambda) = \frac{\sigma\lambda^2}{D_1} + \frac{\gamma}{mD_1}H_2(\lambda)$$

$$H_1(\lambda) = \frac{H_{d1} + \nu(H_{d1}^2 + H_{d2}^2)}{(1+\nu H_{d1})^2 + (\nu H_{d2})^2}$$

$$H_2(\lambda,\nu) = \frac{H_{d2}}{(1+\nu H_{d1})^2 + (\nu H_{d2})^2}$$

and H_{d1} and H_{d2} are given by:

$$H_{d1} = \lambda \left[\frac{\sinh 2\lambda + \sin 2\lambda}{\cosh 2\lambda - \cos 2\lambda}\right] - 1$$

$$H_{d2} = \lambda \left[\frac{\sinh 2\lambda - \sin 2\lambda}{\cosh 2\lambda - \cos 2\lambda}\right]$$

J_0 and J_1 are Bessel functions of first kind and of order 0 and 1 respectively. Remark that the numerical evaluation of the solution requires to calculate a double integral whose integrand is a oscillatory function. When the parameters are such that the period of the integrand is short, classical numerical methods to evaluate this integral fail to give an accurate solution. In that case a special integration algorithm must be used. This one is given later. When facing such problems and given the difficulty there is to handle such complicated analytical solutions, numerical inversion techniques for Laplace transforms may appear more appropriated.

Solution of van Genuchten (1985a)

Previously given solutions are for a Dirichlet condition at the inlet, which means according to the remarks previously made that corresponding solutions may be used to calculate breakthrough curves but does not give the concentration profiles in terms of volume–averaged concentration. We now consider the problem defined by equations [3.55], [3.56], [3.57] where (i=2), with the boundary conditions [3.69], [3.70], [3.73], [3.74], and initial conditions [3.72], [3.75]. Let us recall some of the important hypothesis included.

(1) A third type input boundary condition and a semi infinite profile are the boundary conditions for [3.55],

(2) There is continuity of the concentration at the interface micro–macro–porosity,

(3) Local equilibrium is assumed when modeling the sorption process.

An analytical solution giving the volume–averaged concentration profile in the mobile phase was derived by van Genuchten (1985a). The solution is as follows,

$$C_m(Z,T) = \frac{1}{2} + \frac{2P}{\pi}\int_0^\infty \frac{\exp(\frac{PZ}{2} - z_p Z)}{[(\frac{P}{2} + z_p)^2 + z_m^2]} [(\frac{P}{2} + z_p)\sin(2\gamma\lambda^2 T - z_m Z) - z_m \cos(2\gamma\lambda^2 T - z_m Z)] \frac{d\lambda}{\lambda} \qquad [3.87]$$

where

$$z_p = [\tfrac{1}{2}(r_p + \Omega_1)]^{1/2} \qquad z_m = [\tfrac{1}{2}(r_p - \Omega_1)]^{1/2}$$

$$r_p = (\Omega_1^2 + \Omega_2^2)^{1/2}$$

$$\Omega_1 = \frac{P^2}{4} + \gamma P(1-\beta)R\Psi_1 \qquad \Omega_2 = 2\gamma P\beta R\lambda^2 + \gamma P(1-\beta)R\Psi_2$$

$$\Psi_1 = \frac{3\lambda(\sinh 2\lambda + \sin 2\lambda)}{\cosh 2\lambda - \cos 2\lambda} - 3$$

$$\Psi_2 = \frac{3\lambda(\sinh 2\lambda - \sin 2\lambda)}{\cosh 2\lambda - \cos 2\lambda}$$

In his paper, van Genuchten (1985a) remarked that if one is interested in predicting the effluent concentration for finite lenght columns (Z=1), the following expression giving the flux–average concentration at the outlet should be used.

$$C_e(T) = \frac{1}{2} + \frac{2}{\pi}\int_0^\infty \exp(\frac{P}{2} - z_p)\,\sin(2\gamma_s\lambda^2 T - z_m)\,\frac{d\lambda}{\lambda} \qquad [3.88]$$

---

which is the solution of Rasmuson and Neretnieks (1980) evaluated at (Z=1). Notice also that if $R = R_m = R_{im} = 1$, then we have the solution for a non–reactive tracer.

The concentration profile in the immobile phase can be obtained by first calculating the concentration profiles inside the aggregates, and then evaluating equation [3.57]. Analytical solutions for the diffusion equation applied to aggregates of different shapes are readily available for constant boundary conditions. For time dependant boundary conditions, in our case given by the concentration in the mobile phase, *Duhamel's* theorem can be applied, and we have, Rosen (1952),

$$C_a(\rho,z,T) = \int_0^\infty C_m(z,\lambda)\,\frac{\partial}{\partial T}H(\rho,T-\lambda)\,d\lambda \qquad [3.89]$$

where H(r,t) is the solution of the diffusion problem for a boundary condition, $C_a(0,z,T) = 1$ and a initial condition, $C_a(\rho,z,0) = 0$. For spherical aggregates, $H(\rho,t)$ is as follows,

$$H(\rho,T) = 1 - 2\sum_{n=1}^{\infty}\frac{(-1)^{n+1}}{\sigma_n\rho}\sin(\sigma_n\rho)\exp(-D_s\sigma_n^2 T) \qquad [3.90]$$

where $\sigma_n = n\pi/a$ and in fact $\sigma_n = n\pi$ since in that case $a = 1$. The derivative

$\partial H/\partial t$ is calculated from equation [3.90], and used in [3.89], thus giving,

$$C_a(\rho,z,T) = 2D_s \sum_{n=1}^{\infty} (-1)^{n+1} \sigma_n \frac{\sin(\sigma_n \rho)}{\rho} \int_0^T C_m(z,\lambda) \exp[-D_s \sigma_n^2 (T-\lambda)] d\lambda \qquad [3.91]$$

This expression is used in equation [3.57] to evaluate the concentration in the immobile phase. After integration it follows,

$$C_{im}(z,T) = 6D_s \sum_{n=1}^{\infty} \int_0^T C_m(z,\lambda) \exp[-D_s \sigma_n^2 (T-\lambda)] d\lambda \qquad [3.92]$$

The concentration of the adsorbed phase is easily obtained using adsorption isotherms.

Though, previous solutions are given for a constant input rate, solutions can easily be derived for a finite length pulse input. In this case inlet boundary conditions are, either

$$\underline{\text{First–Type}}: \begin{cases} C(0,t) = 1 & \text{for} \quad 0 \le t < t_0 \\ C(0,t) = 0 & \text{for} \quad t_0 \le t \end{cases}$$

$$\underline{\text{Third–Type}} \quad (C_m - \frac{1}{P} \frac{\partial C_m}{\partial x}) = \begin{cases} 1 & 0 \le t \le t_0 \\ 0 & t \ge t_0 \end{cases}$$

Given the properties of the Laplace transform, the solution for a square pulse is,

$$C_f(z,t) = C(z,t) - C(z,t-t_0)H(t-t_0) \qquad [3.93]$$

where H is the Heaviside's step function, C the solution for constant input rate, and C_f the solution for the finite lenght square pulse. Notice that in fact C_f represents either a flux–averaged concentration (first–type boundary condition), or a volume–averaged concentration (third–type boundary condition).

3.3.2 PLANAR VOIDS AND RECTANGULAR AGGREGATES

The case of planar voids received a great deal of attention in the literature. Contamination risk assessment for nuclear wastes repositories in fractured rocks, induced the first studies and numerical models, **Grisak and Pickens (1980), Grisak et al. (1980), Tang et al. (1981), Sudicky and Frind (1982), Neretnieks et al. (1982), Rasmuson et al. (1982), Huyakorn et al. (1983b), Hodgkinson and Lever (1983), Neretnieks and Rasmuson (1984), Moreno et al. (1985), Moreno and Rasmuson (1986).** The fact that shrinking cracks in clay

soils are geometrically more or less like planar voids, might also increase the popularity of this approach in the field of soil physics. Rectangular aggregates have been considered by **van Genuchten (1985a,b)** in soil leaching models. Numerical as well as analytical solutions have been derived for solute transport through rectangular voids, usually planar cracks, or around rectangular aggregates. Let us first consider the case of transport through planar cracks.

The set of equations modeling solute transport in a plane fissure with simultaneous diffusion and adsorption in the porous matrix, is in fact constituted by equations [3.39] where ϵ_m is taken equal to 1, equation [3.40] where S is easily calculated to be $1/b$ if $2b$ is the aperture of the crack, and equation [3.41] expressed in plane coordinates (1–D). The retardation factor accounting for tracer adsorption at the surface of the crack is defined by equation [3.52a]. Inside the porous matrix the retardation factor is defined by [3.54]. Usually, continuity of the concentration is assumed at the surface of the cracks, **Tang et al. (181), Sudicky and Frind (1982), Neretnieks and Rasmuson (1984), Moreno et al. (1985), Moreno and Rasmuson (1986).** The skin effect could also be considered. Analytical solutions have been derived for the case of a single crack, **Tang et al. (1981)**, and for a set of regularly spaced cracks, **Sudicky and Frind (1982)**. In both cases a first–type boundary conditions and a semi infinite profile are assumed boundary conditions for equation [3.39]. For the case of a single fracture an infinite porous matrix is assumed, while a natural no–flux condition is imposed halfway between two cracks for a set of regularly spaced cracks. Let us remark in addition that the solutions given below correspond to transport equations including a decaying term, λ.

Plane Fracture in a semi–infinite medium. (Tang et al. 1981)

Concentration profile in the fracture.

$$\frac{C}{C_0} = \frac{\exp(\nu z)}{\sqrt{\pi}} \int_l^\infty \exp\left[-\xi^2 - \frac{\nu^2 z^2}{4\xi^2}\right] \exp(-\eta z^2)$$

$$\left\{\exp\left[-\sqrt{\lambda}\, Y\right] \operatorname{erfc}\left[\frac{Y}{2T} - \sqrt{\lambda}\, T\right] + \exp\left[\sqrt{\lambda}\, Y\right] \operatorname{erfc}\left[\frac{Y}{2T} + \sqrt{\lambda}\, T\right]\right\} d\xi \qquad [3.94]$$

where

$$Y = \frac{\nu^2 \beta^2 z^2}{4A\xi^2}$$

$$\nu = v/2D \; ; \; \beta^2 = 4RD/v^2 \; ; \; \eta = \frac{\lambda R}{4D\xi^2}$$

$$T = \left[t - \frac{Rz^2}{4D\xi^2}\right]^{1/2}$$

$$A = \frac{bR}{\sqrt{R_p D_p}}$$

where D is the dispersion coefficient in the fracture, R the face retardation factor,

D_P the diffusion coefficient of the porous matrix, R_P the bulk retardation factor, z the depth, t the time, and λ the decay constant.

Concentration profile in the porous matrix

The concentration profile in the porous matrix at a given depth z and time T is then given by:

$$\frac{C'}{C_0} = \frac{\exp(\nu z)}{\sqrt{\pi}} \int_l^\infty \exp\left[-\xi^2 - \frac{\nu^2 z^2}{4\xi^2}\right] \exp(-\eta z^2)$$

$$\left\{\exp\left[-\sqrt{\lambda}\, Y'\right] \operatorname{erfc}\left[\frac{Y'}{2T} - \sqrt{\lambda}\, T\right] + \exp\left[\sqrt{\lambda}\, Y'\right] \operatorname{erfc}\left[\frac{Y'}{2T} + \sqrt{\lambda}\, T\right]\right\} d\xi \quad [3.95]$$

where Y' is then defined by:

$$Y' = \frac{\nu^2 \beta^2 z^2}{4A\xi^2} + B(x-b) \qquad B = \sqrt{R_a/D_a}$$

Other parameters, ν,η, and T being already defined above.

Case without dispersion

A simplified solution, assuming no dispersion (D=0 in equation [3.39]); flow dominated by convection; is as follows for the concentration in the fracture, Tang et al. 1981,

$$\frac{C}{C_0} = \frac{1}{2} \exp\left(-\frac{\lambda R z}{v}\right)\left[\exp\left(-\frac{\sqrt{\lambda} R z}{vA}\right) \operatorname{erfc}\left(\frac{z}{2vAT'} - \sqrt{\lambda} T'\right) + \exp\left(\frac{\sqrt{\lambda} R z}{vA}\right) \operatorname{erfc}\left(\frac{z}{2vAT'} + \sqrt{\lambda} T'\right)\right] \qquad T'>0 \quad [3.96]$$

where $T' = \left[t - \frac{Rz}{v}\right]^{1/2}$, and the concentration in the porous blocks is given by:

$$\frac{C'}{C_0} = \frac{1}{2} \exp\left(-\frac{\lambda R z}{v}\right)\left[\exp\left(-\sqrt{\lambda}\, W\right) \operatorname{erfc}\left(\frac{W}{2T'} - \sqrt{\lambda} T'\right) + \exp\left(\sqrt{\lambda}\, W\right) \operatorname{erfc}\left(\frac{W}{2T'} + \sqrt{\lambda} T'\right)\right] \qquad T'>0 \quad [3.97]$$

$C'/C_0=0$ for $T'<0$, and $W = Rz/(vA) + B(x-b)$. Remark that when no dispersion is accounted for, no integral evaluation is required to calculated the solution.

Steady–sate case.

The steady state solution of the general problem is also obtained. This one is useful for prediction of maximun penetration distances of the tracer inside the porous blocks. Remark that a steady–state solution can be derived because a decay term, λ, is included in the transport equation. Concentration profiles in the fracture and in the matrix are respectively given by:

$$\frac{C}{C_0} = \exp\left\{\left[v - \left[v^2 + \frac{\psi}{D}\right]^{1/2}\right]z\right\}$$

$$\frac{C'}{C_0} = \exp\left\{\left[v - \left[v^2 + \frac{\psi}{D}\right]^{1/2}\right]z\right\} \exp\left\{ - \left[\frac{\lambda}{D'}\right]^{1/2}(x-b)\right\} \qquad [3.98]$$

where $\psi = \lambda + \frac{\theta(D'\lambda)^{1/2}}{b}$.

Regularly spaced fractures

Let us assume that we have a media made up of porous blocks with width 2B separated by cracks with aperture 2b. Equations for this system are quite the same as for the previous case. The only difference is the boundary condition used at r=B for the diffusion equation in the porous blocks. Instead of a semi–infinite horizontal profile, we impose now, due to the symmetry of the problem, a no–flux condition at r=B. Analytical solutions for this new set of equations were given by, Sudicky and Frind (1982).

Solution in the fracture, Sudicky and Frind (1982)

Concentration profile in the fracture.

$$\frac{C}{C_0} = \frac{2\ \exp(\nu z)}{(\pi)^{3/2}} \int_l^\infty \exp\left[-\xi^2 - \frac{\nu^2 z^2}{4\xi^2} - \frac{R\lambda z^2}{4D\xi^2}\right] \int_0^\infty \frac{\epsilon}{\lambda^2+\epsilon^4/4} \exp(\epsilon_R).$$

$$\left\{\exp(-\lambda T)\left[\frac{\epsilon^2}{2}\sin(\epsilon_1)_{|T} - \lambda\cos(\epsilon_1)_{|T}\right] + \frac{\epsilon^2}{2}\sin(\Omega) + \lambda\cos(\Omega)\right\} d\epsilon\ d\xi \qquad [3.99]$$

where

$$l = \frac{z}{2}\left[\frac{R}{Dt}\right]^{1/2}$$

$$T = t - \frac{Rz^2}{4D\xi^2}$$

$$\Omega = \frac{Y\epsilon}{2}\left[\frac{\sinh(\sigma\epsilon) + \sin(\sigma\epsilon)}{\cosh(\sigma\epsilon) + \cos(\sigma\epsilon)}\right]$$

$$\epsilon_R = \frac{Y\epsilon}{2}\left[\frac{\sinh(\sigma\epsilon) - \sin(\sigma\epsilon)}{\cosh(\sigma\epsilon) + \cos(\sigma\epsilon)}\right]$$

$$\epsilon_1 = \frac{\epsilon^2 t}{2} - \frac{Y\epsilon}{2}\left[\frac{\sinh(\sigma\epsilon) + \sin(\sigma\epsilon)}{\cosh(\sigma\epsilon) + \cos(\sigma\epsilon)}\right]$$

$$Y = \frac{\nu^2 k^2 z^2}{4A\xi^2} \qquad \nu = v/2D$$

$$k^2 = 4RD/v^2 \qquad A = \frac{bR}{\theta\sqrt{R'D'}}$$

$$\sigma = G(B-b) \qquad G = (R'/D')^{1/2}$$

Concentration profile in the porous blocks.

The concentration profile in the porous matrix is also given by **Sudicky and Frind (1982).**

$$\frac{C'}{C_0} = \frac{2\ \exp(\nu z)}{\sigma^2\sqrt{\pi}} \int_l^\infty \exp\left[-\xi^2 - \frac{\nu^2 z^2}{4\xi^2} - \frac{R\lambda z^2}{4D\xi^2}\right] \int_0^\infty \frac{\epsilon}{\lambda^2+\epsilon^4/4} \exp(\epsilon_R).$$

$$\sum_{n=0}^{\infty} (-1)^n(2n+1)\cos\left[\frac{(2n+1)\pi(B-x)}{2(B-b)}\right].\left[\frac{\exp(-\lambda T)}{\pi^4(2n+1)^4/16\sigma^4 + \epsilon^4/4}\right.$$

$$\left\{\frac{\epsilon^2}{2}\left[\frac{\pi^2(2n+1)^2}{4\sigma^2}\sin(\epsilon_1)_{|T} - \frac{\epsilon^2}{2}\sin(\epsilon_1)_{|T}\right]\right.$$

$$-\lambda\left[\frac{\pi^2(2n+1)^2}{4\sigma^2}\cos(\epsilon_1)_{|T} + \frac{\epsilon^2}{2}\sin(\epsilon_1)_{|T}\right] + \exp\left[-\frac{\pi^2(2n+1)^2 t}{4\sigma^2}\right]$$

$$\left.\left[\frac{\epsilon^4}{4}\cos(\Omega') + \frac{\pi^2(2n+1)^2\epsilon^2}{8\sigma^2}\sin(\Omega') + \frac{\pi^2(2n+1)^2\lambda}{4\sigma^2}\cos(\Omega') - \frac{\lambda\epsilon^2}{2}\sin(\Omega')\right]\right\}$$

$$\left.\left. + \frac{4\sigma^2}{\pi^2(2n+1)^2}\left\{1 - \exp\left[-\frac{\pi^2(2n+1)^2 t}{4\sigma^2}\right]\right\}.\left\{\frac{\epsilon^2}{2}\sin(\Omega) + \lambda\cos(\Omega)\right\}\right] d\epsilon d\xi \quad [3.100]$$

---

where Ω' is defined by, $\Omega' = \Omega + \frac{Rz^2\epsilon^2}{8\xi^2}$

Remark that these solutions are quite complicated and that their evaluation requires to integrate a double integral with a oscillatory integrand. Solutions for no dispersion and steady state are also given by Sudicky and Frind (1982) and are somewhat simpler to use.

We present now the solution given by van Genuchten (1985a). The set of equations has already been given in Tab. 3.1, and is only repeated here for user's commodity. We have the following equations:

$$\beta R \frac{\partial C_m}{\partial T} + (1-\beta) R \frac{\partial C_{im}}{\partial T} = \frac{1}{P} \frac{\partial^2 C_m}{\partial Z^2} - \frac{\partial C_m}{\partial Z} \qquad Z \in [0,1]$$

$$(1-\beta) R \frac{\partial C_a}{\partial T} = \gamma_s \frac{\partial^2 C_a}{\partial \rho^2} \qquad \rho \in [0,1]$$

$$C_{im} = \int_0^1 C_a(\rho)\, d\rho$$

and the dimensionless parameters are still defined by:

$$T = \frac{\theta_m V_m t}{\theta L} \qquad Z = \frac{z}{L}$$

$$P = \frac{V_m L}{D_m} \qquad \rho = \frac{r}{a}$$

$$\gamma_s = \frac{D_a \theta L}{a^2 \theta_m V_m R_{im}} \qquad \beta = \frac{\theta_m R_m}{\theta_m R_m + \theta_{im} R_{im}} = \frac{\theta_m R_m}{\theta R}$$

where a is now such that $2a$ is the distance between two cracks or the width of rectangular aggregates. Remark that no reference is made to the aperture of the crack or to the pattern of the macroporosity. In fact that one is lumped into the parameter θ_m. The retardation factor associated with the mobile phase is therefore defined on a mass basis and not as a face retardation factor. It is important to note that a third–type input boundary condition and a semi–infinit profile are assumed. No provision is made for inclusion of a decay process. Given that the transport in the mobile phase is still modeled by equation [3.55] the concentration profile is as for spherical aggregates given by:

Profile in the mobile phase.

$$C_m(Z,T) = \frac{1}{2} + \frac{2P}{\pi} \int_0^\infty \frac{\exp(\frac{PZ}{2} - z_p Z)}{[(\frac{P}{2} + z_p)^2 + z_m^2]} [(\frac{P}{2} + z_p) \sin(2\gamma\lambda^2 T - z_m Z)$$

$$- z_m \cos(2\gamma\lambda^2 T - z_m Z)] \frac{d\lambda}{\lambda} \qquad [3.101]$$

---

where all the parameters are the same as for equation [3.87] except for the followings,

$$\Psi_1 = \frac{\lambda(\sinh 2\lambda - \sin 2\lambda)}{\cosh 2\lambda + \cos 2\lambda}$$

$$\Psi_2 = \frac{\lambda(\sinh 2\lambda + \sin 2\lambda)}{\cosh 2\lambda + \cos 2\lambda}$$

The concentration profile in the rectangular aggregates is then

Concentration profile in the aggregates

$$\frac{C'}{C_0} = \frac{1}{2} + \frac{2}{\pi} \sum_{n=1}^{\infty} \frac{(-1)^n}{(2n-1)} \exp(-\gamma_n^2 T) \cos \frac{\gamma_n(1-\rho)}{\sqrt{\gamma}} + \gamma \int_0^{\infty} \exp(\frac{PZ}{2} - Z\sqrt{\frac{\delta+x}{2}}).$$

$$\left[S_1 \sin(Z\sqrt{\frac{\delta-x}{2}}) + S_2 \cos(Z\sqrt{\frac{\delta-x}{2}}) + S_3 \sin(\lambda T - Z\sqrt{\frac{\delta-x}{2}}) - S_4 \cos(\lambda T - Z\sqrt{\frac{\delta-x}{2}})\right] \frac{d\lambda}{\lambda} \qquad [3.102]$$

---

where $S_{1,2,3,4}$ are defined by:

$$S_1 = 16\gamma \sum_{n=1}^{\infty} \frac{(-1)^{n-1}(2n-1)^3}{(2n-1)^4\pi^2\gamma^2 + \frac{16\lambda^2}{\pi^2}} \cos\left[\frac{(1-\rho)\gamma_n}{\sqrt{\gamma}}\right] \exp(-\gamma_n^2 T)$$

$$S_2 = 16\lambda \sum_{n=1}^{\infty} \frac{(-1)^{n-1}(2n-1)}{(2n-1)^4\pi^2\gamma^2 + 16\lambda^2} \cos\left[\frac{(1-\rho)\gamma_n}{\sqrt{\gamma}}\right] \exp(-\gamma_n^2 T)$$

$$S_3 = S_1|_{T=0} \qquad S_4 = S_2|_{T=0}$$

$$\gamma_n = \frac{(2n-1)\pi\sqrt{\gamma}}{2}$$

$$x = \frac{P^2}{4} + PRH_1(1-\beta) \qquad y = PR\beta\lambda + PRH_2(1-\beta)$$

$$H_1 = \sqrt{\frac{\lambda\gamma}{2}}\left[\frac{\sinh\sqrt{\frac{2\lambda}{\gamma}} - \sin\sqrt{\frac{2\lambda}{\gamma}}}{\cosh\sqrt{\frac{2\lambda}{\gamma}} + \cos\sqrt{\frac{2\lambda}{\gamma}}}\right]$$

$$H_2 = \sqrt{\frac{\lambda\gamma}{2}}\left[\frac{\sinh\sqrt{\frac{2\lambda}{\gamma}} + \sin\sqrt{\frac{2\lambda}{\gamma}}}{\cosh\sqrt{\frac{2\lambda}{\gamma}} + \cos\sqrt{\frac{2\lambda}{\gamma}}}\right]$$

$$\delta = \sqrt{x^2+y^2}$$

3.3.3 SOILS CONTAINING CYLINDRICAL AGGREGATES

The case of cylindrical aggregates received less attention. Analytical solutions are given by Pellet (1966) and van Genuchten (1985a). This case is also considered by Rasmuson (1985a,b), in two studies of aggregate shape effects on transport characteristics. We shall come back later on this problem. In order to model the diffusion process inside the aggegates making use of the cylindrical symmetry, one must assume as for previous rectangular aggregates that the extremities of the cylinders are sealed and thus do not participate in the exchange process. This somewhat limits the usefulness of this approach. Once this assumption made, the set of equations is as given in Tab. 3.1 and recalled here for commodity,

$$\beta R \frac{\partial C_m}{\partial T} + (1-\beta)R \frac{\partial C_{im}}{\partial T} = \frac{1}{P}\frac{\partial^2 C_m}{\partial Z^2} - \frac{\partial C_m}{\partial Z} \qquad Z \in [0,1]$$

$$\frac{\partial C_a}{\partial T} = \frac{\gamma_s}{\rho}\frac{\partial}{\partial \rho}\left(\rho \frac{\partial C_a}{\partial \rho}\right) \qquad \rho \in [0,1]$$

$$C_{im} = 2\int_0^1 \rho C_a(\rho)\, d\rho$$

and the dimensionless parameters are still defined by:

$$T = \frac{\theta_m V_m t}{\theta L} \qquad Z = \frac{z}{L}$$

$$P = \frac{V_m L}{D_m} \qquad \rho = \frac{r}{a}$$

$$\gamma_s = \frac{D_a \theta L}{a^2 \theta_m V_m R_{im}} \qquad \beta = \frac{\theta_m R_m}{\theta_m R_m + \theta_{im} R_{im}} = \frac{\theta_m R_m}{\theta R}$$

where *a* is now the radius of the cylindrical aggregates. The solution is very similar to those derived before.

Analytical solution van Genuchten (1985a)

Profile in the mobile phase

$$C_m(Z,T) = \frac{1}{2} + \frac{2P}{\pi}\int_0^{\infty} \frac{\exp(\frac{PZ}{2} - z_p Z)}{[(\frac{P}{2} + z_p)^2 + z_m^2]} [(\frac{P}{2} + z_p)\sin(2\gamma\lambda^2 T - z_m Z) - z_m \cos(2\gamma\lambda^2 T - z_m Z)] \frac{d\lambda}{\lambda} \qquad [3.103]$$

where all the parameters are the same as for equation [3.87] except for the followings,

$$\Psi_1 = \frac{\lambda\sqrt{8}[Ber(\lambda)Ber'(\lambda) + Bei(\lambda)Bei'(\lambda)]}{Ber^2(\lambda) + Bei^2(\lambda)}$$

$$\Psi_2 = \frac{\lambda\sqrt{8}[Ber(\lambda)Bei'(\lambda) - Bei(\lambda)Ber'(\lambda)]}{Ber^2(\lambda) + Bei^2(\lambda)}$$

where Ber and Bei are tabulated Bessel functions. See for example **Spiegel (1968)**.

3.3.4 HOLLOW CYLINDRICAL MACROPORES

The case of solute transport in cylindrical macropore was first investigated by **Scotter (1978)**. He used an approximated numerical solution of the CDE in the macropore and of the diffusion equation in the porous matrix to simulate chloride and phosphorus transport through channels. An experimental work, de **Cockborne (1980)**, gave further insight on the influence of pore radius and flow velocity on the amount of solute held in the microporosity.

The set of equations modeling the phenomena for a finite radius soil column is given in Tab. 3.1, and repeated here for commodity,

$$\beta R \frac{\partial C_m}{\partial T} + (1-\beta)R \frac{\partial C_{im}}{\partial T} = \frac{1}{P}\frac{\partial^2 C_m}{\partial Z^2} - \frac{\partial C_m}{\partial Z} \qquad Z \in [0,1]$$

$$\frac{\partial C_a}{\partial T} = \frac{\gamma_s}{\rho}\frac{\partial}{\partial \rho}(\rho \frac{\partial C_a}{\partial \rho}) \qquad \rho \in [0,1]$$

$$C_{im} = \frac{2}{\rho_0^2 - 1}\int_0^1 \rho C_a(\rho)\, d\rho$$

and the dimensionless parameters are still defined by:

$$T = \frac{\theta_m V_m t}{\theta L} \qquad Z = \frac{z}{L}$$

$$P = \frac{V_m L}{D_m} \qquad \rho = \frac{r}{a} \qquad \rho_0 = \frac{b}{a}$$

$$\gamma_s = \frac{D_a \theta L}{a^2 \theta_m V_m R_{im}} \qquad \beta = \frac{\theta_m R_m}{\theta_m R_m + \theta_{im} R_{im}} = \frac{\theta_m R_m}{\theta R}$$

where a is now the radius of the cylindrical pore and b the radius of the soil column surrounding the macropore. The analytical solution given by van Genuchten et al. (1984) is expressed in a form similar to those proposed for other geometries.

Analytical solution van Genuchten et al. (1984)

Profile in the mobile phase (third–type B.C)

$$C_m(Z,T) = \frac{1}{2} + \frac{2P}{\pi} \int_0^\infty \frac{\exp(\frac{PZ}{2} - z_p Z)}{[(\frac{P}{2} + z_p)^2 + z_m^2]} [(\frac{P}{2} + z_p) \sin(2\gamma\lambda^2 T - z_m Z) - z_m \cos(2\gamma\lambda^2 T - z_m Z)] \frac{d\lambda}{\lambda} \qquad [3.104]$$

where all the parameters are the same as for equation [3.87] except for the followings,

$$\Psi_1 = \frac{2\lambda[N_1(M_1 - M_2) + N_2(M_1 + M_2)]}{(\rho_0^2 - 1)(N_1^2 + N_2^2)}$$

$$\Psi_2 = \frac{2\lambda[N_1(M_1 + M_2) - N_2(M_1 - M_2)]}{(\rho_0^2 - 1)(N_1^2 + N_2^2)}$$

where M_i and N_i are complicated expressions involving Bessel functions.

$$M_1 = \mathrm{Ber}_1(\rho_0\lambda)\mathrm{Ker}_1(\lambda) - \mathrm{Bei}_1(\rho_0\lambda)\mathrm{Kei}_1(\lambda) - \mathrm{Ker}_1(\rho_0\lambda)\mathrm{Ber}_1(\lambda) + \mathrm{Kei}_1(\rho_0\lambda)\mathrm{Bei}_1(\lambda)$$

$$M_2 = \mathrm{Ber}_1(\rho_0\lambda)\mathrm{Kei}_1(\lambda) - \mathrm{Bei}_1(\rho_0\lambda)\mathrm{Ker}_1(\lambda) - \mathrm{Ker}_1(\rho_0\lambda)\mathrm{Bei}_1(\lambda) + \mathrm{Kei}_1(\rho_0\lambda)\mathrm{Ber}_1(\lambda)$$

$$N_1 = \mathrm{Bei}_1(\rho_0\lambda)\mathrm{Ker}(\lambda) - \mathrm{Ber}_1(\rho_0\lambda)\mathrm{Kei}(\lambda) - \mathrm{Kei}_1(\rho_0\lambda)\mathrm{Ber}(\lambda) + \mathrm{Ker}_1(\rho_0\lambda)\mathrm{Bei}(\lambda)$$

$$N_2 = \mathrm{Bei}_1(\rho_0\lambda)\mathrm{Kei}(\lambda) - \mathrm{Ber}_1(\rho_0\lambda)\mathrm{Ker}(\lambda) - \mathrm{Kei}_1(\rho_0\lambda)\mathrm{Bei}(\lambda) + \mathrm{Ker}_1(\rho_0\lambda)\mathrm{Ber}(\lambda)$$

Ber_1, Bei_1, Ker_1, Kei_1, are tabulated Bessel functions. See Spiegel (1968). The analytical expression for the breakthrough curve is obtained according to equation [3.9]. This expression corresponds to the solution for a first–type input condition evaluated at Z=1.

Profile in the mobile phase (first–type BC)

$$C_m(T) = \frac{1}{2} + \frac{2}{\pi}\int_0^\infty \exp\left(Z\frac{P}{2} - z_p Z\right)\sin(\gamma\lambda^2 T - z_m Z)\frac{d\lambda}{\lambda} \qquad [3.105]$$

The breakthrough curve is immediatly obtained by making (Z=1) in this equation.

When a radially infinite system is assumed, the transport is best modeled by eq. [3.39], where $S(z) = 2/a$, and equation [3.40] is expressed in cylindrical coordinates. The solution for this problem with a first–type input boundary condition is also given by van–Genuchten et al. (1984). The concentration profile in the macropore is given by:

Profile in the mobile phase with first type B.C. and radially infinit soil matrix

$$C_m(z,t) = \frac{1}{2} + \frac{2}{\pi}\int_0^\infty \exp\left(\frac{v_m z}{2D_m} - z_p z\right)\sin\left(\frac{\lambda^2 D_a t}{a^2 R_a} - z_m z\right)\frac{d\lambda}{\lambda} \qquad [3.106]$$

where z_m, z_p and r_p have allready been defined. (See solution for spherical aggregates). Ω_1 and Ω_2 are given by:

$$\Omega_1 = \frac{v_m^2}{4D_m^2} + \frac{2\theta_a D_a \lambda A_1^0}{a^2 D_m \epsilon_f}$$

$$\Omega_2 = \frac{R_m D_a \lambda^2}{a^2 R_a D_m} + \frac{2\theta_a D_a \lambda A_2^0}{a^2 D_m \epsilon_f}$$

and A_1^0 , A_2^0 are defined by

$$A_1^0 = -\frac{Ker(\lambda)Ker'(\lambda) + Kei(\lambda)Kei'(\lambda)}{Ker^2(\lambda) + Kei^2(\lambda)},$$

$$A_2^0 = \frac{Kei(\lambda)Ker'(\lambda) - Ker(\lambda)Kei'(\lambda)}{Ker^2(\lambda) + Kei^2(\lambda)},$$

Assuming no dispersion in the macropore, approximate solutions for the radial concentration profile in the porous matrix are available for both radially

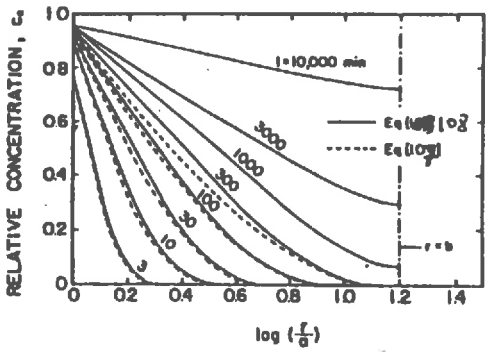

Fig. 3.2 Radial concentration profiles in the porous matrix at various times. The radius of the pore is a and the radius of the column is b [after *van Genuchten et al. 1984b*]

finite and infinite systems.

Case of a radially infinite system.

$$C_a(r,z,t) = 0 \quad t \le t_1$$

$$C_a(r,z,t) = \sqrt{\frac{a}{r}}\exp\left(-\frac{z\theta_a D_a}{a^2 v_m \epsilon_f}\right)\mathrm{erfc}\left(\frac{\eta}{2\sqrt{t_1}}\right) \quad t_1>0 \qquad [3.107]$$

where $t_1 = t - (zR_m/v_m)$

For the case of a radially finite system the solution is obtained under assumption that the concentration in the macropore remains constant after a certain time. That assumption releases the coupling between solute transport in the macropore and diffusion inside the porous matrix. Therefore the problem reduces to the diffusion in a hollow cylinder with a fixed boundary condition. The solution proposed by van Genuchten et al. (1984), is

Case of a radially finite system.

$$C_a(z,r,t) = 0 \qquad t \le t_1$$

$$C_a(r,z,t) = C_m^0(z,t)B(r,t_1) \quad t \ge t_1$$

$$B(r,t_1) = 1 - \pi\sum_{n=1}^{\infty}\exp(-D_a\alpha_n^2 t_1/R_a)J_1^2(\alpha_n b)$$

$$\left[\frac{J_0(\alpha_n r)Y_0(\alpha_n a) - Y_0(\alpha_n r)J_0(\alpha_n a)}{J_1^2(\alpha_n b) - J_0^2(\alpha_n a)}\right] \qquad [3.108]$$

and where the coefficients α_n are the roots of

$$J_0(\alpha_n a)Y_1(\alpha_n b) - J_1(\alpha_n b)Y_0(\alpha_n a) = 0$$

Examples of concentration profiles as calculated by [3.107] or [3.108] are ploted Fig. 3.2.

3.4 INFLUENCE OF PARTICLE SHAPE ON TRANSPORT KINETIC

Equations modeling reactive and non–reactive tracers movement in aggregated media made up of uniformely shaped and sized particles have been derived, and corresponding analytical expressions for breakthrough curves and solute distributions inside mobile and immobile water phases have been given. Being able to model transport phenomena and to obtain the solutions in geometrically simple media, the next natural step, when dealing with materials which as the soil can be made up of mixtures of irregularly shaped and sized aggregates, is to try to answer the two following questions; (1) can any aggregate be approximate from the point of view of the diffusion process by a geometrically simple one? and (2) how are solute distributions and breakthrough curves modified in a media made up of a mixture of regular aggregates? These two problems have been adressed for both batch and flowing systems, using either experimental or modeling approaches.

3.4.1 EFFECTS OF PARTICLE SHAPES: BATCH STUDY

We report here the main results and conclusions of a study conducted by Rao et al. (1982), whose objectives were to determine whether or not uniform spherical aggregates can be used (1) in place of a population of non uniform spherical aggregates and (2) in place of a cubic aggregates. Experiments consisted to immerse previously tracer saturated aggregates into a tracer free solution and to regularly sample the concentration of that solution. Equations modeling this system for regular spherical aggregates with radius a are as follow

$$\frac{\partial C(r,t)}{\partial t} = D\left[\frac{\partial C}{\partial r^2} + \frac{2}{r}\frac{\partial C}{\partial r}\right] \qquad [3.109]$$

$$C(r,0) = C_0, \qquad C(a,t) = C_b(t) \qquad [3.110]$$

$$\overline{C}(t) = (3/a^3)\int_0^a r^2 C(r,t)\, dr \qquad [3.111]$$

where C and $\overline{C}$ are respectively the local and average concentrations inside the aggregates, C_b is the concentration of the batch solution, assumed uniform and equal to 0 at the beginning, and C_0 the initial concentration inside the aggregates. Remark that the concentration of the batch solution is

$$C_b(t) = (\theta_b/\theta_a)[C_0 - \overline{C}(t)]. \qquad [3.112]$$

where θ_b and θ_a are the volume of the batch solution and the volume of void inside the aggregates, respectively. At equilibrium, the concentration is equal inside and outside the aggregates and is given by

$$C_\infty = \theta_a C_0/(\theta_a+\theta_b) \qquad [3.113]$$

An analytical solution giving the average concentration in the aggregates and therefore the batch solution concentration is

$$\overline{C}(t) = C_\infty + (C_0 - C_\infty) \sum_{n=1}^{\infty} \frac{6\beta(\beta + 1)}{9 + 9\beta + q_n^2\beta^2} \exp\left[-\frac{Dq_n^2 t}{a^2}\right] \qquad [3.114]$$

where $\beta = \theta_b/\theta_a$ and the coefficients q_n are the positive roots of: $\tan(q_n) = [3q_n/(3 + \beta q_n^2)]$. To use this solution for modeling diffusion from or into a mixture of aggregates, one needs to calculate an "*equivalent radius*", $\bar{a}$ for that mixture.

Radius averaging procedures

Rao et al (1982) proposed two procedures to determine an equivalent radius. First, remarking that diffusion kinetic depends upon D/a^2, Eq. [3.114], it seems reasonable to look for a weighted average value of that parameter. For a radius class, an immediate weighting candidate coefficient is the ratio of the volume of water contained in that class, noted W_i, to the total volume of water contained in all the classes, noted W_t. Thus, the weighting coefficient, f_i, for the class of aggregates with radius a_i is defined by

$$f_i = \left[\frac{V_i \theta_i}{\sum_{i=1}^{k} V_i \theta_i}\right] = \frac{W_i}{W_t} \qquad [3.115]$$

and $$V_i = n_i(4/3)\pi a_i^3$$

where n_i is the number of aggregates of radius a_i. Therefore, the weighted average value for D/a^2 is

$$\overline{D/a^2} = \sum_{i=1}^{k} [f_i(D/a_i^2)]. \qquad [3.116]$$

If it is assumed that all aggregates in a given class have the same porosity and diffusion coefficient, this expression simplifies to

$$\overline{D/a^2} = D \sum_{i=1}^{k} (V_i/V_t)/a_i^2 = D/\bar{a}^2 \qquad [3.117]$$

and $\bar{a}$ is then given by

$$\bar{a} = \left[\sum_{i=1}^{k} (V_i/V_t)/a_i^2\right]^{-1/2}. \qquad [3.118]$$

An alternative to the above described procedure is to simply define $\bar{a}$ as a

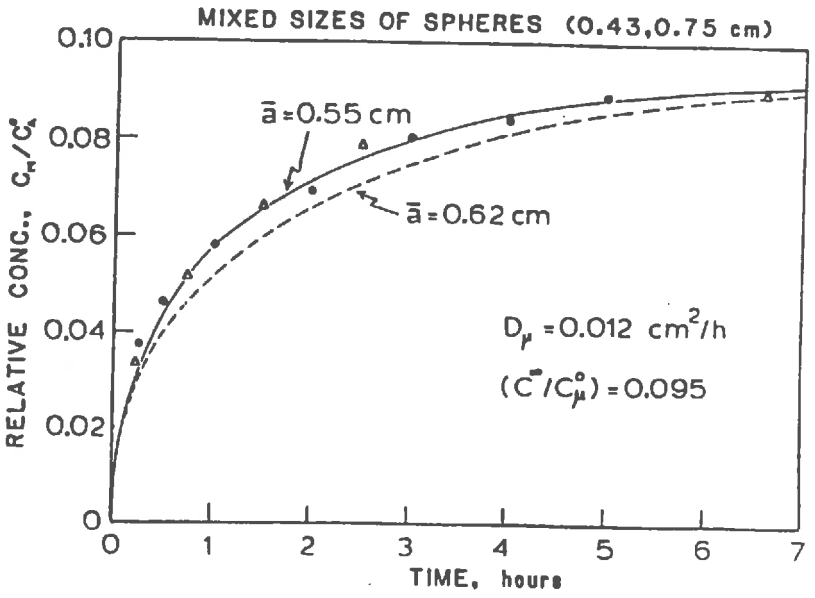

Fig. 3.3 Chloride diffusion out of mixed sized of spherical aggregates. Two sets of data (dots and triangles) are plotted with model predictions obtained with two different averaged–radius. [after *Rao et al. 1982*]

volume–weighted average radius,

$$\bar{a} = \sum_{i=1}^{k} (V_i/V_t)a_i. \qquad [3.119]$$

When dealing with cubic aggregates, one must first define the radius of an equivalent sphere for each cube size and then aplly one of the two procedures above proposed. It is obvious that for a cubic aggregate an equivalent radius may be defined in many ways. The approach chosen by Rao et al. (1982) was to simply calculate the radius such that the cube and the sphere have the same volume. In that case one must notice that for a given volume the surface developed by a cube is greater than the one offered by a sphere. Therefore, at least at the beginning of the process, one can expect the amount of solute transported per unit time from the aggregates to the solution to be greater in the case of the cube. This way to define an equivalent sphere for a cubic aggregate is therefore not very well suited regarding diffusion process. However, it has the advantage to respect the total amount of solute initially present in the aggregates

Results

Figure 3.3, from Rao et al. (1982), presents for a mixture of spherical aggregates, observed and calculated concentration evolutions of the batch solution. Simulated results have been obtained with equation [3.114]. Solid and dashed lines correspond to equivalent radius calculated with equation [3.118] and equation [3.119], respectively. It appears that equation [3.118] gives a better fit.

For cubic aggregates, Figure 3.4(A,B,C,D) present observed and simulated concentrations for three different aggregate sizes and for a mixture of aggregates. The equivalent radius used in equation [3.114] is calculated with equation [3.118]. The good fit of the results is in that case less easy to analyse. Unlike for spherical aggregates where the diffusion coefficient was independently measured, it has been in that case adjusted so as to obtain a best fit for cases A,B and C, (Fig. 3.4). Thus, errors introduced calculating for each cube the radius of the 'equivalent' sphere are in part corrected by the diffusion coefficient. However, a good agreement appears, with somewhat less satisfactory results at large times.

3.4.2 EFFECTS OF PARTICLE SHAPES: COLUMN STUDIES

Rasmuson (1985b) studied the effects of particle shapes, Peclet number, and bed length on breakthrough curves. For respectively, slab, cylindrical, and spherical aggregates, the system of equations considered was almost identical to equation [3.78]–[3.81], where now a parameter α_f is introduced to account for the three possible symmetries. Equations are as follows

$$\frac{\partial C}{\partial t} + v\frac{\partial C}{\partial z} - D\frac{\partial^2 C}{\partial z^2} = -(\partial q/\partial t)/m \qquad [3.120]$$

$$\epsilon_p \partial C_p/\partial t + \partial C_s/\partial t = D_s(\partial^2 C_p/\partial r^2 + \frac{\alpha_f}{r}\partial C_p/\partial r) \qquad [3.121]$$

$$\frac{\partial C_s}{\partial t} = k_{ads}(C_p - C_s/k_a) - k_r C_s \qquad [3.122]$$

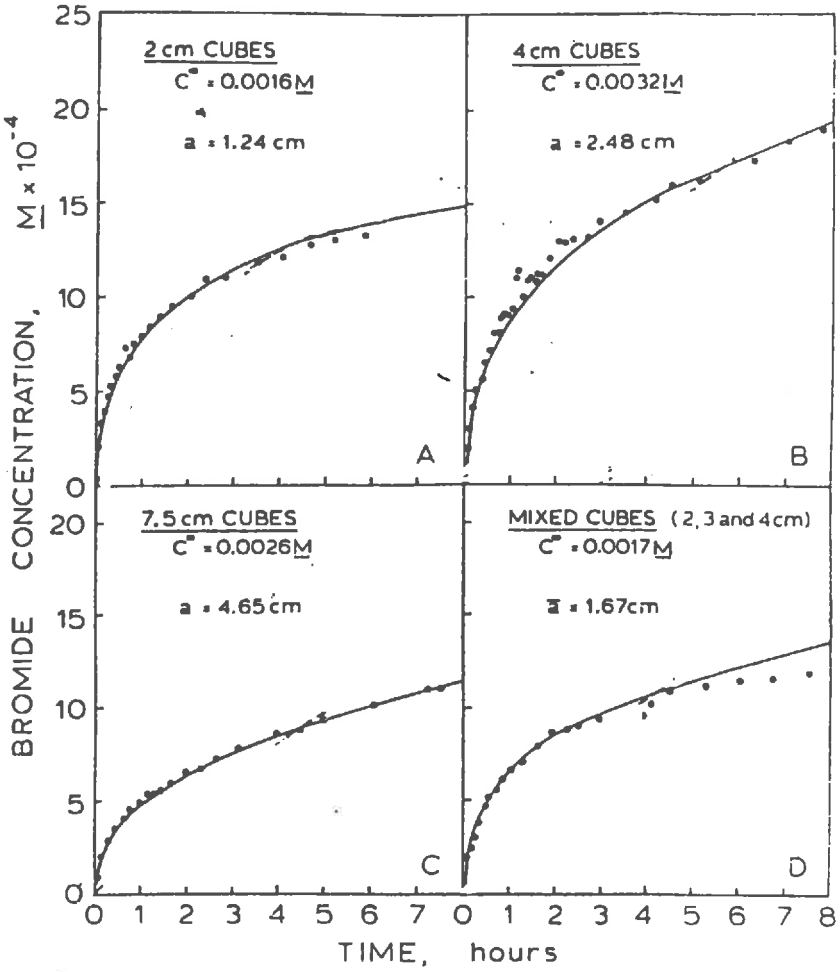

Fig. 3.4 Diffusion of Br out of cubic aggregates. Model prediction (solid line) and data (dots) are plotted for 3 different sizes and a mixture of aggregates [after *Rao et al. 1982*].

$$\frac{\partial q}{\partial t} = \frac{k_f(\alpha_f+1)}{b}\left(C - C_p\Big|_{r=b}\right) \qquad [3.123]$$

where b is the characteristic length of the particles, and α_f is equal to 0, 1, 2 for the plane, cylindrical and spherical symmetries, respectively. In this formulation there is provision for a first order chemical reaction rate modeled by the term, $-k_r C_s$ in [3.122]. Notice that this set of equations is slightly different from the one used by van Genuchten (1985a), since in this case solute adsorption on the solid phase is now modeled by a first order process rather than assuming instantaneous local equilibrium, first part of the right hand side in Eq. [3.122]. One of the consequences is that for cylindrical aggregates the general transient solution cannot be obtained and expressed in terms of tabulated functions. However, this is possible letting $k_{ads} \to \infty$ and $k_r \to 0$ which corresponds to the case of instantaneous equilibrium and no chemical reaction. Remark also that the transport rate from the flowing solution into the aggregates is controled by a boubary layer with mass transfer coefficient, k_f. Equations are solved for a semi–infinit profile and a first type boundary condition at the inlet. The analytical solution for this system of equations is very similar to the solutions already derived by van Genuchten (1985a). In that case the analytical solution is

$$C(z,t)/C_0 = \frac{1}{2} + \frac{2}{\pi}\int_0^\infty \exp\left[\frac{1}{2}P_e - \frac{\sqrt{\sqrt{(x'z^2)^2+(y'z^2)^2} + x'z^2}}{\sqrt{2}}\right] \cdot$$

$$\sin\left[\lambda^2 y - \frac{\sqrt{\sqrt{(x'z^2)^2+(y'z^2)^2} - x'z^2}}{\sqrt{2}}\right]\frac{d\lambda}{\lambda} \qquad [3.124]$$

where

$$z^2x' = P_e\left(\frac{P_e}{4} + \delta H_1\right) \qquad z^2y' = \delta P_e\left(\frac{2\lambda^2}{3R_1} + H_2\right)$$

$$y = \frac{2D_p\epsilon_p}{(k_a+\epsilon_p)b^2}t \qquad P_e = \frac{zV}{D_l}$$

$$\delta = \frac{(\alpha_f+1)D_p\epsilon_p}{b^2}\frac{z}{mV}$$

$$R_1 = \frac{(\alpha_f+1)(k_a+\epsilon_p)}{m} = \frac{k(\alpha_f+1)}{m}$$

Functions H_1 and H_2 are the same as for [3.77] and H_{d1}, H_{d2} are now given in Table 3.2 according to the parameter α_f. Functions H_{d1} and H_{d2} are equal to functions Ψ_1 and Ψ_2 defined by van Genuchten (1985a), equation [3.87] and following, modulo a constant equal to 3 and already included in z^2x'.

In order to compare the breakthrough curves obtained on media made up of different types of aggregates, one must choose the geometrical characteristics

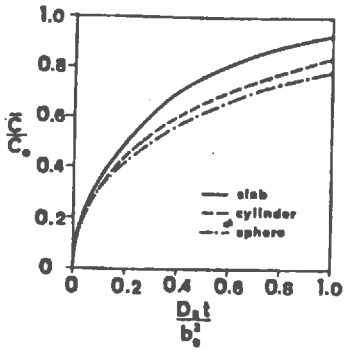

Fig. 3.5 Average relative concentration for a slab and cylinder, both with sealed ends, and for a sphere with the same surface–to–volume ratios [after *Rasmuson 1985*].

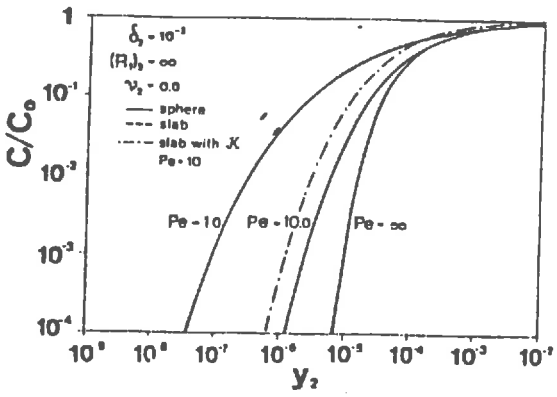

Fig. 3.6 Breakthrough curves for various Peclet numbers and particules shapes. Case of a short contact time, δ_2=1/100. [after *Rasmuson 1985*].

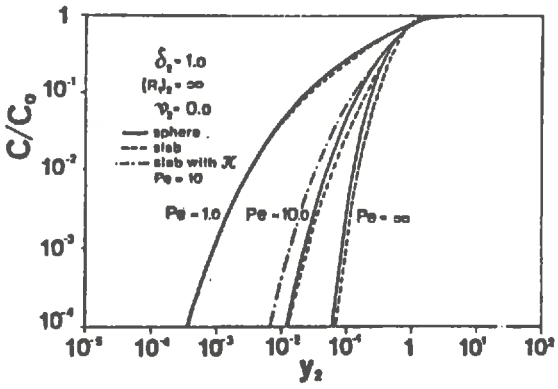

Fig. 3.7 Idem as for Fig.3.6 but for the case of a medium contact time, δ_2=1 [after *Rasmuson 1985*].

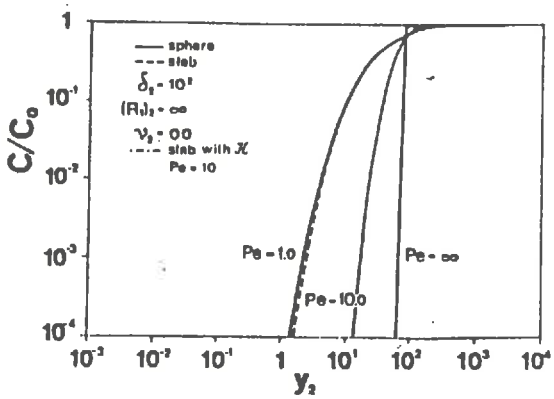

Fig. 3.8 Idem as for Fig. 3.6 but for the case of a long contact time, δ_2=100 [after *Rasmuson 1985*].

of the particles such that they have the same surface to volume ratio (function S'(z) previously defined). Thus taking b_2 the radius of a spherical particle as a reference, corresponding b_i, δ_i and y_i for the two others geometries are given by

$$b_i = b_2(\alpha_f+1)/3 \qquad \delta_i = 3\delta_2/(\alpha_f+1)$$

$$y_i = \left[\frac{3}{\alpha_f+1}\right]^2 y_2$$

With this choice, the global exchange surface of the flow domain is the same and one can expect the breakthrough curves to be identical at early times since adsorption is independent of particle shapes at the beginning of the process. (cf.§3.4.1) Influence of particle shape is expected to appear at medium times while at larger times breakthrough curves are again expected to be same, a limiting case being solute saturation of the particles. Figure 3.5 presents the average concentration for the three geometries as a function of the dimensionless parameter $D_a t/b_0^2$. It can be constated that as expected, there is very little difference at short times and that the slab is more "*effective*" at medium times.

Sensitivity of breakthrough curves to particle geometry and Peclet number is illustrated by Fig. 3.6, 3.7, 3.8, taken from **Rasmuson (1985b)**. The parameter δ_2 defined above has the dimension of (1/L) and in fact is a measure of the bed or column length. All curves are expressed as function of y_2 which is a contact time parameter. For small values of δ_2, which can be viewed as the case of a short column when all other parameters are fixed, and whatever is the Peclet number, no differences can be noticed. Identically, at large times, only a little variation appears. For intermediate times some differences appear which seem to be increasing with the Peclet number while remaining quite small for a Peclet of 1.

3.4.3 SHAPE FACTORS

Shape factor based on evolution of the average concentration

We have discussed the effects of particle shapes on breakthrough curves and showed that at least for batch experiments, cubic aggregates for example, could be approximate by spherical aggregates. For this purpose, an effective radius was simply defined such that the volume of the cube and the volume of the equivalent sphere be equal. It was also shown that any mixture of spherical aggregates or cubic aggregates could be, via an averaging procedure, approximated by uniform spherical aggregates.

Conversion of a cubic aggregate into a spherical one was made on a simple geometry basis and regardless of the diffusion process. Therefore, the equivalence was probably "weak" and as then remarked this weakness taken care of by the fitted diffusion coefficient. **van Genuchten (1985a)** proposed an alternative to transform any of the usual regularly shaped aggregates, sphere, plane sheet, rectangular prism, solid cylindrical and hollow cylinder into any of those.

Again, the basis of the approach was to consider a non–flowing system characterized by a constant external concentration and initially solute free aggregates. For the different geometries above referred, analytical solutions of the diffusion equation with initial condition, C(r,0) = 0 and boundary condition C(a,t) = 1, which correspond to the batch system described above, are available in **Carslaw and Jaeger (1959)**. For this particular problem, average

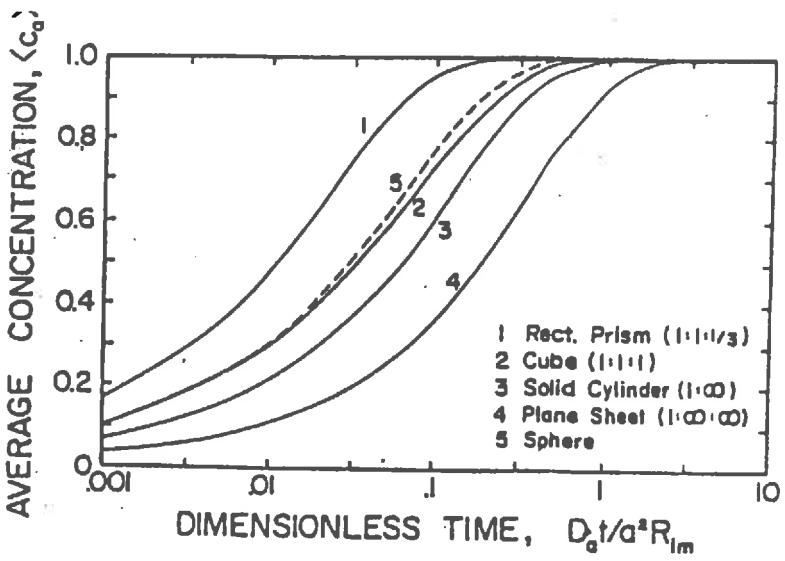

Fig. 3.9 Evolution of the average concentration inside various soil aggegates [after *van Genuchten 1985*].

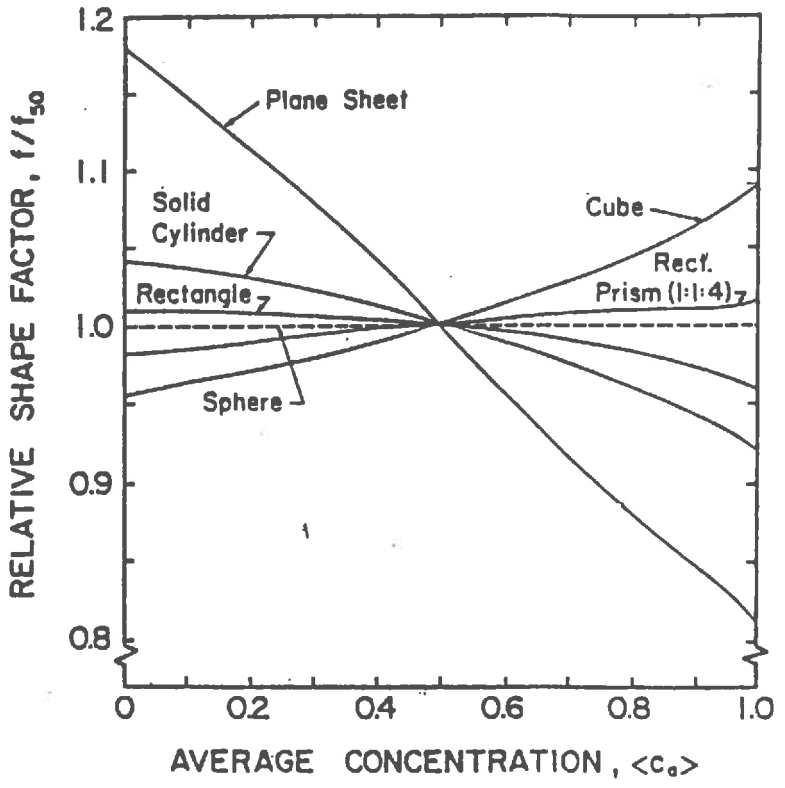

Fig. 3.10 Effect of the average concentration on the relative shape factor for conversion of several aggregates geometries into equivalent spheres [after *van Genuchten 1985*].

concentrations, <C>, function of $T = Dt/a^2$, are given Table 3.3 and plotted Figure 3.9. One can observe that these curves have all the same shape and that if translated they are almost superimposed. Therefore, taking any shape as reference, for example the spherical one, one can almost define for each of other shapes a translation parameter such that the evolution in time of the average concentration is the same for all. In fact, given the physics of the phenomena one cannot expect that parameter to be a constant for a given geometry. It obviously depends on time, and seeking for a constant value only leads to a more or less good approximation. A given value of <C> is attained for two aggregates with different geometries but having the same characteristic length at two different times noted t_1 and t_2. Therefore, we can seek for different characteristic lengths such as to obtain a given average concentration at the same time for both aggregates. It comes the following equalities

$$\frac{Dt_1}{a_1^2} = \frac{Dt_2}{a_2^2}$$

$$a_1 = a_2\sqrt{\frac{t_1}{t_2}} = a_2\sqrt{\frac{T_1}{T_2}} = a_2\, f_{1,2}. \qquad [3.125]$$

We can now define for each value of <C> a parameter, noted $f_{1,2}$, giving the ratio between the characteristic lengths a_1 and a_2 of both aggregate types. Recognizing that the parameter $f_{1,2}$ is concentration or what is equivalent time dependent, van Genuchten (1985a) arbitrarily chose to estimate the scaling factor, now noted f_{50}, at <C>=.5. Table 3.4, taken from van Genuchten (1985a) gives the values of f_{50} to pass from one aggregate geometry to another. Notice for example that the shape factor transforming a cube into a sphere is equal to 1.046, and that with the previous approach it was equal to 1.2406. Noting f the shape factor that is concentration–dependent, Figure 3.10 presents the variations of f/f_{50} as a function of the average concentration when the sphere is the reference. On can observe that values relatively close to one, indicating a weak dependence of f on <C>, are obtained except for the case of a plane sheet. Time variations of the average concentration calculated with the spherical equivalent are plotted together with exact values for some particular cases, Fig.3.11. Good fits are obtained for rectangular prismatic or cubic aggregates, but much less good agreements for geometrical shapes not so close to the sphere. Observe also that at early times the curves are superimposed whatever is the geometry. This is due to the fact that the quantity of solute diffusing into the aggregates is very weakly shape dependent at the beginning of the process, but mostly related to the exchange surface area.

Let us to end outline two properties of this scaling factor. First, it is evident that with the procedure above defined one can transform any aggregate into any other and not only a spherical equivalent. This is accomplished with the following rule, $f_{1,3} = f_{1,2}\, f_{2,3}$, where the subscripts $_{1,2,3}$ refer to any of the shapes listed in Tab. 3.4. From this relation, and given that $f_{1,1} = 1$, it comes $f_{1,2}=1/f_{2,1}$.

However, besides the facts that this shape factor is constant while it is really time–dependent, it has another major inconvenient which is that it is not easily evaluated. As a mater of fact, no analytical expressions can be derived for f, and in order to obtain numerical values one is restricted to numerical inversions of the solutions given in Table 3.3. An other more convenient method based on comparison of Laplace transforms for average concentrations was

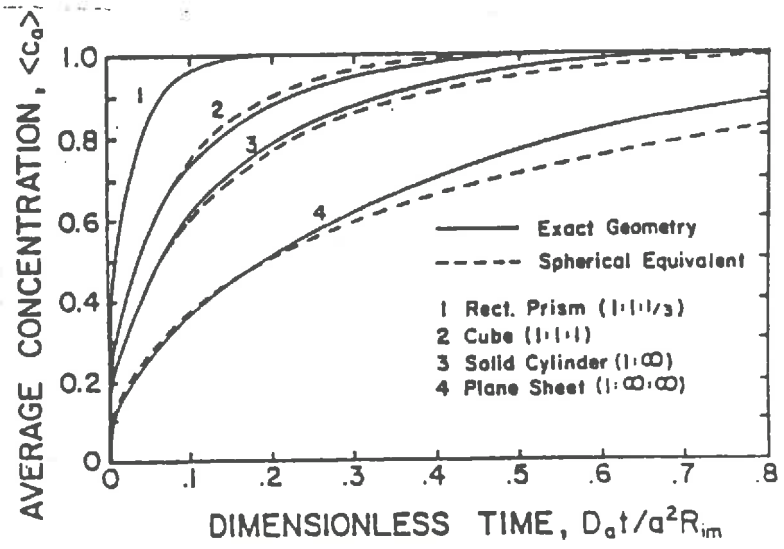

Fig. 3.11 Evolution of the average concentration for various geometries. Calculated with the exact solution (solid line) and with the "spherical equivalent" (dashed line) [after *van Genuchten 1985*].

proposed by van Genuchten and Dalton (1986).

Shape factors obtained from Laplace transforms

Analytical solutions as those presented in Table 3.3 are usually derived by first applying the Laplace transform to the system of equations to remove the time–dimension. Solution obtained in term of Laplace transforms are usually expressed in much more simpler analytical forms than the final ones. The main idea is thus, as the Laplace transform is supposed to carry the same information as the original function, to compare Laplace transforms of average concentrations rather than much more complicated and not easily handled final solutions.

Let us consider the diffusion problems defined by the equations in Table 3.1 with the boundary condition $C_a = C_m$. Respective Laplace transforms for C_a and C_{im} are given in Table 3.5. All these functions depend on γ which is, Eq. [3.60a],

$$\gamma_i = \frac{D_a \theta L}{a_i^2 q R_{im}} \qquad [3.126]$$

where the index $_i$ stands for any particular geometrical shape already defined. With little algebra the following relation is obtained between the parameters γ_i and γ_j corresponding to two different geometries

$$\gamma_i/\gamma_j = (a_i/a_j)^2 \qquad [3.127]$$

Laplace transforms of average immobile concentrations, $\mathcal{L}(C_{im})$, are expressed in terms of hyperbolic functions or Bessel functions. Thus a direct comparison is impossible. However, it is possible to replace, at least for a limited range of argument values, these functions by power series. These can be found in Spiegel (1968). Using the first terms of these developments, comparable expressions are obtained and a relation between γ_1 and γ_2 appears. Let us for example consider the case of transformation of a slab into a sphere. From Tab. 3.5. we have for a spherical aggregate

$$\overline{C}_a(Z,\rho,s) = \frac{\sinh(\rho p)}{\rho \sinh(p)} \overline{C}_m(Z,s)$$

$$\overline{C}_{im}(Z,s) = \left[\frac{3}{p} \coth(p) - \frac{3}{p^2} \right] \overline{C}_m \qquad [3.128]$$

where $p = \sqrt{s/\gamma_s}$ and for a slab

$$\overline{C}_a(Z,\rho,s) = \frac{\cosh(\rho p)}{\cosh(p)} \overline{C}_m(Z,s)$$

$$\overline{C}_{im}(Z,s) = \frac{\tanh(p)}{p} \overline{C}_m(Z,s) \qquad [3.129]$$

where $p = \sqrt{s/\gamma_1}$. We have the following series expansions for the coth and tanh.

$$\coth(p) = \frac{1}{p} + \frac{p}{3} - \frac{p^3}{45} + \frac{2p^5}{945} + \ldots \qquad [3.130]$$

$$\tanh(p) = p - \frac{p^3}{3} + \frac{2p^5}{15} - \frac{17p^7}{315} + \ldots \qquad [3.131]$$

Using the first terms of these series in the expressions giving $\overline{C}_m$ and $\overline{C}_{im}$ it comes for spherical and slab aggregates,

$$\overline{C}_{im} \cong (1 - \frac{s}{15\gamma_s})\,\overline{C}_m \qquad \overline{C}_{im} \cong (1 - \frac{s}{3\gamma_l})\,\overline{C}_m\,, \qquad [3.132]$$

respectively. Thus, equating term to term these two expressions one obtains: $\gamma_s/\gamma_l = 1/5$. Notice that second order terms have been released. One can immediately deduce the relation between a_s and a_l from Eq. [3.127]. It that particular case it comes: $a_s = \cong 2.24\ a_l$. Remark that with the previous method a value of 2.54 was obtained.

Therefore, using this shape factor to convert any aggregate into, a sphere for example, and making also use of the weighting procedure developped by **Rao et al. (1982)**, (cf.§3.4.1), it is possible to transform any mixture of aggregates into an equivalent media, made up of uniform spherical particles, and behaving approximately in the same way as the original one regarding the diffusion phenomena. Besides this method consisting to first transform the media in something "equivalent" and mathematically more tractable, some other approaches have been developped to deal with complex media made up of mixtures of aggregates or particles having different shapes and sizes. Works of **Rasmuson (1985a)** and **Barker (1985a,b)** are presented hereafter.

3.4.4 MIXTURE OF PARTICLES. ANALYTICAL SOLUTION.

Rasmuson (1985a) gave an analytical solution for transport through a bed made up of a mixture of spherical, finite slab and finite cylinder particles. Let us consider a particle size distribution where each particle size group, i, is characterized by a shape factor $\alpha_{f,i}$, a characteristic length b_i and the volume fraction $F(b_i)$ of the total volume of particles. The shape factor α_f takes the values 0,1,2 for, slab, cylindrical and spherical particles, respectively. In addition each group is allowed to have different values of the properties: diffusivity, $D_{p,i}$, adsorption constant, $K_{a,i}$, adsorption rate constant, $k_{ads,i}$, mass transfer coefficient, $k_{f,i}$, chemical reaction rate, $k_{r,i}$, and void fraction, $\epsilon_{p,i}$. The set of equation describing the transport by convection–diffusion in the bed, exchange of solute between liquid phases, surface adsorption and kinetic adsorption on the solid phase inside the particles is as follows,

$$\frac{\partial C}{\partial t} + V\frac{\partial C}{\partial z} - D\frac{\partial^2 C}{\partial z^2} = -\frac{1}{m}\sum_i \frac{\alpha_{f,i+1}}{b_i} F(b_i) N_0^i \qquad [3.133]$$

$$\epsilon_p^i \partial C_p^i/\partial t + N_I^i = \epsilon_p^i D_p^i(\partial^2 C_p^i/\partial r^2 + \frac{\alpha_{f,i}}{r}\,\partial C_p^i/\partial r) \qquad [3.134]$$

$$\frac{\partial C_s^i}{\partial t} + k_{r,i}C_s^i = k_{ads,i}\,(C_p^i - C_s^i/k_{a,i}) = N_I^i \qquad [3.135]$$

$$N_0^i = k_{f,i}\,(C - C_p^i|_{r=b_i})\,. \qquad [3.136]$$

Initial and boundary conditions being

$$C_p^i(b_i,z,t) = C_p^i\big|_{r=b_i} \qquad \frac{\partial C_p^i}{\partial r}(0,z,t) = 0. \qquad [3.137]$$

$$C(0,t) = C_0 \qquad C(\infty,t) = 0 \qquad [3.138]$$

$$C(z,0) = 0 \qquad C_p^i(r,z,0) = C_s^i(r,z,0) = 0. \qquad [3.139]$$

The analytical solution of this system is classicaly obtained by means of Laplace transforms and is as follows

---

$$C(z,t)/C_0 = \frac{1}{2}u_\infty + \frac{2}{\pi}\int_0^\infty \exp\left[\frac{1}{2}P_e - \frac{\sqrt{\sqrt{(x'z^2)^2+(y'z^2)^2} + x'z^2}}{\sqrt{2}}\right]\cdot$$

$$\sin\left[\lambda^2 y - \frac{\sqrt{\sqrt{(x'z^2)^2+(y'z^2)^2} - x'z^2}}{\sqrt{2}}\right]\frac{d\lambda}{\lambda} \qquad [3.140]$$

---

where

$$u_\infty = \exp\left[\frac{1}{2}P_e - \sqrt{P_e\left[\frac{1}{4}P_e + \frac{\delta}{\nu}\sum_i \frac{\gamma^i}{\gamma}\frac{\nu^i}{\nu}F(b_i)X_t^i(0)\right]}\right]$$

$$X_t^i(0) = 1 - \frac{1}{\nu^i g^i(0) + 1}.$$

The functions $g^i(.)$ are given in Table 3.6, $w^i(.) = \sqrt{v^i(.)}$ and

$$\gamma^i = \frac{(\alpha_l^i+1)D_p^i\epsilon_p^i}{(b^i)^2} \qquad \nu^i = \frac{D_p^i\epsilon_p^i}{k_f^i b^i}$$

$$v^i(s) = \frac{s(b^i)^2}{D_p^i}\left[1 + \frac{k_{ads}^i k_a^i}{\epsilon_p^i}\frac{s+k_r^i}{s}\frac{1}{k_a^i(s+k_r^i) + k_{ads}^i}\right]$$

$$v^i(0) = A_i\frac{B^i}{B^i+1}$$

where

$$z^2x' = P_e\left(\frac{P_e}{4} + \delta\sum_i \frac{\gamma^i}{\gamma}F(b^i)H_l^i\right)$$

$$z^2y' = \delta P_e\left(\frac{\lambda^2}{3R_1}A(1+1/R_2) + \sum_i \frac{\gamma^i}{\gamma} F(b^i)H_2^i\right)$$

$$H_1^i = \frac{H_{d1}^i + \nu^i[(H_{d1}^i)^2 + (H_{d2}^i)^2]}{(1+\nu^i H_{d1}^i)^2 + (\nu^i H_{d2}^i)^2}$$

$$H_2(\lambda,\nu) = \frac{H_{d2}^i}{(1+\nu^i H_{d1}^i)^2 + (\nu^i H_{d2}^i)^2}$$

Functions H_{d1}^i and H_{d2}^i with respect to α_f are given in Table 3.7.

$$\phi_1^i = -\sqrt{\left[\frac{l^i - c^i}{2}\right]} \qquad \phi_2^i = +\sqrt{\left[\frac{l^i + c^i}{2}\right]}$$

$$l^i = \sqrt{(c^i)^2 + (d^i)^2}$$

$$c^i = A^i \frac{\left[\frac{k_{ads}^i k_a^i}{k_{ads}^i k_a}\right]^2 \lambda^4 + B^i(B^i+1)}{(B^i+1)^2 + \left[\frac{k_{ads} k_a^i}{k_{ads}^i k_a}\right]^2 \lambda^4}$$

$$d^i = \left[\frac{k_{ads} k_a^i}{k_{ads}^i k_a}\right] A^i \left[\frac{1}{R_2^i} + \frac{1}{(B^i+1)^2 + \left[\frac{k_{ads} k_a^i}{k_{ads}^i k_a}\right]^2 \lambda^4}\right] \lambda^2$$

Dimensionless parameters are

$$\delta = \frac{\gamma z}{mV} = \frac{(\alpha_f+1)D_p\epsilon_p}{b^2}\frac{z}{mV} \qquad B = \frac{k_a k_r}{k_{ads}}$$

$$y = \frac{k_{ads}}{k_a}t \qquad R_1 = \frac{(\alpha_f+1)K}{3m} \qquad R_e = \frac{k_a}{\epsilon_p}$$

$$A = \frac{b^2 k_{ads}}{D_p\epsilon_p} \qquad \nu = \frac{D_p\epsilon_p}{k_f b} \qquad P_e = \frac{zV}{D}$$

and $K = k_a + \epsilon_p$. **Rasmuson (1985a)** compared the breakthrough curves for three Gaussian and two log–normal particle–size distributions. These distributions were chosen so as they have the same expected value. Log–normal distributions were skeewed toward small radii. Therefore, for a given volume of bed, the total outer surface offered by the particles can be quite different. It is obvious that skewing the distributions toward smaller "radii" relatively increases the surface to volume ratio by comparison with a normal distribution. One can therefore expect the skewing to have a strong effect for short contact times and the

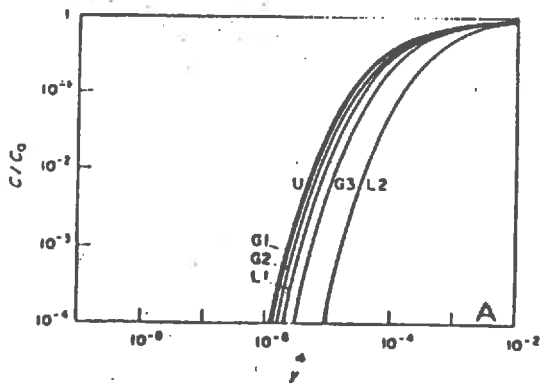

Fig. 3.12A Breakthrough curves for various particule size distri–butions. δ_2=1/100, P_e=10. [after Rasmuson 1985]

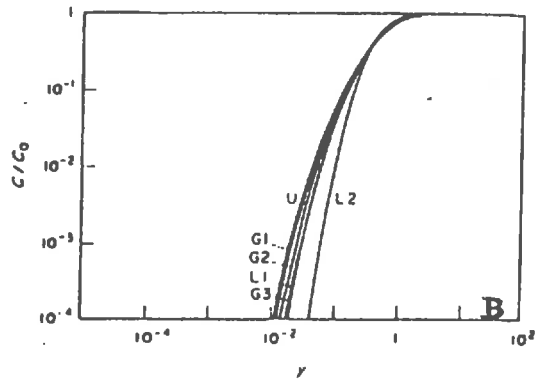

Fig. 3.12B Same as Fig. 3.12A but with δ_2=1. Other parameters are identical. [after *Rasmuson 1985*]

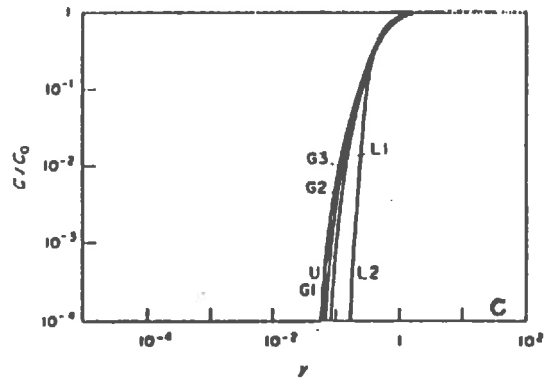

Fig. 3.12C Same as Fig. 3.12B but with P_e=∞. Other parameters are identical. [after *Rasmuson 1985*]

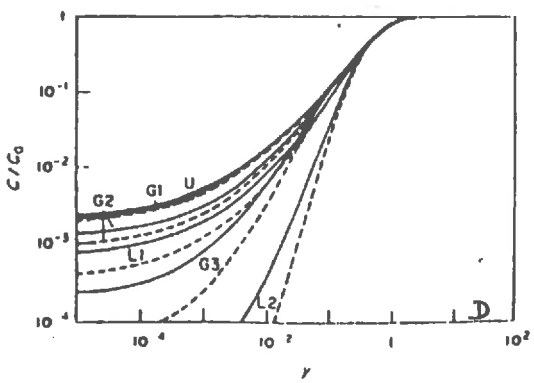

Fig. 3.12B Same as Fig. 3.12B but with ν=.1 Other parameters are identical. k_f independent of the PSD (solid line), accounting for the varying total particule surface (dashed line) [after *Rasmuson 1985*]

presence of small particles to delay initial breakthrough times. Fig 3.12 A,B,C,D taken in **Rasmuson (1985a)**, presents the breakthrough curves obtained for various combinations of the parameters. It can be seen that as far as initial breakthrough times are concerned, the following ranking holds among the distributions; U<G1<G2<L1<G3<L2. Differences are larger for short bed–lengths or what is equivalent short contact times. Curves A,B,C were obtained neglecting the resistence of the liquid film (ν=0) and assuming instantaneous equilibrium between liquid phase concentration inside the particles and adsorbed concentration, (R_1=∞). Those are the assumptions used by **van Genuchten (1985a,b), van Genuchten et al. 1984.** Fig. 3.12D presents the breakthrough curves when the presence of a liquid film is accounted for ($\nu \neq 0$). We still assume, (R_1=∞). In that case differences are much larger. **Rasmuson (1985a)** concludes that narrow Gaussian paricule size distributions have very little effects on breakthrough curves as compared to thoses obtained with a uniform distribution. Calculations show that non–negligible effects due to particle size distributions can be expected for short contact times or for short bed–lengths. More details are available in the paper of Rasmuson (1985a).

3.5 BLOCK–GEOMETRY FUNCTIONS

In the following, we first present some mathematical results which are later used to develop a new solution for the solute transport problem in double porosity media. In particular it will appear that the analytical solutions given for the QSS model and all the geometrically based approaches in the previous paragraphs are in fact particular cases of a more general formulation. Solutions for the set of equations modeling the transport phenomena in double porosity media can be obtained by different techniques. In the following, we start with an approach making use of the Laplace transform and later connect it with more direct solutions techniques leading to a Volterra integro–differential equation. This development is partially based on works of Barker (1985a,b) and Hornung (1987). In fact, the main mathematical tools used in the following belong to the theory of potential and to the theory of eigenvalue problems for self–adjoint operators Courant and Hilbert (1966).

3.5.1 THEORY

Consider a media where two water phases are present. In a first time one can imagine this one as composed of porous blocks Ω with surface Γ, delimitated by a network of cracks. The dependent variable for each phase is a "potential" noted φ_i. The term potential is taken here in its mathematical sense. Physically, it can represent either the piezometric head in a saturated media, the solute concentration, or the temperature. Assume that the following set of equations models the variations of the potential in respectively the mobile and immobile domains, / a gaz conduction

$$S_f(\partial\varphi_f/\partial t) = D\varphi_f - k_f\varphi_f + q \qquad [3.141]$$

$$S_m(\partial\varphi_m/\partial t) = K_m\Delta\varphi_m - k_m\varphi_m \quad \text{in } \Omega \qquad [3.142]$$

$$q(.,t) = -A_v K_m \frac{1}{A}\int_\Gamma \nabla\varphi_m.\vec{n}\, dA = -\frac{1}{a}\nu K_m <\partial\varphi_m/\partial n>_\Gamma \qquad [3.143]$$

$$\varphi_m = \varphi_f \quad \text{on } \Gamma \qquad [3.144]$$

where Δ and ∇ are respectively the Laplacian and gradient operator, D is a differential operator, which can for example be the dispersion–convection operator, $D^*\Delta - v\nabla$, S_f and S_m are the respective porosities of the two regions, k_f and k_m are two decay constants, K_m can be considered as a conductivity or diffusion coefficient, a is the volume to surface ratio of the blocks, ν is the fraction of all space occupied by matrix material, $\partial\varphi/\partial n$ is the normal derivative and $<.>_i$ denotes the average value of a variable over a surface or a volume according to index $_i$. In addition φ_{f0} and φ_{m0} are the two initial conditions. If boundary conditions are supplied for [3.141], then one have a system very similar to the one defined by [3.39], [3.40], [3.41].

In previous chapters several analytical solutions have been proposed for cases where the porous blocks could be given a geometrically simple shape. The standard procedure followed to obtain analytical solutions was to first apply the Laplace transform, then to solve the problem in the Laplace space (solution of a ordinnary differential equation), and at the end to invert that solution to obtain an expression in term of original variables. While the two first stages of the

procedure are relatively straightforward, inversion of the Laplace transform is a lengthy and tedious process leading to complicated expressions which in addition require some precautions during their numerical evaluations.

An other limitation of previous approaches is that natural media must be approximated by regular aggregates or porous blocks. No provision was made and could be made to account for irregular aggregate shapes. We are going to introduce the concept of Block–Geometry Function (BGF) and show how used with numerical inversion procedures for Laplace transform it allows to overcome these difficulties and generalizes previous approaches. We note

$$\mathcal{L}(f)(p) = \bar{f}(p,.) = \int_0^\infty \exp(-pt) f(.,t)\, dt$$

the Laplace transform of a function, f.

The first step is to apply the Laplace transform to equations [3.141] to [3.144]. The folowing set of equations is then readily obtained.

$$S_f(p\bar{\varphi}_f - \varphi_{f0}) - D\bar{\varphi}_f + k_f\bar{\varphi}_f - \bar{q} = 0 \qquad [3.145]$$

$$S_m(p\bar{\varphi}_m - \varphi_{m0}) - K_m\Delta\bar{\varphi}_m + k_m\bar{\varphi}_m = 0 \qquad [3.146]$$

$$\bar{\varphi}_m(.,.,p) = \bar{\varphi}_f(.,p) \quad \text{on } \Gamma \qquad [3.147]$$

$$\bar{q} = -\frac{1}{a}\nu K_m \langle \partial\bar{\varphi}_m/\partial n \rangle_\Gamma \qquad [3.148]$$

The Laplace transform of the interphase transport rate, q, is in fact, modulo a multiplicative constant, an average value of the Laplace transform of the gradient, which one can be derived from the solution of [3.146] and [3.147]. Equations [3.146], [3.147] can be written

$$a^2\Delta\bar{\varphi}_m - x^2\bar{\varphi}_m = \gamma \quad \text{in } \Omega \qquad [3.149]$$

$$\bar{\varphi}_m = \bar{\varphi}_f \quad \text{on } \Gamma \qquad [3.150]$$

where $x^2 = a^2(k_m+S_mp)/K_m$, and $\gamma = -a^2S_m\varphi_{m0}/K_m$. Applying the linear transformation

$$\psi = \frac{1}{\beta\bar{\varphi}_f}\bar{\varphi}_m + \frac{\gamma}{\beta\bar{\varphi}_f x^2} \qquad \text{where } \beta = 1 + \frac{\gamma}{\bar{\rho}_f \lambda^2}$$

one obtains the following problem

$$a^2\Delta\psi - x^2\psi = 0 \quad \text{in } \Omega \qquad [3.151]$$

$$\psi = 1 \text{ on } \Gamma. \qquad [3.152]$$

For any function ψ solution of this sytem of equations, one can define a function

noted B(x), by

$$B(x) = x^{-2}a\langle \partial\psi/\partial n\rangle_{\Gamma} \qquad [3.153]$$

A straightforward application of the divergence theorem leads to $B(x) = \langle\psi\rangle_{\Omega}$

Definition: B(x) is called the Block–Geometry Function assossiated with the problem [3.151], [3.152].

Replacing from [3.153] into [3.148], the Laplace transform of the interphase transport rate can be expressed as a function of B(x),

$$\bar{q} = -\nu[\bar{\varphi}_f(k_m+S_m p) - S_m\varphi_{m0}]B(x). \qquad [3.154]$$

Combining with equation [3.145] its comes the following differential equation

$$D\bar{\varphi}_f = \lambda\bar{\varphi}_f - \mu \qquad [3.155]$$

where

$$\lambda = S_f p + k_f + \nu(k_m+S_m p)B(x) \qquad [3.156]$$

$$\mu = S_f\varphi_0 + \nu S_m\varphi_{m0}B(x) \qquad [3.157]$$

$$x^2 = a^2(k_m+S_m p)/K_m\ . \qquad [3.158]$$

Notice that, when defining the concept of BGF no assumptions have been made regarding the shape of Ω. Remark also that the BGF depends only on the geometry of Ω, (not its abolute size). An important consequence is that the equation modeling the system in the Laplace space, Eq. [3.155], is now a simple second–order differential equation similar to the one obtained for a transport problem in a homogeneous media.

Quasi–steady State Models and BGF.

The quasi–steady state approach has already been presented. The first order physical non–equilibrium model being for example a quasi steady–state approximation of models explicitely accounting for diffusion into the porous blocks. With the notations above defined, this approach corresponds to equations [3.141], [3.144] and

$$S_m(\partial\varphi'_m/\partial t) + k_m\varphi'_m + q/\nu = 0 \qquad [3.159]$$

$$q = \alpha\nu K_m(\varphi'_m - \varphi_f)/a^2 \qquad [3.160]$$

where φ'_m represents an average potential in the porous blocks and α is a dimensionless parameter. Equations [3.141], [3.144], [3.159] and [3.160] can still be reduced to equation [3.155] and followings where the Block–Geometry Function is now defined as

$$B(x) = \alpha/(\alpha+x^2) \qquad [3.161]$$

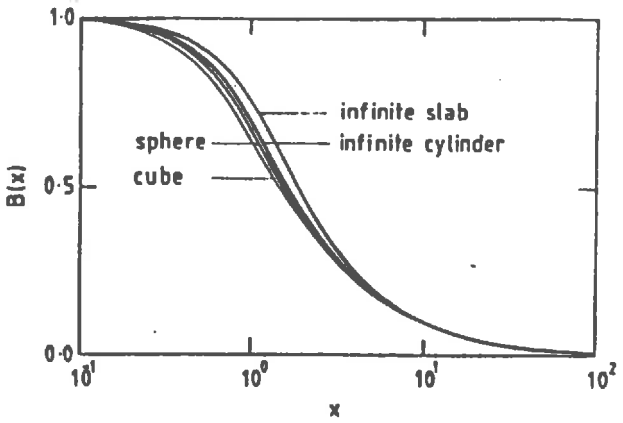

Fig. 3.13 Some examples of BGF for simple aggregate shapes [after *Barker 1985a*].

The fact that quasi–steady state and geometrically based models can be both integrated into the same formulation will provide an interesting way to compare both approaches, and will give some indications on when and how good (or bad) is the quasi–steady state model an approximation of the real transport process. Of course, we implicitely assume that equations [3.141] to [3.143] represent a good model, or at least the best available model, for the physical phenemena under examination. Notice that we do not include the boundary condition defined by Eq. [3.144] in this affirmation, since, as already remarked, the presence of a boundary layer, due to physical or chemical properties, and controling the exchange rate is likely. Introduction of this feature is the subject of the next paragraph.

Block–Geometry Functions and Boundary Layers

Equations modeling the presence of a boundary layer, also often referred as skin effect, film diffusion or film resistance, have been given earlier (see §3.2.2 *Another way to couple macro– and micro–porosity*). With the present notation, transport equations for a model accounting for the skin effect are constituted by [3.141] to [3.143] and the boundary condition [3.144] is now replaced by

$$\varphi_m = \varphi_s \quad \text{on } \Gamma$$

and q verifies

$$q = \beta\nu K_m (\varphi_s - \varphi_f)/a^2 \qquad [3.162]$$

The Laplace transform of the interphase transport rate is still given by equation [3.154] where $\overline{\varphi}_s$ now replaces $\overline{\varphi}_f$. Taking the Laplace transform of [3.162], $\overline{\varphi}_s$ can be expressed as function of $\overline{q}$, and replacing $\overline{\varphi}_s$ by its value in [3.154] leads to the following expression for $\overline{q}$

$$\overline{q} = (\nu K_m/a^2)(\xi - \overline{\varphi}_f)x^2 B_s(x,\beta) \qquad [3.163]$$

where

$$B_s(x,\beta) = B(x)/[1+x^2 B(x)/\beta]$$

and $\xi = S_m\varphi_{m0}/(k_m+S_m p)$.

Remark that if $\beta \to \infty$, (no film resistance), $B_s(x,\beta) \to B(x)$. Thus, the case of continuity of the concentration at the interface can be viewed as a limiting case of a more general formulation using the concept of film resistance. Barker (1985b), called B_s an "*Effective Block–Geometry Function*".

There is a certain analogy between the flux defined by equation [3.162] for the skin–effect model and the flux given by [3.160] for the quasi–steady state model. This degree of redundancy appears clearly when the BGF for the QSS model is written, $B(x)=1/(1+x^2/\alpha)$. This means that the QSS model can be viewed as diffusional model with an effective block–geometry function $B_s(x,\beta)$, where $\beta=\alpha$ and $B(x)=1$. Physically, this means that the QSS model can be viewed as a good representation of situations where the skin controls the exchange process and where the porous matrix has an infinite diffusivity ($B(x)\equiv 1$). Therefore, unless the introduction of the skin is physically required it is redundant to combine skin effect and QSS models.

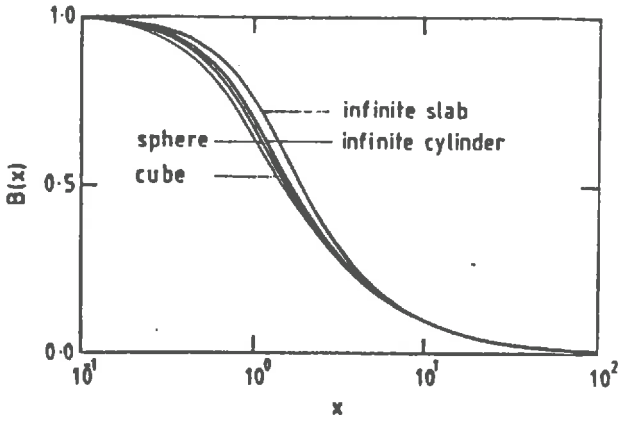

Fig. 3.13 Some examples of BGF for simple aggregate shapes [after *Barker 1985a*].

Block–Geometry Functions. Properties and Examples.

Block geometry functions depend on x and therefore on p. Given equation [3.154] this means that they completely characterize the time–variation of the interphase transport rate. Therefore, diffusion rates inside various aggregates can be qualitatively appreciated by looking at their respective BGF. It is obvious that the same is true regarding the variation of the average concentration inside the aggregates. Block–Geometry functions are easily calculated for simple domains, Ω. Some examples are given in Tab. 3.8 and plotted fig. 3.13. It is easy to verify that the BGF listed in Tab. 3.8 all verify the following properties

(a) $\lim_{x \to 0} B(x) = 1$

(b) $\lim_{x \to 0} B'(x) = 0$

(c) $B'(x) \leq 0$

(d) $B(x) \approx 1/x \quad \text{as } x \to \infty$

These properties do not automatically follow from the definition of B(x). Remark also that the BGF defined for the quasi–steady state model verifies properties (a), (b) and (c), but that when $x \to \infty$ then $B(x) \to \alpha/x^2$ and not $1/x$.

These properties give some insigths into the physical process. First, at small times or with high decay rates, k_m large, the behavior of the physical system is given by the behavior of B(x) when $x \to \infty$. Property (d) shows that all the BGF have the same behavior which means that the solution will not be shape dependent but will only depend on the block surface area per unit volume. This is not the behavior predicted by the BGF for the quasi–steady state model. Identically, at large times a common behavior, including the quasi–steady state model, is predicted which corresponds to the approach of equilibrium between matrix and fracture phases.

Arbitrary Block–Geometry Functions

Looking at the curves plotted on Fig. 3.13 it appears that for example an infinity of other possible BGF could be defined "between" those corresponding to an infinite slab and a cube, respectively. Thus, one can imagine to use parametrized empirical BGF in addition to the few ones already defined for regularly shaped porous blocks. Notice that using arbitrary BGF probably precludes from deriving analytical solutions and thus requires to numerically invert the solution obtained in the Laplace space. It seems reasonable that above properties be required from any BGF candidate. Barker (1985a) proposed three families

(a) All the functions in Tab. 3.8 can be parametrized by a.

(b) $B_k(x) = (1+kx)/(1+kx+kx^2) \quad k>0$

(c) $B_{k,h}(x) = (1+kx^2)/(1+hx^2+kx^3) \quad h>k>0$

Families (a), (b), (c) have 1, 2 and 3 parameters, respectively. Barker (1985b) also remarked that BGF for slabs, spheres and cylinders (see Tab. 3.8) can all be expressed in terms of modified Bessel functions

$$B(x) = \frac{I_{\mu/2}(\mu x)}{x I_{\frac{1}{2}\mu-1}(\mu x)} \qquad [3.164]$$

where μ = 1,2,3 for slabs, cylinders and spheres, respectively. Eq. [3.164] represents an infinite familly of functions which may be useful as empirical BGF.

Block–Geometry Functions and Composite Media.

Regarding, the problem of media made up of a mixture of blocks split into N classes, each characterized by their parameter a_i (volume to surface ratio), and BGF, $B_i(x)$,it is still possible to define a BGF for this mixture and this one is given by

$$B(x) = \sum_i P_i B_i(x a_i/a)$$

where P_i is the proportion of matrix volume occupied by blocks of type i, and a is given by

$$a = \left[\sum_i P_i/a_i\right]^{-1}$$

It is readily verified that the BGF above defined also verifies properties (a), (b), (c), (d). Barker (1985a) remarked that such BGF can considerably differ from those shown Fig. 3.13. However, it is interesting to remark that a BGF verifying properties (a), (b), (c), (d) exists for such a system and consequently that the behavior of a composite complex media can still be modeled with the approach previously developed. Therefore, for a given system, there is some hope to find a BGF by fitting procedures. One clearly see here that all the information usually carried by the solution of the diffusion equation in the porous block is now all contained in the BGF. The resolution of the diffusion equation in the porous blocks is no longer required.

Solution Procedures

At this point, analytical solutions of equation [3.155] with appropriated boundary conditions can be easily obtained. When D is the convection–dispersion operator these solutions already exist for particular one– two– or three–dimensional problems. Barker (1985a) remarked that analytical inversion of these expressions is not easy if not impossible in certain cases due to the complexity of B(x). Numerical inversion algorithms allow to overcome this problem. An other important advantage of numerical algorithms is that, given the possibility to quickly change the BGF or to use any reasonnable expression for it, they release the problem consisting to handle several complicated analytical solutions and the constraint consisting to only consider geometrically simple aggregates. This will be explained in more details later. A review of numerical algorithms for Laplace transform inversion is given §3.5.2. Let us also remark that if analytical solutions of [3.155] cannot be derived for some reasons, it is still possible to obtain by means of standard numerical techniques, finite differences or finite elements, an approximate solution and to apply the inversion algorithm to this one. This approach has been applied with success to different heat transfer problems in homogeneous media, Chen et al. (1987).

Time dependent Block–Geometry Functions and Direct Solutions

From equation [3.154] or [3.163] one can see that in fact $\overline{q}$ is expressed as a product of Laplace transforms. Let us define a function noted $B_t(t)$ by

$$B(x) = \int_0^\infty \exp(-x^2 t) B_t(t)\, dt$$

which means that $B(x)$ is the Laplace transform of $B_t(t)$ with respect to x^2. From equation [3.154] where $\overline{\varphi}_s$ replaces $\overline{\varphi}_f$ and after some manipulations $q(t)$ is given by

$$q(t) = L^{-1}[\overline{q}(p)] = \nu S_m \varphi_{m0} L^{-1}[B(x)] - \nu k_m L^{-1}[\overline{\varphi}_s(p) B(x)] - \nu S_m L^{-1}[p\overline{\varphi}_s(p) B(x)]$$

where L is the Laplace transform operator and L^{-1} its inverse. It is easily shown that

$$L^{-1}[B(x)](t) = \frac{K_m}{a^2 S_m} \exp(-k_m t/S_m)\, B_t\left(\frac{K_m t}{a^2 S_m}\right)$$

Using the convolution theorem, $L^{-1}[L(f)L(g)] = L^{-1}[L(f*g)] = f*g$, and usual formulas for Laplace transform it comes

$$q(t) = \frac{\nu K_m}{a^2} \exp(-k_m t/S_m) \left\{ (\varphi_{m0} - \varphi_{s0}) B_t\left(\frac{K_m t}{a^2 S_m}\right) - \right.$$

$$\left. \int_0^t \left[\frac{\partial \varphi_s}{\partial t} + \frac{k_m}{S_m} \varphi_s \right] \exp(-k_m t/S_m)\, B_t\left[\frac{K_m (t-u)}{a^2 S_m}\right] du \right\} \qquad [3.165]$$

If the skin effect is not accounted for, φ_f replaces φ_s in equation [3.165]. A similar expression is obtained if we start with [3.163] instead of [3.154] and $B_t(t)$ is replaced by a function $B_{st}(t)$. Barker (1985b) remarked that no relationship seems to appear between B_t and B_{st}.

If one knows $B_t(t)$, expression [3.165] is very useful for numerical modeling without making use of Laplace transform. Again, it is clear that the time dependent Block–Geometry function $B_t(t)$ carries all the information regarding the exchange process between the two phases. As an example, let us consider the case of solute transport modeling in densely fractured or aggregated media. Assuming that initial concentrations are equal to 0 in both phases, and that $k_m=0$ (no decay), the initial system of equations ([3.141] to [3.144]) is then reduced to

$$S_f \frac{\partial \varphi_f}{\partial t} = K_f \Delta \varphi_f - v \nabla \varphi_f - \frac{\nu K_m}{a^2} \int_0^t \frac{\partial \varphi_s}{\partial t}(u)\, B_t\left[\frac{K_m (t-u)}{a^2 S_m}\right] du\,. \qquad [3.166]$$

Such an equation is usually referred as a *Volterra partial integro–differential equation*. Notice that the variation of concentration in the immobile phase and consequently the exchange process between the two phases is modeled by a convolution integral. A certain analogy can be remarked when comparing with the coupling terms used by **Huyakorn et al. (1983a)** for water flow modeling in saturated fractured media. (Infinite sum of convolution integrals with an exponential in place of $B_t(t)$). (cf Equations [1.35], [1.36], [1.38]). This analogy is not surprising and will be clearly explained in the following paragraph. $B_t(t)$ is here analogous to what is known as a "*Memory Function*" in the field of leaky aquifers flow modeling, **Herrera and Rodarte (1973)**, Herrera (1974), **Herrera and Yates (1977)**.

If we want to use this approach we need to know B_t or at least to know some properties of $B_t(t)$. In the following we derive a general definition for $B_t(t)$, and give some of its properties.

Let us consider the case of diffusion inside porous blocks with initial concentration φ_{m0}, without decay and with a known and constant external concentration φ_s. In that case, equation [3.165] gives q(t) as

$$q(t) = -\nu K_m(\varphi_{m0}-\varphi_s)B_t(\frac{K_m t}{a^2 S_m})/a^2$$

and we have also

$$q(t) = -\nu K_m <\partial\varphi_m/\partial n>_\Gamma$$

Thus, $B_t(t)$ and the average gradient over Γ are related by

$$B_t(\frac{K_m t}{a^2 S_m}) = a<\partial\varphi_m/\partial n>_\Gamma/(\varphi_{m0}-\varphi_s). \qquad [3.167]$$

Consider now the problem (P) defined by

$$S_m\frac{\partial\psi}{\partial t} = K_m\,\Delta\psi \qquad \text{in } \Omega \text{ and}$$

$$\psi = 1 \text{ on } \Gamma \qquad \psi(0,x) = 0$$

These are in fact the equations describing solute transport inside an aggregate Ω, with a unit concentration at its surface and a zero initial concentration. A general solution of this problem can be sought of the form: $\psi(.,t) = f(.)g(t)$ where g(t) is

$$g(t) = \exp(-\beta K_m t/S_m).$$

Then, f must be a solution of $\Delta f = -\beta f$ and must verify f=1 on Γ. This is a particular case of a Sturm–Liouville eigenvalue problem. The Laplace operator being self–adjoint, we know, **Courant and Hilbert (1966)**, that the eigenvalues of this problem constitute a denumerable sequence β_i and that the eigenfunctions f_i constitute a complete orthogonal system. Noting $V(\Omega)$ the volume of Ω, the f_i functions can be normalized by

$$f_i = f_i / \| f_i \|_2^2 = f_i / [V(\Omega) \langle f_i^2 \rangle_\Omega]$$

and any general solution of the eigenvalue problem can be expressed as an infinite linear combination of the f_i,

$$f(.) = \sum_i \alpha_i f_i(.) .$$

The coefficients α_i are determined such that f verifies the initial condition of (P). Hence, they are the composantes of φ_{m0} in the basis (f_i) and are given by:

$$\alpha_i = \varphi_{m0} \langle f_i \rangle_\Omega V(\Omega)$$

Therefore, the general solution $\psi(.,t)$ of (P) is given by

$$\psi(.,t) = \sum_i \frac{\langle f_i \rangle_\Omega}{\langle f_i^{\,2} \rangle_\Omega} \exp(-K_m t \beta_i / S_m) \varphi_{m0}(.)$$

ψ constitutes the solution of (P) which is the homogeneous problem associated with Eq. [3.142] and [3.144]. At this point a direct application of *Duhamel's theorem* would lead to an expression of $(\partial\varphi_m/\partial t)$ under the form of a convolution integral. As we already noticed, a simple application of the divergence theorem allows to replace the term q appearing in Eq. [3.141] by the time derivative $(\partial\varphi_m/\partial t)$. Thus, by means of the solution of the homogeneous problem and of Duhamel's theorem, we can combine equations [3.141] and [3.142] to obtain an integro–differential equation. The other possibility is to calculate the average gradient over $\partial\Omega$ from above expression. Noting $b_i = a^2\beta_i$ and using [3.166] we derive the following formula for B_t

$$B_t(t) = \sum_i b_i \frac{\langle f_i \rangle_\Omega^2}{\langle f_i^{\,2} \rangle_\Omega} e^{-b_i t} = \sum_i c_i e^{-b_i t} \qquad [3.168]$$

An important property expressed by this formula is that time dependent block–geometry functions can always be expressed as an infinite sum of exponentials. It will be seen in the following that this property is fundamental when it comes to design efficient numerical schema to integrate equations such that [3.166]. Some example of $B_t(t)$ functions are given in Tab. 3.9. For these particular cases, the correspondance with the analytical solutions given Tab. 3.3 is obvious. $B_t(t)$ functions can be shown to verify the following properties, Barker(1985b)

(a) $B_t(t) \approx 1/\sqrt{\pi t}$ as $t \to 0$

(b) $dB_t(t)/dt \leq 0$

(c) $\lim_{t \to \infty} B_t(t) = 0.$

These properties cannot be obtained directly from the definition given above, Eq. [3.168]. They can be obtained from an other expression of $B_t(t)$ derived by the method of images and the fundamental solution of the heat equation. (See for example **Herrera and Rodarte (1973)** for a particular case or **Carslaw and Jaeger (1959)**). **Hornung (1987)** gives the following result, very similar to property (a). For spherical aggregates, $\rho(t)$, the solution of the homogeneous problem given Tab. 3.3, is closely approximated by the function:

$$\rho'(t) = \sqrt{1-\exp(-\pi^2 Dt)}$$

and in particular we have the following properties

$$\lim [\rho(t)-\rho'(t)] = 0 \quad \text{when } t \to 0 \text{ and } t \to \infty$$

$$\lim_{t\uparrow 0} [\rho(t)/\rho'(t)] = \pi\sqrt{\pi}/6 \approx 1.08$$

$$\lim_{t\uparrow \infty} [\frac{1-\rho(t)}{1-\rho'(t)}] = 1.22$$

We actually dont know if similar approximations hold for other geometries. These results are of practical interest since they allow to replace the sum of convolution integrals by a simple integral with a controlled error. This is the occasion to remark that even if the BGFs, $B(x)$ and $B_t(t)$, are "equivalent", the approach based on the Laplace transform has from a computational point of view the advantage to use simpler expressions for the BGF. In the direct approach, even with the possible approximation of $B_t(t)$ given above, will remain in many cases the problem of the evaluation of an infinite sum of convolution integrals.

Remark that the function B_t for the quasi–steady state model is $\alpha\exp(-\alpha t)$ and tends to α as t tends to zero. Thus at early times different behaviors are predicted by the QSS model and geometrically based models. This was a qualitative result also derived from BGF using the Laplace formulation of the problem.

Proceeding in a way similar to that used with block–geometry functions defined with the Laplace variable, it is possible to define a function $B_t(t)$ for a media made up of a mixture of porous blocks belonging to N classes each of which characterized by a volume to surface ratio, a_i, and a function, $B_{ti}(t)$. This function is given by

$$B_t(t) = \sum_i P_i(a/a_i)^2 B_{ti}(ta^2/a_i^2)$$

$$a^{-1} = \sum_i P_i/a_i$$

Parametrization of Time–dependent BGF.

Although, this is not remarked by **Barker (1985b)**, it is probably possible to use parametrized $B_t(t)$ functions. First, from equation [3.166], it appears clearly that for a given geometry, a is a possible parameter. Secondly, one

remarks that for the functions given Tab. 3.9, c_ns' coefficients are constant and therefore that $B_t(t)$ can be written

$$B_t(t) = c \sum_n e^{-b_n t}$$

Hence, for a given set of coefficients b_n, c appears as a second candidate to parametrize $B_t(t)$. This gives a two–parameters function. For a given physical situation, one can use the b_n's corresponding to a theoretical aggregate whose shape is the closest to the the real ones and adjust the parameters *a* and c. Usually, only the very first terms of the series are used due to the very quick convergence of the exponential series. Therefore, if we only use the first or the first two terms we get three– or four–parameters families. It is also evident that if we deal with short time transport processes, $B_t(t)$ can be taken in first approximation equal to $1/\sqrt{\pi t}$. The notion of "short time" is of course relative to the transport coefficient, diffusion or conductivity, in the porous matrix. The higher the value of the transport coefficient, the shorter the period of time this approximation can be consider a good one. The results given above regarding the approximation of the solution of the homogeneous problem also suggest some parametrizations.

3.5.2 RESOLUTION TECHNIQUES.

Though analytical solutions could be derived from equation [3.155] and the expressions given for the Block–Geometry Functions, this is not the most intelligent use it can be made of these. Beside the fact that the BGFs theory offers a general frame for transport modeling problems in densely fractured media, one of the main advantage it offers is that it releases the geometrical constraint and thus eliminates the part of the problem consisting to solve the diffusion equation for particular geometries. Thus, to take full advantage of the possibility to use arbitrary BGF and for example to fit these functions, one must use numerical techniques to invert analytical or numerical solutions obtained in the Laplace space. It is clear that with this approach a single numerical code is sufficient and that the block of the program defining the BGF only has to be change from one case to the other. Identically, if we use the time–dependent block geometry function approach leading to partial integro–differential equations, specific numerical techniques are required to handle such equations. In the following we give a review of different algorithms and methods to numerically invert Laplace transforms or to integrate equations such that [3.166].

A Method to solve Integrodifferential Equations

We are giving here some ideas and a numerical algorithm usually employed in the field of leaky aquifers flow modeling to treat such equations. A complete review of numerical techniques to solve integro–differential equations arising in the field of flow modeling in leaky aquifers and applicable to this case is given in Herrera (1976). Considering equation [3.166], one sees that evaluation of the convolution integral normaly requires to know at a given time t all the past history of functions φ_f or φ_s. This means that if the variables t and u cannot be decoupled in $B_t(t-u)$ one have to keep at hand all the information on φ_f or φ_s to be able to calculate the convolution integral. Effectively, since one of the function under the integral sign depends on the upper bound of the integral one have to carry out at each new time step the integration from 0 to the actual time. Fortunately, it has been shown that $B_t(t)$ can allways be expressed as a

sum of exponentials, which allows to decouple the contributions of u and t. Hence, the terms function of t can be carried out of the integral sign. The problem is then to truncate the infinit sum. A rigorous procedure to construct a familly of functions B_{tn} that approximate B_t is developed in **Herrrera and Yates (1977)**. These functions essentially retain the first n terms of the infinite series and have in addition a Dirac's delta function located at the origin, the mass of which accounts for truncated terms. Hence, each of the functions B_{tn} preserves what is called the "*yield*", which means that they verify the following condition

$$\int_0^\infty B_t(t)dt = \int_0^\infty B_{tn}(t)dt.$$

Thus, keeping only n terms of the series, equation [3.149] becomes

$$S_f \frac{\partial \varphi_f}{\partial t} = K_f \Delta \varphi_f - v\nabla \varphi_f - \sum_{i=1}^{n} c_i \exp\left(\frac{K_m b_i t}{a^2 S_m}\right) \frac{\nu K_m}{a^2} \int_0^t \frac{\partial \varphi_s}{\partial t}(u) \exp\left(\frac{-K_m b_i u}{a^2 S_m}\right) du$$

$$- A_n \frac{\nu K_m}{a^2} \int_0^t \frac{\partial \varphi_s}{\partial t}(u)\delta(t-u)\, du$$

Notice that the second integral on the right hand side is equal to $\partial\varphi_s/\partial t$ evaluated at u=t. Therefore, using a classical step by step integration algorithm, the remaining integral is simply evaluated by adding to its value at the previous time step the contribution of the current one. A complete derivation of discrete equations for a Crank–Nicholson schema is given in **Herrera and Yates (1977)** (see annex 3 for details). A second order in time accurate algorithm is also proposed in **Hornung (1987)**, (see also annex 3). A somewhat similar method was also used by **Bibby (1981)**, but his algorithm was not including the δ Dirac's function. The method developped by **Herrera and Yates (1977)** is in fact very general and said to be " *more appropriate than most of the methods specifically devised for transport modeling in fissured media.*", **Barker (1985b)**.

Numerical Inversion of the Laplace Transform

Many algorithms are available for numerical inversion of Laplace transform. Our purpose in this paragraph is to give some references where the reader will find most appropriate methods. Before starting this discusion we recall that if we deal with a convection–dispersion problem, the Laplace transform of the potential in the mobile phase is usually of the form: $L(\varphi_f)(s)=[\exp(a-\sqrt{f(s)})]/s$ where f(s) is a complicated function of s, classicaly involving ratios and square roots of hyperbolic or Bessel functions. Therefore, one should be carefull when assessing the quality of a method from results obtained on simple test problems.

A very easy to implement algorithm is the one given by **Stehfest (1970)**. Applied to some test problems, and in particular to the inversion of $F(s)=\sqrt{\pi/2}\exp(-1/2s)/s$ it seems to give an accuracy of about 1%. This algorithm was used by **Moench and Ogata (1981)** for a radial flow problem. The solution was displaying some oscillations and inaccuracies at large times as compared with the

analytical solution. This method should only be used for debugging purpose.

In a study of different theoretical solute transport problems in fissured media **Barker (1982)** used an algorithm due to **Durbin (1974)**. **Durbin (1974)** obtained a very good agreement for a case involving a combination of hyperbolic functions. **Valocchi (1985)** in his study of the validity of the LEA, (see §3.6.4) also used the same algorithm to evaluate the moments of the breakthrough curves from their expressions in the Laplace space. This algorithm largely improves the original method of **Dubner and Abate (1968)**. A very similar method was proposed by **Crump (1976)**. This last algorithm is particularly well suited to handle oscillating functions. A very good accuracy is obtained in the case of damped oscillatory functions. These two methods are recommended by **Barker (1985b)**, as well as a method due to **Talbot (1979)** for its high accuracy and efficiency.

Lately, an algorithm based on an expansion of the function f, solution of the inverse problem, in series of Laguerre polynoms and Poisson functions have been proposed, **McCoy (1987)**. The coefficients are simply function of the moments of f, which are easily obtained from F, the Laplace transform of f, by

$$M_n = \lim_{s \to 0} (-1)^n d^n F / ds^n$$

The moments M_n can be evaluated numerically or by means of a code performing algebra operations, (MACSYMA, MUMATH, ..). This method seems to be able to give correct results for exponential functions but is not recommended for oscillatory functions.

Hsu and Dranoff (1987), proposed an algorithm based on Fast Fourier Transform. They compared their numerical solution with the analytical one given by **Rosen (1952)** for the problem of solute transport in media made up of spherical aggregates. (See §3.2.2 *An other way to couple macro– and micro–porosity* for the definition of the problem and §3.3.1 for the analytical solution.) A very good agreement is obtained with a relative error lower that .001%. In addition it seems that their solution is very little sensitive to the number of terms used to calculated the FFT and to the size of the time increment. This algorithm is in fact the one proposed by **Durbin (1974)** and improved for the evaluation of the Fourier coefficients.

The reader interested in a review of these methods and more details should refer to **Davies and Martin (1979)**. See also for an improved method, De Hoog et al. (1982). It is difficult to recommend a particular algorithm, but it seems that one should preferentially use those of **Durbin (1974)**, **Crump (1976)**, **Talbot (1979)** and **Hsu and Danoff (1987)**. However, it would be interesting and probably a good precaution to first test these methods against the various analytical solutions presented before.

3.5.3 CONCLUSIONS

As remarked, the concept of Block–Geometry Function appears at two levels. First, applying the Laplace transform to the set of equations defining the problem, the BGF appears as the average of the Laplace transform of the potential over a porous block, or what is equivalent as the Laplace transform of the interphase transport rate per unit storage capacity of the matrix per unit difference in initial "potential", Eq. [3.154]. In that case, a simple differential equation modeling the transport phenomena results in the Laplace space, the coefficients of which depend among others parameters on the BGF. It is also obvious that BGFs naturally appear as Laplace transforms. Therefore, applying

the Laplace transform inverse operator to equation [3.154], a relation is obtained between the interphase transport rate and a function defined as a time–dependent Block–Geometry Function. For both types, independent definitions and properties have been given.

The connection with the solution of the homogeneous problem associated with the diffusion equation modeling solute movement inside the aggregates has been underlined. It is important to remark that in fact, we mainly used the properties of regularity and linearity of the Laplace operator. For example these properties allowed us to express the solution in a general form without having to introduce assumptions regarding the geometry of Ω.

The theoretical frame developed in the previous sections offers a general and attractive tool for transport modeling in materials presenting two distinct domains where water, solute or heat transport rates are ruled by different equations. It has been shown that all previous approaches, quasi–steady state model, geometrically based models, skin effect model, can be integrated in the frame of BGFs. Beside that, it is important to remark that with the formulation obtained with the BGF we no longer have to assume a simple geometrical shape for the porous blocks or more generally for the immobile water phase. All the information on the interphase transport rate depending on the geometry is now concentrated in the BGF. Thus, this one appears as a characteristic of the geometry of the porous media, characteristic which can probably be obtained by identification or parameter fitting techniques. As important is the fact that by means of numerical inversion methods for Laplace transforms, we can use as complicated BGFs as we want to characterize a porous media, BGFs for which analytical inversion of the solutions of the problem are unlikely to be possible. Thus, for problems where initial and boundary conditions allow to derive analytical solutions in the Laplace space, the combination of arbitrary BGF and numerical techniques for inverting Laplace transforms provide a powerful tool for transport modeling.

When the geometry or initial or boundary conditions do not allow to derive analytical solutions for [3.155], it is still possible either to use numerical solutions of that equation, or to use equation [3.141] where q is given by [3.165]. In this last case we have to solve a partial integro–differential equation. Remark that a certain formal analogy exist between equation [3.166] for example and equation [3.25]. The interphase coupling term is now much more complicated and in fact the interphase transport phenomena is no longer approximated by a first order process as it is the case in the usual quasi–steady state model. Here again the time–dependent Block–Geometry Function completely characterizes the geometry of the porous blocks. Thus, as for the BGFs, it seems reasonable to try to obtain B_t by means of fitting techniques.

It appeared that the block geometry function concept allows to compare quasi–steady state (QSS) and geometrically based models. As the QSS model is usually viewed as an approximation of those, it is important to know when this approximation can be considered valid. The general problem of relating macroscopic models (QSS or LEA) to geometrically based models is adressed in the following paragraphs.

3.6 MACROSCOPIC MODELING APPROACHES.

3.6.1 INTRODUCTION

As noted at the beginning of this report, first approaches to solute transport modeling were based on the simple CDE. Later it was recognized that the physics of the transport process was not well described by the LEA. Progressively, more and more complicated models, more realistically simulating the physical and chemical processes taking place during solute transport, were introduced. So, successively appeared the first order non–equilibrium model accounting with a relatively simple equation for solute exchange between two water phases and later, models based on geometrical conceptualizations of the porous media explicitely simulating the diffusion process from one phase to the other. At each step more detailed informations on the media were required to make use of these models. An other problem was that additional parameters were introduced whose links with the physical process were not always very clear or were quite complicated.

Models such as the quasi–steady state model given §3.2.2 or the LEA model (Local Equilibrium Assumption model) given by equation [3.1] are because of their relative simplicity attractive and easily coupled with other transport models. So an important task is to estimate when these simplified approaches can be used instead of more rigorous but also more complicated models based on a geometrical conceptualizations of porous blocks.

A trend in the last two or three years has been to use the information gathered from complicated and detailed models to obtain more useful expressions for the parameters to be used in simpler models. Therefore arises the problem to identify the real dependence on flow characteristics and geometry of parameters such that α for the QSS model or the dispersion coefficient for the LEA models. The problems consisting to define conditions such that two different models are "equivalent" and/or to seek for relations linking model parameters to flow and domain characteristics has been mainly envisaged in the last years by Rao et al. (1980a), Raats (1981, 1984), van Genuchten (1985b), van Genuchten and Dalton (1986), Barker (1985a,b), Valocchi (1985), Parker and Valocchi (1986). At the light of the previous results obtained with the BGF theory and as we now dispose of a general and relatively simple formulation for the transport problem in inhomogeneous media, it is clear that some of these studies dealing with particular cases are of somewhat limited interest. Therefore, we shall only briefly review the various results presented in the literature.

The first step has been in a first time to link QSS and diffusional models and then to go back one step further to the LEA model. Many ways have been employed to compare the different models and derive equivalent coefficients. They are generally based on the comparison of solutions in batch systems or on the comparison of breakthrough curves. In the following, before dealing with these particular cases, we first present a general method having as starting point the partial integro–differential equation derived before and giving some insight into the relations existing between the different models.

3.6.2 ZEROTH– AND FIRST–ORDER APPROXIMATIONS OF DIFFUSIONAL MODELS

The quasi steady state model has already been presented, without justifications, as an approximation of more rigorous models explicitely simulating the diffusion process inside the aggregates. We are going to show that in fact the QSS model is a "*first–order*" approximation of these models and quantify the error made by neglecting "*higher order*" terms. We stated that the transport

process is modeled by a partial integro–differential equation such as [3.166]. We also showed that the function $B_t(t)$ referred as BGF or "memory" function can always be expressed as a series of exponential terms, eq. [3.168]. With these properties, the general partial integro–differential equation modeling the transport process can be symbolically written

$$M(\varphi_f) = -\int_0^t \frac{\partial \varphi_f}{\partial t}(u) \sum_{i=0}^{\infty} c_i e^{-b_i(t-u)}\, du \qquad [3.169]$$

where M is the differential operator $(S_f\partial/\partial t - D_f\Delta + v\nabla)$. Notice that since the integral on the right hand side describes the time variation of the concentration in the immobile phase, M is equivalent to : $-\partial\varphi_m/\partial t$. Taking the Laplace transform of this equation and using its basic properties, in particular the formula for a convolution product, yields

$$\overline{M} = -sL(\varphi_f)(s) \sum_{i=0}^{\infty} \frac{c_i}{s+b_i}. \qquad [3.170]$$

It can be shown by different ways that the series in equation [3.170] can always be written under the form $\Sigma\ \gamma_i s^i$ where each γ_i depends on all the b_j and c_j coefficients. Therefore, applying the inverse Laplace operator to

$$\overline{M} = -sL(\varphi_f)(s) \sum_{i=0}^{\infty} \gamma_i s^i \qquad [3.171]$$

and making use of the fact that if $c(0)=0$, $L(d^ic/dt^i) = s^iL(c)$ it comes

$$M(\varphi_f) = -\left\{ \sum_{i=0}^{\infty} \gamma_i \frac{\partial^i}{\partial t^i} \right\} \frac{\partial \varphi_f}{\partial t} \qquad [3.172]$$

Before using this result let us derive an other relation. An other possibility is, in equation [3.171], to divide the left hand side by the series so as to keep on the right hand side, the Laplace transform of the time derivative only. It is then possible with relatively little algebra to obtain an expression of the form

$$-sL(\varphi_f)(s) = \overline{M} \sum_{n=0}^{\infty} \beta_i s^i \qquad [3.173]$$

Then applying the inverse operator to this equation it comes

$$\frac{\partial \varphi_f}{\partial t} = -\left\{ \sum_{i=0}^{\infty} \beta_i \frac{\partial^i}{\partial t^i} \right\} M(\varphi_f) \qquad [3.174]$$

In equations [3.172] and [3.174] it is assumed by convention that $\partial^0/\partial t^0$ is the identity operator. The time variation of the mass of solute in the immobile zone is now directly related to the various time derivatives of the concentration in the mobile phase. Considering [3.172] one sees that if we drop all the terms but the first one in the series, we obtain a model where the variation of the concentration in the immobile phase (left hand side) is linearly related to the variation of the concentration in the mobile phase, which traduces the establishment of an intantaneous equilibrium between the two phases. Therefore, the instantaneous equilibrium model corresponds to a zeroth–order approximation of the diffusional model. This conclusion is also straightforwardly derived from equation [3.174].

Still considering equation [3.172], if we conserve the first two terms in the series we introduce a second derivative for φ_f. This means that we add to the instantaneous storage term (first derivative), an inertie term which is the simplest way to account for the inertie of the porous blocks in the process of uptaking or releasing solute. This results in a modified dispersion coefficient in the CDE. An example of application to spherical aggregates, is given below, (§3.6.4).

Conserving the first and second terms of the series in equation [3.174] can be easily shown to correspond to use a first–order linear differential equation, identical to the one used in the QSS model to describe the interphase transport rate. From equation [3.174] we have

$$\frac{\partial \varphi_f}{\partial t} = -\beta_1 M(\varphi_f) - \beta_2 \frac{\partial}{\partial t}[M(\varphi_f)]. \qquad [3.175]$$

But as $M(\varphi_f) \approx -\partial \varphi_m/\partial t$ it comes

$$\frac{\partial \varphi_m}{\partial t} \approx \frac{1}{\beta_2}[\varphi_f - \beta_1 \varphi_m] \qquad [3.176]$$

which effectively models the variation of concentration in the immobile phase as a first–order process. Thus, the QSS model can be viewed as a first–order approximation of diffusional models. Remark that the LEA model with a modified dispersion coefficient and the QSS model constitute both first–order approximations of the diffusional model. Which one is the best is not an easy question to answer to. It is probably cases dependent

3.6.3 BACK TO THE QUASI–STEADY STATE MODEL

The quasi–steady state model uses in particular a parameter α which one controls the exchange rate between the mobile and immobile zones. Assumptions behind this model are in particular, uniform concentration in both phases at a given level and realization of an instantaneous equilibrium inside the "stagnant zones" when a change in concentration occurs in the interface mobile–immobile water. It is obvious that in media where the immobile phase has a significantly non–nul thickness, as it is the case for fissured or aggregated media, transverse gradients exist and that equilibrium inside the immobile phase is never attained unless the concentration in the mobile phase remains constant over a sufficiently

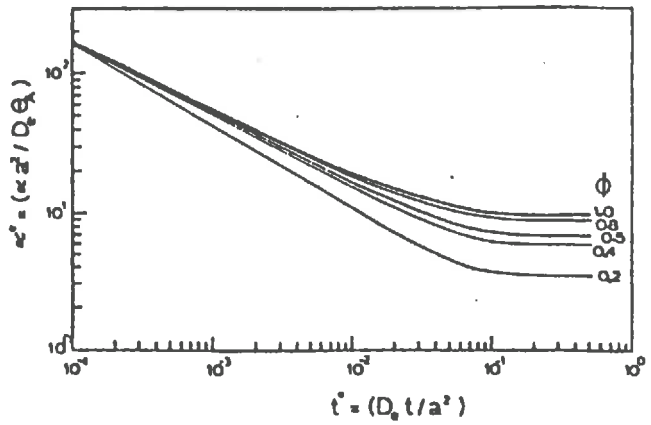

Fig. 3.14 Evolution of the dimensionless parameter α^* function of $t^*=D_et/a^2$. The results are plotted for various values of ϕ (see Eq. 3.77) [after *Rao et al. 1980*].

long period of time.

Consequently, description of the exchange rate by a first–order process is only valid if the "thickness" of the stagnant zones is small enough. This notion is in fact relative to the average time needed to obtain the equilibrium for a given perturbation at the interface. Therefore, when this conceptual model is applied to aggregated media, the fact that the basic assumptions are not verified must in some ways be integrated in the parameter α.

Dependence of α on flow and media parameters

The problem of relating α to media characteristics was first adressed by Rao et al (1980b). They used two models, namely the spherical diffusion model and the quasi–steady state model, to describe diffusion out of spherical aggregates in a batch experiment. Using analytical solutions of these two models and matching the expressions, the following expression was derived for α

$$\alpha = \frac{D\phi\theta_a}{a^2}\frac{\sigma_1}{\sigma_2} \qquad [3.177]$$

where D is the diffusion coefficient inside the aggregates, θ_a is the volumetric water content of the aggregates, θ_m is the volumetric water content external to the aggregates, a is the radius of the spheres, $\phi = \theta_m/(\theta_a+\theta_m)$, and σ_1 and σ_2 are given by:

$$\sigma_1 = \sum_{n=1}^{\infty} \frac{6\beta(\beta+1)q_n^2}{9+9\beta+q_n^2\beta^2} \exp\left(-\frac{Dq_n^2 t}{a^2}\right) \qquad [3.178]$$

$$\sigma_2 = \sum_{n=1}^{\infty} \frac{6\beta(\beta+1)}{9+9\beta+q_n^2\beta^2} \exp\left(-\frac{Dq_n^2 t}{a^2}\right) \qquad [3.179]$$

where q_n are the roots of

$$\tan(q_n) = \frac{3q_n}{3+\beta q_n^2}$$

and $\beta = \theta_m/\theta_a$. It appears clearly that α depends not only on the shape and size of the aggregates but also on time. A plot of $\alpha(t)$ in dimensionless variables is given Fig. 3.14 for different values of ϕ. Clearly α decreases untill it reaches a constant value equal to

$$\alpha = D\theta_a\phi q_1^2/a^2 \quad \text{for} \quad Dt/a^2 > 0.1\ . \qquad [3.180]$$

This means that the larger the size of the aggregates and/or the lower the diffusion coefficient, the higher the time at which α becomes constant. To fix the ideas let us consider a diffusion coefficient of about 10^{-6} cm^2s^{-1}, which is a reasonnalble values for the Nitrate diffusion coefficient in soil, and aggregates with radius .5 cm. Under these conditions, the value of t after which α is constant is approximately equal to 7 hours. Remark the quadratic dependence on the radius of the aggregates, Eq. [3.177]. (Note Equations [3.180] implicitely define a

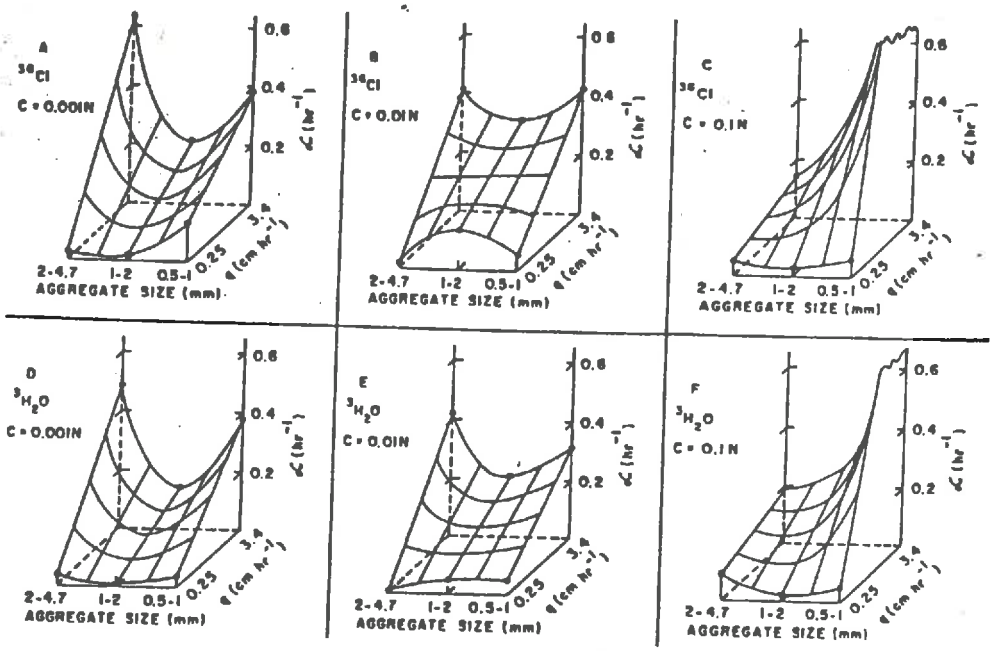

Fig. 3.15 The mass transfer coefficient α as a function of aggregate size and flux for solutions of ^{36}Cl and $^{3}H_2O$ at various concentrations [after *Nkedi–Kizza et al. 1983*].

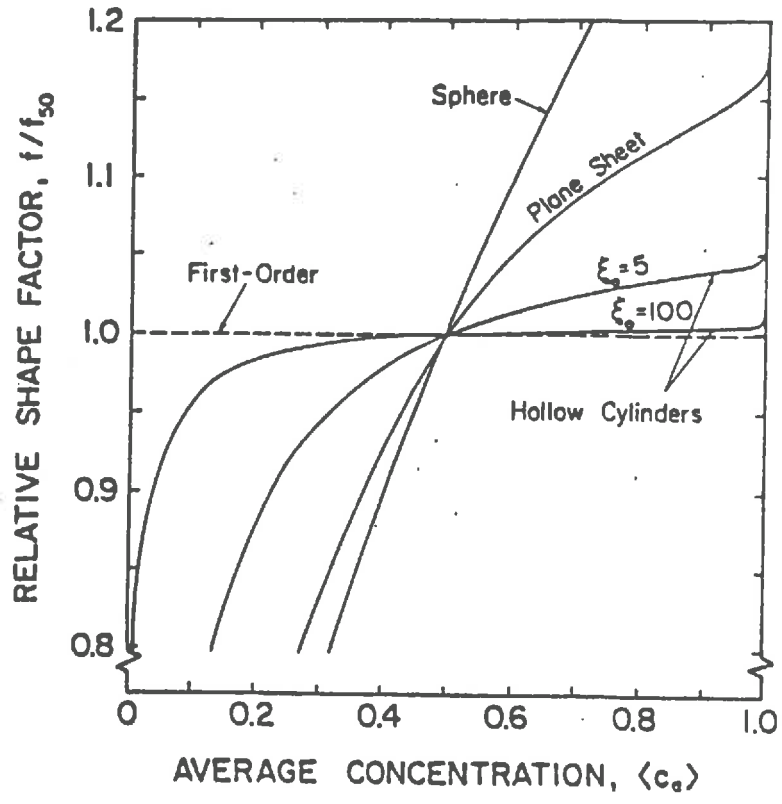

Fig. 3.16 Effect of the average concentration on the relative shape factor used to derive the mass transfer coefficient of an "equivalent" first–order rate model [after *van Genuchten 1985*].

region of equivalence for both models. It is clear from these equations, dependence of α on time, that the QSS model is a poor approximation at "early times". The same conclusion has already been derived from respective BGFs for these two models.

For non–batch systems, the dependence of α on flow and media characteristics is more complicated. From a study by Nkeddi–Kizza et al. (1983) where the different parameters of the QSS model were fitted to a series of column experiments, one can conclude that α increases with the velocity, but no simple relation seems to arise regarding the dependence of α upon aggregate size while it is the case for batch experiments. This may be due to incertitudes in fitted parameters as well as to the poor adequacy of the QSS model. It also appears a dependence of α upon the concentration which is not explained. In fact as it can be constated on Fig. 3.15, the dependence of α upon the various parameters is rather complicated and seems to preclude from deriving relationships between α and these parameters.

van Genuchten (1985b) also proposed a method to relate α to aggregate shapes. This method is very similar to the one he derived to pass from one aggregate shape to another. (cf §3.4.3) A solution of [3.33] in a system where C_m is constant (C_m=1) and the initial concentration equal to 0 is given by:

$$C_{im}(T_1) = 1 - \exp(-T_1) \quad \text{with} \quad T_1 = \frac{\alpha t}{\theta_{im} R_{im}} \qquad [3.181]$$

The method consists to seek for a parameter α such that equation [3.181] describes solute accumulation inside a given aggregate. Let's for example consider the case of a spherical aggregate. If we consider T_1 as the characteristic time of a reference aggregate we can look for an α such that the average concentration inside the sphere, $<C_a>$ be equal to C_{im} (Eq. [3.181]) at a given time. Again α is time– or concentration–dependent and α is arbitrarily defined such that the average concentration $<C_a> = .5$ is attained at the same time for both aggregates. Hence, we can use the table of parameters f previously defined, Tab 3.4, and for example, the parameter α to approximate a media made up of spherical aggregates with radius a_s is given by:

$$\alpha = \frac{D_a \theta_{im}}{f_{s,1}^2 a_s^2} \qquad [3.182]$$

It follows that dimensionless parameters ω (dimensionless parameter for α) and γ_s (dimensionless diffusion coefficient for the aggregates), see equations [3.28] and [3.60a,b] for definitions, are related by

$$\omega = \frac{(1-\beta)R\gamma_s}{f_{s,1}^2} \approx 22.4(1-\beta)R\gamma_s \qquad [3.183]$$

Similar equations apply to conversions from other aggregate geometries. See Table 3.4 for values of $f_{i,j}$. For a hollow cylindrical macropore the following relation holds

$$\omega = \frac{(1-\beta)R\gamma_p}{(\xi_0-1)^2 f_{p,1}^2} \qquad [3.184]$$

Fig 3.16 illustrates the dependence of the parameter f upon average concentration

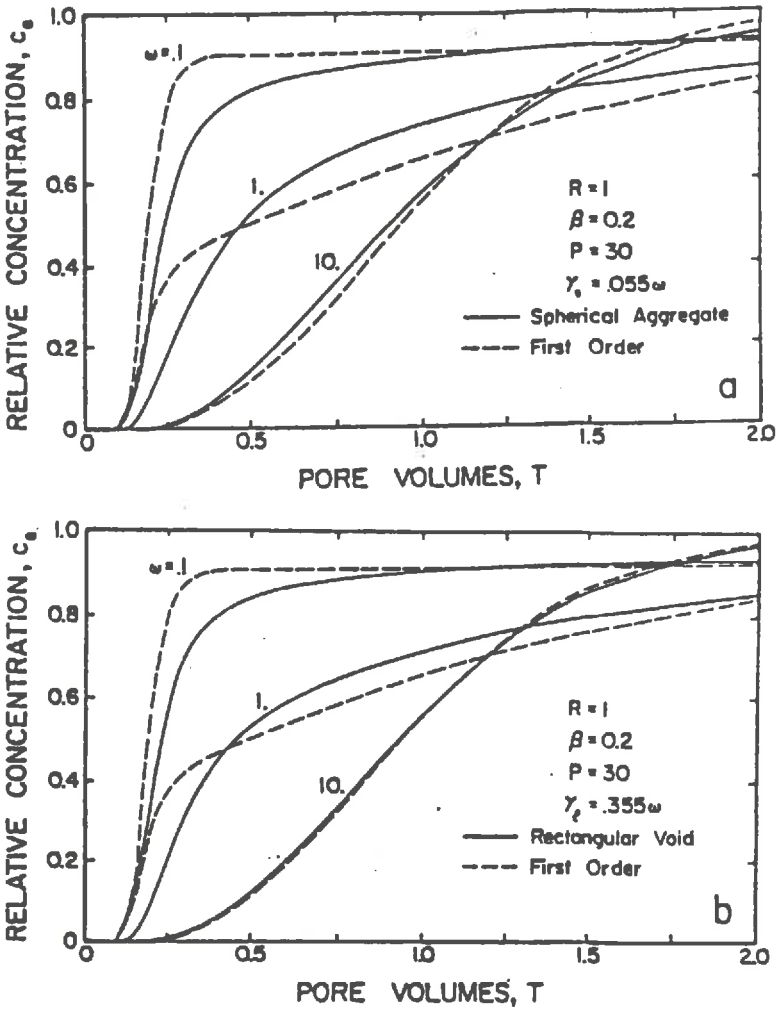

Fig. 3.17 Breakthrough curves obtained with the approximate first–order rate model and exact solutions for (a) spherical aggregates and (b) rectangular voids [after *van Genuchten 1985*].

inside the aggregates. It can be seen that except for the case of a hollow cylindrical macropore, the first order model only poorly approximates the reality. This is more explicitely illustrated by Fig 3.17 and 3.18 presenting various breakthrough curves obtained for different aggregate shapes using either the exact solution or the one obtained with the first order "equivalent" model. A derivation of ω based on a comparison of Laplace transforms of immobile concentrations obtained for both approaches is also possible and leads to similar results. For more details see van Genuchten and Dalton (1986)

For the particular case of spherical aggregates, Parker and Valocchi (1986) derived an expression for ω by matching the second order moments of breakthrough curves obtained with the QSS model and with the model using spherical aggregates. (cf. Eq. [3.55]–[3.60] for the definition of the problem and equations [3.87]–[3.88] for the analytical solution.) More details can be found in the following paragraph (§3.6.4) concerning the technique used to calculate the moments. They derived the following expressions

$$\omega = 15\gamma_s R(1-\beta) \qquad \text{or} \quad \alpha = 15 D_a \theta_{im}/a^2 \,. \qquad [3.185]$$

The first expression is similar to the one derived by van Genuchten (1985b) in which where the coefficient was approximately equal to 22.4 instead of 15, (Eq. [3.183]).

The same expression was obtained by Raats (1984) in the case of spherical aggregates using a development of the operator in the mobile phase. His method was a particular case of the general discussion on the relations between macroscopic and geometrically based models proposed above, (see §3.6.2).

By means of BGFs, Barker (1985a,b) also looked at how good is the QSS model an approximation of geometrically based models. As already presented, one of the main result is that the BGFs assossiated with QSS and geometrically based models do not behave in the same way when $x \to \infty$ which indicates that at early times the QSS model is not a good approximation of geometrically based models. This is in agreement with previous conclusions. The BGF theory predicts that at large times the QSS model becomes a good approximation. A natural way to obtain the parameter α to be used in equation [3.160] at large times is to compare the respective BGFs when $x \to 0$. (Attention, the meaning of α is not the same here and in [3.185]). This is done by equating their respective Mac–Laurin series in the vicinity of 0. One finds

$$\alpha = -2/B''(0) \qquad [3.186]$$

which for examle gives α = 3, 2, 5/3, 1.377... for slab, cylinders, spheres and cubes, respectively. An other alternative proposed by Barker (1985b) is to compare the long–time behavior of the respective $B_t(t)$ functions. As they are all expressed as series of exponential terms, (cf Tab 3.9 and Eq. [3.168]), a possible choice is to take only the first term of the series and to choose $\alpha = b_1$. In that case one obtains α = 2.47, 1.45, 1.1, .82 for slab, cylinders, spheres and cubes, respectively. Which ones are the best is here also a question without simple answer.

Remarks and Perspectives

At this point it is important to remark that all above studies try to

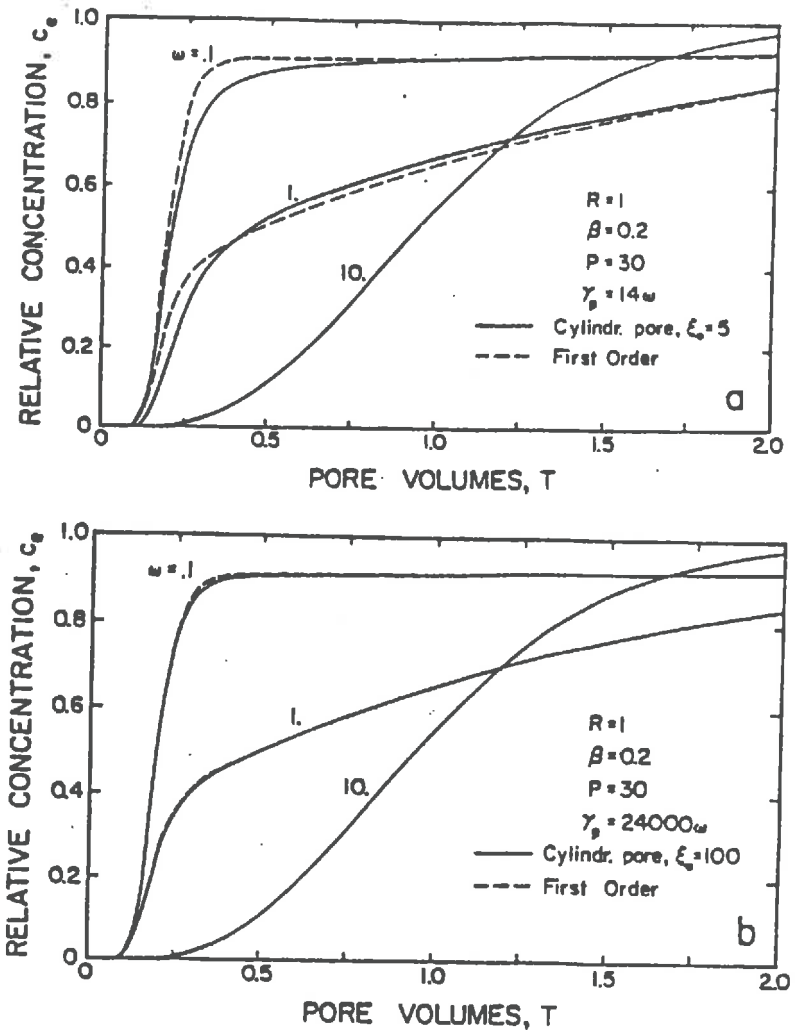

Fig. 3.18 Breakthrough curves obtained with the approximate first–order rate model and exact solutions generated with the cylindrical macropore model for two values of ξ_0 [after *van Genuchten 1985*].

replace α, a time–dependent and very poorly understood parameter, by a constant, simply in order to simplify the mathematical formulation and to reduce the amount of calculation effort required to solve the problem. A very important result of the BGF theory is that the complicated initial set of equations is, precisely via the introduction of a BGF, reduced to a simple ordinary differential equation or to a partial integro–differential equation. These equations are no more complicated to solve than those of the QSS model but have the advantage to retain the complexity of the interphase exchange process through the time–dependent BGF involved in the convolution integral or directly in the BGF appearing in the coefficients of the equation in the Laplace space. Much more, we are no longer restricted to make a choice regarding the shape of the aggregates. Thus the block geometry functions and α play a very similar role. However, it seems that unlike α the BGF does not depends on the characteristics of the flow. This is probably due to the very crude nature of the QSS model which leads to, at the same time, lump into a constant parameter, geometrical and time–dependent properties. At the light of BGFs' intrinsic properties, it will perhaps be more easy to relate the BGF to mesurable characteristics of soil structure than we have so far been able to understand and quantify the relationships between α and soil or/and flow parameters. This problem may very well be a consequence of the poor representation of the interphase diffusion process provided by the first order equation. Consequently the following question arises: Shouldn't we preferentially look at the relations between BGFs and soil geometrical characteristics rather than go on focusing on the meaning of α that we know is anyway a pisaller? One should be aware that while α can only be determined from dynamic experiments, the BGF for a representative volume of soil, can be obtained from a simple batch experiment. (A representative volume of soil being a sample offering a representative mixture of aggregate shapes that can be present in the soil profile.) This simply comes from the definition of the BGF, Eq. [3.151]–[3.153] or Eq. [3.167]. Thus, BGFs can be obtained by applying fitting techniques either to the problem expressed in original variables or expressed in terms of Laplace transforms. Compared to tracer experiments on laboratory soil columns or in the field, advantages in terms of time, cost and simplicity are evident. Of course, BGFs can also be obtained from dynamic experiments. In particular, if a boudary layer approach is elected for the modeling of the interphase tranport rate, dynamic experiments are probably required in order to fit the transport parameter involved in this formulation, β in Eq. [3.162].

van Genuchten (1985b) remarked that many information have been gathered over the years, Brewer (1964), Baver et al. (1972) regarding soil aggregation, soil structure, aggregate shapes, sizes, types, etc.. As BGFs only depend on the geometry of the porous blocks, direct links could probably be found between BGFs and soil morphological properties.

3.6.4 BACK TO THE *LEA* MODEL

The simplest solute transport model based on the CDE is the LEA model. The main advantage of this model over others is that it requires only two parameters, the retardation factor and the dispersion coefficient. In addition relatively simple analytical solutions are available for steady–state flows and for more complicated unsteady cases, numerical solutions can still quite easily be obtained. We showed in §3.6.2 that the simple LEA model is a zeroth–order approximation of diffusional model. We also showed that by retaining one more term in the series one obtains a model with a modified dispersion coefficient, which ~~now~~ ~~constitutes~~ a first–order approximation. The problem is ~~thus~~ to define "when" a LEA based model can be used in place of first–order or

diffusional models and how good is the approximation. We already reported in paragraph 3.1 ("*Adsorption isotherms and Retardation factors*"), that a rather "qualitative" condition was that chemical reaction rates should be faster than flow rates. In the following we report two studies conducted by **Valocchi (1985)** and **Parker and Valocchi (1986)** defining some constraints on the validity of LEA and first–order physical nonequilibrium models applied to structured porous media.

Moments Analysis

In both papers, evaluation of equivalence between the different models is carried out by "comparing" the breakthrough curves. If we consider them as distributions, a "measure" of their "differences" is provided by comparing their various moments. Usually, the comparison is limited to the first three moments, expectation, variance and skewness. For a pulse–like input, the nth moment of the breakthrough curve is given by

$$M_n = \int_0^\infty T^n \, C(L,T) \, dT \qquad [3.187]$$

Remark that the total mass of solute leaving the soil column is proportional to M_0. Thus the nth central normalized moment μ_n is given by

$$\mu_n = \left[\int_0^\infty (T-\mu_1)^n C(L,T) \, dT\right] / \left[\int_0^\infty C(L,T) \, dT\right]. \qquad [3.188]$$

The main problem arising when evaluating these expressions is that analytical expressions for breakthrough curves are under the form of complicated integral involving complicated analytical functions, (e.g. the various analytical solutions presented before), thus precluding from obtaining analytical expressions for the moments. This obstacle is overcome by making use of a formula due to **Aris (1958)** that relates the moments to the derivatives of the Laplace transform of the function. In our case, Laplace transforms of the breakthrough curves are easily obtained and expressed as relatively simple functions, hence allowing to obtain analytical expressions for the moments. The formula due to **Aris (1958)** is

$$M_n = (-1)^n \lim_{p \uparrow 0} \left[\frac{d^n}{dp^n} \overline{C}(L,p)\right]. \qquad [3.189]$$

Valocchi (1985) gives the different expressions of the Laplace transform of the breakthrough curve for the LEA model, the first–order physical non–equilibrium model, a kinetic chemical non–equilibrium model and the spherical aggregates model, respectively. One must remark that the chemical nonequilibrium model used is only a particular case of a more general one proposed by **Nkedi–Kizza et al. (1984)** that was shown to be mathematically equivalent to the physical nonequilibrium model. In the model used by **Valocchi (1985)** all adsorption sites are assumed to be of the kinetic type. Consequently, it seems that there is a certain degree of redundancy among the various models he analysed. The first three moments and Laplace transforms of the breakthrough curves for the various models are given in Tabs. 3.10 and 3.11, respectively.

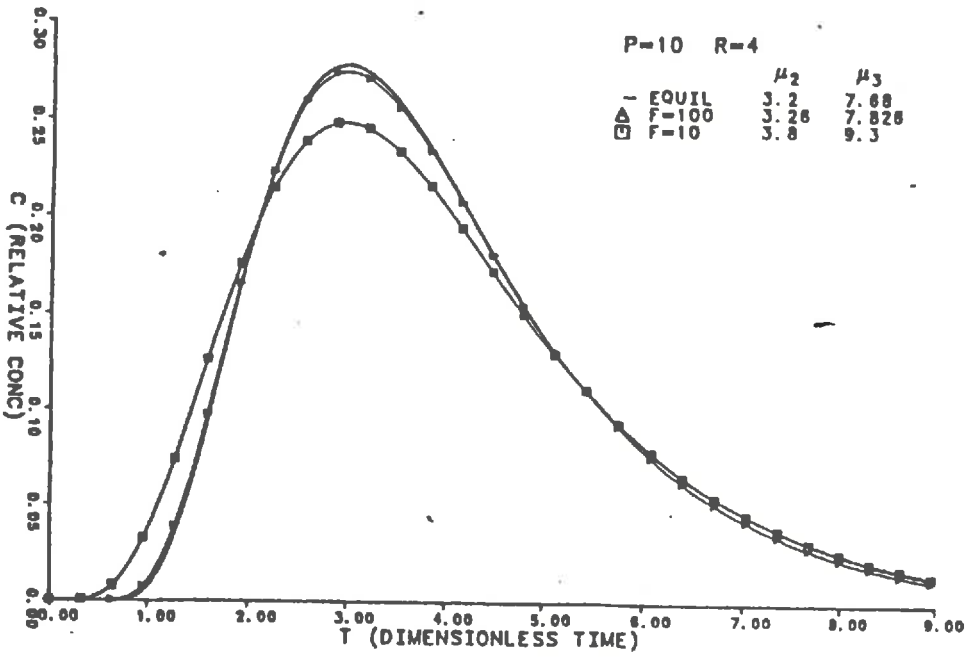

Fig. 3.19 Comparison of equilibrium and linear chemical nonequilibrium breakthrough curves for a Dirac impulse. Parameters of interest are indicated on the graph [after *Valocchi 1985*].

As the first moments are all equal one can conclude that the mean breakthrough time is not influenced by the type of nonequilibrium model. As well, higher order moments are very similar which indicates that the type of nonequilibrium model does not greatly influence the shape of the breakthrough curve. Valocchi (1985) proposes to use the following formula to evaluate the differences between the moments obtained for the various nonequilibrium models and the LEA model, respectively.

$$\epsilon_n = \frac{\mu_n{}^{ne} - \mu_n{}^{e}}{\mu_n{}^{e}} \qquad [3.190]$$

where $_{ne}$ and $_{e}$ refer to nonequilibrium and equilibrium models, respectively. The index $_{n}$ refers to the moment order. In this study moments of order 2 and 3 are considered. In terms of original variables we have the following expressions.

Chemical Nonequilibrium Model

$$\epsilon_2 = \frac{P}{F}\frac{(R-1)}{R^2} \qquad \epsilon_3 = \frac{P}{F}\frac{(R-1)}{R^2}\left[1+\frac{P}{F}\frac{1}{2R}\right] \qquad [3.191]$$

Spherical Aggregates Model

$$\epsilon_2 = \frac{P}{\gamma}(1-\beta)^2/15 \qquad \epsilon_3 = \frac{P}{\gamma}(1-\beta)^2\left[1+\frac{P}{\gamma}\frac{(1-\beta)}{21}\right]/15 \qquad [3.192]$$

Physical Nonequilibrium Model

$$\epsilon_2 = \frac{P}{\omega}(1-\beta)^2 \qquad \epsilon_3 = \frac{P}{\omega}(1-\beta)^2\left[1+\frac{P}{\omega}\frac{(1-\beta)}{2}\right] \qquad [3.193]$$

Among the nondimensional variables used above, P, ω, β, γ and R have already been defined, (cf equations [3.28] and [3.58]–[3.60]), and F is given by $F=k_rL/v$ where k_r is the reverse rate coefficient in the chemical nonequilibrium model. Of course, for a given nonequilibrium model, the smaller the coefficients ϵ_n the better an approximation is the LEA model. This is illustrated fig. 3.19. The various expressions derived for ϵ_2 and ϵ_3 show that the ratios P/F and P/ω can be viewed as index of equilibrium for a given R. In fact the ratio P/F gives an idea of how "close" are reaction and flow rates. One sees that the smaller the ratio P/F the smaller will be the coefficients ϵ_n. This means that for a given reaction rate the smaller the Peclet number, which is a measure of the transport rate, the better an approximation is the LEA. Thus comparing the moments, we end up with the already proposed intuitive condition that if the flow rate is small as compared to the chemical reaction rate, then the LEA model can be employed to simulate the transport of reactive substances. Setting bounds on the moments or on the ratios P/F and P/ω is let to the subjective appreciation of the modeler. As an example, considering Fig. 3.19, the LEA model can probably be considered as a good approximation of the nonequilibrium model for F=100, but as a bad one for F=10. From above expressions one can see that

(1) If P and R are fixed, the chemical nonequilibrium model tends to the LEA model when F increases.

(2) If F and R are fixed, the chemical nonequilibrium model tends to the LEA model when P decreases

The same conclusions hold for the physical nonequilibrium model if F is replaced

by ω and R by β.

Derivation of an Equivalent Dispersion Coefficient

When P increases and R is kept fixed, the second moments of the various models all tend to a unique expression, $2XR^2/P$. It means that all the breakthrough curves tend to a Gaussian distribution with mean XR and variance $2XR^2/P$. Consequently, under these conditions the transport of a reactive solute can be modeled by a CDE equation with appropriate coefficients. These coefficients, velocity and dispersion, can be obtained from the moments. Following an analysis due to Aris (1958) and Turner (1972), Valocchi (1985) gives the following expressions for effective velocity and dispersion.

$$v_{eff} = vX \frac{\theta_m}{\theta}(\mu_1')^{-1} \qquad [3.194]$$

$$\frac{D_{eff}}{vL} = \frac{1}{2}\frac{\theta}{\theta_m}\frac{\mu_2}{\mu_1'}\left[\frac{v_{eff}}{v}\right]^2 \qquad [3.195]$$

where, v is the velocity, θ is the global water content, and θ_m is the water content of the mobile phase. Using expressions of the moments in Tab. 3.10 one sees that the same effective velocity is obtained for all the models,

$$v_{eff} = \frac{v}{R}\frac{\theta_m}{\theta} \qquad [3.196]$$

while the following expressions are derived for the effective dispersion coefficient.

Physical Nonequilibrium Model

$$D_{eff} = \frac{D}{R}\frac{\theta_m}{\theta} + \frac{(1-\beta)^2(\theta_m v)^2}{R\alpha\theta} \qquad [3.197]$$

Spherical Aggregates Model

$$D_{eff} = \frac{D}{R}\frac{\theta_m}{\theta} + \frac{(1-\beta)^2(\theta_m v a)^2}{15D_a R\theta\theta_{im}} \qquad [3.198]$$

Chemical Nonequilibrium Model

$$D_{eff} = \frac{D}{R} + \left[\frac{v}{R}\right]^2\frac{(R-1)}{R}\frac{1}{f} \qquad [3.199]$$

The common factor $D\theta_m/(\theta R)$ is the effective dispersion coefficient for the equilibrium model.

Notice that for the chemical nonequilibrium model, θ_m is equal to θ. It is important to remark that the Peclet number must be large enough in order to use these coefficients with some success in a CDE since this development relies on the hypothesis that P is large enough to have a Gaussian–like BTC. It means that very long soil columns or high velocities are required. Notice also that the notion of large Peclet number is relative to the retardation factor as they have contrary effects when they vary in the same direction. In the study of Valocchi (1985), a

value of 1000 for P is said to be sufficient. However, no value is given for R and we assume that it is for a value of 4 as used elsewhere in that paper. In the same study, with R=4 a Peclet number of 10 (upper bound) is required so as the LEA closely approximates the chemical nonequilibrium model. Therefore, between these two extreme values of P (10 and 1000) for which the LEA model can be apllied with appropriated equivalent dispersion coefficients, a large gap exists where none of these approaches gives a really satisfactory approximation.

We already shown, §3.6.2, that conserving the second order term in equation [3.172] led to a modified dispersion coefficient with which the LEA model constitutes a first–order approximation of diffusional models such as for example the spherical aggregates model. The general methodology presented in that paragraph can be applied to any BGF. Raats (1984) obtained an expression for D_{eff} equivalent to [3.198]. van Genuchten and Dalton (1986) used a very similar method to derive effective dispersion coefficients for other simple aggregate shapes. First they take the Laplace transform of the equation describing the transport in the mobile phase and replace the term involving the immobile concentration by its value taken in Tab. 3.5. One obtains

$$RsL(C_m) = \frac{1}{P_m}\partial^2 L(C_m)/\partial Z^2 - \partial L(C_m)/\partial Z - (1-\beta)Rs\left[\frac{3}{s}\coth(s) - \frac{3}{s^2}\right]L(C_m)$$

That term, which might also be in the form of a Bessel function, is replaced by its approximation at the first–order. For the spherical aggregate this one is given equation [3.132]. Taking the inverse of the Laplace transform it appears a second derivative for the mobile concentration. Replacing the time derivative by the convection–dispersion operator and neglecting the terms of higher order it remains a second order space derivative. The global coefficient of the second order space derivative is then

$$D_e = D\phi_m + \frac{(1-\phi_m)\, a^2 v^2 R_{im}^2}{15DR^2} \qquad [3.200]$$

with $\phi_m = \theta_m/\theta$. It is readily verified that this expression is equivalent to the one given by equation [3.198]. Following the same method, effective dispersion coefficients are derived for slabs, cylindrical aggregates and a hollow cylindrical macropore. The various coefficients are given in Tab. 3.12. For spherical aggregates, Parker and Valocchi (1986) derived the same expression by means of moments analysis.

Moments expressions for the LEA model and diffusional models can be found in Tab. 4.10. Let us note P_e the Peclet number for the LEA model and P_m the Peclet number associated with a diffusional model. If we want the two models to be equivalent, their second moments must be equal. Then, consider for example the case of spherical aggregates, equating the second moments gives

$$\frac{2XR^2}{P_e} = \frac{2XR^2}{P_m} + \frac{2X(1-\beta)^2R^2}{15\gamma}.$$

Let us note P_{im} the additional dispersion due to solute diffusion inside the immobile phase. If we define $1/P_{im} = (1-\beta)^2/15\gamma$, we have the relation: $1/P_e = 1/P_{im} + 1/P_m$. Expressions for $1/P_{im}$ are easily derived for any other geometry. Notice that $1/P_{im} \to 0$ thus provides an index of validity for the monocontinuum approach.

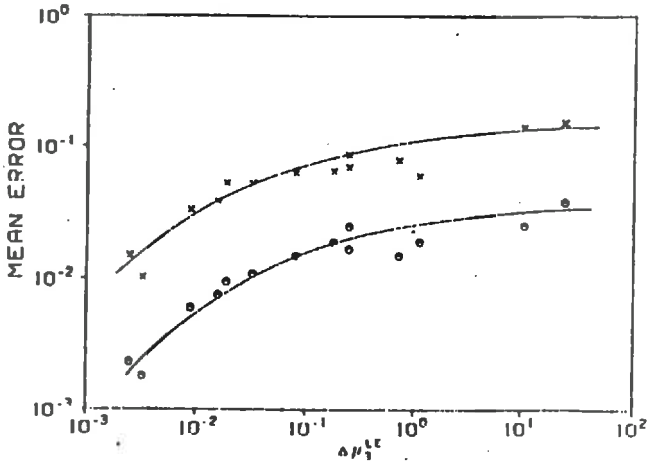

Fig. 3.20 Observed mean error versus third–moment deviation between spherical diffusion model and LEA model for a broad range of parameter values (see Table below), Dirac injections (×) and continuous injections (o) [after *Parker and Valocchi 1986*].

Case	X	γ	β	R	P_m	P_{lm}	P_e
1a	1.0	0.03	0.1	1.0	30.0	0.50	0.49
1b	1.0	0.30	0.1	1.0	30.0	5.00	4.29
1c	1.0	3.00	0.1	1.0	30.0	50.0	18.75
2a	1.0	0.3	0.01	1.0	30.0	4.55	3.95
2b	1.0	0.3	0.50	1.0	30.0	8.99	6.92
2c	1.0	0.3	0.99	1.0	30.0	451.30	28.13
3a	1.0	0.1	0.1	1.0	30.0	1.66	1.57
3b	1.0	0.1	0.1	10.0	30.0	16.66	10.71
3c	1.0	0.1	0.1	100.0	30.0	166.66	25.42
4a	1.0	1.0	0.1	1.0	1.0	16.66	0.94
4b	1.0	1.0	0.1	1.0	10.0	16.66	6.25
4c	1.0	1.0	0.1	1.0	100.0	16.66	14.28
5a	0.01	10.0	0.1	1.0	30.0	166.66	25.42
5b	0.10	10.0	0.1	1.0	30.0	166.66	25.42
5c	1.00	10.0	0.1	1.0	30.0	166.66	25.42

Parameter combinations used to define the points in Fig. 3.20 [after *Parker and Valocchi 1986*].

An estimation of the approximation error between the LEA equivalent model and the original diffusional model can be obtained for the two methods above proposed. Retaining one more term in the developement of $L(C_{im})$, van Genuchten and Dalton (1986) obtained the following estimation

$$E = \frac{2(1-\beta)}{15\gamma_s}\left[\frac{1}{P} + \frac{2-7\beta}{105\gamma_s R}\right]\frac{\partial^3 C}{\partial Z^3} \qquad [3.201]$$

while calculating the absolute value of the difference between the third moments, Parker and Valocchi (1986) obtained

$$\Delta_{\mu_3}^{le} = \frac{4(1-\beta)}{5X^2\gamma R}\left|\frac{1}{P} + \frac{2-7\beta}{105\gamma R}\right| \qquad [3.202]$$

Although the two expressions are very similar, the last expression is not an estimation of the error. However, Parker and Valocchi (1986) showed that for a set of various conditions the mean error E defined by

$$E = \frac{1}{n}\sum_{i=1}^{n}|Y_i^{sd} - Y_i^{le}| \qquad [3.203]$$

was related to $\Delta_{\mu_3}^{le}$. Fig. 3.20 presents a Log–Log plot of E function of $\Delta_{\mu_3}^{le}$ for a Dirac and a continuous input, respectively. Remark that the Dirac input seems to correspond to the most constraining situation. By means of the same technique exposed above, an expression for $\Delta_{\mu_3}^{fo}$ can be derived for the QSS model.

$$\Delta_{\mu_3}^{fo} = \frac{2(1-\beta)}{175(X\gamma R)^2} \qquad [3.204]$$

It then appears that $\Delta_{\mu_3}^{le}$ and $\Delta_{\mu_3}^{fo}$ are related by

$$\Delta_{\mu_3}^{le} = \left|\frac{12}{P_m P_{im} X^2} - \frac{14\beta-4}{3}\Delta_{\mu_3}^{fo}\right| \qquad [3.205]$$

This expression indicates that the QSS model and the LEA model with its modified dispersion coefficient do not provide equivalent first–order approximations. If the nonequilibrium behavior is pronounced the LEA model may perform better than the QSS model depending on the value of $\Delta_{\mu_3}^{fo}$. If nonequilibrium conditions are weak then the QSS model performs better. At the limit when $\gamma \to \infty$ then $\Delta_{\mu_3}^{fo} \to 0$ while $\Delta_{\mu_3}^{le}$ is still different from 0. Parker and Valocchi (1986) obtained, for certain combinations of the parameters, good agreements between the BTC calculated for the spherical aggregate model and those derived from the "equivalent LEA model". From the expression of the

moments given Tab. 3.10, one sees that if $\beta \to 1$ or if γ is large $\mu_3^{sd} \longrightarrow \mu_3^{le}$.

Notice that making R=1 in above formula gives the dispersion coefficient to be used for nonreacting solutes transport. Using a different reasoning, Passioura (1971), in his paper "Dispersion in aggregated media", derived the same expression for a media made up of spherical aggregates. He assumed that by analogy with a capillary tube the dispersion coefficient could be written

$$D = D_m + kv^2a^2/D_m \qquad [3.206]$$

Then, assuming that steady–state holds in the mobile phase, and considering a plane moving with velocity v, any flux of matter through this plane can only be the result of lateral variation in concentrations. The flux through that plane is then given by

$$F = \epsilon_a u(c_m - c_a)/\epsilon_t \qquad [3.207]$$

where ϵ_t and ϵ_a are respectively the total and intraaggregate porosities and u is given by: $u = v\epsilon_m/\epsilon_t$. Assuming that the flow is mainly convective and that we can neglect second order terms, large Peclet number, c_a is obtained by solving the diffusion equation in a sphere of radius a with zero initial condition and surface condition $k_1 t$. At large times ($t > .3a^2/D_a$) c_a is approximated by

$$c_a = k_1(t - a^2/15D_a) \qquad [3.208]$$

and it comes

$$F = \frac{\epsilon_a}{\epsilon_t} \frac{u^2 a^2}{15D_a} \frac{\partial c_m}{\partial x} \qquad [3.209]$$

which means that the transfer is controlled by an effective dispersion coefficient. It is important to remark that two assumptions are at the base of this result. First the flow is mainly convective, which is an assumption present in the study of Valocchi (1985) and secondly the coefficient $a^2/15D_a$ in the approximation of C_a is obtained if t is large enough.

3.6.5 CONCLUSIONS

We reviewed two classicaly used macroscopic modeling approaches, LEA and QSS models. We have emphasized on their relationships with diffusional models and showed that they constitute zeroth– and first–order approximations of these models. Approximations of parameters, α for the QSS model and D for the LEA model, have been expressed as functions of geometrical and diffusional characteristics of the aggregates. Many approaches have been proposed to carry out these derivations, (1) comparison of solutions in batch systems, (2) moments analysis of breakthrough curves, (3) comparison of Block Geometry Functions either in terms of Laplace or original variables, (4) development of the convolution product in the partial integro–differential equation in a series of time derivatives by means of Laplace transform. These derivations have highlighted the limitations of macroscopic models when applied to aggregated media. For example the fact the QSS model might not perform better than the LEA model when strong nonequilibrium conditions exist clearly shows that the first–order equation modeling the transport between both phases is a poor representation of

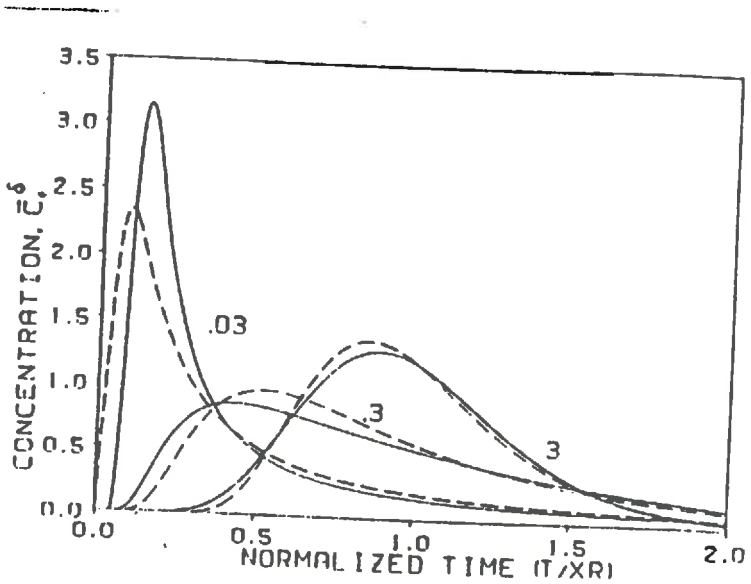

Fig. 3.21 Comparison of breakthrough curves (flux–averaged) obtained with the spherical aggregate model (solid lines) and the "equivalent" LEA model (dashed lines) for a Dirac injection. Values of γ indicated on the curves, and other parameters as for cases 1a, 1b, 1c (see Fig. 3.20 and accompanying table) [after *Parker and Valocchi, 1986*].

the real diffusional process. Comparisons have been carried out between the breakthrough curves obtained with diffusional models and with their QSS or LEA "equivalents", van Genuchten (1985b), Valocchi (1985), van Genuchten and Dalton (1986), Parker and Valocchi (1986). Some of those are given in this report, fig. 3.17, 3.18, 3.19, 3.21. One can see that the quality of the agreement is very case dependent. In fact a large number of parameters; geometry, Peclet number, γ, R, play a role and the agreement depends in a complex way on the combination used. For example fig. 3.18 shows that the QSS model is a good approximation of the diffusional model for a cylindrical macropore while Fig. 3.17 shows that for spherical aggregates or rectangular voids and with the same flow conditions (R, β and P identical), the agreement is in many cases unacceptable. We know that for pronounced nonequilibrium conditions the LEA model may perform better than the QSS model to approximate the spherical aggregate model. This means that for low values of ω we shall obtain a slightly better approximation with the QSS model but that for intermediate values a large gap remains. Therefore, simply choosing which macroscopic model should be used as function of aggregates geometry or soil structure is not an easy task. Much more we do not always have acceptable physical conditions, flow parameters, diffusion characteristics, aggregate sizes, to use a macroscopic model, QSS or LEA.

From all studies and modeling approaches it clearly seems to emerge that models based on a first–order representation of the interphase transport rate should poorly perform on strongly aggregated or structured media. Among all the papers reporting and modeling solute transport experiments we reviewed, we only found seven experiments conducted on undisturbed soil monoliths. Among those, only one, White et al. (1986), is concerned with a quite strongly structured soil ($20mm<\phi_{agg}<100mm$). That experiment was analysed with a transfer function model. Others undisturbed soil monoliths can be classified as weakly structured. See for example, Seyfried and Rao (1987), Schulin et al. (1987), Jardine et al. (1988). All others experiments are concerned with soil laboratory columns packed with disturbed soil or small aggregates, usually with diameters between 0.5 and 4.0 mm. Results from a study of Rao et al. (1980a), where large spherical artificial aggregates were included in a homogeneous sand show the limitations of the QSS model as compared to the spherical aggregate model. Experimental breakthrough curves and those simulated with both models are presented fig. 3.22 and 3.23. One clearly sees that the QSS model gives less good an agreement than the spherical aggregate model, especially when the velocity and/or the radius of the aggregates increase. In particular, while the tailing is perfectly reproduced by the spherical aggregate model, quite poor a fit is obtained with the QSS model. These experiments also lead to the qualitative conclusion that the strongly structured is the soil the poorly will perform the QSS model. This conclusion is in agreement with previous theoretical deductions.

In some papers, the LEA model has been used with a modified dispersion coefficient as proposed §3.6.4. Rao et al. (1980a), using the formula proposed by Passioura (1971), obtained a good aggreement for the first of their experiments (small aggregates and low velocity), the only one to verify the conditions given above. Schulin et al. (1987), also used an equivalent dispersion coefficient derived from the QSS model. They obtained satisfactory agreements between simulated and observed breakthrough curves for the low velocity experiments conducted with Tritium. For Bromide, one can observe in their data that the agreement gets better when the Peclet number increases as required by the theory, §3.6.4. However, for their experimental conditions, the Peclet number was never large enough so as the LEA model could be used with some success.

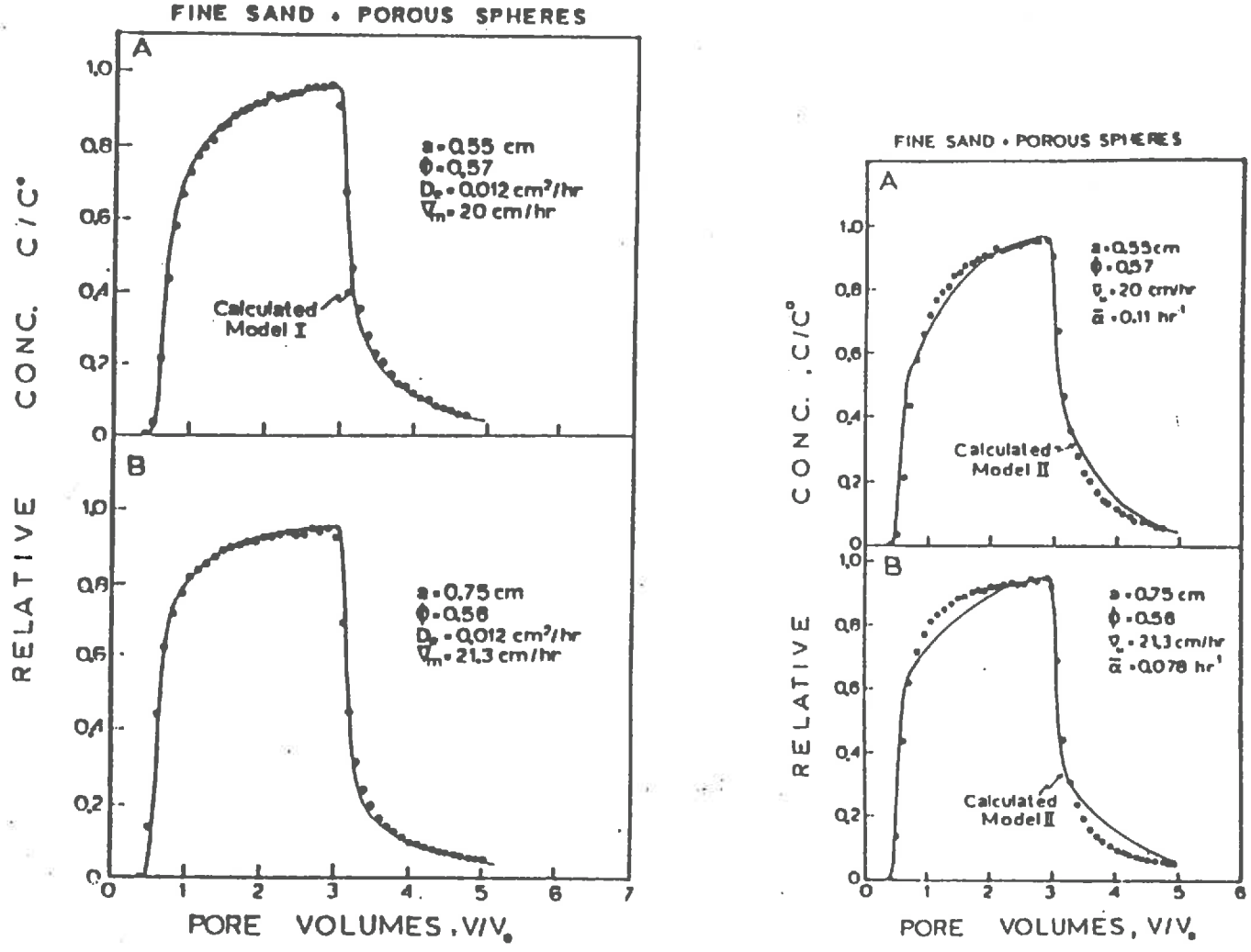

Fig. 3.22 Comparison of experimental and simulated breakthrough curves for a sand containing porous spheres with radii of .55 and .75 cm respectively. Calculations used the spherical aggregate model (Model I), left part of the graph, and the First–Order physical nonequilibrium model (Model II), right part of the graph [after *Rao et al., 1980*].

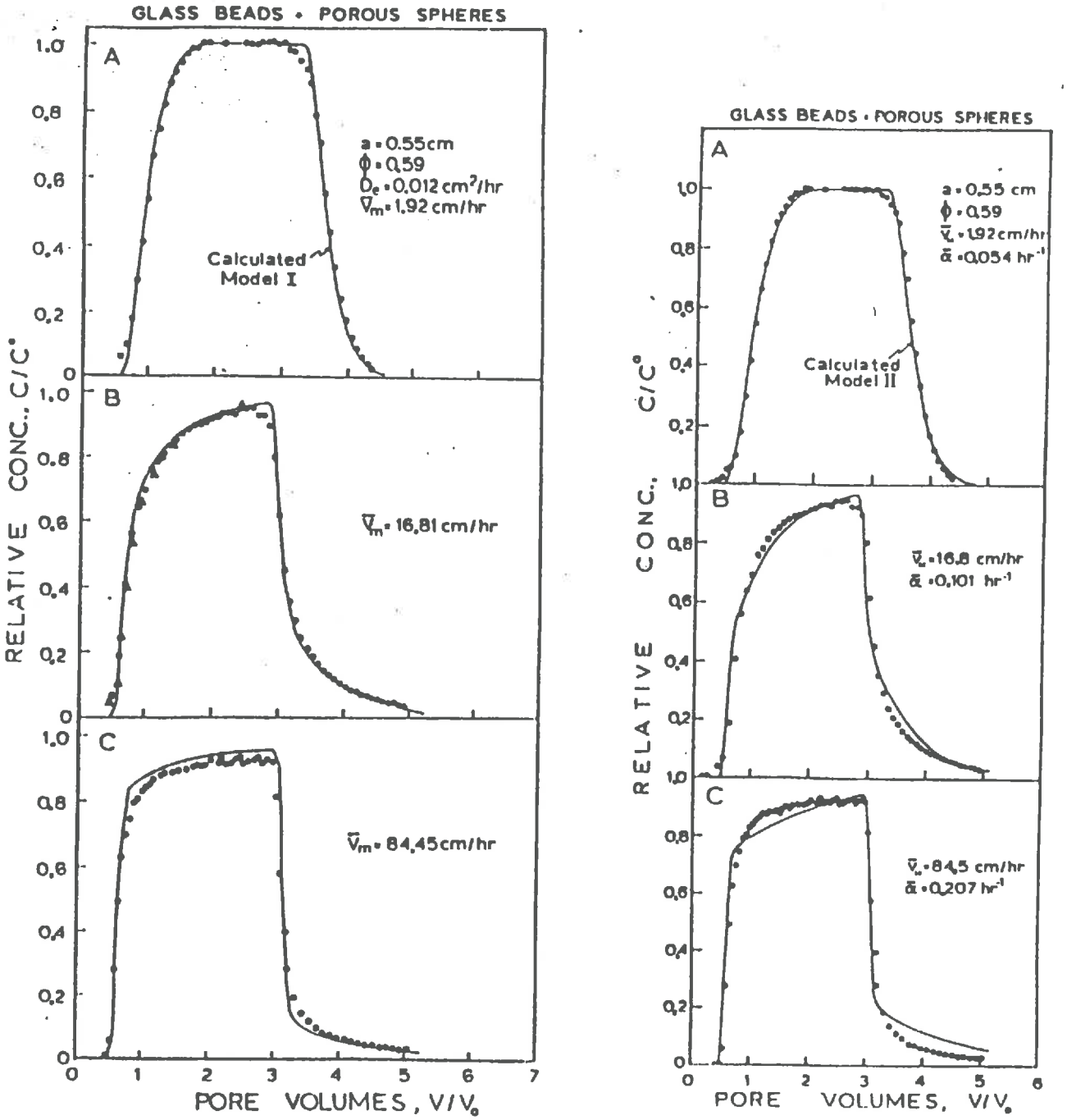

Fig. 3.23 Comparison of experimental and simulated breakthrough curves for a media made up of glass beads and porous spheres with radius of .55 cm. Calculations used the spherical aggregate model (Model I), left part of the graph, and the First–Order physical nonequilibrium model (Model II), right part of the graph. Results are presented for three different velocities [after *Rao et al., 1980*].

Beside the deterministic modeling approaches developed in this chapter, some other techniques have been employed to model and analyse field as well as column tracer experiments. The following chapter treats of the *Transfer Function* approach and of its applications to te problem of solute transport modeling in heterogeneous media.

4. TRANSFER FUNCTION MODELS – STOCHASTIC MODELING

Pople have been studying the problem of solute transport in porous media from different points of view and with different objectives in mind. Some were purely cognitional such as identification of physical processes at different scales (which equations appropriately model the phenomena) or theoretical study of the pheneomena (origin of the dispersion for example); while others were more applications oriented, fertilizers movement prediction and pollution risks assessment for example. Another obvious discrimination is provided by the modeling scale. Until now, this report has been dealing with deterministic modeling studies, in particular based on the CDE, and has been focusing on the relations existing between soil structure and solute transport. Beside their mechanistic character, the models presented before have also in common a deterministic character, since we were interested in modeling the physical phenomena at a scale where first, transport characteristics (dispersion, velocity, retardation factors, decay constant,...) could be considered as perfectely known and sufficiently homogeneous over the soil volume, and second, physical and chemical phenomena were sufficiently well identified so as we were able to write equations at our modeling scale. For example, remark that we implicitely assumed the validity of the CDE as an equation accurately modeling the transport of disolved substances through porous media.

In this report, no attention has been until now paid to the spatial variability of transport coefficients. In the past years many approaches have been proposed to deal with this problem. They rely mainly on the use of deterministic models whose coefficients are supposed randomly distributed in space. Average and standard deviations of relevant variables, for example concentration at a given depth, can be derived if the probability density functions of the parameters are known. Unfortunately, due to the large number of simulations required to estimate means and variances, these approaches are restricted to simple models. In the following we describe a new approach, called Transfert Function, aiming at predicting solute transport at the scale of the field and characterized by the fact that none of the physical or chemical mechanisms taking place during the transport are specifically modeled. Rather, the system is considered as a "black box", transforming an input signal.

4.1 INTRODUCTION

Solute movement in saturated and unsaturated media has been for years now modeled by means of the convection–dispersion equation. That equation proved to be a useful tool to analyse laboratory experiments, but part of its basis are of entirely empirical nature. Sposito et al. (1986) remarked, *"In respect to modeling studies, the basic issue has not been adressed as to wether the CDE with fitted values of its dispersion coefficient provides an intrinsically sound physical description of solute transport through soil and aquifer materials or instead generates only a mathematical model with enough adjustable parameters to describe solute breakthrough curves having a sigmoid character."* In the past few years many papers tried to propose a rigorous derivation of the CDE based on microscopic or molecular principles. While, momentum, mass and energy stochastic equations can be derived at the pore scale, the problem is, given the various possible levels of randomness, to derive averaging laws allowing to pass from a pore scale to a REV scale, then to the laboratory column scale and ultimately to the field scale. A very interesting and clear review of the different approaches proposed in the litterature to derive stochastic partial differential equations for solute transport can be found in Cushman (1987). Regarding solute transport modeling through soil materials, a rigorous derivation of the CDE still

remains an open research problem. The transfer function model, hereafter noted TFM, proposed by Jury (1982, 1986) is an example of stochastic transport model whom the convection dispersion equation is a particular case, Sposito et al. (1986).

In his paper, Jury (1982) mainly invoques two reasons to model solute transport with a transfer function and hence abandon deterministic and mechanistic models. Respectively, were advanced the facts that natural soils are heterogeneous at field scale (spatial variability), and that local scale heterogeneities in soil structure (cracks, dead roots, worm holes, strongly structured soils,...) are present. So, one of the main reasons at the base of his choice was that because of local heterogeneities, deterministic transport models will fail, and consequently approaches based on deterministic models used with stochastic parameters, like the scaling approach of Dagan and Bresler (1979), should be rejected. Let us remark that the progresses made during the last years in developing deterministic solute transport models for heterogeneous media tends to weaken and give less weight to this assumption.

4.2 THEORY

The transfer function model proposed by Jury (1982) can be introduced by different ways. In particular, a new and more general formulation was described by Jury et al. (1986). Identically, Cushman (1987) remarks that the TFM was a particular case of a stochastic convective model developed by Simmons (1982). In the following, rather than presenting the model as particular case of more complicated approaches, we first describe the initial reasoning followed by Jury (1982) and then discuss the connections of the TFM with other models.

4.2.1 INITIAL APPROACH

The initial development of the TFM by Jury (1982), is based on the following assumption.

H 1: *The displacement of a solute molecule is controled by the amount of water applied at the soil surface independently of the rate or mode of application.*

This assumption relies for a large part on the work of Wierenga (1977) in which it was demonstrated that solute displacement under transient flow conditions was primarily function of the amount of water applied. The validity of this hypothesis can be discussed, given that Jury (1982) does not reject the possibility of convective transfer through large heterogeneities and that the theoretical work of Wierenga (1977) was based on the CDE which may not be applicable in many field situations as demonstrated by many experiments.

This paragraph could have been also titled "*The TFM or the resurgence of the RTD*", so much is the TFM closely related to the notion of Residence Time Distribution (RTD). This notion was introduced by Danckwertz (1953) to analyse laboratory column breakthrough curves. At each point of a field and for a given application of solute and water, a RTD can be determined. Obviously, owing to the spatial variability of the media these distributions will not be identical, but it will be possible to estimate from those the probability for a given concentration to reach a given depth. This is precisely the starting point of the TFM.

Definition: Let us note $F_1(I)dI$ the probability that the injected tracer reaches the depth l for a dose of water between I and $I+dI$. $F_1(I)$ is the probability density function, hereafter noted pdf.

Hence, by definition, the probability that the tracer reaches the depth l

after a net amount of water, I, has been applied is

$$P_l(I) = \int_0^\infty F_l(I')\, dI' \qquad [4.1]$$

Our problem is now to determine $F_l(I)$. Given (H1), we can use the global amount of water applied I, in place of the time. Hence, our "time" of reference will be I=0. Assume that we apply a δ–pulse of tracer at I=0 followed by an application of a net amount of water I, free of tracer. The function $F_l(I)$ is precisely the average normalized concentration measured at depth l. So, after a Dirac–like input and application of a sufficiently large amount of water, an estimation of $F_l(I)$ can be obtained by sampling the field at depth l and at different times, provided that the application of water was uniform. This can also be expressed by: if the input concentration was $C_{in}=C_0\delta(0)$ and after application of an amount of water I, the average concentration at $Z=l$ will be $C_l=C_{in}F_l(I)$. If the input concentration is not of the Dirac–type but varies with the amount of water applied, the average concentration at l can be obtained by superposition of an infinity of Dirac input $C_{in}(I')\delta(I')$. We obtain

$$C_l(I) = \int_0^\infty C_{in}(I-I')F_l(I')\, dI'. \qquad [4.2]$$

The upper bound of the integral is taken equal to infinity since $C_{in}=0$ for $I'>I$.

This approach can be extended to spatially variable input rates. Let's assume that the intake rate is not uniform or that the application of water is not uniform. The probability for a point to receive water at a rate i can be described by a probability density function $G(i)$. This one expresses that the probability for the application rate at a point to be between i and $i+di$ is $G(i)di$. If we assume that at any point in the field the rate of application is constant in time, then at a given location the probability for a tracer to reach the depth l between times t and $t+dt$ for a Dirac input is

$$F_l(I)\,dI = F_l(it)\,idt \qquad [4.3]$$

So, the probability at the scale of the field for a tracer to reach the depth l between times t and $t+dt$ will be given by integrating over all the values of i found in the field, the joint probability density function, $G(i)iF_l(it)$. Hence, we define a new pdf, noted $H_l(t)$ by:

$$H_l(t) = \int_0^\infty G(i)F_l(it)\,idi \qquad [4.4]$$

which for a nonuniform input plays the same role as F_l do for a homogeneous input. Here also notice that the integration is taken over $[0,\infty]$, but that in fact intake rates, i, only spread over a finite lenght interval outside of which G is identically null. Following the same reasoning as for a uniform distribution of water, the concentration at depth l for a Dirac input is $C_l(t)=H_l(t)C_{in}$ and for a time dependent input concentration is given by

$$C_l(t) = \int_0^\infty C_{in}(t-t')H_l(t')\,dt' = \int_0^\infty\int_0^\infty C_{in}(t-t')G(i')i'F_l(i't')\,dt'\,di'. \quad [4.5]$$

We now have all we need to predict the concentration at depth l. But this is of little interest since l is precisely the depth at which the field was sampled. In order to extend the predictive capability of the model to other depths, another assumption is required. Jury (1982) introduces here the following strong hypothesis.

H 2: *If an amount of water I is required to move the solute pulse to the depth l, then an amount nI is required to move the same pulse to depth nL.*

Making this assumption means that the probability density function F_l in which are lumped all the physical and chemical phenomena conditioning the transport of solute through the layer [0,l] is valid for any layer [z,z+l]. In terms of stochastic models, this linear dependence of the pdf on the amount of water applied is equivalent to assume that an invariant probability distribution for the velocity applies at each depth z. A question arising is then: Isn't this invariance of the probability distribution for velocity implying the vertical homogeneity of the soil? For example it is highly probable that crack density or soil structure will vary with depth. In that case what are the effects on the pdf, and in particular isn't that strongly limitating the range of applicability and usefulness of the TFM? In his discussion, Jury (1982) only envisaged the case of strongly layered soils and concluded that a new pdf has to be calibrated for each layer or that a single pdf is sufficient if the calibration is made at the bottom of the system. Results of an experiment illustrating this problem and the limits of the TFM are given §4.3.

Accepting the second hypothesis (H2), the probability to move the tracer to a depth z after an amount of water I has been applied is

$$P_z(I) = P_l(Il/z) = \int_0^{Il/z} F_l(I')dI' \quad [4.6]$$

Hence, the pdf F_z, associated with the depth z, is related to the reference pdf $F_l(I)$ by

$$F_z(I) = (l/z)\,F_l(Il/z) \quad [4.7]$$

The average concentration at depth z as a function of I or t follows immediately by replacing F_l by F_z in equations [4.2] and [4.5]. One obtains respectively for, spatially uniform and variable applications

$$C_z(I) = \int_0^\infty C_{in}(I-I')(l/z)F_l(I'l/z)\,dI' \quad [4.8]$$

$$C_z(t) = \int_0^\infty C_{in}(t-t')\int_0^\infty (l/z)iG(i)F_l(it')\,dt'\,di \quad [4.9]$$

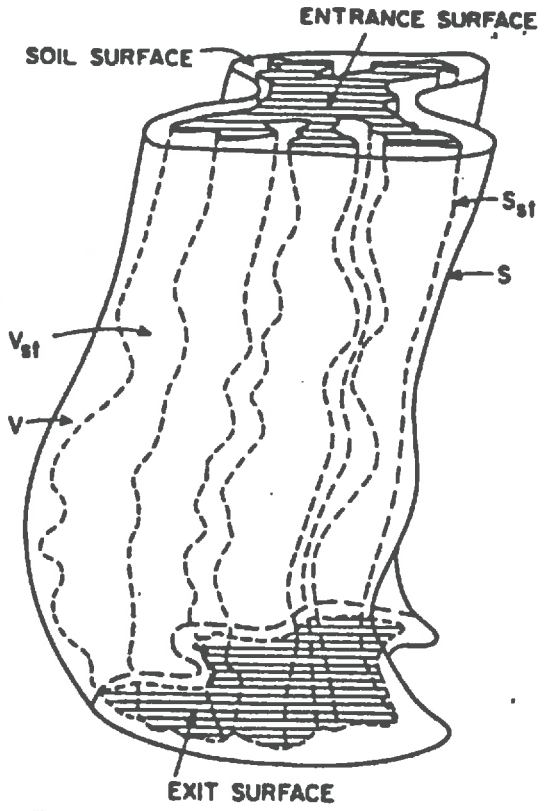

Fig. 4.1 Schema of a macroscopic unit of soil for the TFM [after *Jury et al., 1986*].

It follows from these expressions that if an analytical or discrete expression is known for F_I, and G if needed, a simple analytical or numerical integration will give the time and space distributions of the average concentration over the field. An extension of these results to the case of solutes undergoing adsorption or first–order decay is presented in Annex 4. Jury (1982) presents some theoretical calculations carried out with a lognormal expression for F_I and a uniform input rate. F_I is as follows

$$F_I(I) = \exp \frac{-[\ln(I)-\mu]^2/\sigma^2}{\sqrt{2\pi}\sigma I} \qquad [4.10]$$

where μ is the mean of the lognormal distribution and σ^2 its variance. In that case, analytical expressions for $C_z(I)$, solution of Eq. [4.8], are obtained in the form of *erf* functions. For a continuous application of solute and a square input one obtains respectively,

$$C_{out}(Z,I) = \frac{C_0}{2}\left\{1+\text{erf}\left[\frac{\ln(IL/Z)-\mu}{\sqrt{2}\sigma}\right]\right\} \qquad [4.11]$$

$$C_{out}(Z,I)=\frac{C_0}{2}\left\{\text{erf}\left[\frac{\ln(IL/Z)-\mu}{\sqrt{2}\sigma}\right]-\text{erf}\left[\frac{\ln(I-\Delta I)L/Z-\mu}{\sqrt{2}\sigma}\right]\right\} \qquad [4.12]$$

where ΔI is such that $C_{in}=0$ for $I>\Delta I$. His simulations illustrated how asymmetry and tailing of breakthrough curves are influenced by the velocity distribution.

4.2.2 DEVELOPMENTS

Lately, Jury et al. (1986) and Sposito et al. (1986) proposed a new and more general derivation of the TFM. This one is more enlightening regarding the relations of the TFM with the CDE. Figure 4.1 gives a sketch of a macroscopic unit of soil volume through which the transport will take place. The surface S bounding V is chosen far enough such that no solute flux will occur through S during the period the solute transport will be monitored. Inside V, is a volume V_{st}, termed "effective solute transport volume", including all the fluid that is active in the transport process. This volume can be seen as the mobile phase in two–region models. It is obvious that the surface S_{st} bounding that volume has a very complex shape changing with time and likely also depending on the mode of application or water intake rates at the soil surface. The solid phase is considered as a potential sink or source for solute . Intersection of S_{st} with the soil surface defines an "entrance surface", while its intersection with the bottom of the soil volume defines an "exit surface". One more time, no particular physical or chemical mechanisms are specifically envisaged. Jury et al. (1986) make the following assumptions; (1) *Solute may enter the transport volume through the entrance surface, (2)It may appear in the transport volume as the result of desorption from the solid phase or contiguous liquid phases not participating to the transport, (3) It may be the result of chemical, physical or biological processes wholly occuring within the transport volume.* Equivalenty, (1) *Solute may disappear from the transport volume through the exit surface, (2)It may disappear as the result of sorption on the solid phase or diffusion into contiguous liquid phases not participating to the transport, (3) It may disappear as the result of chemical, physical or biological processes wholly occuring within the*

transport *volume.* Whatever physical, chemical or biological mechanisms acting during the transport process, one can define two important time variables for any solute molecule transported through the soil unit. First, noted T', the time at which it first appeared in the transport volume, V_{st}. T' is called the *input time.* Second, noted T, its lifetime, that is the time lag between its appearance in the transport volume and disappearance from the entire soil unit. Here, it is assumed that when a molecule disappears it is permanently.

Jury et al. (1986) assume that these two characteristic times are random variables whose statistical properties can be defined through a normalized joint probability density function $p(\tau,t')$. This means that the probability for a molecule to enter the system between t' and $t'+dt'$ and to have a lifetime between τ and $\tau+d\tau$ is $p(\tau,t')d\tau dt'$. Two probability density functions called marginal pdfs, can be defined from $p(\tau,t')$, and associated with the entry time and the lifetime, respectively. By definition, the marginal pdf associated with the entry time and noted Q_{in} is given by

$$Q_{in}(t') = \int_0^\infty p(\tau,t')d\tau \qquad [4.13]$$

Physically speaking, Jury et al. (1986) give the following definition for Q_{in}. Q_{in} represents the rate at which solute enters the transport volume at the first time, normalized by the total solute input. It is important to notice the restriction, "at the first time" since a solute molecule can enter the flow, then leave it because of adsorption on the solide phase or diffusion into immobile water regions and then later re–enter the transport volume if diffusion from immobile regions or desorption from the solide phase are possible. Remark also that the time spent by the molecule adsorbed on the solid phase or in the stagnant zones is part of its lifetime since the molecule is still in the soil unit though not in the transport volume, V_{st}. One sees also that integrating Q_{in} over all the input times leads to a value of 1 since $p(\tau,t')$ is a normalized pdf. It results, still by definition, that the conditional probability density function for the lifetime is

$$g(\tau|t') \equiv \frac{p(\tau,t')}{Q_{in}(t')} \qquad [4.14]$$

$g(\tau|t')$ is called a conditional probability function since the lifetime is supposed to depend on the entry time. This can be expressed by: given an entry time t'=T', the probability that the lifetime T lies within $[\tau,\tau+d\tau]$ is given by $g(\tau|t')d\tau$. Physically it means that, for a molecule having entered the transport volume at t' the probability to disappear from the soil unit between τ and $\tau+d\tau$ is $g(\tau|t')d\tau$. When considering the system at a time t, we are interested in knowing the probability for a molecule having entered the transport volume at time T' still to be in the soil unit at our observation time. In term of probability what we want to calculate is the probability for the lifetime to be greater than t–T', which insures that the molecule is still within the soil unit, given that this molecule had to be already in the transport volume at T'<t. Given the joint probability density function $p(\tau,t')$ this probability is

$$P\{T>t-T'|T'<t\} = \int_0^t \int_{t-t'}^{\infty} p(\tau,t')\, d\tau dt' \qquad [4.15]$$

which reads: the probability for a molecule having entered the transport volume at $t'<T$ to have a lifetime, T, greater than $t-T'$ is equal to ... We can use the relations derived above to express this in a slightly different form. It comes

$$P\{T>t-T'|T'<t\} = \int_0^t \left[\int_0^{\infty} p(\tau,t')d\tau - \int_{t-t'}^{\infty} p(\tau,t')dt' \right]$$

$$= \int_0^t Q_{in}(t')dt' - \int_0^t \int_0^{t-t'} g(\tau|t')Q_{in}(t')d\tau dt'. \qquad [4.16]$$

The first term on the right hand side of [4.16] can be interpreted as the total mass of solute injected in the system up to time t. Since $g(\tau|t')d\tau$ is the conditional probability that a molecule having entered the transport volume at t' desappears from the soil unit between τ and $\tau+d\tau$, the second integral on the right hand side gives the total amount of solute that have already left the soil unit at time t. Consequently, equation [4.15] can be viewed as a mass–conservation equation. Taking the derivative with respect to time one obtains an expression of the net rate of solute accumulation in the transport volume.

$$\frac{dP}{dt} = Q_{in}(t) - \int_0^t g(t-t'|t')Q_{in}(t')dt' \qquad [4.17]$$

From this equation, we can formally define the transfer function equation

$$Q_{out}(t) = \int_0^t g(t-t'|t')Q_{in}(t')dt' \qquad [4.18]$$

where $g(t-t'|t')$ is logically called the lifetime density function. Effects on solute lifetime, of all the processes, diffusion, dispersion, convection, decay, sorption, biological transformations, etc..., occuring in a representative volume of soil are all lumped into g.

After application of the transformation $t-t' \longrightarrow t'$ in the right hand side, equation [4.18] is an example of first type Volterra equation. (Notice the analogy with the formulation derived in §3.5). Q_{out} represents the inhomogeneous term, Q_{in} is the kernel and g is the homogeneous term. Identification of g can be done by inversion of [4.18] if the homogeneous and inhomogeneous terms are known. For a Dirac input characterized by $Q_{in}(t') = k\delta(0)$, the lifetime density function is $g(t|0)=Q_{out}(t)/k$, and for a step input characterized by $Q_{in}(t')=Q_{in}(0)$, g is defined by $g(t|0)=(dQ_{out}/dt)/[Q_{in}(0)]$, Jury et al. (1986). If the form of the kernel is not simple, one have to use numerical techniques.

Jury et al. (1986) recognized that if the solute enters or leaves the transport volume only through respectively the entrance and exit surfaces which is the case of a relatively nonreactive solute (e.g., a halide ion), then Q_{in} and Q_{out} can be expressed as products of the solute flux concentration C by the solution flow rate, i. Under these assumptions equation [4.18] becomes

$$C_{ex}(t) = \int_0^\infty g(t-t'|t') \frac{i_{en}(t')}{i_{ex}(t)} C_{en}(t')\, dt' \qquad [4.19]$$

Under steady–state flow conditions this equation reduces to

$$C_{ex}(t) = \int_0^\infty g(t-t'|t')\, C_{en}(t')\, dt' \qquad [4.20]$$

Since under these conditions the cumulative amount of water applied, I, and the time are related by: $I=i_0 t$, equation [4.20] can be written

$$C_{ex}(t) = \int_0^I F(I-I'|I')\, C_{en}(I')\, dI' \qquad [4.21]$$

where $F(I-I'|I') \equiv g(t-t'|t')/i_0$. Assuming that the solute lifetime is independent of the input time I', F(I–I'|I') reduces to F(I–I'), and equation [4.21] becomes

$$C_{ex}(t) = \int_0^I F(I-I')\, C_{en}(I')\, dI' \qquad [4.22]$$

One recognizes here the initial form of the transfer function model developed in the previous paragraph.

4.2.3 RELATIONS WITH MODELS BASED ON THE CDE

Let us consider the case of a steady–state flow. It is shown, **Mysels (1982)**, that the solution of the simple CDE for a initial concentration equal to zero and an input concentration $C_{in}(t)$ can be written

$$C(L,t) = \int_0^\infty C_{in}(t-t')F_1(t')\, dt' \qquad [4.23]$$

where L is the observation depth and F_1 is

$$F_1(t) = \frac{L}{2t\sqrt{\pi D t}} \exp[-(L-vt)^2/(4Dt)] \qquad [4.24]$$

This result can be obtained by application of *Duhamel's* theorem. Remark also that in Eq. [4.23] the concentration is a flux–averaged concentration. So, from these expressions it is obvious that the CDE is a particular case of TFM whose travel time pdf is the function F_1 given above, Eq. [4.24]. The TFM with its lognormal pdf defined as in Eq. [4.10] can then be compared with the CDE by looking at the first moments of their respective pdfs. Simmons (1982) and Jury and Sposito (1985) remarked that the predictions of the two models will nearly superimpose at the depth where the pdfs were calibrated. At other depths, mean and variances of the two pdfs give a qualitative idea of the respective behavior of the two models. Respective means and variances for the two pdfs are

$$E_z[t] = \int_0^\infty \tau F_z(\tau)\, d\tau = \begin{cases} L/v & (CDE) \\ \exp(\mu+\sigma^2/2) & (TFM) \end{cases} \qquad [4.25]$$

$$var_z[t] = \int_0^\infty \{\tau - E_z[t]\}^2 F_z(\tau) d\tau = \begin{cases} 2DZ/v^3 & (CDE) \\ (Z/L)^2 \exp(2\mu+\sigma^2)[\exp(\sigma^2-1] & (TFM) \end{cases} \qquad [4.26]$$

It appears that the variance depends linearly on the depth for the CDE and on the square of the depth in the case of the TFM. Thus, the TFM will predict much more spreading of the signal with increasing depths of penetration.

The same kind of analysis can be conducted for the two–region models which account for physical or chemical non–equilibrium conditions by means of first–order processes. See, §4.2.2 and equations [4.32]–[4.35]. These models were expressed in terms of resident concentration, (volume–averaged concentrations). After expressing these equations in terms of flux–averaged concentration C_f, Sposito et al. (1986) showed that the flux concentration at the exit of a soil column of lenght L could be expressed as

$$C_{f1}(L,T) = \int_0^T C_{en}(T') \frac{\partial C_f}{\partial T}(L, T-T')\, dT' \qquad [4.27]$$

where $C_{en}(T)$ is the flux concentration imposed at the top of the column and C_f is the solution for a unit flux concentration at the input. This results also from a direct application of *Duhamel's* theorem. Comparing equations [4.27] and [4.20], we can define a travel time pdf $g_1(T)$ evaluated at X=1 by

$$g_1(T) = \frac{\partial C_f}{\partial T}(1,T) \qquad [4.28]$$

Hence, the travel time pdf is the time derivative of the flux concentration at the exit of the soil column. In that case, as for the simple CDE, a strikingly similarity appears between the TFM and the notion of RTD. Noting E(T) the RTD, we have for an input $C_{en}(t)$, Schweich et Sardin (1983),

$$C_f(1,T) = \int_0^T C_{en}(\tau) E(T-\tau)\, d\tau \qquad [4.29]$$

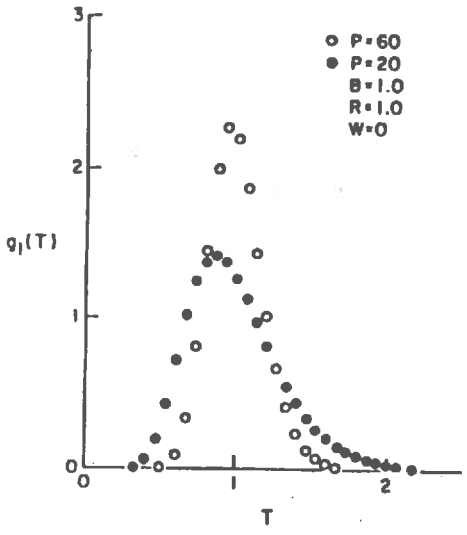

Fig. 4.2 Travel time pdf for the CDE model and for two Peclet numbers. [after *Sposito et al. 1986*]

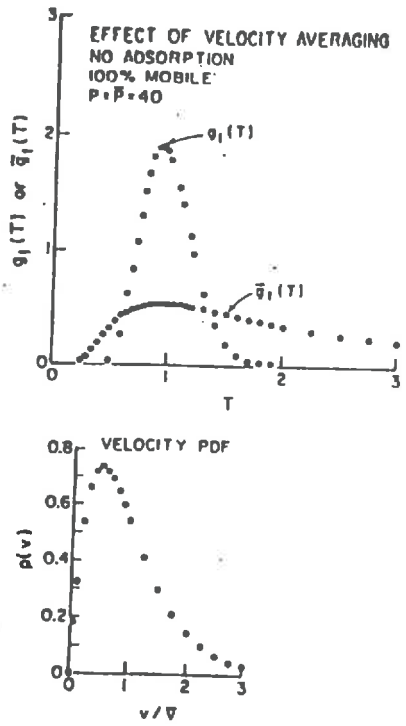

Fig. 4.3 Velocity distribution obeying a γ–distribution (bottom). Comparison of the pdf with that obtained for the CDE model (top) [after *Sposito et al. 1986*]

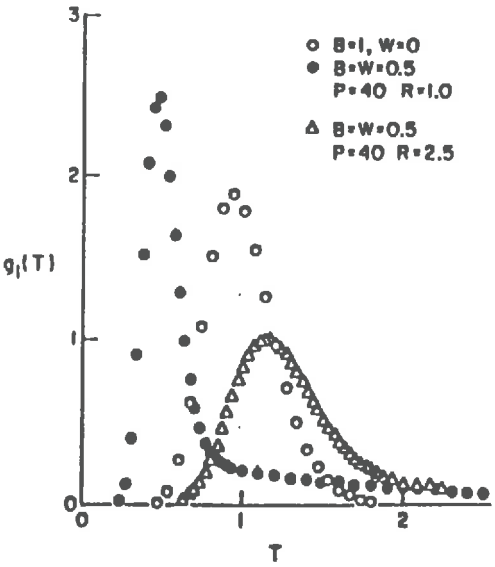

Fig. 4.4 Graphs of the travel time pdf for the two–region CDE model for various values of β and ω [after *Sposito et al. 1986*].

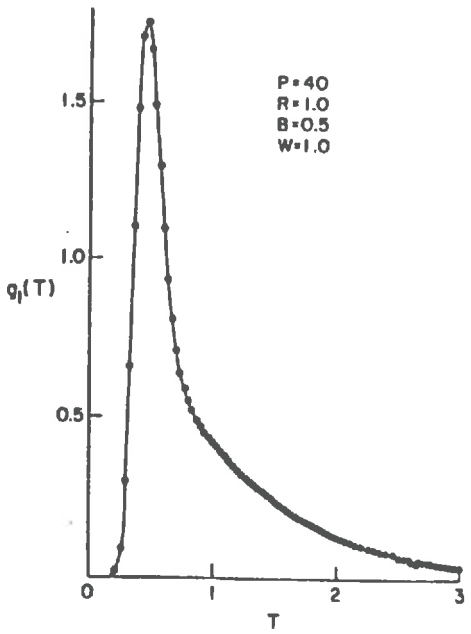

Fig. 4.5 Graph of the travel time pdf showing the effect of increasing the transport rate between mobile and immobile phases [after *Sposito et al. 1986*]

It appears immediatly that $E(T) = \partial C_f/\partial T = g_1(T)$. The similarity between the RTD and the lifetime pdf is obvious.

Applying the Laplace transform to both sides of equation [4.22], and making use of the convolution theorem, one gets

$$\mathcal{L}(C_{f1})(s) = \mathcal{L}(G)(s)\,\mathcal{L}(\partial C_f/\partial T)(s) = \mathcal{L}(G)\,\mathcal{L}(g_1) \qquad [4.30]$$

where $\mathcal{L}$ is the Laplace tranform operator. This equation expresses that the Laplace transform of the lifetime pdf is directly related to the Laplace transform of the breakthrough curve. In particular this last one being easily obtained, the moments of the lifetime pdf are easily calculated by means of equation [3.189]. Sposito et al. (1986) show that in term of flux concentration, applying the Laplace transform to the two–region model leads to the differential equation

$$\beta Rs\left[1+\frac{(1-\beta)\,\omega/\beta}{(1-\beta)Rs+\omega}\right]\overline{C}_{f1}(X,s) = \frac{1}{P}\frac{\partial^2\overline{C}_{f1}}{\partial X^2} - \frac{\partial\overline{C}_{f1}}{\partial X} \qquad [4.31]$$

where $\overline{C}_{f1} = \mathcal{L}(C_{f1})$. Hence, according to Eq. [4.30], $\mathcal{L}(G)\,\mathcal{L}(g_1)$ is solution of Eq. [4.31]. The solution of [4.31] being

$$\overline{C}_{f1}(s)=\overline{G}(s)\exp\left\{\frac{P}{2}\frac{1}{2}\left[P^2+4\beta RPs\left[1+1+\frac{(1-\beta)\,\omega/\beta}{(1-\beta)Rs+\omega}\right]\right]^{1/2}\right\} \qquad [4.32]$$

a comparison of Eq. [4.32] and Eq. [4.30] leads to

$$\mathcal{L}(g_1)(s) = \exp\left\{\frac{P}{2}\frac{1}{2}\left[P^2+4\beta RPs\left[1+1+\frac{(1-\beta)\,\omega/\beta}{(1-\beta)Rs+\omega}\right]\right]^{1/2}\right\} \qquad [4.33]$$

As said before the mean and variance of the solute lifetime are obtained by applying formula [3.189] to Eq. [4.33]. In term of dimensionless variables it comes

$$E[T]=R \qquad var[T]=\frac{2R^2}{P}\left[1+\frac{(1-\beta)^2P}{\omega}\right] \qquad [4.34]$$

These expressions were already obtained by Valocchi (1985). Effects of different model parameters on the mean and variance of the solute lifetime pdf can be easily analysed in a way similar Valocchi (1985) proceeded to evaluate the range of validity of the LEA model when varying some parameters (See §4.6.4). Some trivial conclusions are obtained such that; E[T] increases if (1) positive sorption increases, (2) pore water velocity decreases, (3) there is anion exclusion. Similarly, it is concluded that var[T] increases if (1) pore water velocity decreases, (2) dispersion increases, (3) positive adsorption increases. Inversely, var[T] decreases in response to anion exclusion or to any other parameter variation or mechanism tending to reduce the role of immobile zones. Sposito et al. (1986) used a numerical algorithm, Talbot (1979), to invert Eq. [4.33]. Fig. 4.2 illustrates the effects of varying the Peclet number for the classical CDE. Remark the displacement of the maximun toward the mean, E[T]=1, and the simultaneous diminution of the tailing due to an increased convective character of the transport. The authors also show how the introduction of velocity heterogeneities modifies the shape of $g(t)$. Fig. 4.3 (bottom) illustrates the case

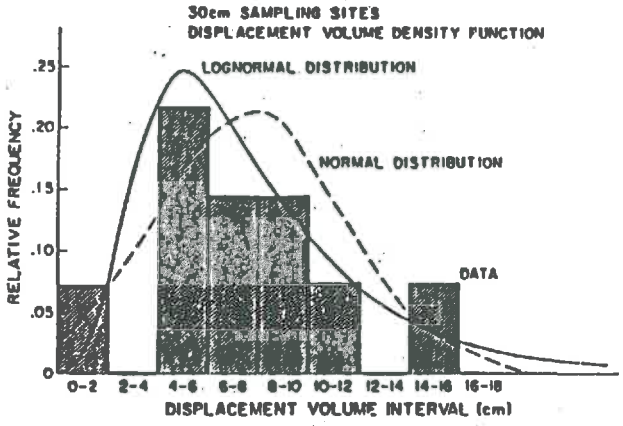

Fig. 4.6 Measured distribution of the relative probability of occurrence of solute displacement to 30 cm depth after a given net input of water [after *Jury et al. 1982*].

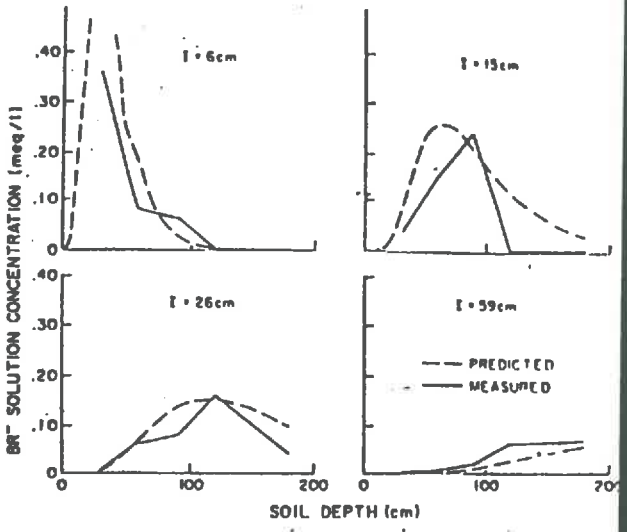

Fig. 4.8 Predicted and average of field measured concentration profiles after application of various net amounts of water [after *Jury et al. 1982*].

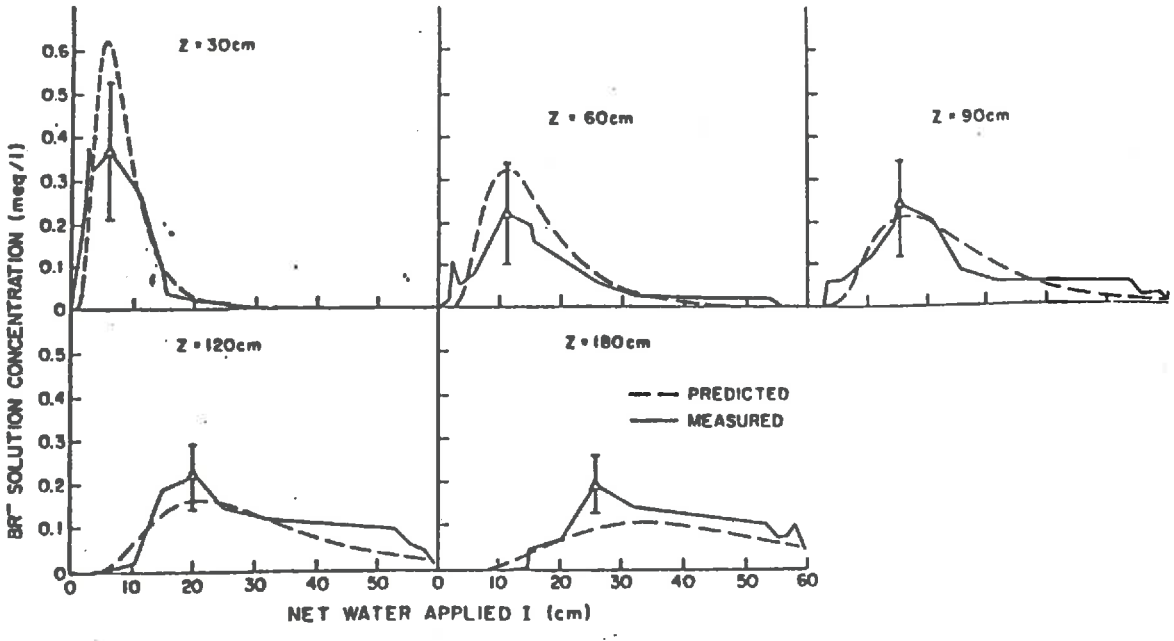

Fig. 4.7 Comparison of predicted and measured breakthrough curves at various depths as function of the net amount of water applied [after *Jury et al. 1982*]

of a velocity distribution obeing a gamma pdf. In the upper part of the figure, notice the loss of symmetry and the long time tailing of the travel time pdf $\bar{g}_1$ derived with the gamma distribution as compared with the pdf g_1 obtained for the classical CDE. Effects due to variations in β and ω are presented Fig. 4.4 and 4.5. Comparing the triangles and the black dots in Fig. 4.4, one remarks that increasing the retardation factor compensates the tailing effect and lack of symmetry due to the presence of an immobile phase. This is a striking illustration of the correlation existing between R and ω in the QSS model.

4.3 APPLICATION TO EXPERIMENTS ANALYSIS

Following the publication of the TFM of Jury (1982) and its extension Jury et al. (1986), several papers appeared using the TFM to analyse solute movement at the scale of undisturbed soil columns as well as at the scale of the field. The first study by Jury et al. (1982) had for objective to test the TFM on a large scale solute transport experiment. The experiment consisted in following in time and space (14 solution samplers at 30 cm depth over a 0.64 hectare field), the movement of a δ–input of Bromide followed by 93 mm of water distributed over 100 days. The pdf $F_1(I)$ (see Eq. [4.1]) was calibrated on the maxima of the breakthrough curves obtained at 30 cm depth by means of the solution samplers. Figure 4.6 presents the distribution of the amount of water applied, I, at which the maxima were reached. A normal and a lognormal pdf were fitted to this experimental distribution. As it can be observed on Fig. 4.6, the lognormal distribution offers a better fit. Breakthrough curves at 60, 90, 120 and 180 cm depth as well as concentration profiles at different times were then calculated using equation [4.11]. Figure 4.7 taken from Jury et al. (1982) allows to compare observed and calculated breakthrough curves at various depths. Calculated and field–averaged concentration profiles are displayed Fig. 4.8. It seems that for that situation, homogeneity of the soil structure throughout the profile in particular, the pdf determined at 30 cm depth can be used to calculate the behavior of the solute pulse at deeper depths. Table 4.1 presents the various recovery percentages (14 sampling sites) obtained by integrating in time the breakthrough curves observed at 30, 60, 90, 120 and 180 cm depths. Notice the large inter–sites variability but the reasonable means.

	Site Number														
Depth, cm	1	2	3	4	5	6	7	8	9	11	12	13	14	15	Average
30	41	50	54	121	96	132	142	81	33	55	84	95	115	59	83
60	84	30	62	103	61	64	115	29	57	49	67	91	126	178	80
90	146	50	100	43	113	110	162	33	180	124	122	126	105	100	108
120	80	65	134	69	117	126	115	158	106	215	76	68	163	149	117
180	3	85	213	123	110	50	126	141	113	111	131	138	63	104	108 (116*)

Percent recovery is $100 \int_0^{t'} C(z, I)\, dI/C_0 \Delta I$.
*Neglecting site 1.

Tab. 4.1 Recovery percentage per site and depth of measurement of the breakthrough curve [after *Jury et al. 1982*].

An important problem arising when calibrating the pdf is to determine the number of sampling sites needed to achieve a given level of precision in the estimated mean and variance of the pdf to be fitted. The first question to answer to is: Are we interested in extreme values of the distribution ? These values can be very important if we deal with tracers for which it is essential to predict the

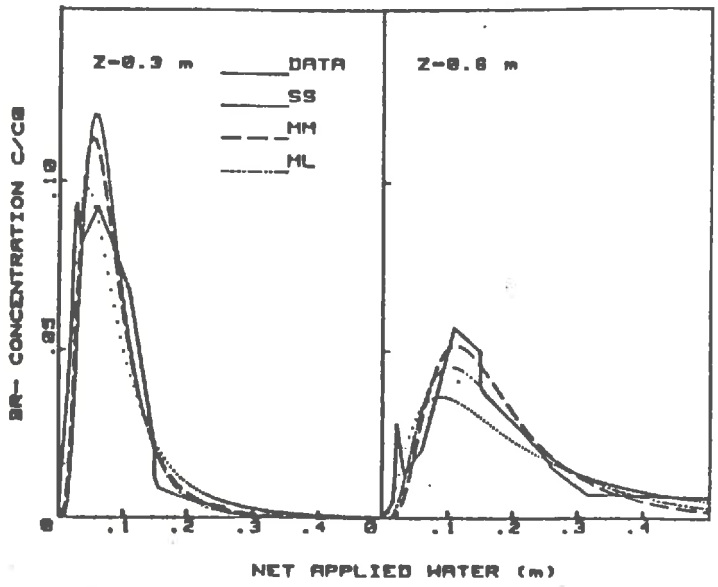

Fig. 4.9 Lognormal travel time pdf fitted with three different optimization techniques. Case of a Br transport experiment conducted on a loamy sand [after *Jury et al. 1985*]

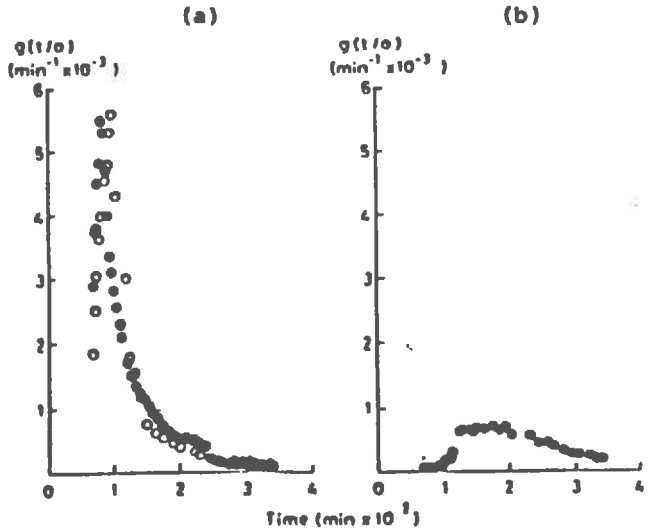

Fig. 4.10 Measured travel time pdf for Br transport through a clay soil at two adjacent field sites [after *White et al. 1986*]

probability that small quantities will reach the groundwater table. In the case of the experiment reported by **Jury et al. (1982)**, the mean and variance were respectively, μ=E[lnI]=1.91 and var[lnI]=0.56. The theoretical bounds for a 1% error were I_{min}<1.84 and I_{max}>24.7. Hence, as the minimum and maximum values recorded were 1.75 and 15 respectively, the maximun travel time expected to occur 1 over 100 times was not contained in the 14 samples population. **Jury et al. (1982)** calculated that with 14 samples the mean travel time was only estimated at ±35%.

The same set of data was also analysed by **Jury and Sposito (1985)**. In particular, three different optimization techniques, minimization of the sum of square of the differences (SS), moments method (MM) and maximum likelihood (ML) were used to fit the pdf F_1 to a lognormal distribution. The breakthrough curves and concentration profiles simulated with the three different lognormal distributions presented non–negligeable discrepancies. This is illustrated Fig. 4.9. According to the authors these differences are a consequence of the fact that the travel–time pdf they used (lognormal distribution) was not physically accurate, otherwise the same set of parameters, mean and variance, should have been obtained by using different optimization techniques. In particular, this result shows that the distribution of velocities is not always lognormal. It also indicates that even if a fit to a lognormal distribution seems good it should be used with precautions, and perhaps the simulated results obtained with the lognormal distribution compared to those obtained with a numerical integration technique directly using the observed distribution of travel times.

Beside the loamy sand on which this experiment was conducted, the TFM has been applied to various field and column tracer experiments, most of them conducted on the same clay soil, (Evesham clay, Typic Haplaquent). These studies are reported in **White (1985)**, **White et al. (1986a)**, **White et al. (1986b)**, **White (1987)**, **Dyson and White (1987)**. A characteristic of these studies is that they apply the TFM to laboratory column or small field plot as opposed to the experiment of **Jury et al. (1982)** conducted at the scale of the field.

In each of these papers a lognormal travel time pdf was fitted to observed breakthrough curves. This was done as follows. If the input is considered of Dirac–type, we already noticed that $g(t|0)=Q_{ext}/k$ where k is a normalizing constant such that the integral of $g(t)=1$. If we note $C(t)$ the concentration of the effluent and $V_{ext}(t)$ the cumulative drainage at the bottom of the column or of the field plot, the travel time pdf is easily obtained with $Q_{ext}(t)$ approximated by $Q_{ext}'(t)=C(t)dV_{ext}(t)/dt$. Figure 4.10 shows two examples of travel time pdf obtained for two differents plots, located in the same field, treated with an identical δ–input of Bromide, **White et al. (1986a)**. While the breakthrough curve recorded on the first plot shows evidences of rapid transfer, the second presents a skewed but much more homogeneous distribution of travel times. Let us define the *median travel time* t_m, as the time at which the probability for a molecule to have left the soil volume is .5. Notice that t_m is not the expected value of the pdf g. The median time gives an idea of the average travel time. Values of respectively 110 and 170 mn were calculated for the two plots. If we assume that the Bromide is a perfect tracer of water flow, then the median time t_m can be used to calculate an average fluid velocity v_m and a porosity θ_t participating in the transport. If q_0 is the input rate, we have

$$v_m=L/t_m \qquad \theta_t=q_0/v_m$$

Remark that if we have a steady flow, then $g(t|0)=q_0C_{ext}/k$ and can be expressed in terms of the cumulative amount of water applied, I. We can write, $F_1(I|0)=g(t|0)/q_0=C_{ext}(I)/k$. If F_1 is fitted to a lognormal pdf with mean μ, then

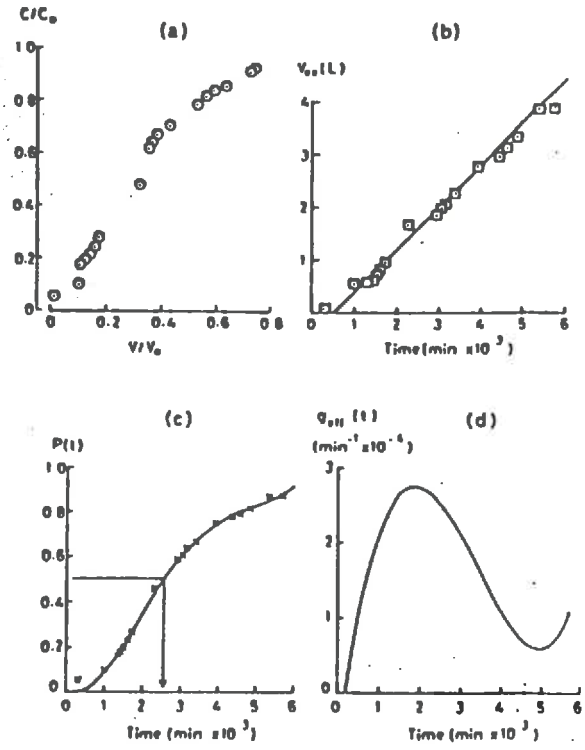

Fig. 4.11A Chloride transport through an undisturbed core of clay soil. Initially wet sample. Input rate of 1.3 mm/h. (a) Experimental breakthrough curve. (b) Cumulative effluent volume. (c) Integral of the travel time pdf. (d) Fitted travel time pdf [after *White et al. 1986*]

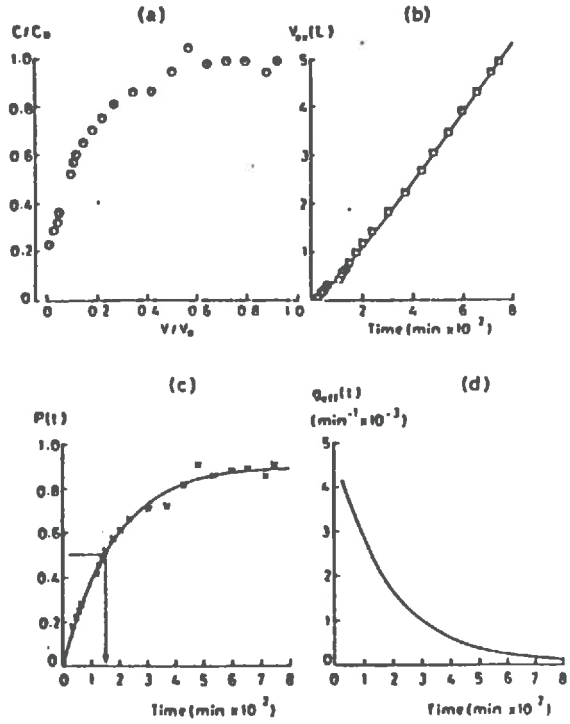

Fig. 4.11B Chloride transport through an undisturbed core of clay soil. Initially dry sample. Input rate of 12 mm/h. (a), (b), (c), (d) as above. [after *White et al. 1986*]

θ_t is given by: θ_t=exp(μ)/L. In a first approximation θ_t can be related to the mobile phase in a two–region model and of course to the transport volume defined §4.2.2.

Laboratory experiments with step inputs were also performed on soil columns taken from the same field plots as above, White et al. (1986a). Two cylindrical columns with diameters and lenghts of about 23 cm, and contrasted initial water contents, .414 and .350, were irrigated at rates of 1.3 and 12 mm/h, respectively. For these conditions we have

$$g(t|0) = [dQ_{ext}(t)/dt]/Q_{ent} \qquad [4.35]$$

where $Q_{ext}(t)$ is approximated as already explained above. Figure 4.11A,B show the various data and fitted distributions for the lower and higher application rate, respectively. First, it should be remarked that the two pdfs fitted for each column are quite different. Origins of these differences should probably be related to differences in initial water contents and/or irrigation rates. Large differences in soil structure are unlikely since both columns were sampled at very close locations and in the same horizon. These experiments show in particular the dependence of the pdf on the input rate and initial water content. Hence, even at the location it has been calibrated, the TFM cannot be used as a predictive tool unless input and initial conditions are not to far from the ones used during the calibration experiment. This means that for very contrasted climatic conditions, for example a succession of very dry periods and stormy events, the TFM based on a travel time pdf calibrated during a steady state experiment will perform very poorly. This means also that the notion of average fluid velocity does not make a lot of sense under these conditions, but this is obvious. That was also remarked by Jury et al. (1982). These conclusions could be expected since for these unsaturated flow conditions, the TFM implicitely integrates very rawly the strongly non–linear physical interactions existing between mobile and immobile water phases, in particular the phenomena of solute uptake by porous blocks due to water flow in addition to the diffusion process. Thus, one probably cannot expect the pdf to be independent of initial water content and input rate. It is also very interesting to remark that for this soil, the travel time pdfs observed in the field and on undisturbed soil columns in the laboratory are quite different. This can be partially explained by the fact that two different tracers were used, in the field Bromide which is a perfect tracer of water movement and for laboratory columns Chloride which is subject to anion exclusion, this phenomena reducing the transport volume. Also, cannot be eliminated the possibility that the results obtained at the scale of the laboratory column are perhaps not extrapolable to the scale of the field plot. This appears to be very likely since the field plots were squares of 2 by 2 meters while the laboratory colums were cylinders with diameters of about 23 cm. Hence, the differences in travel time pdf may very well be related to the different scales at which the transport phenomena was observed. It seems that passing from one scale to the other is not a problem of changing transport parameter values but of changing the shape of the pdf.

The links between the CDE and TFM have been underscored in the previous paragraphs. In order to compare these two modeling approaches, Dyson and White (1987) analysed with the CDE and the TFM a series of laboratory tracer experiments carried out on undisturbed soil columns. The same soil as above was used. Steady–state flow experiments consisted to obtain the breakthrough curves for various step input of $CaCl_2$ at rates varying from 0.3 to 3 cm/h. Eighteen undisturbed soil columns with diameter of about 22 cm and height 15 cm were used. Chloride concentation profiles were also measured for 8

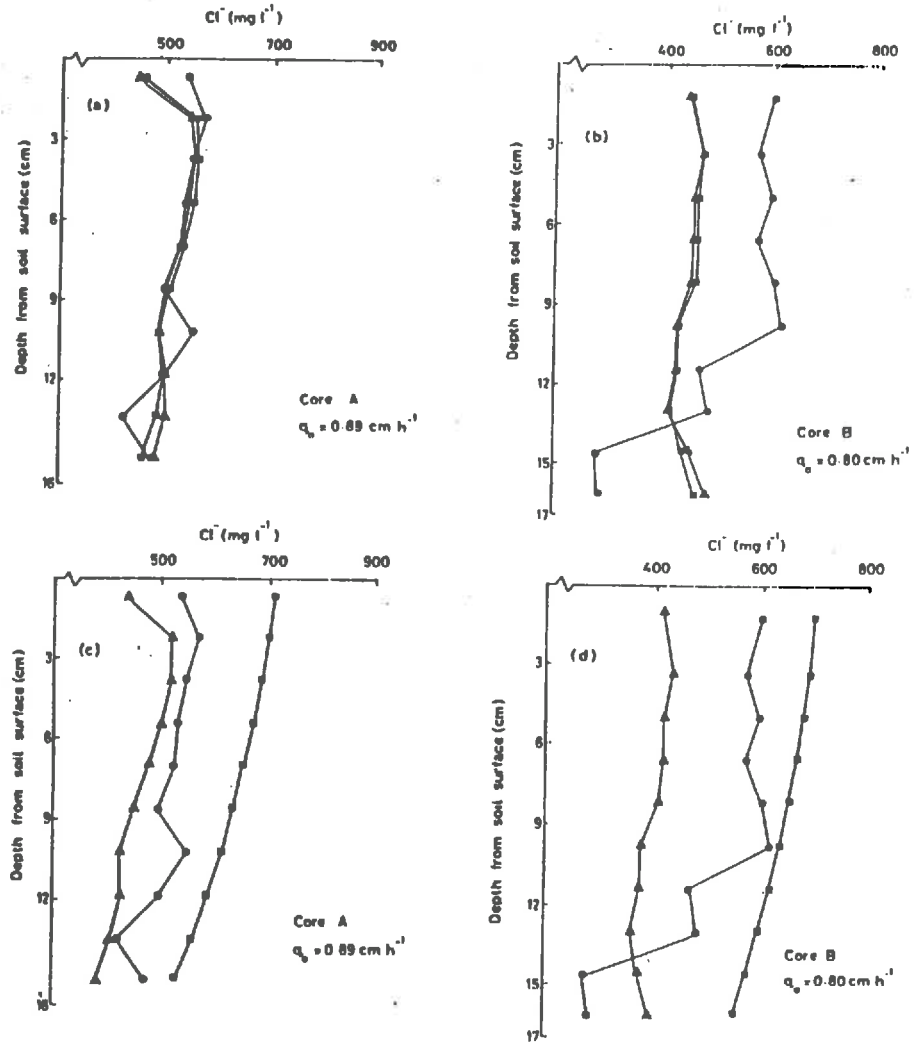

Fig. 4.12 Measured (dots) and predicted volume–averaged concentration profiles for two undisturbed soil cores with different structures. (a) and (b), predictions based on Eq. [4.41] for the TFM (squares) and CDE (triangles). (c) and (d) see explanation in the text [after *Dyson and White 1987*]

Irrigation intensity ($cm\ h^{-1}$)	TFM		CDE	
	v ($cm\ h^{-1}$)	D ($cm^2\ h^{-1}$)	v ($cm\ h^{-1}$)	D ($cm^2\ h^{-1}$)
0.282	0.702	3.04	0.704	2.81
0.362	0.888	2.69	0.889	2.55
0.571	1.29	5.56	1.39	5.24
0.801	2.33	10.4	2.33	9.68
0.886	2.21	9.09	2.21	8.47
1.12	2.70	41.5	2.66	35.1
1.40	3.14	34.8	3.13	25.3
1.72	4.30	29.4	4.32	26.3
2.31	5.38	95.8	5.44	75.5
2.81	6.29	44.8	6.34	39.8

Tab. 4.2 Values of v and D derived from the TFM and the CDE.

columns. Let us recall that for a lognormal travel time pdf

$$F_I(I) = \exp \frac{-[\ln(I)-\mu]^2/\sigma^2}{\sqrt{2\pi}\ \sigma I} \qquad [4.36]$$

where μ the mean of the lognormal distribution and σ^2 its variance, the concentration at any depth Z is given by

$$C(Z,I) = \frac{C_0}{2}\left\{1+\mathrm{erf}\left[\frac{\ln(IL/Z)-\mu}{\sqrt{2}\sigma}\right]\right\} \qquad [4.37]$$

The concentration at the outlet is obtained by making Z=L. Analytical solutions for the CDE in terms of flux–averaged concentration with a step input have been given at the beginning of Chap. 3, Eq. [3.14]. In the present case one have R=1.

An equally good fit between calculated and observed breakthrough curves was obtained with the CDE or the TFM provided that the velocity in the CDE was not taken equal to the flux divided by the water–filled pore volume. Adjustement made allowing the dispersion only to vary were giving very bad results. This means, as expected for this structured soil, that not all the water present in the porosity participated in the transport. A strong correlation seemed to hold between the velocity and the dispersion coefficient. The non linear relation $D=4.1(\pm 0.16)v^{1.42(\pm 0.12)}$ provided a fit with a correlation coefficient of 0.889. Notice that the relation is not linear which seems to agree with the fact the linearity is commonly accepted for pore water velocities lower than 1 cm/d, Sposito et al. (1986). The dispersivity was estimated to be of about 4.1 cm which also revealed the wide range of pore velocities. This value is also slightly higher than those of about 3 cm/day or less usually found for field experiments.

We gave, §4.2.2, Eqs. [4.25] and [4.26], the expressions for the mean and variance of the travel time distributions respectively associated with the CDE and the TFM. By equating the two means, a value of the velocity can be calculated function of the mean and variance of the pdf fitted for the TFM. Identically, by equating the variances a value of the dispersion coefficient can be derived. These substitutions respectively give

$$v = L \exp[-(\mu+\sigma^2/2)] \qquad [4.38]$$

$$D = L^2\exp[-(\mu+\sigma^2/2)][\exp(\sigma^2)-1]/2. \qquad [4.39]$$

Table 4.2 gives the values of the velocity and dispersion coefficient calculated with above formula or obtained by fitting the solution of the CDE, Eq. [3.14], to experimental breakthrough curves. It appears that the velocities obtained by both methods are very close but that the TFM predicts larger dispersion coefficients, especially for velocities above 1.1 cm/h. Thus, as said before the predictions superimpose at the depth of calibration since the breakthrough curves are equally well reproduced, but the fact that the dispersion coefficient predicted with the TFM is larger means that at deeper depths the signal simulated with this coefficient will be more spreaded.

Figures 4.12a,b presents two examples of calculated and measured resident concentration profiles. In particular, the second sample noted Core B in the

graph, presents a sharp change in concentration at about 10 cm depth which the authors explained by a change of the soil structure. This figure illustrates clearly the fact that a perfect fit can be obtained for the breakthrough curves whit at the same time a very bad prediction of the resident concentration profile. This also shows that if the pdf used in the TFM is fitted at a depth such that the solute already traveled through layers of different "characteristics", may be a correct prediction of the breakthrough curve will be obtained at the scale of the field and this is not certain, but a certainly very bad prediction of the resident concentrations will follow. Of course the same is true for the CDE if a velocity and a dispersion coefficient independent of the depth are used. It is obvious that this incapacity to predict resident concentrations is a serious limitation to the use of the model since for example subsequent irrigations will be simulated with a false initial situation. Correct predictions of at the same time the breakthrough curves and the resident concentration profiles can only be obtained by fully accounting for the dependence of model parameters on depth in the CDE or by fitting as many travel time pdfs as necesary to account for profile heterogeneity.

From a theoretical point of view, it appears that ignoring the physical characteristics of the system, average transport parameters can still be found such that the CDE or the TFM will correctly predict the breakthrough curves. Thus, in that case these two models appear as pure mathematical models without physical background. Since the breakthrough curves were equally well reproduced by both models we can also conclude that the information included in a breakthrough curve is not sufficient to decide of the physical validity of a model. Comparisons with measures taken inside the system must absolutely be included in the estimation process.

The solution of the CDE used to analyse these experiments is expressed in term of flux–average concentration. Different methods can be employed to convert the results in a resident concentration profile. The authors proceeded as follows. We note $J(0,t)=i_0C_0$ the input flux and $J(z,t)=C_{ex}(t)I_0(z)$ the flux at a depth z where $I_0(z)$ is the drainage rate at depth z and i_0 the input rate. Since $I_0(L)$, the drainage rate at the bottom of the column may be different from i_0 due to water uptake by the sample, the drainage rate at any depth z is calculate as

$$I_0(z) = I_0(L) - \frac{L-z}{L}[I_0(L)-i_0] \qquad [4.40]$$

which means that the uptake of water by the porous matrix during the tracer experiment is equally distributed all along the soil column. The average resident concentration between two depths z_1 and z_2 is then

$$C_r(z_1,z_2,t) = \frac{\int_0^t [I_0(z_1)C_{ex}(z_1,t)-I_0(z_2)C_{ex}(z_2,t)]}{\pi a^2[z_2-z_1]\theta_v'} \qquad [4.41]$$

where a is the radius of the column and θ_v' is the estimated volumetric water content.

An other way to calculate the resident concentration is to use Eq. [3.2] or what is equivalent use the resident concentration profile given by Eq. [3.6]. But, since all the water is not active in the transport process this solution will lead to an overestimation of the concentration and will violate the mass balance unless it is applied with a porosity corresponding to the effective transport volume. Figure 4.11c,d, black squares, presents the case where all the water is assumed to

articipate in the transport process. The overestimation and violation of the mass–balance appear clearly. The authors then derived an average porosity effective in the transport as follows. Let τ be the mean travel time defined by

$$\tau = \int_0^\infty t g(t|0)\, dt \qquad [4.42]$$

Remark that τ is not the median time τ_m, used before and which was defined as the time at which the probability for a molecule to have left the soil column is .5. Noting q_0 the rate of application of the tracer, the porosity effective in the transport can then be estimated by

$$\theta_{st} = q_0 \tau / L \qquad [4.43]$$

Notice that since τ is different from τ_m, θ_{st} is different from θ_t calculated previously. For these experiments θ_{st} was estimated to be .41 (±.06) while θ_t was estimated to be .29 (±.07). Using θ_{st}, the profile with black triangles were predicted, Fig. 4.11c,d. Quite large differences are still present. One of the conclusions immediately arising is that when only a part of the water participates in the transport process, it is impossible to pass from a flux–averaged to a volume–averaged formulation of the CDE by means of Eq. [3.2]. According to the authors, this is due to the fact that the porosity effective in the transport process and derived from probabilistic considerations is interpreted in a mechanistic sense. It probably exists a value of the porosity such that a good prediction of the volume–averaged concentration is obtained from [4.6]. This experiment shows that this value cannot be derived from the median travel time or the mean travel time.

4.4 CONCLUSIONS.

If our objective is the prediction of chemical species movement in porous media, and thus our criteria to judge of the usefulness of a modeling approach its predictive capability, then one of the main conclusions of this study is that the TFM approach does not have that predictive capability, unless an extensive and carefull calibration of the model is conducted at the site where it will be used. Due to its lack of physical background, it is difficult if not impossible to relate the travel time pdf modeling the transport to the characteristics of the soil. The experiments reported above have illustrated the large dependence of the travel time pdf to be calibrated, on soil structure, initial water content, flow intensities, type of solute, scale of the experiment, etc... Hence, similarly with the difficulties that arose with the equation, relating the flux and the water content in the macroporosity, used in kinematic wave approach, the main problem is that the travel time pdf does not depend on the characteristics of the soil only.

Now, if we look at the problem from a theoretical point of view, the comparison of the TFM with more classical approaches such that the simple CDE or two–region models have highlighted the fact that the CDE is a particular case of TFM. Experiments have also illustrated the fact that using the TFM as well as the CDE, correct predictions of the breakthrough curves can be obtained with at the same time a poor prediction of the resident concentration profile. This of course comes from disregarding physical properties and internal variability of the system. In particular one can conclude that the simple good fit of a breakthrough curve is not sufficient to decide of the validity of a physical model. In consequence, the predictive capability of any solute transport model when

applied to a natural soil profile cannot and must not be appreciated just by looking at how good is the fit with experimental breakthrough curves. Inclusion of variables internal to the system appears to be a requirement for future experiments designed for solute transport model evaluations.

Although the last formulation of the TFM allows the modeling of reactive tracers transport, it has only been applied to nonreactive solutes (Bromide, Chloride, Tritium, Nitrate) since the evaluation of Q_{in} and Q_{out} necessary to the identification of g (see Eq.[4.18]) is possible only if appearance and disappearance of the solute occur through respectively the entrance and exit surfaces of the soil unit. This constitutes a serious limitation to the use of the TFM. We also notice that the pdfs fitted to a breakthrough curve for a particular experiment have never been used to predict later transport experiments. In the same order of idea, the TFM has never been applied to analyse experiments involving square pulse inputs or successive leachings.

All experiments reported in the literature and analysed with the TFM and the classical CDE show that the breakthrough curves are equally well reproduced by both models. However, no estimation of the respective predictive capabilities of the two models has been made or at least reported in the literature. Actually, there is no experimental evidence allowing to say that one or the other is best suited for solute transport modeling. It seems that the TFM is slightly more general since the CDE is a particular case of TFM. On an other hand, models accounting much more accurately than the simple CDE for the physical and chemical mechanisms acting during solute transport in heterogeneous media have been developed in the past few years. These models presented in the previous chapter proved that they could accurately simulate complex transport processes through laboratory columns made up of aggregates. An other advantage of models based on the CDE is that some of their parameters can be related to the physical and chemical properties of the media. The TFM has been originally developed to deal with tracer movement at the scale of the field where the CDE seemed to fail. Applying the TFM to column experiments only adds to an already abundant literature and certainly does not add to our knowledge and understanding of the phenomena.

The main problem when using the TFM is that all the physical and chemical effects are lumped into one "parameter". Hence, it is impossible to assess the relative importance of each of the mechanisms, physical, chemical, which by opposition can be done with a mechanistic model. Thus, this lack of determinism precludes from assessing the range of system parameters (soil structure, initial water content, application rate, etc...) where a fitted pdf can be considered valid. In particular, as opposed to determinist models presented before, no relation, qualitative or quantitative, can be established between the "properties" of the media and the parameters of the model.

Regarding the identification of the travel time pdf, most of the time a lognormal distribution is used. This choice was initially suggested by the fact that many experimental studies reported a lognormal distribution of velocities for undisturbed materials. Among the few field or laboratory experiments analysed with the TFM, it already appears that the lognormal distribution is not always a good choice. The paper by Jury and Sposito (1985) clearly illustrates the large differences that may appear between lognormal pdf obtained by various optimization techniques, thus suggesting that a lognormal model is not the right one to describe the distribution of travel times. In these cases, a dicrete travel time pdf derived from the experimental breakthrough curve must be used.

5. COUPLED TRANSFER. CONCLUSIONS AND PERSPECTIVES.

Coupled Transfer

Several models have been presented for saturated flow modeling in heterogeneous or fractured media, (see §1). These models are based on a double porosity approach consisting to distinguish between two continua with different hydraulic properties and in each of which water flow is modeled by different equations. Interaction between these two continua is modeled with a distributed source/sink term related to the density of fissuration and the geometry of porous matrix blocks, **Duguid and Lee (1977)**, **Huyakorn et al. (1983)**. An other approach based on a detailed geometrical description of the heterogeneities was also propsosed by **Narasimhan (1982d)**. If we consider that the flow is correctly modeled with these approaches, we can derive, from the respective solutions, the velocity distribution at any time and any location in the two continua. Then, solute transport in each continuum can be modeled with a CD type equation. In fact, it suffices to use the equations developed paragraph 3.2.2, assuming in addition that the velocity is now space and time dependent. The same type of coupling between the two continua can be employed, (continuity of the concentration or film diffusion). As well, the same choice of geometrical conceptualization for the porous blocks is possible, prismactic, spherical, cylindrical. An example of such transport model, although not coupled with water flow modeling, is given by **Huyakorn et al. (1983b)**. The coupling with any of the saturated flow models presented above is only matter of informatics work and do not pose any conceptual problems.

For saturated–unsaturated flow conditions, it clearly appeared in the previous paragraphs that the main problem was to correctly predict the flow of water in the macropore continuum. Several different approaches have been presented attempting to derive a macroscopic law relating the flux and the water content in the heterogeneities. In all the cases but one, **Germann (1985)**, the interaction with the porous matrix during the experiments makes it difficult to judge of the quality of the flow model for the macropore continuum. However, since we have at our disposition several models predicting the flux of water in that continuum, it is possible to built a coupled tranfer model based on a CDE for solute transport.

For the case of a single crack or macropore, an equation for the flow in the pore or the crack is not required. So a more accurate modeling is possible. Water flow and solute transport in the porous matrix can be modeled with the equations classicaly used for a homogeneous porous media. The flow of water in the pore can be estimated fom the uptake of water by the matrix and the input at the entry of the pore estimated from the runoff at the soil surface. The transport of solute in the macropore can then be calculated with a CDE coupled with the transport in the matrix. This approach has never been developed, but the model proposed by Yeh and Luxmoore (1980) for water flow in a macropore was coupled with solute transport in the pore and in the porous matrix.

Let us recall here that the flow in the macropore was modeled with the following equation

$$\beta' \frac{\partial \psi}{\partial t} = \nabla.(K \frac{d\varphi}{d\ell} \vec{n}_\ell) \qquad [5.1]$$

when the pore is saturated and by

$$\frac{\partial \theta}{\partial t} = \frac{dz}{d\ell} \vec{n}_\ell \nabla K \qquad [5.2]$$

when the pore is unsaturated. φ, ψ, θ are, the total head, the pressure head, and the water content, respectively, in the pore. ℓ is the distance from a reference point and $\vec{n}_\ell$ is the unit vector along the logitudinal direction of the pore. β' is the compressibility of water and K is the equivalent hydraulic conductivity. Expressions for the conductivity of a cylindrical macropore or a crack have been given paragraph 2.2.

The chemical transport is modeled in the macropore and in the porous matrix with the same equation

$$\theta R_d \frac{\partial c}{\partial t} = -\nabla.(\vec{v}c) + \nabla.(\theta[D].\nabla c) - (\frac{\partial \theta}{\partial t} + \theta\lambda R_d)c - (K_w\theta + K_s\rho_b K_d)c + M \qquad [5.3]$$

where c is the concentration in the macropore or in the porous matrix, $\vec{v}$ is the velocity, [D] is the dispersion tensor, λ is a decay constant, R_d is the retardation factor, K_w is the first order degradation rate through the disolved phase, K_s is the first order degradation rate throug the adsorbed phase, ρ_b is the bulk density, and M is an artificial sink/source term. The velocity is either obtained from Darcy's law for the porous matrix, or from the flux and the water content in the macropore. The retardation factor is defined on a mass basis for the porous matrix

$$R_d = 1 + \rho_b K_d/\theta \qquad [5.4]$$

where K_d is the distribution coefficient. For the flow in the macropore, the distribution coefficient is replaced by a surface distribution coefficient, K_a, and R_d is now given by

$$R_a = 1 + K_a/\theta \qquad [5.5]$$

and

$$R_a = 1 + K_a/(\theta W) \qquad [5.6]$$

for a pore and a crack, respectively. W is the aperture of a crack. Continuity of the concentration is assumed at the interface matrix/macropore. Notice that the transport is two–dimensional in the porous matrix and one–dimensional in the macropore. This model was used by the authors to demonstrate the deep migration of solute that occurs when the macropore participates in the infiltration process.

Considering now a complete soil profile containing heterogeneities, there is at our knowledge only one model available, named AGTHEM, and documented by Fong and Appelbaum (1980), and Hetrick et al. (1982). This model still considers two superposed macroscopic continua. The soil profile is divided into a finite number of layers, across the boundary of which the flows in the macropore and micropore continua are governed by the following set of rules:

1– Flow rate within the macropores is rapid and not governed by geometrical factors. At each time step, the amount of water flowing from one layer to the next is the lesser of the amount of water contained in the layer and of the amount of water that can be accepted by the underlying layer. So, no equation is required to model the flow in the macropore continuum.

2– Flow from macropore to porous matrix is controled by the hydraulic properties of the soil. Richards equation is solve for plane and cylindrical symmetries in order to evaluate the amount of water uptaken by the porous

matrix.

3– Flow from porous matrix to macropores results from the building of a positive pressure head in the matrix.

4– Flow from one layer to the other in the matrix obeys Darcy's law.

Regarding solute movement, instanataneous mixing is assumed in the macropore continuum inside a layer. Diffusion and hydrodynamic dispersion are not simulated. It is also assumed that chemicals enter the porous matrix by mass flow. Solute movement by diffusion inside the porous matrix is not accounted for. This means in particular, that the establishment of an instantaneous equilibrium inside a layer is assumed. When solute is transported from the porous matrix into the macropore, instanataneous mixing with the solution already present in the macropore is also assumed. This model is therefore considerably simpler than the one presented before, and mainly based on mass balance considerations.

Conclusions and Perspectives

It is now well recognized that in many situations the soil profile can barely be considered as an homogeneous porous medium. Most of the time, natural materials present at least two kinds of porosity. A macroporosity, also referred as structural porosity, corresponding to large voids of many origins, and a microporosity, also referred as textural porosity, and determined by the organization of soil particles. Water flow in these two domains does not obey the same physical laws. In consequence, Richards' equation which proved to be a good model of water movement in homogeneous porous media often leads to poor descriptions of water distribution and fluxes when applied to undisturbed materials. Hence, wether modeled for irrigation practices, groundwater recharge, runoff control, etc..., or to be used in solute transport calculations, modeling of water flux and soil water content distributions can no longer mainly rely on Darcy's law and Richards' equation. Some years ago the scientific community seemed to acknowledge the need for an improved water flow modeling approach accounting for convective transport in the macropore continuum and for the interactions with the porous matrix. Since and quite surprisingly, a very small number of models have been proposed, with a somewhat larger number of experimental studies. If we neglect the models restricted to a single crack or pore and of little applicability, only two models have been published, namely the kinematic wave approach developed by Germann and Beven, and the double porosity model lately proposed by Jarvis and Leeds–Harrison. Also, while for years, hundreds of experiments have been conducted to test Richards' equation, we remarked that except for the experiments conducted by Germann and Beven in order to test their models, nobody else tried or at least reported field or laboratory experiments analysed with the kinematic wave approach. It is actually to early to judge of the popularity of the model proposed by Jarvis and Leeds–Harrison.

By opposition, transport modeling in structured media has been largely studied and improved in the past few years. In fact this may appear somewhat illogical since solute movement modeling requires the knowledge of water flux. So, we are actually in a situation where we have at our disposition a relatively good modeling tool for solute movement in structured media but where we are missing one of the main parameter required to make use of this tool: water flux in the macropore continuum. In consequence and without any doubt, our capacity to handle all the problems we are facing regarding water management, and which will become more important and crucial in a near future, hinge upon our capacity to model water flow in heterogeneous media. Problems such that, management of groundwater recharge, optimization of irrigations and more generally of water

utilization, estimation of soil infiltrability and runoff risks assessment, optimization of solute applications and of leaching strategies, groundwater pollution and deep migration of chemical species, all strongly depend on the quality of water flux estimation.

What are the reasons for this state of the research in the domain of water flow modeling, what are the problems and difficulties encountered and what should our efforts aim at ?

Considering the soil as a double porosity media and accepting Richards' equation to model water flow in the microporosity, the first idea is to try to derive an equation for the macropore continuum. At least one formulation have been proposed. **Germann and Beven** derived an expression where the flux and the water content are related by a power law ($Q=a\theta^b$). This law was derived from geometrical consideration and scaled to account for soil tortuosity. Experiments showed that the two parameters, a and b, could not be considered as soil dependent only. It appeared that boudary conditions and at a lesser degree initial conditions strongly influenced these two parameters. In addition, it was difficult to relate the parameters to qualitative properties of the soil structure. Notice that the same expression is in fact used by **Yeh and Luxmoore**. In all other models, water flow in the macroporosity is not explicitely simulated. In the model of **Jarvis and Leeds–Harrison** the flux in the macropore continuum is calculated from mass balance considerations. This way to proceed seems to be the more promissing given the difficulties encountered in the characterization of the macropore continuum from the point of view of water flow, (e.g. the limitations of the power law). This last algorithm could in our opinion be generalized to any heterogeneity profile and in a way such that it would only require soil structure characteristics easily estimated or measured with standard procedures, (e.g. structural porosity,...).

The second problem, but vry closely related with the former, is to model the interaction between soil matrix and structural porosity. This is done in a relatively simple way in the models proposed by **Germann and Beven**, and at our opinion probably too crudely. The treatment proposed by **Jarvis and Leeds–Harrison** and based on the sorptivity seems much more appropriate and accurate although they introduce some questionable simplifications (e.g. linearity of the sorptivity function of water content). An other obvious limitation is due to the assumption of plane cracks. We presented (e.g. §3.4.2 and Fig. 3.5) some results for solute uptake by aggregates of various geometries. These results showed clearly the influence of aggregate shapes on solute uptake rates function of time. The same kind of behavior can be expected for water uptake. Thus, water flow rates from the macropore continuum into the microporosity depend not only on the percentage of the exchange surface used by the flow but also on the geometry of the porous blocks. At first, it seems that a cylindrical or spherical formulation of Richards' equation would be more appropriate than the conventional (1–D plane symmetry) formulation. This becomes particularly true when the size of aggregates decreases, and/or when the flow in the macropore lasts a long time, in which cases the geometry becomes very quickly an important factor. The notion of "long time" is of course relative as it was for solute transport (e.g. relative to soil water diffusivity and aggregate geometry). Calculations similar to what has been done for solute uptake by aggregates could give some insights on that problem.

Any model for water flow in the macroporisity requires a ceratin degree of "characterization" of the macropore continuum. Among the different variables required, some can be easily measured, for example a structural porosity profile. Others such as the global exchange surface between micro– and macroporosity as a function of depth have been so far obtained from hypothesis on the geometry of

the system, (e.g. plane cracks and spacing and widths of the cracks), Jarvis and Leeds–Harrison. Mathematical techniques for distributed parameters identification could be usefull for that particular problem. In particular, they could give the real exchange surface as a function of depth, and in fact more likely and depending on the formulation of the model, the parameter, a (§3.5.1), which is the volume to surface ratio of the porous blocks or aggregates, (not the parameter of the power law of Germann and Beven). It has been well established now that this parameter depends on the flow rate, and probably also on the lower boundary condition and structural porosity profile. An upper bound of that parameter, saturated flow, could probably be obtained from saturated solute tracer experiments. Solute uptake by porous blocks has the enormous advantage to be modeled by a linear differential operator, Laplace operator, which allows to derive solutions without constraints on the geometry, (see §3.5.1). Thus, the geometry of the porous media, parameter a, can be easily characterized, what does not appear to be simple for water flow without making some strong assumptions of the geometry itself.

Although the distribution of a with depth seems to be the main parameter controling water flow in a structured porous media, one must not neglect the structural porosity profile which may for certain flow conditions become an important composante of soil water storage capacity. Also, in many soils, structural heterogeneities have a dynamic character. Hence, depending on soil swelling and/or shrinking properties it may sometimes be necessary to characterize this dynamics, and to account for it in models.

It seems clear now that one of the main problem we are facing when modeling water flow in structured soils is that model parameters depend in particular on flow characteristics, initial and boundary conditions, duration of the phenomena, etc... For some flow conditions one parameter can be preponderant while for other boundary conditions or time durations, an other parameter becomes preponderant. Hence, it is difficult to define a global approach that could be applied in every case. The sensitivity of the model to parameters changes with initial, and boundary conditions. For example, if we consider the case of infiltration, application rates at the soil surface of course directly determine the value of a and its evolution with time while on an other hand the intial situation and the duration of the input will determine the time at which the volume of the structural porosity will become important. In other words, model parameters, even if they appear to be directly related to soil characteristics and geometry, are not soil dependent only, while it is the case for the conventional porous media approach where hydraulic properties of a given soil can theoretically be defined once and for all and used for any flow problem. For example we could see a as a model parameter as $K(\psi)$ or $\psi(\theta)$ are. But, by opposition with classical hydraulic charcteristics, a depends on initial and boundary conditions and not on a variable characteristic of the system such that θ of ψ. This is important for future research since it appears that to model water flow in the macropore continuum we should characterize a soil with respect to the constraints that will be applied for a given initial situation and not regard the material as having intrinsic properties as it is classicaly done. Notice that classical hydraulic characteristics are still required to evaluate the uptake of water by the aggregates and thus are still playing a very important role. At first it seems that such a characterization cannot be achieved by direct measurement techniques, but probably will require the use of mathematical identification techniques. Thus, in–situ experiments are necessary and can barely be replaced by laboratory experiments for obvious reasons related to the problems of sampling soil cores with a volume sufficient to represent the overall profile.

For transient unsaturated flow conditions, solute uptake by the porous blocks results from a mass–flow component related to water uptake and a diffusion component. Their relative importance depends on initial conditions, diffusion coefficients and hydraulic characteristics. If we consider an infiltration, it is obvious that in the early stages of the process, solute uptake due to water uptake is the main component of the flux of solute into the porous matrix and that the participation of diffusion is probably negligible. This is particularly true for species with low diffusion coefficient. At long times, when the rate of water uptake decreases, diffusion becomes a more important component of the intake of solute by the aggregates. Here also, a model would allow to assess and quantify the relative importance of the main parameters: initial situation, diffusion coefficient, hydraulic characteristics, geometry of the aggregates. In conclusion, water uptake rate by the porous block will probably be in most situation the principal phenomena controling the quantity of solute retained and adsorbed by the aggregates. This should encourage us to focus on an improved prediction of water uptake rates by the porous matrix and water flux in the macropore continuum.

REFERENCES

Addiscott, T. M., Simulating diffusion within soil aggregates: a simple model for cubic and other regularly shaped aggregates, *J. Soil Sci., 33,* 37–45, 1982.

Ammozegar–Fard, A., D. R. Nielsen, and A. W. Warrick, Soil solute concentration distributions for spatially varying pore water velocities and apparent diffusion coefficient, *Soil Sci. Soc. Am. J., 46,* 3–9, 1982.

Anderson, J., and R. Thunvik, Predicting mass transport in discrete fracture networks with the aid of geometrical fielf data, *Water Resour. Res., 22,* 1941–1950, 1986.

Anderson, J., and B. Dverstorp, Conditional simulations of fluid flow in three–Dimensional networks of discrete fractures, *Water Resources Res., 23,* 1876–1886, 1987.

Aris, R., On the dispersion of linear kinematic waves, *Proc. R. Soc. London,* Ser. A, 245, 268–277, 1958.

Babcock, R. E., D. W. Green and R. H. Perry, Logitudinal dispersion mechanisms in packed beds, *A.I.Ch.E.J., 12(5),* 922–926, 1966.

Barenblatt, G. I., Iu. P. Zheltov, and N. Kochina, Basic concepts in the theory of seepage of homogeneous liquids in fissured rocks, *Prikl. Mat. Mekh, 24,* 852–864, 1960.

Barker, J. A., Laplace transform solutions for solute transport in fissured aquifers, *Adv. Water Resources, 5,* 98–104, 1982.

Barker, J. A., Block–geometry functions characterizing transport in densely fissured media, *Journal of Hydro., 77,* 263–279, 1985a.

Barker, J. A., Modeling the effects of matrix diffusion on transport in densely fissured media, *Proceedings of the 18th IAH congres,* CAMBRIDGE, 250–269, 1985b.

Baver, L. D., W. H. Gardner, and W. R. Gardner, *Soil Physics,* 4th ed., John Wiley and Sons, New York, 1972.

Beacher, G. B., and N. A. Lanney, Trace length biases in joint surveys, in *Proc. of the 19th U.S. Symposium on Rock Mechanics,* p. 56–65, 1978.

Beven, K. and P. F. Germann, Water flow in soil macropores 2. A combined flow model, *J. Soil Science, 32,* 15–29, 1981.

Beven, K. and P. F. Germann, Macropores and water flow in soils, *Water Resour. Res., 18,* 1311–1325, 1982.

Beven, K. and P. F. Germann, A distribution function model of channelling flow in soil based on kinematic wave theory, *Proceeding of the ISSS symposium on water and solute movement in heavy clay soils, Wageningen,* 89–100,1985.

Bibby, R., Mass transport of solutes in dual–porosity media, *Water Resour. Res., 17,* 1075–1081, 1981.

Biggar, J. W., and D. R. Nielsen, Miscible displacement: II Behavior of tracers, *Soil Sci. Soc. Am. Proc., 26,* 125–128, 1962.

Black, J. H. and K. L. Kipp, Jr, Movement of tracers through dual–porosity media. Experiments and modeling in the cretaceous chalk, England, *Journal of Hydro., 62,* 287–312, 1983.

Blake, G., E. Schilting, and U. Zimmerman, Water recharge in a soil with shrinkage cracks, *Soil Sci. Soc. Am. Proc, 37,* 669–672, 1973.

Bovardsson, G., On the temperature of water flowing trough fractures, *J. of Geophysical Res., 74,* 1987–1992, 1969.

Bouma, J., Field measurement of soil hydraulic properties characterizing water movement through swelling clay soils, *J. Hydr., 45,* 149–158, 1980.

Bouma, J., Soil morphology and preferential flow along macropores, *Agricultural Water Manag., 3,* 235–250, 1981.

Bouma. J., Measuring the hydraulic conductivity of soil horizons with continuous macropores, *Soil Sci. Soc. Am. J., 46,* 438–441, 1982.

Bouma, J., and J. L. Anderson, Water and chloride movement through soil columns simulating pedal soils, *Soil Sci. Soc. Am. J., 41,* 766–770, 1977.

Bouma, J., A. Jongerius, O. Boersma, A. Jager, and D. Schoonderbeek, The function of different types of macropores during satutated flow through four swelling soil horizons, *Soil Sci. Soc. Am. J., 41,* 945–950, 1977.

Bouma, J., and L. W. Dekker, A case study on infiltration into dry clay soil. I. Morphological observations, *Geoderma, 20*: 27–40, 1978.

Bouma, J., and J. H. M., Wosten, Flow patterns during extended saturated flow in two undisturbed swelling clay soils with different macrostructures, *Soil Sci. Soc. Am. J., 43,* 16–22, 1979.

Bouma, J., C. F. M. Belmans, and L. W. Dekker, Water infiltration and redistribution in a silt loam subsoil with vertical worm channels, *Soil Sci. Soc. Am. J., 46,* 917–921, 1982.

Bouma, J. and J.H.M. Wosten, Characterizing ponded infiltration in a dry cracked clay soil, *Jounal of Hydrology, 69,* 297–304, 1984.

Brandt, A., E. Bresler, N. Dinner, I. Ben–Asher, J. Heller, and D. Goldberg, Infiltration from a trickle source, I. Mathematical models, *Soil Sci. Soc. Am. Proc., 35*: 675–682, 1972.

Brenner, H., The diffusion model of longitudinal mixing in beds of finite length. Numerical values, *Chem. Eng. Soc., 17*:229–243, 1962.

Bresler, E. and G. Dagan, Solute transport in unsaturated soil at field scale. II application, *Soil Sci. Soc. Am. J., 43*, 467–472, 1979.

Brewer, J., *Fabric and Mineral analysis of Soils.* John Wiley & Sons, New York, 1964.

Broadbent, S. R., and J. M. Hammersley – Proc. Camb/ Phil. Soc. 53, 629, 1957.

Cameron, D. R., and A. Klute, Convective–Dispersive solute transport with a combined equilibrium and kinetic adsorption model, *Water Resour. Res, 13,* 183–188, 1977.

Carslaw, H. S., and J. C. Jaeger, *Conduction of heat in solids. Oxford University Press* 1959.

Castillo, E., G. M. Karadi, and R. J. Krizeck, Unconfined flow through jointed rock, *Water Resour. Bull.*, 8(2), 266–281, 1972a.

Castillo, E., R. J. Krizeck, and G. M. Karadi, Comparison of dispersion characteristics in fissured rocks, *Proc. Symp. Fundam. Transp. Phenom.* Porous Media, 2nd, 778–797, 1972b.

Charbeneau, R. J., Kinematic models for soil moisture and solute transport, *Water Resour. Res., 20*, 699–706, 1984.

Chen, H., T. Chen, and C. Chen, Hybrid Laplace transform/finite element method for one–dimensional transient heat conduction problems, *Comp. Meth. in Appl. Mech. and Eng., 63,* 83–95, 1987.

Coat, K. H., and B. D. Smith, Dead end pore volume and dispersion in porous media, *Soc. Petrol. Eng. J., 4*, 73–84, 1964.

Courant, R., and D. Hilbert, *Method of mathematical physics.* Vol. 1, pp 561, Interscience pub., New york, 1966.

Courant, R., and D. Hilbert, *Method of mathematical physics.* Vol. 2, pp 830 Interscience pub., New york, 1966.

Crump, K. S., Numerical inversion of Laplace transforms using a Fourier series approximation, *J. Ass. Comp. Mach., 23,* 89–96, 1976.

Cushman, J. H., Development of stochastic partial differential equations for subsurface hydrology, *Stochastic Hydrology and Hydraulics, 1,* 241–262, 1987.

Dagan, G. and E. Bresler, Solute transport in unsaturated soil at field scale, I, Theory, *Soil Sci. Soc. Am. J., 43*, 461–466, 1979.

Dankwerts, P. V., Continuous flow systems, *Chem. Eng. Sci., 2*, 1–13, 1953.

Davidson, M. R., A Green–Ampt model infiltration in a cracked soil, *Water Resour. Res., 20,* 1685–1690, 1984.

Davidson, M. R., Numerical calculation of Saturated–Unsaturated infiltration in a cracked soil, *Water Resour. Res., 21,* 709–714, 1985.

Davidson, M. R., Asymptotic infiltration into a soil which contains cracks or holes but whose surface is otherwise impermeable, *Transport in Porous Media, 2,* 165–176, 1987.

Davis, G. B., A Laplace transform technique for the analytical solution of a diffusion–convection equation over a finite domain, *Appl. Math. Modeling, 9,* 69–71, 1985.

Davies, B., and B. Martin, Numerical inversion of the Laplace transform: A survey and comparison of methods, *J. Comp. Phys., 33,* 1–32, 1978.

DeAngelis, D. L., G. T. Yeh, and D. D. Huff., An integrated compartmental model for describing the transport of solute in a fractured porous medium. ORNL/TM–8983, *Environmental science division, Pub. No. 2292,* 1984.

Deans, H. H., A mathematical model for dispersion in the direction of flow in porous media, *Soc. Pet. Eng., 3*:49–52, 1963.

de Cockborne, A–M., Transfert des nitrates en mileieux poreux sature en presence d'une porosite structurale, 92 pp., *thesis* Grenoble, 1980.

De Hoog, F. R., J. H. Knight, and A. N. Stokes, An improved method for numerical inversion of Laplace transform, *SIAM J. Statist. Comp., 3,* 357–366, 1982.

De Smedt, F., and Wierenga, P. J., A generalized solution for solute flow in soils with mobile and immobile water, *Water Resour. Res., 15,* 1137–1141, 1979.

Dixon, D. M., and A. E. Peterson, Water infiltration control: a channel system concept, *Soil Sci. Soc. Am. Proc., 35,* 968–973, 1971.

Dixon, R. M., Controlling water infiltration in bimodal porous soils: air–earth interface concept, *Proceeding of the 2nd Symposium IAHR–ISSS,* GUELPH, 1972.

Domenico, P. A., and G. A. Robbins, A dispersion scale effect in model calibrations and field tracer experiments, *J. of Hydro., 70,* 123–132, 1984.

Dubner, R., and J. Abate, Numerical inversion of Laplace transforms by relating them to the finite Fourier cosine transforms, *J. Ass. Comp. Mach., 15,* 115– , 1968.

Duguid, J. O. and P. C. Y. Lee, Flow in fractured porous media, *Water Resour. Res., 13,* 558–566, 1977.

Durbin, F., Nunerical inversion of Laplace transforms: efficient improvement to Dubner and Abate's method, *Computer J., 17,* 371–376, 1974.

Dyson, J. S., and R. E. White, A comparison of the convection–dispersion equation and transfer function model for predicting chloride leaching through an undisturbed, structured clay soil, *Journal of Soil Science, 38*, 157–172, 1987.

Edwards, A. L., TRUMP: A computer program for transient and steady state temperature distributions in multidimensional systems, report, *Natl. Tech. Inf. Serv., Nat. Bur. of Standards*, Springfield, Va., 1969.

Edwards, W. M., R. R. van der Ploeg, and W. Ehlers., A numerical study of the effects of noncapillary–sized pores upon infiltration, *Soil Sci. Soc. Am. J., 43*, 851–856, 1979.

Ehlers, W., Observation of earthworm channels and infiltration on tilled and untilled loess soil, *Soil Sci., 119*, 242–249, 1975.

Elsworth, D., A model to evaluate the transient Hydraulic response of three–dimensional sparsely fractured rock masses. *Water Resour. Res., 22*, 1809–1819, 1986.

Evans, R. D., A proposed model for multiphase flow through naturally fractured reservoirs, *Soc. of Petr. Eng. J.*, p 669–680, Oct. 1982.

Fong, L., and H. R. Appelbaum, Macropore–mesopore model of water flow through aggregated porous media, p 56, *ORNL/MIT–312, Oak Ridge National Lab.*, Oak Ridge, TN., 1980.

Gartling, D. K. and R. K. Thomas, A statistically based numerical model for heat conduction in fractured rack masses, *Int. J. Num. Meth. in Geom., 8*, 567–588, 1984.

Gaudet, J–P., Transferts d'eau et de solutes dans les sols non–satures. Mesure et simulation, *These de Docteur d'Etat, Universite de Grenoble, 230pp.*, 1978.

Germann, P. F., and K. Beven, Water flow in soil macropores. I An experimental approach, J. *Soil Science, 32*, 1–14, 1981a.

Germann, P. F., and K. Beven., Water flow in soil macropores. III A statistical approach, *J. Soil Science, 32*, 31–39, 1981b.

Germann, P. F., and K. Beven, Kinematic wave approxination to infiltration into soils with sorbing macropores, *Water Resour. Res., 21*, 990–996, 1985.

Germann, P. F., and M. S. Smith, Kinematic wave approximation to the transport of escherichia coli in the vadose zone, *Water Resour. Res.*, (to appear) 1987.

Germann, P. F., Kinematic wave approach to infiltration and drainage into and from soil macropores, *Trans. ASAE.* 1985.

Gershon, N. D., and A. Nir, Effects of boundary conditions of models on tracer distribution in flow through poroud mediums, *Water Resour. Res., 5,* 830–839, 1969.

Gillham, R. W., E. A. Sudicky, J. A. Cherry, and E. O. Frind, An advection–diffusion concept for solute transport in heterogeneous unconsolidated geological deposits, *Water Resour. Res., 20,* 369–378, 1984.

Goltz, M. N., Three–dimensional analytical modeling of diffusion–limited solute transport, pp 172, *PhD Stanford University, Dep of Civil Eng.*, 1986.

Green, R. E., P. S. C. Rao, and J. C. Corey, Solute transport in aggregated soils: tracer zone shape in relation to pore–velocity distribution and adsorption, in: *Proc. 2nd Symp. Fundam. of Trans. in Porous Media*, IAHR–ISSS, Guelph. 7–11 August 1972. Vol.2: 732–752, 1972.

Grisak, G. E., and J. F. Pickens, Solute transport through fractured media, 1. The effect of matrix diffusion, *Water resour. Res., 16,* 719–730, 1980.

Grisak, G. E., J. F. Pickens, and, J. A. Cherry, Solute transport through fractured media, 2. Column study of fractured till, *Water Resour. Res., 16,* 731–739, 1980b.

Grisak, G. E., and J. F. Pickens, An analytical solution for solute transport through fractured media with matrix diffusion, *J. of Hydrology, 52,* 47–57, 1981.

Guyon, E., J–P. Hulin, and R. Lenormand, Application de la percolation a la physique des milieux poreux, *Annales des Mines, 5–6*, 17–40, 1984.

Hallaire, V., Retrait vertical d' un sol argileux au cours du dessechement. Mesures de l' affaissement et consequences structurales, *Agronomie, 7,* 631–637, 1987.

Hasegawa, S. and T. Sato, Water uptake by roots in cracks and water movement in clayed subsoil, *Soil Sci., 143,* 381–386, 1987.

Herrera, I., Integrodifferential equations for systems of leaky aquifers and applications 2. Error analysis of approximate theories, *Water Resour. Res., 10,* 811–820, 1974.

Herrera, I., A review of the integrodifferential equations approach to leaky aquifers mechanics, *Adv. Groundwater Hydrol.,* 1976.

Herrera, I., and L. Rodarte, Integrodifferential equations for systems of leaky aquifers and applications 1. The nature of approximate theories, *Water Resour. Res., 9,* 995–1004, 1973.

Herrera, I., and R. Yates, Integrodifferential equations for systems of leaky aquifers and applications 3. A numerical method of unlimited applicability, *Water Resour. Res., 13,* 725–732, 1977.

Hetrick, D.M, J. T. Holdeman, and R. J. Luxmoore, AGTHEM: Documentation of modifications to the Terrestrial Ecosystem Hydrology Model (TEHM) for agricultural applications, p. 115, ORNL/TM–7856, Oak Ridge National Loboratory, Oak Ridge, TN., 1982.

Higashi, K. and T. H. Pigford, Analytical models for migration of radionuclides in geological sorbing media, *J. of Nuclear Sci. and Tech., 17,* 700–709, 1980.

Hirt, C. W., and F. H. Harlow, A general corrective procedure for the numerical solution of initial value problems, *J. Comp. Phys., 2,* 114–119, 1967.

Hogdkinson, D. P., and D. A. Lever, Interpretation of a field experiment on the transport of sorbed and non–sorbed tracers through a fracture in crystalline rock, *Radioctive Waste Management and the Nuclear Fuel Cycle, 4,* 129–158, 1983.

Hodgkinson, D. P., D. A. Lever, and T. H. England, Mathematical modeling of radionuclide transport through fractured rock using numerical inversion of Laplace transforms: Application to INTRACOIN level 3, *Ann. Nuclear Energy, 11,* 111–122, 1984.

Hoogmoed, W. B., and J. Bouma, A simulation model for predicting infiltration into cracked clay soil, *Soil. Sci. Soc. Am. J., 44,* 458–461, 1980.

Hornung, U., Miscible displacement in porous media influenced by mobile and immobile water, *Tech. Rep. 102, Dep. of Math., Arizona State Univ.,* Dec. 1987.

Hosanski, J. M., F. Bernaudat, E. Ledoux, and A. Ribstein, Transferts thermiques en milieux fissures, *Annales des Mines, 5–6,* 93–102, 1984.

Hsu, J. T., and J. S. Dranoff, Numerical inversion of certain Laplace transforms by the direct application of fast Fourier transform (FFT) algorithm, *Comput. Chem. Engng., 11,* 101–110, 1987.

Hursh, C. R., Report of the subcomitte on subsurface flow, *Eos Trans. AGU, 25,* 743–746, 1944.

Huyakorn, P. S., B. H. Lester and C. R. Faust, Finite element techniques for modeling groundwater flow in fractured aquifers, *Water Resour. Res., 19,* 1019–1035, 1983a.

Huyakorn, P. S., B. H. Lester and J. W. Mercer, An efficient finite element technique for modeling transport in fractured porous media 1. Single species ransport, *Water Resour. Res., 19,* 841–854, 1983b.

Huyakorn, P. S., and K. Nilkuha, Solute transient transport equation using an upstream finite element scheme, *Appl. Math. Modeling, 3,* 7–17, 1979.

James, R. V., and J. Rubin, Applicability of the local equilibrium assumption to transport through soil of solutes affected by ion exchange, in *Chemical Modeling of Aqueous Systems,* edited by E. A. Jenne, pp. 225–235, American Chemical Society, Washington, D.C., 1979.

Jardine, P. M., G. V. Wilson, and R. J. Luxmoore, Modeling the transport of inorganic ions through undisturbed soil columns from contrasting watersheds, Submitted to *Soil Sci. Soc. Am. J.* 1988.

Jarvis, N. J., and P. B. Leeds–Harrison, Modelling water movement in drained clay soil. I. Description of the model, sample output and sensitivity analysis, *Journal of Soil Science, 38,* 487–498, 1987a.

Jarvis, N. J., and P. B. Leeds–Harrison, Modelling water movement in drained clay soil. II. Application of the model in Evesham series clay soil, *Journal of Soil Science, 38,* 499–509, 1987b.

Jarvis, N. J., P. B. Leeds–Harrison, and J. M. Dosser, The use of tension infiltrometers to assess routes and rates of infiltration in a clay soil, *Journal of soil Science, 38,* 633–640, 1987.

Jouanna, P., and C. Louis, Ecoulements dans les milieux fissures. Methodologie d'etude et de modelisation, *Annales des Mines, 5–6,* 41–50, 1984.

Jury, A. W., Solute travel–time estimates for tile drained fields, I, Theory, *Soil Sci. Soc. Am. Proc., 39,* 1020–1024, 1975a.

Jury, A. W., Solute travel–time estimates for tile drained fields, II, Application to experimental studies, *Soil Sci. Soc. Am. Proc., 39,* 1024–1028, 1975b.

Jury, A. W., Simulation of solute transport using a transfer function model, *Water Resour. Res., 18,* 363–368, 1982.

Jury, A. W., L. H. Stolzy, and P. Shouse, A field test of the transfer function model for predicting solute transport, *Water Resour. Res., 18,* 369–375, 1982.

Jury, W. A., and T. M. Collins, Stochastic versus deterministic models for solute movement in the field, In: *Proc. of the Symp. on Unsaturated Flow and Transport Modeling,* Seattle, 1982.

Jury, W. A., and G. Sposito, Field calibration of solute transport models for the unsaturated zone, *Soil Sci. Soc. Am. J., 49,* 1331–1341, 1985.

Jury, W. A., G. Sposito and R. E. White, A transfer function model of solute transport through soil 1. Fundamental concepts, *Water Resour. Res., 22,* 243–247, 1986.

Kanchanasut, P., D. R. Scotter, and R. W. Tillman, Preferential solute movement through larger soil voids. II Experiments with saturated soil, *Aust. J. Soil Res., 16,* 269–276, 1978.

Kissel, D. E., J. T. Ritchie and E. Burnett, Chloride movement in undisturbed clay soil, *Soil Sci. Soc. Am. Proc, 37,* 21–24, 1973.

Kneale, W. R., and R. E. White, The movement of water through cores of dry (cracked) clay–loam graaland topsoil, *J. Hydro., 67,* 361–365, 1984.

Knighton, R. E., and R. J. Wagenet, Simulation of solute transport using a continuous time Markov process. 1. Theory and steady state application, *Water Resour. Res., 23(10)*, 1911–1916, 1987.

Knighton, R. E., and R. J. Wagenet, Simulation of solute transport using a continuous time Markov process. 2. Application to transient field conditions, *Water Resour. Res., 23(10),* 1917–1925, 1987.

Kreft, A., On the boundary conditions of flow through porous media and conversion of chemical flow reactors, *Bull. Acad. Polonaise des Sci. 29,* 521–529, 1981.

Kreft, A., and A. Zuber, On the physical meaning of the dispersion equation and its solutions for different initial and boundary conditions, *Chem. Eng. Sci., 33,* 1471–1480, 1978.

Lai, S., and J. J. Jurinak, Cation adsorption in one–dimensional flow through soils: A numerical solution, *Water Resour. Res.*, 8, 99–107, 1972.

Lafolie, F., R. Guennelon, and M. Th. van Genuchten, Analysis of water flow under trickle irrigation. I Theory and numerical solution, Submitted to *Soil Sci. Soc. Am. J.*, 1988.

Lapidus, L., and N. R. Amundson, Mathematics of adsorption in beds. VI The effect of longitudinal diffusion in ion exchange and chromatographic columns, *J. Phy. Chem., 56*, 984–988, 1952.

Lawes, J. B., J. H. Gilbert, and R. Warington, On the amount and composition of the rain and drainage water collected at Rothamsted, *Williams, Clowes and Sons Ltd.*, London 1882.

Leblois, E., Etude de quelques aspects de la dispersion hydrodynamique en milieu poreux fissure. pp 117, *These presente a* l'Universite Louis Pasteur de Strasbourg. 1986.

Lewis, D. T., Subgroup designation for three udolls in southeastern Nebraska, *Soil Sci. Soc. Am. Proc, 41*, 940–944, 1977.

Lindstrom, F. T., R. Haque, V. H. Freed, and L. Boersma, Theory on the movement of some herbicide in soils; Linear diffusion and convection of chemicals in soils, *Env. Sci. Technol., 1*:561–565, 1967.

Lindstrom, F. T., and M. N. L. Narasimham, Mathematical theory of a kinetic model for dispersion of previouly distributed chemicals in a sorbing porous medium, *SIAM J. Appl. Math., 24*, 496–510, 1973.

Long, J. C. S., J. S. Remer, C. R. Wilson, and P. A. Witherspoon, Porous media equivalents for networks of discontinuous fractures, *Water Resour. Res., 18,* 645–658, 1982.

Long, J. C. S., and P. A. Witherspoon, The relationship of the degree of interconnection and permeability in a fracture network, *J. Geophys. Res., 90(B4),* 3087–3098, 1985.

Long, J. C. S., P. Gilmour, and P. A. Witherspoon, A model for steady fluid flow in random three–dimensional networks of disc–shaped fractured, *Water Resour. Res., 21(8),* 1105–1115, 1985.

Long, J. S.C., and D. M. Billaux, The use of geostatistics to incorporate spatial variability in the modeling of flow through fracture networks, *Rep. 21439,* Lawrence Berkeley Lab., Berkeley, Calif., 1986.

McCoy, B. J., Approximate polynomial expansion method for inverting Laplace transforms of impulse responses, *Chem. Eng. Comm., 52,* 93–103, 1987.

McGarry, D., and K. W. J. Malafant, A cumulative mass coordinate to etermine water profile changes in variable volume soil, *Soil Sci. Soc. A. J., 51,* 850–854, 1987.

McMahon, M. A., and G. W. Thomas, Chloride and tritiated water flow in disturbed and undisturbed soil cores, *Soil Sci. Soc. Am. Proc., 38,* 727–732, 1974.

Maloszewsky, P., and A. Zuber, On the theory of tracer experiments in fissured rocks with a porous matrix, *J. of Hydrology, 79,* 333–358, 1985.

de Marsily, G., Influence of the spatial distribution of velocities in porous media on the form of solute transport, *Proceeding of the symposium on unsaturated flow and transport modeling,* Seattle, 1982.

de Marsily, G., Methodes et domaines d'application de la mecanique des fluides en milieux poreux et fissures, *Annales des Mines, 5–6,* 5–10, 1984.

de Marsily, G., Flow and mass transport in fractured rocks: conectivity and scale effect, *Proceeding of Hydrogeology of rocks of lowm permeability,* Tucson, 1985.

Mathab, M. A., D. B. Bolstad, J. R. Alldredge, and R. J. Shanley, Analysis of fracture orientations for input in structural models of discontinuous rock, *Rep. Invest. U.S. Bur. Mines, 7669,* 76pp., 1972.

Matheron, G. and, G. de Marsily, Is transport in porous media always diffusive ? A counterexample, *Water Resour. Res., 16,* 901–917, 1980.

Matheron, G., L'emergence de la loi de DARCY, *Annales des Mines, 5–6,* 11–16, 1984.

Moench, A. F., Double porosity models for a fissured reservoir with fracture skin, *Water Resour. Res., 20,* 831–846, 1984.

Moench, A. F., and A. Ogata, A numerical inversion of the Laplace transform solution to radial dispersion in a porous medium, *Water Resour. Res., 17,* 250–252, 1981.

Moreno, L., I. Neretnieks, and T. Ericksen, Analysis of some laboratory tracer runs in natural fissures, *Water Resour. res., 21,* 951–958, 1985.

Moreno, L., and A Rasmuson, Contaminant transport through a fractured porous rock: Impact of the inlet boundary condition on the concentration profile in the rock matrix, *Water Resour. Res, 22,* 1728–1730, 1986.

Mysels, K. J., Diffusion–controlled adsorption kinetics. General solution and some applications, *J. Phys. Chem., 86,* 4648–4651, 1982.

Narasimhan, T. N., The significance of the storage parameter in saturated–unsaturated groundwater flow, Water Resour. Res., 15, 569–576, 1979.

Narasimhan, T. N., Physics of saturated–unsaturated subsurface flow, *Geological Soc. of A.,* Special paper 189, 1982a.

Narasimhan, T. N., Numerical modeling in Hydrology, *Geological Soc. of A.,* Special paper 189, 1982b.

Narasimhan, T. N., Simulation of consolidation in partially saturated soil materials, *Symposium on unsaturated flow and transport modeling.* Seattle March 23–24, 1982c.

Narasimhan, T. N., Multidimensional numerical simulation of fluid flow in fractured porous media, *Water Resour. Res., 18,* 1235–1247, 1982d.

Narasimhan, T. N., Fundamentals of transport phenomena in porous media, *NATO ASI Series, Series E: Applied Sciences No. 82,* Martinus Nijhoff publishers, Boston, 1984.

Narasimahan T. N. and P. A. Witherspoon, An integrated finite difference method for analysing fluid flow in porous media, *Water Resour. Res., 12,* 57–64, 1976.

Narasimhan, T. N. and P. A. Witherspoon, Numerical model for Saturated Unsaturated flow in deformable porous media 1. Theory, *Water Resour.Res., 13,* 657–664, 1977.

Narasimhan, T. N., P. A. Witherspoon and A. L. Edwards, Numerical model for saturated–unsaturated flow in deformable porous media 2. The algorithm, *Water Resour. Res., 14,* 255–261, 1978.

Narasimhan, T. N., and P. A. Witherspoon, Numerical model for saturated–unsaturated flow in deformable porous media 3. Applications, *Water Resour. Res., 14,* 1017–1034, 1978.

Neretnieks, I., T. Eriksen, and P. Tahtinen, Tracer movement in a single fissure in granitic rock: Some experimental results and their interpretation, *Water Resour. Res., 18,* 849–858, 1982.

Neretnieks, I., and A. Rasmuson, An approach to modeling radionuclide migration in a medium with strongly varying velocity and block sizes along the flow path, *Water Resour. Res., 20,* 1823–1836, 1984.

Nieber, J. L., Simulation of infiltration into cracked soils, *Paper presented at the 1981 summer meeting of the ASAE,* ORLANDO, 1981.

Nielsen, D. R., and J. W. Biggar, Miscible displacement in soils. I. Experimental information, *Soil Sci. Soc. Am. Proc., 25,* 1–5, 1961.

Nkedi–Kizza, P., P. S. C. Rao, R. E. Jessup, and J. M. Davidson, Ion exchange and diffusive mass transfer during miscible displacement through an aggregated oxisol, *Soil Sci. Soc. A. J., 46,* 471–476, 1982.

Nkedi–Kizza, P., J. W. Biggar, M. Th. van Genuchten, P. J. Wierenga, H. M. Selim, J. M. Davidson, and D. R. Nielsen, Modeling tritium and chloride 36 transport through an aggregated oxisol, *Water Resour. Res., 19,* 691–700,1983.

Nkedi–Kizza, P., J. W. Biggar, H. M. Selim, M. Th. van Genuchten, P. J. Wierenga, J. M. Davidson, and D.R. Nielsen, On the equivalence of two conceptual models for describing ion exchange during transport through an aggregated oxisol, *Water Resour. Res., 20,* 1823–1836, 1984.

Noorishad, J. and M. Mehran, An upstream finite element method for solution of transient transport equation in fractured porous media, *Water Resour. Res., 18,* 588–596, 1982.

Novakowski, K. S., G. V. Evans, D. A. Lever, and K. G. Raven, A field example of measuring hydrodynamic dispersion in a single fracture, *Water Resour. Res., 21,* 1165–1174, 1985.

Oddson, J. K., J. Letey, and, L. V. Weeks, Predicted distribution of organic chemicals in solution and adsorbed as a function of position and time for various chemical and soil properties, *Soil Sci. Soc. Am. Proc., 34:* 412–417, 1970.

Ogata, A., Mathematics of dispersion with linear absorption isotherm. Fluid movement in earth materials, *Geological survey professional paper 411–H,* 1964.

Parker, J. C., and M. Th. van Genuchten, Flux–Averaged and Volume –Averaged concentrations in continuum approaches to solute transport, *Water Resour. Res., 20,* 866–872, 1984.

Parker, J. C., and A. J. Valocchi, Constraints on the validity of equilibrium and first order kinetic transport models in structured soils, *Water Resour. Res., 22,* 399–407, 1986.

Parlange, J. Y., and J. L. Starr, Dispersion in soil column: Effect of boundary conditions and irreversible reactions, *Soil Sci. Soc. Am. J., 42,* 15–18, 1978.

Passioura, J. B., Hydrodynamic dispersion in aggregated media 1. Theory, *Soil Science, 111,* 345–351, 1971.

Passioura, J. B. and D. A. Rose., Hydrodynamic dispersion in aggregated media 2. Effects of velocity and aggregate size, *Soil Science, 111,* 345–351, 1971.

Pearson, J. R. A., A note on the "Danckwerts" boundary conditions for continuous flow reactors. *Chem. Eng. Sci., 1*0:281–284, 1959.

Pellet, G. L., Longitudinal dispersion, intraparticule diffusion and liquid phase mass transfer during flow through multiparticules system, *Tappi, 49(2)*, 75, 1966.

Philip, J. R., Kinetics of sorption and volume change in clay–colloid pastes, *Aust. J. of Soil Res., 6*:249–267, 1968.

Philip, J. R., Hydrostatics and Hydrodynamics in swelling soils, *Water Resour. Res., 5,* 1070–1077, 1969.

Pruess, K. and T. N. Narasimhan, A practical method for modeling fluid and heat flow in fractured porous media, *Society of Pet. Eng. J.,* 14–26, 1985.

Quisenberry, V. L., and R. E. Phillips, Percolation of surface–applied water in the field, *Soil Sci. Soc. Am. J., 40,* 484–489, 1976.

Raats, P. A. C., Transport in structured porous media. *Proceedings of Euromech 143*, Delft, 1981.

Raats, P. A. C., Tracing parcels of water and solutes in unsaturated zones, In: *Pollutants in Porous Media*, Ed. B. Yaron, G. Dagan, and J. Goldshmid, Springer–Verlag, 1984.

Rao, P. S. C., J. M. Davidson, R. E. Jessup, and H. M. Selim, Evaluation of conceptual models for describing nonequilibrium adsorption–desorption of pesticides during steady flow in soils, *Soil Sci. Soc. Am. J., 43*, 22–28, 1979.

Rao, P. S. C., D. E. Rolston, R. E. Jessup, and J. M. Davidson, Solute transport in aggregated porous media: theoretical and experimental evaluation, *Soil Sci. Soc. Am. J., 44,* 1139–1146, 1980a.

Rao, P. S. C., R. E. Jessup, D. E. Rolston, J. M. Davidson, and D. P. Kilcrease, Experimental and mathematical description of non–adsorbed solute transfer by diffusion in spherical aggregates, *Soil Sci. Soc. Am J., 44,* 684–688, 1980b.

Rao, P. S. C., R. E. Jessup, and T. M. Addiscott, Experimental and theoretical aspects of solute diffusion in spheres and nonspherical aggregates, *Soil Sci., 133,* 342–349, 1982.

Rasmuson, A., Diffusion and sorption in particles and two–dimensional dispersion in a porous medium, *Water Resour. Res., 17,* 321–328, 1981a.

Rasmuson, A., Exact solution of a model for diffusion and transient adsorption in particles and longitudinal dispersion in packed beds, *Am. Inst. of Chemi. Engineers, 27,* 1032–1035, 1981b.

Rasmuson, A., Migration of radionuclides in fissured rock: Analytical solutions for the case of constant source strength, *Water Resour. Res., 20,* 1435–1442, 1984.

Rasmuson, A., The effect of particles of variables size, shape, and properties on the dynamics of fixed beds, *Chemical Eng. Science, 40,* 621–629, 1985a.

Rasmuson, A., The influence of particle shape on the dynamic of fixed beds, *Chemical Eng. Science, 40*, 1115–1122, 1985b.

Rasmuson, A., and I. Neretnieks, Exact solution of a model for diffusion in particules and longitudinal dispersion in beds, *A.I.Ch.E. J., 26,* 686–690, 1980.

Rasmuson, A., and I. Neretnieks, Migration of radionuclides in fissured rocks: The influence of micropore diffusion and longitudinal dispersion, *J. of Geophysical Res., 86,* 3749–3758, 1981.

Rasmuson, A., T. N. Narasimhan, and I. Neretnieks, Chemical Transport in a fissured rock: Verification of a numerical model, *Water Resour. Res., 18,* 1479–1492, 1982.

Ritchie, J. T., D. E. Kissel, and E. Burnett, Water movement in undisturbed swelling clay soil, *Soil Sci. Soc. Am. Proc., 36*, 874–879, 1972.

Rosen, J. B., Kinetics of a fixed bed system for solid diffusion into spherical particles, *The Journal of Chemical Physics, 20,* 387–394, 1952.

Schulin, R., P. J. Wierenga. H. Fluhler and J. Leuenberger, Solute transport through a stony soil, *Soil Sci. Soc. A. J., 51*, 36–42, 1987.

Schumacher, W., Die Physik des Boden, Berlin, 1864.

Schwartz, F. W., L. Smith and A. S. Crowe, A stochastic analysis of macroscopic dispersion in fractured media, *Water Resour. Res., 19,* 1253–1265, 1983.

Schwartz, F. W. and L. Smith, A new continuum approach for modeling dispersion in fractured media, *IAH Meeting*, Tucson, 1985.

Schweich, D. and M. Sardin, Interactions Physico–Chimiques en presence d'un ecoulement. In: *Les mecanismes d'interaction solide–liquide et leur modelisation: applications aux etudes de migration en milieux aqueux.* IAEA–TECDOC–367, 1986.

Scotter, D. R., Preferential solute movement through larger soil voids, I. Some computations using simple theory, *Aust. J. Soil Res., 16,* 257–267, 1978.

Selim, H. M., J. M. Davidson, and R. S. Mansell, Evaluation of a two–site adsorption–desorption model for describing solute transport in soils, *Proc. Summer Comp. Simul. Conf.,* 12–14 July 1976, Washington D. C. p 444–448.

Selim, H. M., R. Schulin, and H. Fluhler, Transport and ion exchange of Calcium and Magnesium in an aggregated soil, *Soil Sci. Soc. Am. J., 51*:876–884, 1987.

Seyfried, M. S., and P. S. C. Rao, Solute transport in undisturbed columns of an aggregated tropical soil: Preferential flow effects, *Soil Sci. Soc. Am. J., 51,* 1434–1444, 1987.

Shaffer, K. A., D. D. Fritton, and D. E. Baker, Drainage water sampling in a wet dual–pore soil system, *J. Envir. Qual., 8,* 241–246, 1979.

Shapiro, A. M., and J. Andersson, Steady state fluid response in fractured rock: A boundary element solution for a discrete fracture continuum model, *Water Resour. Res., 19,* 959–969, 1983.

Shapiro, A. M., and J. Andersson, Simulation of steady state flow in three–dimensional networks using a boundary element method, *Adv. Water Resour., 8,* 106–110, 1985.

Shuford, J. W., D. D. Fritton, and D. E. Baker, Nitrate nitrogen and chloride movement through undisturbed field soil, *J. Env. Qual., 6,* 255–259, 1977.

Simmons, C. S., A stochastic–convective transport representation of dispersion in one–dimensional porous media systems, *Water Resour. Res., 18,* 1193–1214, 1982.

Simpson, T. W. and R. L. Cunningham, The occurance of flow channels in soils, *Journal of Env. Qual., 11,* 29–30, 1982.

Skopp, J. and A. W. Warrick, A two–phase model for the miscible displacement of reactive solutes in soils, *Soil Sci. Soc. Am. Proc., 38,* 545–550, 1974.

Skopp, J., W. R. Gardner, and E. J. Tyler, Solute movement in strcutured soils Two–Region model with small interaction, *Soil Sci. Soc. am. J., 45,* 837–842, 1981.

Smettem, K. R. J. and N. Collis–George, Prediction od steady–state ponded infiltration distribution in a soil with vertical macropores, Journal of Hydrology, 79, 115–122, 1985a.

Smettem, K. R. J. and N. Collis–George, Statistical characterization of soil biopores using a soil peel method, Geoderma, 1985b.

Smettem, K. R. J. and N. Collis–George, The influence of cylindrical macropores on steady–state infiltration in a soil under pasture. *J. of Hydrology, 79,* 107–114, 1985c.

Smiles, D. E., Infiltration into a swelling material, *Soil Sci., 117,* 140–147, 1974.

Smiles, D. E., and Rosenthal M. J., The movement of water in swelling materials, *Aust. J. of Soil Res., 6*: 237–248, 1968.

Smith, R. E., Approximate soil water movement by kinematic characteristics, *Soil Sci. Soc. Am. J., 47,* 3–8, 1983.

Smith, L. and F. W. Schwartz, Mass transport 1. A stochastic analysis of Macroscopic dispersion, *Water Resour. Res., 16,* 303–313, 1980.

Smith, L. and F. W. Schwartz, An analysis of the influence of fracture geometry on mass transport in fractured media, *Water Resour. Res., 20,* 1241–1252, 1984.

Smith, L., C. W. Mase, F. W. Schwartz, and D. Chorley, A numerical model for transport in networks of planar fractures, *in Proc. IAH Meeting,* Tucson, 1985.

Southworth, G. R.,K. W. Watson, and J. L. Keller, Comparison of models that describe the transport of organic compounds in macroporous soil. *Env. Toxicology and Chemistry, 6,* 251–257, 1987.

Spiegel, M. R., Mathematical handbook of formulas and tables, *Schaum's Outline Series,* McGraw–Hill, 1968.

Sposito, G., R. E. White, P. R. Darrah, and W. A. Jury, A transfer function model of solute transport through soil 3. The Convection–Dispersion equation, *Water Resour. Res., 22,* 255–262, 1986.

Stehfest, H., Numerical inversion of Laplace transform, Algorithm 368, *Comm. of the ACM, 13,* 47–49, 1970.

Streltsova, T. D., Hydrodynamics of Groundwater flow in a fractured formation, *Water Resour. Res., 12,* 405–414, 1976.

Sudicky, E. A., and E. O. Frind, Contaminant transport in fractured porous media: Analytical solutions for a system of parallel fractures, *Water Resour. Res., 18,* 1634–1642, 1982.

Talbot, A., The accurate numerical inversion of Laplace transforms, *J. Inst. Math. Appl., 23,* 97– , 1979.

Tang, D. H., E. O. Frind, and E. A. Sudicky, Contaminant transport in fractured porous media: Analytical solution for a single fracture, *Water Resour. Res., 17,* 555–564, 1981.

Thomas, G. W., and R. E. Phillips, Consequence of water movement in macropores, *J. Env. Qual., 2,* 149–152, 1979.

Topp, G. C., and J. L. Davis, Detecting infiltration of water through soil cracks by time domain reflectometry, *Geoderma, 26,* 13–23, 1981.

Trudgill, S. T., A. M. Pickles and K.R.J. Smettem, Soil–water residence time and solute uptake 2. Dye tracing and preferential flow predictions, *Journal of Hydrology, 62,* 279–285, 1983.

Tsang, Y. W. and P. A. Witherspoon, Effects of fracture roughness on fluid flow through a single deformable fracture, *Proceeding of the 17th IAH international congress,* Tucson, 1985.

Turner, G. A., The flow structure in packed bed, *Chem. Eng. Sci. 7:* 156–165, 1958.

Turner, G. A., *Heat and concentration waves,* Academic, New York, 1972.

Valocchi, A. J., Validity of the local equilibrium assumption for modeling sorbing solute transport through homogeneous soils, *Water Resour. Res., 21,* 808–820, 1985.

van Genuchten, M. Th., J. M. Davidson, and P. J. Wierenga, An evaluation of kinetic and equilibrium equations for the prediction of pesticide movement through porous media, *Soil Sci. Soc. Am. J., 38*, 29–35, 1974.

van Genuchten, M. Th., and P. J. Wierenga, Mass transfert studies in sorbing porous media I. Analytical solutions, *Soil Sci. Soc. Am. J., 40*, 473–480, 1976.

van Genuchten, M. Th., and P. J. Wierenga, Mass transfert studies in sorbing porous media II. Experimental evaluation with Tritium ($^3H_20$), *Soil Sci. Soc. Am. J., 41*, 272–278, 1977.

van Genuchten, M. Th., and P. J. Wierenga, Mass transfert studies in sorbing porous media III. Experimental evaluation with 2,4,5–T, *Soil Sci. Soc. Am. J., 41*, 278–284, 1977.

van Genuchtem, M. Th., and P. J. Wierenga, Numerical solutions for convective dispersion with intra–aggregate diffusion and nonlinear adsorption, pp 275–291. In: G. C. van Steenkiste (ed.) *System simulation in water resource*, North Holland Publ. Comp., Amsterdam.

van Genuchten, M. Th., One–dimensional analytical transport modeling, *Proceedings of the Symposium on unsaturated flow and transport modeling* Seattle, 1982.

van Genuchten, M. Th., and J. C. Parker, Boundary conditions for displacement experiments through short laboratory soil columns, *Soil Sci. Soc. Am. J., 48,* 703–708, 1984.

van Genuchten, M. Th., D. H. Tang, and R. Guennelon, Some exacts and approximated solutions for solute transport through large cylindrical macropores, *Water Resour. Res., 20,* 335–346, 1984.

van Genuchten, M. Th., A general approach for modeling solute transport in structured soils, *Memoires IAH, Vol 17*, 513–526, 1985a.

van Genuchten, M. Th., Solute transport processes in structured soils, In: *Proceedings of the 5th AGU*, Fort Collins, Colorado, 1985b.

van Genuchten, M. Th. and F. N. Dalton, Models for simulting salt movement in aggregated field soils, *Geoderma, 38*, 165–183, 1986.

Villermaux, J., and P. M. van Swaay, Modele representatif de la distribution des temps de sejour dans un reacteur semi–infini a dispersion axiale avec zones stagnantes, *Chem. Eng. Sci., 24:* 1097–1111, 1969.

Wang, J. S. Y., and T. N. Narasimhan, Hydrologic mechanisms governing fluid flow in partially saturated, fractured, porous medium, *Water Resour. Res., 21,* 1861–1874, 1985.

White, R. E., The analysis of solute breakthrough curves to predict water redistribution during unsteady flow through undisturbed structured clay soil, *Journal of Hydrology, 79,* 21–35, 1985.

White, R. E., A transfert function model for the prediction of Nitrate leaching under field conditions, *Journal of Hydrology, 92,* 207–222, 1987.

White, R. E., S. R. Wellings and J. P. Bell, Seasonal variations in nitrate leaching in structured clay soils under mixed land use. *Agricultural Wat. Manag., 7,* 391–410, 1983.

White, R. E., G. W. Thomas, and M. S. Smith, Modelling water flow through undisturbed soil cores using a transfer function model derived from ^3HOH and Cl transport, *Journal of Soil Sci., 35,* 159–168, 1984.

White, R. E., J. S. Dyson, R. A. Haigh, W. A. Jury, and G. Sposito, A transfer function model of solute transport through soil 2. Illustrative applications, *Water Resour. Res., 22,* 248–254, 1986a.

White, R. E., J. S. Dyson, Z. Gerstl, and B. Yaron, Leaching of herbicides through undisturbed cores of a structured clay soil, *Soil Sci. Soc. Am. J., 50,* 277–283, 1986b.

Wierenga, P. J., Solute distribution profiles computed with steady–state and transient water movement models, *Soil Sci. Soc. Am. J., 41,* 1050–1054, 1977.

Wilson, C., An investigation of laminar flow in fractured porous rocks, *Ph. D. dissertation,* 178pp., Univ. of. Calif., Berkeley, 1970.

Witherspoon, P.A., J. S. Y. Wang, K. Iwai, and J. E. Gale., Validity of Cubic law for fluid flow in a deformable rock fracture. Water Resour. Res., 16, 1016–1024, 1980.

Yeh, G. T., and R. J. Luxmoore, Chemical transport in macropore–mesopore media under partially saturated conditions, *Proceedings of the symposium on unsaturated flow and transport modeling,* Seattle, 1982.

APPENDIX 1

Numerical Solution of Solute Transport Equations in an Aggregated Media.

In the following we give a numerical scheme proposed by Huyakorn et al. (1983b). In their model, solute transport in the macropore continuum is modeled with the following equation

$$\frac{\partial}{\partial x_m}(D_{mn}\frac{\partial c}{\partial x_n}) - v_m\frac{\partial c}{\partial x_m} = \frac{\partial c}{\partial t} + \lambda c - (\frac{1-\epsilon}{\epsilon})\Gamma \qquad [A1.1]$$

which is a generalization of Eq. [3.39] to a multidimensional domain. They assume that the porous blocks are either spherical with radius, a, or infinite paralelepipeds with width, $2a$, delimitated by parallel cracks with aperture $2b$. Solute movement inside the porous blocks is modeled with the diffusion equation. We note c' the concentration inside the porous blocks and D' the diffusion coefficient. The leakage term, Γ, is then given by

$$\Gamma = -\frac{1}{a}(D'\frac{\partial c'}{\partial z'}\Big|_{z'=a}) \qquad [A1.2]$$

$$\Gamma = -\frac{3}{a}(D'\frac{\partial c'}{\partial r'}\Big|_{r'=a}) \qquad [A1.3]$$

for the parallelepipeds and the spheres, respectively. The gradient in above formula will be obtained from the solution of the diffusion equation in the porous blocks. For the parallelepipeds, c' verifies

$$\frac{\partial}{\partial z'}(D'\frac{\partial c'}{\partial z'}) = \varphi' R'\frac{\partial c'}{\partial t} + \lambda\varphi' R' c' \qquad [A1.4]$$

and for a sphere the diffusion equation is

$$\frac{1}{r^2}\frac{\partial}{\partial r}(D'r^2\frac{\partial c'}{\partial r}) = \varphi' R'\frac{\partial c'}{\partial t} + \lambda\varphi' R' c' \qquad [A1.5]$$

where φ' is the porosity of the porous blocks, λ is a constant which can be used to model radioactive decay or chemical reactions. R' is the retardation factor defined by

$$R' = 1 + \rho_s(1-\varphi')k_d/\varphi' \qquad [A1.6]$$

where ρ_s is the solid density and k_d the distribution coefficient.

The boundary conditions for the macropore continuum are given by:

$c = \bar{c}$ on a part B_1 of the boundary and

$$(-D_{mn}\frac{\partial c}{\partial x_j} + v_m c)n = -\bar{q}.\bar{c}$$

on the rest of the boundary. n is the outward unit normal vector, $\bar{c}$ is the

concentration of the solute entering the system through B_1, and $\bar{q}$ is the inward liquid flux. For the diffusion equation in the porous blocks, the boundary conditions are

$c' = c$ at the surface of the blocks

$\frac{\partial c'}{\partial .} = 0$ at the center of the spheres or on the plane of symmetry of the

parallelepipeds. Initial concentrations are assumed constant in space and respectively equal to c_0 and c'_0. The solution of this set of equations presents two main difficulties. First the resolution of the convection–dispersion equation, and second the evaluation of the leakage term, Γ. Many works have been devoted to the obtention of an oscillation–free solution of the CDE which at the same time minimizes the numerical diffusion and preserves the accuracy. It is well known that the problems arise from the convective term, and that mainly two remedies are available. One is to used a decentered approximation of the first–order derivative terms, which leads to uncentered finite–difference formula or asymmetric weighting functions for a finite element based solution. The other one is to use a Lagrangian representation of the phenomena which eliminates the convective term. The present finite element based solution uses an upstream weighted residual approximation technique presented by Huyakorn and Nilkua (1979). In this approach, a set of asymmetric functions, W_i, is used to weight the spatial terms in place of the basis functions N_i as it is the case with the standard Galerkin technique. Assuming that there is n nodes in the macropore continuum, and applying the weighting technique it comes

$$\int_\Omega W_i\left[\frac{\partial}{\partial x_m}\left(D_{mn}\frac{\partial c}{\partial x_n}\right) - v_m\frac{\partial c}{\partial x_n}\right]dR - \int_\Omega\left[\frac{\partial c}{\partial t} + \lambda c - m\Gamma - q(c^*-c)\right]N_i = 0$$

$$\text{for } i=1,..,n \qquad [A1.7]$$

Applying Green's theorem and assuming that $c = \Sigma N_i c_i$ leads to the following set of ordinary differential equations

$$\sum_{j=1}^{n}\int_\Omega\left[D_{mn}\frac{\partial W_i}{\partial x_m}\frac{\partial N_j}{\partial x_n} - v_m W_i\frac{\partial N_j}{\partial x_m}\right]c_j dR + \int_\Omega N_i N_j\frac{dc_j}{dt}dR +$$

$$\int_\Omega N_i(\lambda N_j c_j - m N_j\Gamma_j)\,dR - \int_{\partial\Omega} W_i D_{mn}\frac{\partial c}{\partial x_n}n_n\,d\gamma = 0 \qquad [A1.8]$$

The last integral which is taken over the boundary, $\partial\Omega$, is easily evaluated with the aid of the boundary condition. We have

$$-\int_{\partial\Omega} W_i D_{mn}\frac{\partial c}{\partial x_n}n\,dB = \int_{\partial\Omega} W_i\bar{q}(c-\bar{c})\,dB \qquad [A1.9]$$

If a standard one–step schema is used to integrate in time, the following set of differential equations comes

$$\sum_{j=1}^{n}(\theta H_{ij} + \frac{M_{i\,j}}{\Delta t} + \theta\lambda M_{ij})c_j^{\,k+1} - mM_{ij}\Gamma_j^{\,k+\theta}$$

$$+ \theta\overline{M}_{ij}c_j^{\,k+1} = F_i \quad i=1,2,..,n \qquad [A1.10]$$

where Δt is the time increment, and k and k+1 refer to previous and current time levels, respectively. θ is a time weighting factor equal to 1 or 1/2 for an implicit and a Cranck–Nicholson schema, respectively. The coefficients of the mass and stiffness matrices are equal to

$$H_{ij} = \int_{\Omega}\left[D_{mn}\frac{\partial W_i}{\partial x_m}\frac{\partial N_j}{\partial x_n} - v_m W_i\frac{\partial N_j}{\partial x_m}\right]dR \qquad [A1.11]$$

$$M_{ij} = \int_{\Omega} N_i N_j\, dR \qquad [A1.12]$$

$$\overline{M}_{ij} = \int_{\Omega} q_n W_i N_j\, dR \qquad [A1.13]$$

$$F_i = (\theta-1)(H_{ij} + \lambda M_{ij})c_j^{\,k} +$$

$$\left[\frac{M_{i\,j}}{\Delta t}\right]c_j^{\,k} + \overline{M}_{ij}c_j^{\,k}(\theta-1) + \overline{M}_{ij}\bar{c}_j^{\,k} \qquad [A1.14]$$

$$\Gamma_j^{\,k+\theta} = \theta\Gamma_j^{\,k+1} + (1-\theta)\Gamma_j^{\,k} \qquad [A1.15]$$

Integrals appearing in coefficients expressions can be evaluated numerically, Gauss quadrature, or analytically. In order to solve the system of equations for $\{c^{k+1}\}$, an evaluation of $\{\Gamma^{k+\theta}\}$ is required. Since a discrete approximation of the concentration gradient at the surface of the porous blocks would lead to a poor estimation of Γ, especially at early and medium times, **Huyakorn et al. (1983), Lafolie et al. (1988)**, the authors elected to calculate Γ from the Galerkin finite element solution of the diffusion equation. This is described in the following. First, a standard Galerkin procedure, with linear basis functions is applied to the diffusion equation. For the plane symmetry, prismatic blocks, and after application of Green's formula it comes

$$\int_0^a D'\frac{\partial N_i}{\partial z'}\frac{\partial N_j}{\partial z}c_j'\,dz' + \int_0^a \varphi' R' N_i N_j\frac{dc_j'}{dt}dz' + \int_0^a \varphi' R' N_i N_j c_j' dz'$$

$$-D'\frac{\partial c'}{\partial z'}\Big|_{z'=a} = 0 \quad i = 1,2,..,n' \qquad [A1.16]$$

where n' is the number of nodes. After evaluation of the integrals and using a one–step time integration formula one obtains the following tridiagonal set of equations,

$$\beta_1 {c_1}'^{k+1} + \gamma_1 {c_2}'^{k+1} = d_1$$

$$\alpha_i {c_{i-1}}'^{k+1} + \beta_i {c_i}'^{k+1} + \gamma_i {c_{i+1}}'^{k+1} = d_i \quad i=2,3,..,n'-1$$

$${c_{n'}}'^{k+1} = c_j{}^{k+1} \qquad [A1.17]$$

Notice that such a system of equations is associated with each node j in the macropore continuum. The parameters $\alpha_i, \beta_i, \gamma_i$ and d_i are defined by

$$\alpha_i = \theta\alpha_i^* + \varphi' R' \Delta z_{i-1}'/(6\Delta t)$$

$$\gamma_i = \theta\gamma_i^* + \varphi' R' \Delta z_i'/(6\Delta t)$$

$$\beta_i = \theta\beta_i^* + \varphi' R' (\Delta z_{i-1}' + \Delta z_i')/(3\Delta t)$$

$$d_i = (\theta-1)(\alpha_i^* {c_{i-1}}'^k + \beta_i^* {c_i}'^k + \gamma_i^* {c_{i+1}}'^k) + \frac{\varphi' R}{6\Delta t}$$

$$\cdot[(\Delta z_{i-1}'){c_{i-1}}'^k + 2(\Delta z_{i-1}' + \Delta z_i'){c_i}'^k + (\Delta z_i'){c_{i+1}}'^k]$$

$$\alpha_i^* = \frac{-D'}{\Delta z_{i-1}'} + \frac{\lambda\varphi' R' \Delta z_{i-1}'}{6}$$

$$\gamma_i^* = \frac{-D'}{\Delta z_i'} + \frac{\lambda\varphi' R' \Delta z_i'}{6}$$

$$\beta_i^* = \frac{D'}{\Delta z_{i-1}'} + \frac{D'}{\Delta z_i'} + \frac{\lambda\varphi' R'}{3}(\Delta z_{i-1}' + \Delta z_i') \quad i=2,3,..,n'-1$$

$$\beta_1 = \theta\beta_1^* + \varphi' R' \Delta z_1'/(3\Delta t)$$

$$\gamma_1 = \theta\gamma_1^* + \varphi' R' \Delta z_1'/(6\Delta t)$$

$$\beta_1^* = \frac{D'}{\Delta z_1'} + \frac{\lambda\varphi' R' \Delta z_1'}{3}$$

$$\gamma_1^* = \frac{-D'}{\Delta z_1'} + \frac{\lambda\varphi' R' \Delta z_1'}{6}$$

and the spatial increments are: $\Delta z_i' = z_{i+1}' - z_i'$; $i=1,2,..,n'-1$.

For the spherical symmetry, the tridiagonal set of equations is obtained in a similar way. For all elements but the first one, r^2 is approximated by an average of r_i^2 and r_{i-1}^2. For the first element the integration is explicitely

performed and the element matrices obtained are as follows,

$$[E]^e = \int_0^{r_1} r^2 D' \left\{\frac{\partial N}{\partial r}\right\}\left\{\frac{\partial N}{\partial r}\right\}^T dr = \frac{D' r_1}{3}\begin{bmatrix} 1 & -1 \\ -1 & 1 \end{bmatrix}$$

and

$$[M]^e = \int_0^{r_1} r^2 \{N\}\{N\}^T dr = \frac{r_1^3}{60}\begin{bmatrix} 2 & 3 \\ 3 & 5 \end{bmatrix}$$

Two algorithms are proposed by the authors for the overall solution of the problem. First, an iterative algorithm consisting in

(1) – At the begenning of a time step, obtain an estimation, by means of an extrapolation formula (Eq. [A1.18] below), of the concentration at the surface of the porous blocks.

(2) – Obtain from that value and the solution at the previous time step an extimation of the leakage term, Γ, from Eq. A1.17.

(3) – Use this estimation to solve the problem in the macropore continuum, Eq. A1.10.

(4) – Solve the problem in the porous blocks with the Dirichlet condition furnished by the concentration in the macropore continuum,

(5) – An improved estimation for the concentration in the porous blocks and hence for Γ is obtained.

The iterative process consisting of stages (2), (3), (4) is then repeated until negligible changes in the concentration inside the porous blocks are obtained. According to the authors, one or two iterations are sufficient to obtain the convergence. At the begenning of a new time step, the extrapolation formula used to update the concentration in the porous blocks and to start the iterative algorithm is

$$c_j'^{k+1} = c_j'^{k} + (c_j'^{k} - c_j'^{k-1}) \frac{\log(t_{k+1}/t_k)}{\log(t_k/t_{k-1})} \qquad [A1.18]$$

A direct solution scheme is also proposed. In equation, Eq. A1.16, a flux term appears which is in fact directly related to the leakage term, Γ. So, rather than solving the diffusion equation in the porous blocks with Dirichlet condition, the tridiagonal set of equations is written

$$\beta_1 c_1'^{k+1} + \gamma_1 c_2'^{k+1} = d_1$$

$$\alpha_i c_{i-1}'^{k+1} + \beta_i c_i'^{k+1} + \gamma_i c_{i+1}'^{k+1} = d_i \quad i=2,3,..,n'-1$$

$$\alpha_{n'} c_{n'-1}'^{k+1} + \beta_{n'} c_{n'}'^{k+1} = d_{n'} - \Gamma_j^{k+\theta} \qquad [A1.19]$$

Using the first part of Thomas' algorithm, forward elimination, the following expression is obtained relating the leakage term Γ and the concentration at the interface

$$-\Gamma_j^{k+\theta} = l_{n'}c_j'^{k+1} + (\alpha_{n'}g_{n'-1} - d_{n'})_j \quad j=1,2,..,n \qquad [A1.20]$$

where l and g are coefficients resulting from the forward elimination. This equation is used to eliminate the leakage term from Eq. A1.10. Then, the concentration in the macropore continuum is obtained and a backward substitution in the set of equations (Eq. A1.19) gives the solution in the porous blocks. The forward and backward stages of Thomas' algorithm are given below.

Forward elimination

$l_1 = \beta_1$

$u_{i-1} = \gamma_{i-1}/l_{i-1} \qquad i=2,3,..,n'$

$l_i = \beta_i - \alpha_i u_{i-1} \qquad i=2,3,..,n'$

$g_1 = d_1/l_1$

$g_i = (d_i - \alpha_i g_{i-1})/l_i \quad i=2,3,..,n'$

Notice that the right hand side of Eq. A1.10 is now

$$F_i^* = F_i - mM_{ij}(\alpha_{n'}g_{n'-1} - d_{n'})_j$$

Backward Substitution

The backward substituation to obtain the solution in the porous blocks is simply

$$c_{n'}'^{k+1} = c_j^{k+1}$$

$$c_i'^{k+1} = g_i - u_i c_{i+1}'^{k+1} \quad i = n'-1, n'-2, \ldots,1$$

The solution obtained with above procedures have been compared with the analytical solution given by **Tang et al.** (1981) (see page 86) for transport in plane fractures. A very good agreement is obtained for the concentration profile along the fracture and inside the porous matrix. Calculations were also carried out to evaluate the errors induced by assuming a one dimensional transport in the porous matrix where a trully two–dimensional approach is required. Comparisons with the results of **Grisak and Pickens** (1980) and **Noorishad and Mehran** (1982) who employed a two dimensional formulation of the diffusion process inside the porous blocks show that the agreement is within 1%. The authors also claim that the solution is little sensitive to the size of space and time increments.

APPENDIX 2

Numerical solution of an Integrodifferential Equation.

We give here an algorithm to treat the time derivatives and the convolution product appearing in equations such that Eq. [3.166]. We disregard is this annex the spatial approximation of the convection–dispersion operator which can be carried out with finite difference or finite element approximations.

The integro–differential equations apearing in the modeling of solute transport in aggregated media can be symbolically written

$$\theta_m \frac{\partial C_m}{\partial t} - \theta_{im} \int_0^t d\rho(t-s)/dt \, \frac{\partial C_m}{\partial t}(s)\, ds = A[C_m(t)] + b \qquad [A2.1]$$

where ρ is a function referred as "*Memory Function*", and related to the function B_t in equation [3.166]. For above formulation, ρ is in fact the solution of the diffusion equation with homogeneous boundary and initial conditions, and the convolution product stands for the time derivative of the average immobile concentration. A[.], in the right hand side of Eq. [A2.1] is the spatial convection–dispersion operator and b corresponds to a possible sink/source term. The development of the following algorithm uses the fact that ρ can be expressed as an infinit sum of exponentials. To derive a discrete time integration formula, Hornung (1987) first integrates by parts equation [A2.1]. This leads to

$$\theta_m \frac{\partial C_m}{\partial t} - \theta_{im} \int_0^t \rho(t-s)\, \frac{\partial^2 C_m}{\partial t^2}(s)\, ds + \theta_{im}\, \rho(0)\, \frac{\partial C_m}{\partial t}(t) - \theta_{im}\rho(t)\, \frac{\partial C_m}{\partial t}(0) = A[C_m(t)] + b \qquad [A2.2]$$

At time t+h, this expression reads

$$\theta_m \frac{\partial C_m}{\partial t} - \theta_{im} \int_0^{t+h} \rho(t+h-s)\, \frac{\partial^2 C_m}{\partial t^2}(s)\, ds + \theta_{im}\, \rho(0)\, \frac{\partial C_m}{\partial t}(t+h) - \theta_{im}\rho(t+h)\, \frac{\partial C_m}{\partial t}(0) = A[C_m(t+h)] + b \qquad [A2.3]$$

In the following we use C_j and C'_j in place of $C_m(t_j)$ and $\partial C_m/\partial t(t_j)$, respectively. (t_j) is the time series discretizing the time interval. With this discretization of time, above equation is approximated by

$$\theta_m C'_{j+1} - \theta_{im} \sum_{i=1}^{j} \frac{C'_i - C'_{i-1}}{h} \int_{t_{i-1}}^{t_i} \rho(t_{j+1}-s)\, ds - \theta_{im} \frac{C'_{j+1} - C'_j}{h} \int_{t_j}^{t_{j+1}} \rho(t_{j+1}-s) ds +$$

$$\theta_{im}\, C'_{j+1} - \theta_{im}\, \rho_{j+1} C'_0 = A[C_{j+1}] + b \qquad [A2.4]$$

Using the fact that,

$$\int_{t_{i-1}}^{t_i} \rho(t_{j+1}-s)\, ds = \int_{t_{j-i-1}}^{t_{j-i+2}} \rho(s)\, ds\,, \qquad [A2.5]$$

the approximation

$$C_{j+1} = C_j + \frac{h}{2}(C'_{j+1} + C'_j) \qquad [A2.6]$$

and rearraging, it comes

$$(\theta_m + \theta_{im} - \frac{\theta_{im}}{h}\int_{t_0}^{t_1} \rho(s)ds - \frac{h}{2}A)C'_{j+1} = A[C_j + \frac{h}{2}C'_j] +$$

$$[(1-\delta_{0j})\frac{\theta_{im}}{h}\int_{t_1}^{t_2} \rho(s)ds - \frac{\theta_{im}}{h}\int_{t_0}^{t_1} \rho(s)ds]C'_j$$

$$-\frac{\theta_{im}}{h}\sum_{i=1}^{j-1}\left[\int_{t_{j-i}}^{t_{j-i+1}} \rho(s)ds - \int_{t_{j-i+1}}^{t_{j-i+2}} \rho(s)ds\right]C'_i +$$

$$\left[\theta_{im}\rho_{j+1} - (1-\delta_{0j})\frac{\theta_{im}}{h}\int_{t_j}^{t_{j+1}} \rho(s)ds\right]C'_0 + b \qquad [A2.7]$$

where δ_{0j} is equal to 1 if j=0 and 0 otherwise. Notice that Eq. [A2.5] is a property of $\rho(t)$ fundamental for the development of Eq. [A2.7]. If the time increment, h, is constant, integrals involving the function ρ can be calculated once and for all. Above formula relates the time derivative of the concentration in the mobile phase at time, t+h, left hand side, to the spatial operator, first term of the right hand side and to the history of the phenomena through all the time variations already experienced by C, all other terms in the rigth hand side. Remark that, due to the properties of ρ, the overall contribution of the C_i' only needs to be saved and not individual C_i'. To complete the procedure, a finite difference or finite element approximation must be carried out to approximate A[.]. We give hereafter another algorithm.

The following algorithm due to Herrera and Yates (1977) proceeds in a slightly different way to take advantage of the particular properties of $\rho(t)$. For numerical calculations, the infinit sum of exponential appearing in $\rho(t)$ must first be approximated by a finite sum. Here also we consider the problem of time integration only, and disregard the spatial approximation. Consider the

convolution product

$$\int_0^t \rho(t-s)\,\frac{\partial C_m}{\partial t}(s)\,ds \qquad [A2.8]$$

where ρ is given by:

$$\rho(s) = \sum_{i=0}^{\infty} c_i e^{-b_i s} \qquad [A2.9]$$

This convolution product appears for example in Eq. [3.166]. Notice that since ρ is a sum of exponential, it does not make any difference if ρ or $d\rho/dt$ appear in the convolution product. The generality of what follows is preserved. The method proposed by **Herrera and Yates (1977)**, consist to construct a familly of functions ρ_n such that

$$\int_0^{\infty} \rho(s)\,ds = \int_0^{\infty} \rho_n(s)\,ds \qquad [A2.10]$$

and of course presenting only a finit number of terms in the summation. Since a simple direct truncation of the infinit sum would violate this requirement, the authors propose to derived ρ_n in the following way.

First we integrate by parts equation [A2.8]; which gives

$$\int_0^t \rho(t-s)\,\frac{\partial C_m}{\partial t}(s)\,ds = \left[\bar{\rho}(t-s)\frac{\partial C_m}{\partial t}(s)\right]_{s=0}^{t} - \int_0^t \bar{\rho}(t-s)\,\frac{\partial^2 C_m}{\partial t^2}(s)\,ds \qquad [A2.11]$$

where $\bar{\rho}(t)=\int_0^t \rho(s)ds$. Given that $\rho(0)=0$ and that $\frac{\partial C_m}{\partial t}(0)=0$, it remains

$$\int_0^t \rho(t-s)\,\frac{\partial C_m}{\partial t}(s)\,ds = -\int_0^t \bar{\rho}(t-s)\,\frac{\partial^2 C_m}{\partial t^2}(s)\,ds. \qquad [A2.12]$$

Notice that $\bar{\rho}$ is also an infinit sum of exponentials. We note $\bar{\rho}_n$ the function corresponding to the sum of the first n terms. Thus, the convolution integral above is approximated by

$$\int_0^t \rho(t-s)\,\frac{\partial C_m}{\partial t}(s)\,ds \approx -\int_0^t \bar{\rho}_n(t-s)\,\frac{\partial^2 C_m}{\partial t^2}(s)\,ds. \qquad [A2.13]$$

Integrating by parts one more time the integral on the right hand side it comes

$$-\int_0^t \bar{\rho}_n(t-s)\,\frac{\partial^2 C_m}{\partial t^2}(s)\,ds = -\left[\frac{\partial C_m}{\partial t}(s)\bar{\rho}_n(t-s)\right]_{s=0}^{t} + \int_0^t \bar{\rho}_n'(t-s)\,\frac{\partial C_m}{\partial t}(s)\,ds \quad [A2.14]$$

where ' denotes the derivation. Notice that now $\bar{\rho}(0)$ is not equal to 0. Hence, it comes

$$-\int_0^t \bar{\rho}_n(t-s)\,\frac{\partial^2 C_m}{\partial t^2}(s)\,ds = -\frac{\partial C_m}{\partial t}(t)\bar{\rho}_n(0) + \int_0^t \bar{\rho}_n'(t-s)\,\frac{\partial C_m}{\partial t}(s)\,ds\,. \quad [A2.15]$$

Integrating [A2.9], the following expression is obtained for $\bar{\rho}$,

$$\bar{\rho}(t) = K - \sum_{i=0}^{\infty} \frac{c_n}{b_n} e^{-b_n t} \quad [A2.16]$$

where $K = \bar{\rho}(0)$. Notice that $\bar{\rho}(\infty) = \bar{\rho}_n(\infty)$ and that $\bar{\rho}_n(0) = \sum_{i=n+1}^{\infty} \frac{c_n}{b_n}$. We note $\bar{\rho}_n(0) = A_n$. We can now define a function ρ_n such that the initial convolution product, Eq. [A2.8], is approximated by:

$$\int_0^t \rho_n(t-s)\,\frac{\partial C_m}{\partial t}(s)\,ds = -\frac{\partial C_m}{\partial t}(t)\bar{\rho}_n(0) + \int_0^t \bar{\rho}_n'(t-s)\,\frac{\partial C_m}{\partial t}(s)\,ds\,. \quad [A2.17]$$

Remarking that we have the following relation,

$$\frac{\partial C_m}{\partial t}(t)\bar{\rho}_n(0) = \int_0^t \bar{\rho}_n(0)\,\frac{\partial C_m}{\partial t}(s)\,\delta(t-s)\,ds \quad [A2.18]$$

where δ is the Dirac–function, it comes

$$\int_0^t \rho_n(t-s)\,\frac{\partial C_m}{\partial t}(s)\,ds = \int_0^t \bar{\rho}_n'(t-s)\,\frac{\partial C_m}{\partial t}(s) - \bar{\rho}_n(0)\,\frac{\partial C_m}{\partial t}(s)\,\delta(t-s)ds \quad [A2.19]$$

from which we define the function ρ_n by

$$\rho_n(t) = \bar{\rho}_n'(t) - \bar{\rho}_n(0)\delta(t) = -A_n\delta(t) + \sum_{i=0}^{n} c_i e^{-b_i t} . \qquad [A2.20]$$

Remark that ρ_n has in addition to the trucated sum a Dirac–function located at the origin with a mass accounting for the truncated terms. So defined, ρ_n verifies Eq. [A2.10]. Using this function ρ_n in place of the function ρ in the convolution product leads to a transport equation of the form

$$L[C_m] - A_n \frac{\partial C_m}{\partial t}(t) - \sum_{i=0}^{n} c_i e^{-b_i t} \int_0^t e^{b_i s} \frac{\partial C_m}{\partial t}(s)ds = S \frac{\partial C_m}{\partial t}(t) \qquad [A2.21]$$

where $L[C_m]$ is the spatial operator. With this algorithm, all we have to save from one time step to another are the n integrals corresponding to the n terms retained in the truncated sum. When time integration is performed, the integrals on the left hand side are easily updated by adding to their current value the contribution of the current time step. So as in the previous algorithm, the global contribution of previous time derivatives only has to be saved and not the individual values. For example, if the spatial discretization has N nodes, and if we keep n terms in the sum, only Nn values will be stored. Notice also that with this algorithm we are free to use any time step we want. Typical values of n for transport in leaky aquifers are between 0 and 5. In fact, since when t increases the error decreases, one can use large values (<5) at the beginning and smaller values later, (0 or 1). According to **Herrera et al.** a value of 0 is most of the time sufficient. Also, it is intersting to remark that for short times we have at our disposition some simple approximations for ρ. Thus, it seems that a main problem in any numerical algorithm will be to decide when to shift from a short time approximation to a sum of exponentials and how many terms should be used. Since an estimation of the error can be obtained, estimation of A_n, we should be able to decide at any time of the number of terms to be kept.

APPENDIX 3

Some extensions of the TFM to adsorbed solutes or species undergoing a decay process.

In paragraph 4.2, equations [4.8] and [4.9] give the average concentration profile for a solute that does not interact with the porous matrix and/or does not undergo any decay process. These results can be easily extended to the case of solutes with a linear adsorption isotherm, or undergoing a decay process.

Extension to adsorbed chemicals.

If we assume an adsorption process with a linear adsorption isotherm, a partition coefficient K and a local equilibrium, the breakthrough time for a molecule of that chemical is, **Jury and Collins (1982)**,

$$t_a = Kt' \qquad [A3.1]$$

where t' is the breakthrough time for a molecule of nonreacting tracer under the same flow conditions. Assuming that the partition coefficient is a random variable with density function p(K), the average concentration profile is then,

$$C_a(z,t) = \int_0^\infty C_{in}(t-Kt') \int_0^\infty \int_0^\infty (l/z) F_1(it') i G(i) p(K)\, dK\, di dt' \qquad [A3.2]$$

Extension to First Order Decay

If we assume that the rate of decay of the chemical is R, then the breakthrough concentration at depth z, will be

$$C(z,t,t',R) = H(t-t')C_{in}(t-t')e^{-Rt'} \qquad [A3.3]$$

where t' is still the breakthroug time of a nondecaying tracer and H is the heaviside function. If we assume that R is a random variable with density function q(R) then the averaged concentration profile willbe given by

$$C_d(z,t) = \int_0^\infty C_{in}(t-t') \int_0^\infty \int_0^\infty (l/z) F_1(it') i G(i) q(R) e^{-Rt'}\, dK\, di dt' \qquad [A3.2]$$

Tab. 3.1. Diffusion Equation, Average Immobile Concentration and Surface to Volume Ratio for various aggregates.

Aggregate Type	Immob. Liquid Phase Equation	Average Immob. Phase Conc.	Function S'
Spherical Aggregates	$\frac{\partial C_a}{\partial T} = \frac{\gamma_s}{\rho^2}\frac{\partial}{\partial \rho}(\rho^2 \frac{\partial C_a}{\partial \rho})$	$C_{im}=3\int_0^1 \rho^2 C_a d\rho$	$S'=\frac{3}{r}$
Rectangular Aggregates	$\frac{\partial C_a}{\partial T} = \gamma_s \frac{\partial^2 C_a}{\partial \rho^2}$	$C_{im} = \int_0^1 C_a d\rho$	$S'=\frac{1}{a}$
Cylindrical Aggregates	$\frac{\partial C_a}{\partial T} = \frac{\gamma_s}{\rho}\frac{\partial}{\partial \rho}(\rho \frac{\partial C_a}{\partial \rho})$	$C_{im}=2\int_0^1 \rho C_a d\rho$	$S'=\frac{2}{r}$
Hollow Cylindrical Macropores	$\frac{\partial C_a}{\partial T} = \frac{\gamma_s}{\rho}\frac{\partial}{\partial \rho}(\rho \frac{\partial C_a}{\partial \rho})$	$C_{im}=\frac{2}{\rho_0^2-1}\int_0^{\rho_0} \rho C_a d\rho$	$S'=\frac{2r}{r^2-r_0^2}$

–Solute transport in the mobile region is in all cases above modeled by the following equation:

$$\beta R \frac{\partial C_m}{\partial T} + (1-\beta) R \frac{\partial C_{im}}{\partial T} = \frac{1}{P}\frac{\partial^2 C_m}{\partial Z^2} - \frac{\partial C_m}{\partial Z} \qquad Z \in [0,1]$$

and dimensionless parameters, T,R,Z,β,ρ,γ_s are defined by equations [4.58], [4.59], [4.60]

– $\rho_0 = r/r_0$. See also eq. [4.61].

– Useful boundary and initial conditions are given in the text.

Tab. 3.2 Functions H_{d1} and H_{d2} for various aggregate geometries

Geometry	H_{d1}	H_{d2}
Spherical	$\lambda\left[\frac{\sinh 2\lambda + \sin 2\lambda}{\cosh 2\lambda - \cos 2\lambda}\right] - 1$	$\lambda\left[\frac{\sinh 2\lambda - \sin 2\lambda}{\cosh 2\lambda - \cos 2\lambda}\right]$
Cylinder with sealed ends	$\lambda\left[\frac{ac+bd-ad+bc}{c^2+d^2}\right]$	$\lambda\left[\frac{-ac-bd-ad+bc}{c^2+d^2}\right]$
Slabs with sealed ends	$\lambda\left[\frac{\sinh 2\lambda - \sin 2\lambda}{\cosh 2\lambda + \cos 2\lambda}\right]$	$\lambda\left[\frac{\sinh 2\lambda + \sin 2\lambda}{\cosh 2\lambda + \cos 2\lambda}\right]$

$-\ a = \mathrm{Ber}_1(\sqrt{2}\lambda),\ b = \mathrm{Bei}_1(\sqrt{2}\lambda),\ c = \mathrm{Ber}_0(\sqrt{2}\lambda),\ d = \mathrm{Bei}_0(\sqrt{2}\lambda)$

Tab. 3.3 Local and average concentrations inside aggregates of various geometries. $C|_{t=0} = 0$, $C|_{\Gamma} = 1$.

SPHERICAL AGGREGATES

Local Concentration

$$C(t,\rho) = 1 + \frac{2}{\pi\rho}\sum_{n=1}^{\infty}\frac{(-1)^n}{n}\sin(\rho\pi n)e^{-DTn^2\pi^2}$$

Average Concentration

$$<C>(T) = 1 - \frac{6}{\pi^2}\sum_{n=1}^{\infty}\frac{e^{-DTn^2\pi^2}}{n^2}$$

where $T = DT/a^2$. a is the radius of the sphere and $\rho \in [0,1]$ is the normalized radius.

PLANE SHEET

$\Omega = [-a,a]\times]-\infty,\infty[\times]-\infty,\infty[$.

Local concentration

$$C(T,x) = \sum_{n=0}^{\infty}(-1)^n \operatorname{erfc}\left[\frac{(2n+1)\,a - x}{2\sqrt{Dt}}\right] + \sum_{n=0}^{\infty}(-1)^n \operatorname{erfc}\left[\frac{(2n+1)\,a + x}{2\sqrt{Dt}}\right]$$

Average Concentration

$$<C>(T) = 2\sqrt{T}/\sqrt{\pi} + 4\sqrt{T}\sum_{n=1}^{\infty}(-1)^n \operatorname{ierf}(\frac{n}{\sqrt{T}})$$

INFINITE BEAM WITH RECTANGULAR SECTION

$\Omega = [-a,a]\times[-b,b]\times]-\infty,\infty[$

Local concentration

$$C(t,x,y)=1-\frac{16}{\pi^2}\sum_{n=0}^{\infty}\sum_{m=0}^{\infty}\frac{(-1)^{n+m}}{(2n+1)(2m+1)}e^{-\frac{Dt\pi^2}{4}\{[\frac{2n+1}{a}]^2+[\frac{2m+1}{b}]^2\}}\cos\frac{(2n+1)x\pi}{2a}\cos\frac{(2m$$

Average Concentration

$$<C(t)> = 1-\frac{4^3}{\pi^4}\sum_{n=0}^{\infty}\sum_{m=0}^{\infty}\frac{1}{(2m+1)^2(2n+1)^2}e^{-\frac{Dt\pi^2}{4}\{[\frac{2n+1}{a}]^2+[\frac{2m+1}{b}]^2\}}$$

RECTANGULAR PRISM

$\Omega = [-a,a]\times[-b,b]\times]-c,c[$

Local concentration

$$C(t,x,y)=1-\frac{64}{\pi^3}\sum_{n=0}^{\infty}\sum_{m=0}^{\infty}\sum_{l=0}^{\infty}\frac{(-1)^{n+m+l}}{(2n+1)(2m+1)(2l+1)}e^{-t\alpha}\cos\frac{(2n+1)x\pi}{2a}\cos\frac{(2m+1)y\pi}{2b}\cos\frac{(2l+1}{2}$$

where $\alpha = \frac{D\pi^2}{4}\left[\frac{(2l+1)^2}{a^2}+\frac{(2m+1)^2}{b^2}+\frac{(2n+1)^2}{c^2}\right]$

Average Concentration

$$<C(t)> = 1-\frac{8^3}{\pi^6}\sum_{n=0}^{\infty}\sum_{m=0}^{\infty}\sum_{l=0}^{\infty}\frac{e^{-t\alpha}}{(2l+1)^2(2m+1)^2(2n+1)^2}$$

INFINITE CYLINDER

$\Omega = [0,a]\times]-\infty,\infty[$ (Cylindrical Symmetry)

Local concentration

$$C(r,t) = 1 - \frac{2}{a}\sum_{n=1}^{\infty} \frac{e^{-D\alpha_n{}^2 t}}{\alpha_n J_0(a\alpha_n)} J_0(r\alpha_n)$$

and where α_n's are the positive roots of $J_0(a\alpha_n) = 0$.

Average Concentration

$$<C(T)> = 1 - 4\sum_{n=1}^{\infty} \frac{e^{-a^2\alpha_n{}^2 T}}{a^2\alpha_n{}^2}$$

FINITE LENGTH CYLINDER

$\Omega = [0,a]\times[-b,b]$ (Cylindrical Symmetry)

Local concentration

$$C(t,r,z) = 1 - \frac{8}{\pi a}\sum_{n=0}^{\infty}\sum_{m=0}^{\infty} \frac{(-1)^n J_0(r\alpha_m)}{(2n+1)\alpha_m J_1(a\alpha_m)} \cos\frac{(2n+1)\pi z}{2b} e^{-Dt[\alpha_m{}^2+(2n+1)^2\pi^2/4b^2]}$$

and where α_m's are the positive roots of $J_0(a\alpha) = 0$.

Average Concentration

$$<C(T)> = 1 - \frac{32}{a^2\pi^2}\sum_{n=0}^{\infty}\sum_{m=0}^{\infty} \frac{e^{-Ta^2\alpha_m{}^2}\ e^{-Ta^2(2n+1)^2\pi^2/4b^2}}{\alpha_m{}^2(2n+1)^2}$$

where $T = Dt/a^2$

INFINITE HOLLOW CYLINDER

$\Omega = [a,b]\times]-\infty,\infty[$ (Cylindrical Symmetry)

Local concentration

$$C(r,t) = 1 - \pi \sum_{n=1}^{\infty} e^{-D\alpha_n^2 t} \frac{J_1^2(b\alpha_n)[Y_0(r\alpha_n)J_0(a\alpha_n) - Y_0(a\alpha_n)J_0(r\alpha_n)]}{[J_0^2(a\alpha_n) - J_1^2(b\alpha_n)]}$$

and where α_n's are the positive roots of

$$\alpha[J_0(\alpha a)Y_1(b\alpha) - Y_0(\alpha a)J_1(b\alpha)] = 0$$

Let $\rho = r/a$ and $\rho_0 = b/a$.

Average Concentration

$$\langle C(t)\rangle = 1 - \frac{2\pi}{\rho_0^2 - 1} \sum_{n=1}^{\infty} \frac{e^{-D\alpha_n^2 t} J_1^2(\rho_0\alpha_n)}{J_0^2(\alpha_n) - J_1^2(\rho_0\alpha_n)} \frac{1}{\alpha_n} \left\{ \rho_0 \left[J_0(\alpha_n)Y_1(\alpha_n\rho_0) - Y_0(\alpha_n)J_1(\alpha_n\rho_0) \right] + \left[Y_0(\alpha_n)J_1(\alpha_n) - J_0(\alpha_n)Y_1(\alpha_n) \right] \right\}$$

Tab. 3.5 Laplace transforms of local and average concentrations $C(t,.)\big|_{t=0} = 0$ and $C(t,.)\big|_{\Gamma} = C_m(t,.)$.

Geometry	Local Concentration $\overline{C}_a(s,r)$	Average Concentration $\overline{C}_{im}(s,r)$
Plane	$\frac{\cosh(pr)}{\cosh(p)}\overline{C}_m$	$\frac{\tanh(p)}{p}\overline{C}_m$
Cylindrical	$\frac{I_0(pr)}{I_0(p)}\overline{C}_m$	$\frac{2I_1(p)}{pI_0(p)}\overline{C}_m$
Spherical	$\frac{1}{r}\frac{\sinh(pr)}{\sinh(p)}\overline{C}_m$	$\left[\frac{3}{p}\coth(p)-\frac{3}{p^2}\right]\overline{C}_m$
Hollow	$\frac{K_0(pr)I_1(pb)-K_1(pb)I_0(pr)}{K_0(pa)I_1(pb)+K_1(pb)I_0(pa)}\overline{C}_m$	$\frac{2[K_1(pa)I_1(pb)-K_1(pb)I_1(pa)]}{p[I_0(pa)K_1(pb)+I_1(pb)K_0(pa)]}\overline{C}_m$

where in every case p is such that: $p^2 = s/\gamma$

Tab. 3.6 Functions g for the analytical solution of transport through a mixture of particules.

Geometry	α_f	$g^i(s)$
Plane	0	$w^i(s)\tanh(w^i(s))$
Cylindrical	1	$w^i(s)\frac{I_1[w^i(s)]}{I_0[w^i(s)]}$
Spherical	2	$w^i(s)\coth(w^i(s)) - 1$

Tab. 3.7 Functions H_{d1} and H_{d2} for different geometries and first–order kinetic adsorption.

Geometry	H_{d1}	H_{d2}
Plane	$\frac{\varphi_2\sinh 2\varphi_2 - \varphi_1\sin 2\varphi_1}{\cosh 2\varphi_2 + \cos 2\varphi_1}$	$\frac{-\varphi_1\sinh 2\varphi_2 - \varphi_2\sin 2\varphi_1}{\cosh 2\varphi_2 + \cos 2\varphi_1}$
Cylindrical	"	"
Spherical	$\frac{\varphi_2\sinh 2\varphi_2 + \varphi_1\sin 2\varphi_1}{\cosh 2\varphi_2 - \cos 2\varphi_1} - 1$	$\frac{-\varphi_1\sinh 2\varphi_2 + \varphi_2\sin 2\varphi_1}{\cosh 2\varphi_2 - \cos 2\varphi_1}$

Tab. 3.8 Block–Geometry Functions and volume to surface ratio for some simple aggregate shapes.

Geometry	a	B(x)
Infinite Slab	$\frac{d}{2}$	$\tanh(x)/x$
Cylindrical	$\frac{R}{2}$	$I_1(2x)/xI_0(2x)$
Spherical	$\frac{R}{3}$	$(\coth 3x)/x - \frac{x^{-2}}{3}$
Parallelepiped	$\frac{XYZ}{2(XY+YZ+ZX)}$	See (a) below
Hollow Cylinder	$\frac{R_2^1 - R_1^2}{2R_1}$	$\frac{1}{x}\left[\frac{K_1(Z_1)I_1(Z_2) - I_1(Z_1)K_1(Z_2)}{I_0(Z_1)K_1(Z_2)+K_0(Z_1)I_1(Z_2)}\right.$

where $Z_i = R_i x/a$

(a) The BGF for the rectangular parallelepiped is

$$B(x) = \frac{512}{\pi^6} \sum_{l} \sum_{m} \sum_{n} [\alpha_{lmn}/(\alpha_{lmn}+x^2)]l^{-2}m^{-2}n^{-2}$$

where the summation is made over positive odd integers and

$$\alpha_{lmn} = a^2\pi^2(l^2/X^2+m^2/Y^2+n^2/Z^2).$$

The cube is a special case with X=Y=Z=6a.

(b) The BGF for the quasi–steady state model is $B(x) = \alpha/(\alpha+x^2)$.

Tab. 3.9 Time–Dependent Block Geometry Functions.

Geometry	a	B(x)	$B_t(t)$ c_n	b_n
Infinite Slab	$\frac{d}{2}$	$\tanh(x)/x$	2	$(2n-1)^2\pi^2/4$
Cylindrical	$\frac{R}{2}$	$I_1(2x)/xI_0(2x)$	1	$\lambda_n^2/4$
Spherical	$\frac{R}{3}$	$(\coth 3x)/x - \frac{x^{-2}}{3}$	2/3	$n^2\pi^2/9$
Parallelepiped	$\frac{XYZ}{2(XY+YZ+ZX)}$	See (a) below	See (b) below	
QSS Model	/	$\alpha/(\alpha+x^2)$	See (c) below	

where λ_n is the n^{th} positive root of $J_0(\lambda) = 0$.

(a) The BGF for the rectangular parallelepiped is

$$B(x) = \frac{512}{\pi^6} \sum_{l} \sum_{m} \sum_{n} [\alpha_{lmn}/(\alpha_{lmn}+x^2)](lmn)^{-2}$$

$$\alpha_{lmn} = a^2\pi^2(l^2/X^2+m^2/Y^2+n^2/Z^2).$$

(b) The time–dependent BGF is given by

$$B_t(t) = \frac{512}{\pi^6} \sum_{l} \sum_{m} \sum_{n} \alpha_{lmn}(lmn)^{-2}\exp(-\alpha_{lmn}t)$$

where for (a) and (b) the summation is made over positive odd integers.

(c) The time–dependent BGF for the QSS model is

$$B_t(t) = \alpha\exp(-\alpha t)$$

Tab. 3.10 First, Second and Third Moments of the breakthrough curve for various equilibrium and nonequilibrium transport models.

	LEA	Spherical Aggregates	Quasi–Steady State	Chemical Nonequilibriu
μ_1'	XR	XR	XR	XR
μ_2	$\frac{2XR^2}{P}$	$\frac{2XR^2}{P}+\frac{2X(1-\beta)^2R^2}{15\gamma}$	$\frac{2XR^2}{P}+\frac{2X(1-\beta)^2R^2}{\omega}$	$\frac{2XR^2}{P}+\frac{2X(R-1}{F}$
μ_3	$\frac{12XR^3}{P^2}$	$\frac{12XR^3}{P^2}+\frac{4X(1-\beta)^2R^3}{5P\gamma}$	$\frac{12XR^3}{P^2}+\frac{12X(1-\beta)^2R^3}{P\omega}$	$\frac{12XR^3}{P^2}+\frac{12X(R-1}{PF}$
		$+\frac{4X(1-\beta)^3R^3}{105\gamma^2}$	$+\frac{6X(1-\beta)^3R^3}{\omega^2}$	$\frac{6X(R-1)}{F^2}$

Tab. 3.11 Laplace transform of the breakthrough curve for various transport models

Model	Laplace Transform of the Breakthrough Curve.
Spherical Aggregate	$\overline{C}_e(p)=A\exp\left\{\frac{XP}{2}\left[1-\left[1+\frac{4}{P}(\beta Rp+G(p))\right]^{1/2}\right]\right\}$
Physical Nonequilibrium	$\overline{C}_e(p)=A\exp\left\{\frac{XP}{2}\left[1-\left[1+\frac{4}{P}(\beta Rp+H(p))\right]^{1/2}\right]\right\}$
Chemical Nonequilibrium	$\overline{C}_e(p)=A\exp\left\{\frac{XP}{2}\left[1-\left[1+\frac{4p}{P}\left[1+\frac{F(R-1)}{p+F}\right]\right]^{1/2}\right]\right\}$
Local Equilibrium	$\overline{C}_e(p)=A\exp\left[\frac{XP}{2}\left[1-\left[1+\frac{4Rp}{P}\right]^{1/2}\right]\right]$

A is the flux concentration applied at the surface of the column
F is the coefficient in the first–order rate chemical process.
β is defined Eq. [3.60b]

$$G(p)=3\gamma\sqrt{\frac{p}{\gamma}}\coth\sqrt{\frac{p}{\gamma}}$$

$$H(p)=\frac{(1-\beta)R\omega p}{(1-\beta)Rp+\omega}$$

$\gamma'=\gamma/[R(1-\beta)]$ and γ is the coefficient given Eq. [3.60a] multiplied by R_{im}.
ω is defined Eq. [3.28].

Table 3.12 Effective Dispersion Coefficients for various aggregate shapes

Geometry	Dispersion Coefficient
Slab	$D_e = D_m\phi + \frac{(1-\phi)\, a^2 v^2 R_{im}^2}{3 D_a R^2}$
Cylinder	$D_e = D_m\phi + \frac{(1-\phi)\, a^2 v^2 R_{im}^2}{8 D_a R^2}$
Spherical	$D_e = D_m\phi + \frac{(1-\phi)\, a^2 v^2 R_{im}^2}{15 D_a R^2}$
Cyl. Macropore	$D_e = D_m\phi + \frac{(1-\phi)\, b^2 v^2 R_{im}^2}{4 D_a R^2} [2\ln(\frac{b}{a})-1]$
QSS Model	$D_e = D_m\phi + \frac{(1-\phi)^2 v^2 R_{im}^2 \theta}{\alpha R^2}$

$\phi = \theta_m / \theta$.
In each case, a, is the characteristic dimension of the aggregate and f
cylindrical macropore b is the radius of the soil column.